STRUCTURAL STUDIES WITH THE ELECTRON MICROSCOPE

BY

JOHN L. HUTCHISON.

DEPARTMENT OF CHEMISTRY

UNIVERSITY OF GLASGOW.

THESIS SUBMITTED FOR THE DEGREE OF

DOCTOR OF PHILOSOPHY.

OCTOBER, 1970.

ProQuest Number: 11011951

All rights reserved

INFORMATION TO ALL USERS
The quality of this reproduction is dependent upon the quality of the copy submitted.

In the unlikely event that the author did not send a complete manuscript
and there are missing pages, these will be noted. Also, if material had to be removed,
a note will indicate the deletion.

ProQuest 11011951

Published by ProQuest LLC (2018). Copyright of the Dissertation is held by the Author.

All rights reserved.
This work is protected against unauthorized copying under Title 17, United States Code
Microform Edition © ProQuest LLC.

ProQuest LLC.
789 East Eisenhower Parkway
P.O. Box 1346
Ann Arbor, MI 48106 – 1346

SUMMARY

The use of the electron microscope in the study of ionic processes in solution has not been previously reported. In the present work, the hydrolysis products of zirconyl chloride was examined by high resolution electron microscopy. Characterization of various hydrates of zirconyl chloride was carried out, using X-ray and electron diffraction. The hydrolysis was brought about by the reflux of aqueous solutions of zirconyl chloride. Removal of samples of the colloid at various stages of hydrolysis, and subsequent examination of the solids obtained by rapid dehydration of the samples, using an atomiser, has enabled structural units consistent in size with a proposed tetrameric cation $\left[Zr(OH)_2 4H_2O\right]_4^{8+}$ to be resolved in the electron microscope. Single-crystal filaments of chrysotile asbestos were used as a supporting network for the particles, and their lattice images used as a magnification calibration.

Later stages of the hydrolysis produced polymerization of these tetrameric species, and ageing finally produced monoclinic zirconia. The structure and properties of the crystalline zirconia particles is discussed, and evidence from other physical techniques is presented. A suggested mechanism relating the various structures is supported by pH measurements obtained during the hydrolysis.

A preliminary study of the hydrolysis of thorium (IV) showed a chain structure in the early stages of the reaction, the chains being similar in diameter to the $\left[Th(OH)_2\right]_n^{2n+}$ chains present in basic thorium salts.

A high-resolution electron microscope study of Chrysotile was carried out and the characteristics of fibres from various sources is discussed.

ACKNOWLEDGEMENTS

This work was carried out in the Physical Chemistry Department, under the direction of Professor J. Monteath Robertson.

I would like to thank my supervisors Dr. J.R. Fryer and Dr. R. Paterson for their constant help and guidance throughout the course of this work, particularly during the writing of this thesis, and I am also grateful to Miss E. Morrison for her patience in transforming handwritten sheets into typescript.

I would like to express my thanks to Dr. D.D. McNicol of this Department for his assistance in the N.M.R. work, and for many useful discussions. I also thank Dr. D. Webster of Johnson-Matthey, Ltd. for practical help in Surface Area measurement.

Finally, I thank the Science Research Council for financial support and also my colleagues in the Electron Microscopy group, in particular Dr. T. Baird, for their help and assistance at all times.

JOHN L. HUTCHISON.

PART 1

AN ELECTRON MICROSCOPE STUDY OF THE HYDROLYSIS OF Zr (IV).

DIALOGUES IN CHEMISTRY,

INTENDED FOR THE

INSTRUCTION AND ENTERTAINMENT

OF

YOUNG PEOPLE:

IN WHICH THE

FIRST PRINCIPLES

OF THAT

SCIENCE

ARE FULLY EXPLAINED.

TO WHICH ARE ADDED

QUESTIONS AND OTHER EXERCISES

FOR THE

EXAMINATION OF PUPILS.

BY THE REV. J. JOYCE,

AUTHOR OF SCIENTIFIC DIALOGUES,
IN SIX VOLUMES.

A NEW EDITION CORRECTED, WITH ADDITIONS.

IN TWO VOLUMES.

VOL. I.

LONDON:

PRINTED FOR J. JOHNSON,
NO. 72, ST. PAUL'S CHURCH-YARD.

1809.

called Gadolinite, from Professor Gadolin, who discovered it. Its specific gravity is nearly five times that of water, which is almost equal to that of some of the metals, and it has been thought to be a metallic oxyde; but it is generally considered as the substance, which connects the earths with the metals. It may be fused with borax, and with it forms a kind of glass.

Charles. What is GLUCINA?

Tutor. It is obtained from the beryl or emerald, a transparent stone, of a green colour, found crystallized in the mountains of Siberia. The word glucina is derived from the Greek, signifying sweet, because it gives a saccharine taste to all the acids with which it combines.

Charles. What are the properties of this earth?

Tutor. It is a soft white powder, very light, and without taste or smell: it has the property of adhering to the tongue. It has no action on vegetable colours, and is infusible by heat

Charles. What is ZIRCONIA?

Tutor. It is obtained from a precious stone, called *jargon*, or *zircon*, found in the island of Ceylon, from which it derives its name. It is found also in the hyacinth.

James. What are the properties of this earth?

Tutor. It has the form of fine white powder, free from taste or smell. It is soluble in acids, but not in liquid alkalies: It does not combine with them in fusion. Being exposed to a strong heat, zircon fuses, assumes a light grey colour, and such a degree of hardness, on cooling, as to strike fire with steel, and to scratch glass.

SILICA, or siliceous earth is obtained from quartz, flint, rock crystal, and many other stones, found in almost every part of the world.

Charles. Do flints and such hard substances contain an earth?

Tutor. They do; and it is obtained by mixing in a crucible one part of pounded flints and three of potass, and then applying a heat sufficient to melt the mixture. The

INTRODUCTION

ZIRCONIUM 1
POLYMERIC Zr(IV) IONS 1
HYDROUS ZIRCONIA 7
CRYSTALLINE ZrO_2 10
CRYSTALLINE HYDRATES
OF $ZrOCl_2$ 14

INTRODUCTION

ZIRCONIUM: The chemistry of zirconium, discovered in 1789, has been well known for its complexity. In particular, information about aqueous zirconyl species was for a long time confusing and often contradictory, as Connick and McVey (1949) pointed out. Most of the early work on zirconium was concerned with identification of solid phases and this information was collected as a monograph by Venable (1921). Subsequent data was collected by Pascal (1931) and Blumenthal (1954) attempted to correlate the mass of data then available, and to this end a "system of zirconium chemistry" was presented. Blumenthal gave a more detailed account of zirconium chemistry in a book (1959), although many new and significant facts have emerged since then.

Zirconium has found wide usage in the oxide form, being thus used as a refractory, in the development of corrosion-resistant furnace linings (Hoyashi and Doihara, 1968). It has also been used as an opacifying pigment in enamels, although the thermal failure of such enamels was an early cause for concern before the various polymorphic transitions of ZrO_2 were demonstrated by Cöhn and Tolksdorf (1930).

More recently, interest has been directed towards aqueous zirconium chemistry and to the structural relationships between aqueous Zr (IV) species and hydrous zirconia, especially since hydrous zirconia has been shown to be an ion exchange medium (Amphlett, McDonald and Redman, 1958; Britz and Nancollas, 1969).

POLYMERIC Zr (IV) IONS: The hypothesis that Zr (IV) polymerizes on hydrolysis has been held for a long time, although detailed descriptions of the processes involved were often contradictory, when different approaches were used. As early as 1898, Venable and Baskerville, in the course of studies of zirconyl chloride, noted the formation of "hydrogeles" /

/ "hydrogeles" in aqueous Zr (IV) solutions, although they were unable to explain their formation. That polymerization took place in Zr (IV) solutions was first suggested by Ruer (1905) and Venable and Jackson (1920) on the basis of conductivity changes in the solutions. Further evidence of polymeric Zr (IV) ions in aqueous solution was obtained from freezing point studies by Adolf and Pauli (1921), who also suggested that each zirconium atom was attached on average to three hydroxyl groups. The idea that a monomeric ZrO^{++} ion predominated in aqueous solutions over a wide range of acidity was, however, still held by some workers (e.g. Chauvenet, 1920), although a variety of techniques were now providing additional evidence for polymerization (Britton, 1925, Jander and Jahr, 1935).

Laubengayer and Eaton (1940), using electrolysis and polarography suggested, from a high average polarographic deposition potential for Zr, of 1.7 volts, that complex Zr (IV) ions in solution had reasonable stability, whilst the variation in the potential with pH seemed to indicate changes in the nature of the complex ions with changing conditions, in general agreement with earlier observations (Adolf and Pauli, 1921). Small polymers were also indicated from measurements of the hydrolysis of $ZrCl_4$ in acid solutions by Kraus and Tyree (1949), and from the rate of Zr (IV) uptake by ion exchange resins by Lister and McDonald (1952). Connick and McVey (1949), however, pointed out that, at that time, no definite identification of a single Zr (IV) complex had been possible, all the data then available being capable of more than one interpretation. Furthermore, the techniques normally used in such investigations, e.g. freezing point lowering, spectrophotometric analysis, etc., were not ideally suitable, because of the tendency for hydrolysis to take place in aqueous Zr (IV) solutions. By measuring the equilibrium between Zr (IV) in an aqueous phase and an organic phase incorporating a chelating agent, thenoyltrifluoroacetone, it was shown that, at low Zr (IV) concentrations, the average species in 2M perchloric acid was between Zr^{4+} and $Zr\ (OH)^{3+}$. These results however were not accurate, /

/ accurate, due to the presence of some unidentified impurity, although some of the irregularities were consistent with there being polymeric species present at low acidity.

Extending this work, Connick and Reas (1951) suggested that polymers began to form at Zr (IV) concentrations of approximately 2 x 10^{-3}M in 2M perchloric acid and at 2 x 10^{-4}M in 1M perchloric acid. The polymers were thought to form a continuous series from a dimer with between three and five hydroxyl groups attached. This "continuous polymerization" hypothesis was first presented by Graner and Sillen (1947) for Bi (III) hydrolysis. Again, however, the presence of some "impurity" cast doubt upon the exact interpretation of the data.

Further work by Zielen and Connick (1956) confirmed that the Zr (IV) monomer in 1 and 2M perchloric acid was Zr^{4+} and showed that polymerization began at 5 x 10^{-4}M Zr in 2M acid, and at 10^{-4}M Zr in 1M acid. At concentrations up to 0.02M Zr, trimers and probably tetramers were present in the solution. There was, however, no evidence for the dimers proposed earlier by Connick and Reas (1951).

Ultra-centrifuge studies by Kraus and Johnson (1953), of 0.05 and 0.12 M Zr (IV) in 1M perchloric acid/sodium perchlorate solution suggested a degree of polymerization of about three. They found no evidence for the higher polymers, as suggested by Connick and Reas (1951). Johnson and Kraus (1956) found a degree of polymerization of 3.5 for 0.05 M Zr (IV) in M $HCl/NaClO_4$. This, corresponding to trimers or tetramers, agreed with the findings of Zielen and Connick (1956), while Williams-Wynn (1959) was also able to propose a degree of polymerization of approximately four, for Zr (IV) in 1.5M HCL, on the basis of diffusion coefficient measurements. Turbidity measurements by Angstadt and Tyree (1962) gave evidence for a trimeric Zr (IV) species in 2.8 M HCl, in general agreement with other results, although a value of six Zr (IV) ions per aggregate in 0.75 M HCl was rather higher than values /

/ values obtained by other workers (e.g. Johnson and Kraus, 1956).

The first direct evidence for polymeric zirconyl ions was obtained for a solid, rather than for a solution of a zirconyl salt. Clearfield and Vaughan (1956), in an X-ray structure analysis of crystalline $ZrOCl_2 8H_2O$, showed that Zr (IV) species to be a complex in which four Zr atoms, located at the corners of a slightly distorted square, were linked along each edge by two hydroxyl bridges, one above and one below the plane of the square. Four water molecules were also bound to each Zr atom, so that the eight oxygen atoms around it formed a distorted square anti-prism, as shown in figure 1. No evidence was found for Zr-Cl bonds in the complex itself. This complex cation $\left[Zr\ (OH)_2 .\ 4H_2O\right]_2^{8+}$, the stable species in zirconyl chloride octahydrate, was in the same weight range as the polymers proposed by Johnson and Kraus (1956), on the basis of their ultracentrifuge measurements, and there was speculation as to whether or not the cyclic cation remained intact in solution. This speculation was resolved by Muha and Vaughan (1960) who were able to explain low-angle scattering curves from an aqueous solution of $HfOCl_2 . 8H_2O$ if a cation similar to that found in the crystalline solid, was assumed to be present. For solutions of zirconyl chloride, additional low-angle scattering implied that a more highly polymerized species was also present, giving rise to larger inter-atomic distances. The proposed tetrameric species is shown in figure 2 and is very similar to that found in the crystalline state.

In an extensive study of aqueous zirconyl solutions, Ermakov, Marov and Belyeva (1963) arrived at similar conclusions to those of Clearfield, Muha and Vaughan (1956, 1960). The same workers also noted small, but systematic variations in conductivity, and freezing-point depressions of such solutions, with respect to time, and thus detected a slight ageing effect in the solutions.

Matijevic /

FIGURE 1

Projection of one unit cell of $ZrOCl_2 8H_2O$ on (001), showing the cyclic tetramer $\left[Zr(OH)_2 4H_2O\right]_4^{8+}$. Bonds in the tetramer are shown as solid lines.

(after Clearfield & Vaughan 1956)

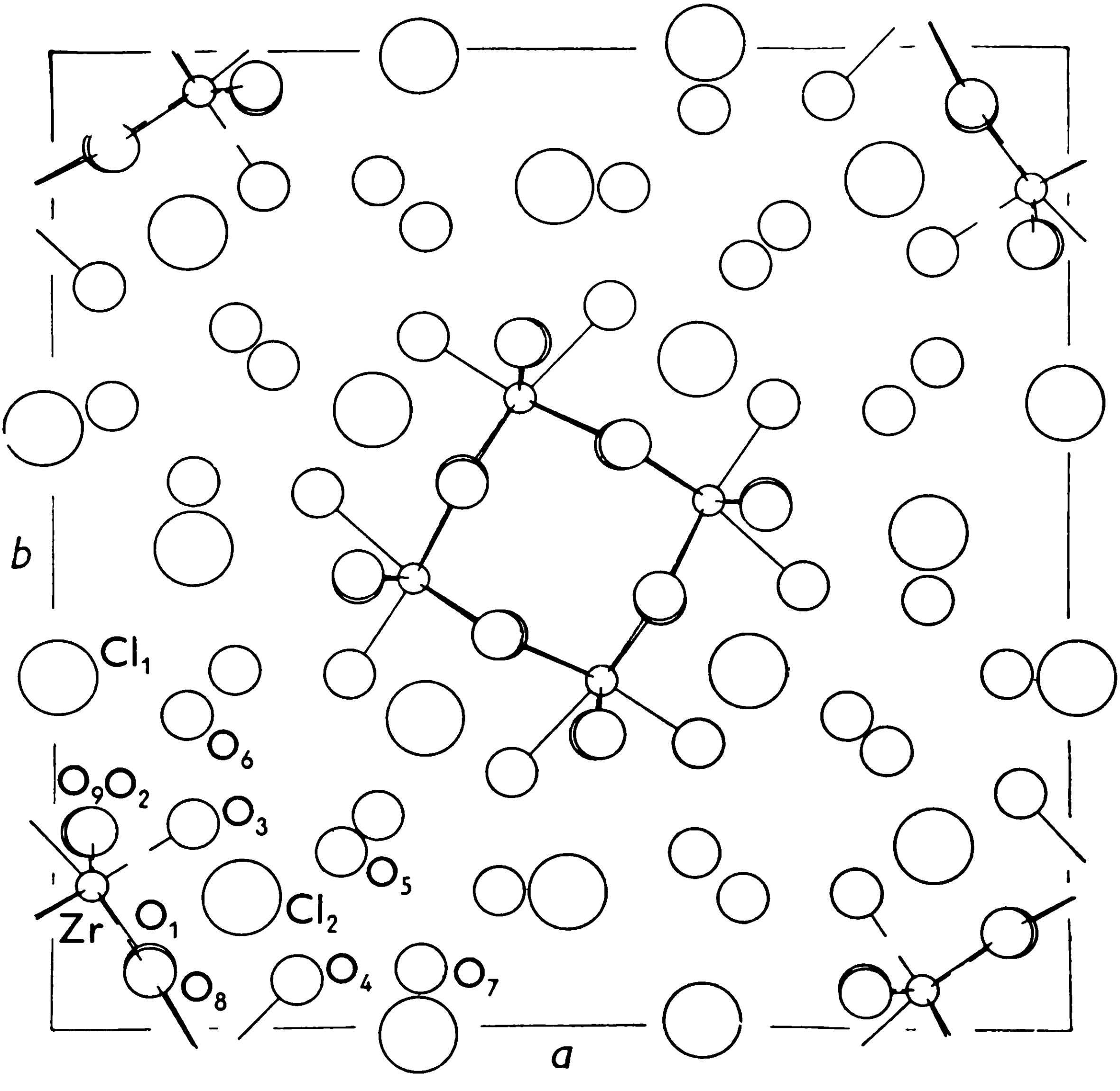
Cl$_1$
O$_6$
O$_9$O$_2$
O$_3$
O$_5$
Zr
O$_1$
Cl$_2$
O$_4$
O$_7$
O$_8$
b
a

FIGURE 2

Structure proposed for tetrameric cation in zirconyl chloride solutions.

(after Muha & Vaughan 1960)

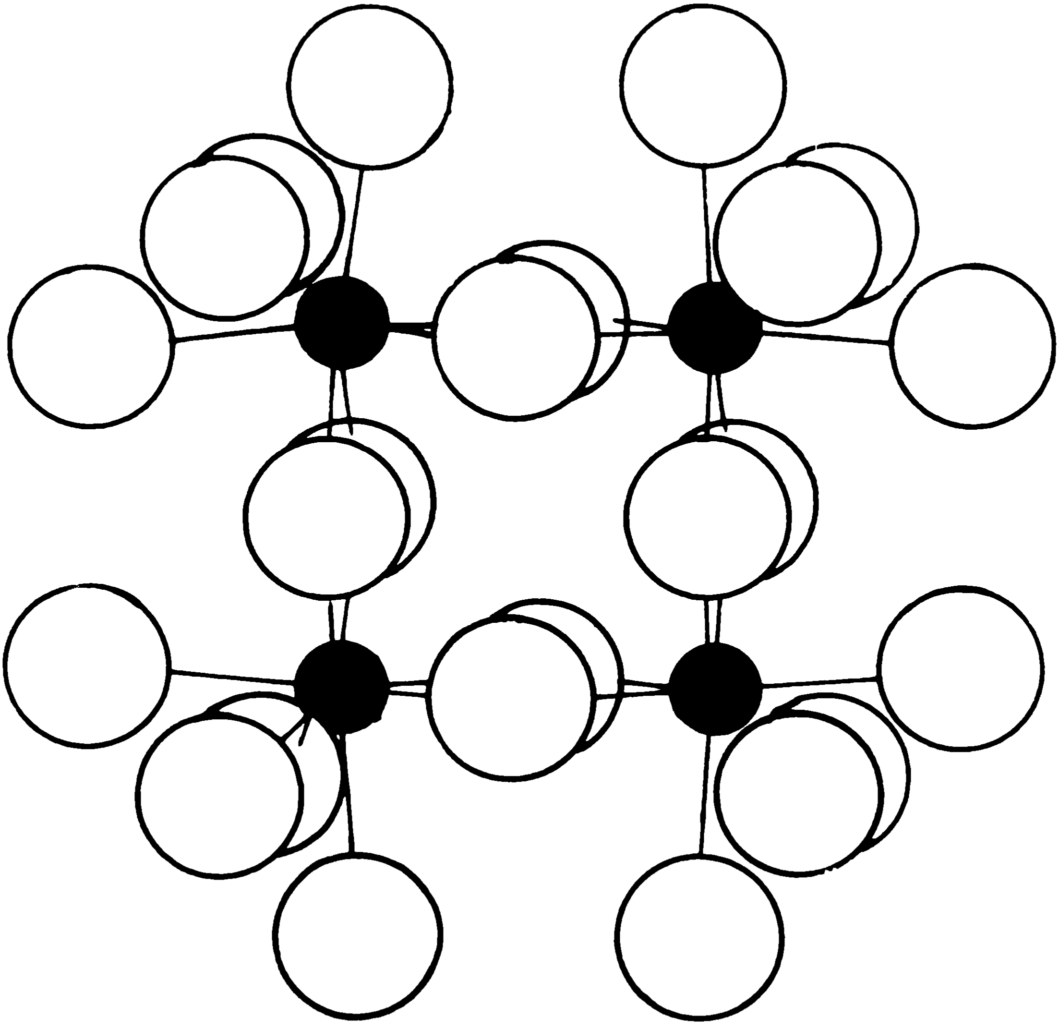

/ Matijević, Mathai and Kerker (1962), using surface chemistry techniques to determine the charge on solute Zr (IV) ions, were also able to demonstrate an ageing effect, the nature of the solute changing slowly with time.

Using extremely accurate potentiometric measurements, Roy (1968) postulated several Zr (IV) complexes in perchloric acid. At acid concentrations between 4 x 10^{-2}M and 2 x 10^{-1}M, and Zr concentrations between 10^{-3}M and 4 x 10^{-2}M, he proposed the following as being possible complexes in solution:-

a)
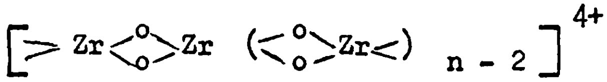

$$\left[> \mathrm{Zr} < \substack{O \\ O} > \mathrm{Zr} \; \left(< \substack{O \\ O} > \mathrm{Zr} < \right)_{n-2} \right]^{4+}$$

, n being from 3 to 5

b)
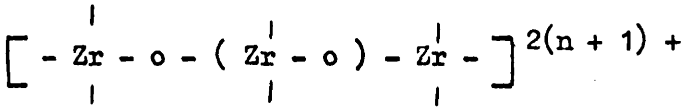

$$\left[- \overset{|}{\underset{|}{\mathrm{Zr}}} - O - \left(\overset{|}{\underset{|}{\mathrm{Zr}}} - O \right) - \overset{|}{\underset{|}{\mathrm{Zr}}} - \right]^{2(n+1)+}$$

He rejected b) and presented a) as being the most likely complex under the conditions of the experiments which he carried out.

HYDROUS ZIRCONIA: "Hydrous Zirconia" is the term commonly applied to the gelatinous amorphous precipitate which is formed on the addition of base to Zr (IV) solutions. Because the precipitate may retain significant amounts of anions, it begins to form before complete neutrality is attained (Larsen and Gammil, 1950, Tananaev and Bokmelder, 1958). Foreign anions may be replaced by hydroxyl groups by washing the precipitate with water, or dilute base.

By means of infra-red studies Fish, Kindness and Landes (1959) and Cabannes - Ott (1960) sought evidence for the presence of hydroxyl groups in hydrous zirconia. However, any hydroxyl stretching frequencies were masked by a broad water absorption band, and no conclusive evidence was found in these studies.

Thomas and Owens (1935) prepared sols by dialyzing mixtures of hydrous zirconia /

/ zirconia and zirconyl chloride solutions. Addition of potassium salts to these sols resulted in large increases in pH, which the authors interpreted as evidence for the displacement of hydroxyl groups from the zirconia by the added anions. Thomas (1934) demonstrated that aged, or boiled sols showed a much smaller pH increase than freshly prepared sols. He considered these zirconia sols to be composed of polymeric systems, the metal atoms being bound by hydroxyl bridges. Oxolation, the process whereby these bridges became oxide or "oxo" bridges was brought about by either prolonged ageing or boiling.

Other studies carried out at about the same time confirmed an ageing effect in zirconia sols. Prakash (1932, 1933) found that the "diamagnetic property" of zirconium hydroxide increased with ageing. He also studied the effect of temperature on the setting time of "zirconium hydroxide jellies". Specific conductivity was shown to increase with age (Sharma and Dhar 1932), whilst Robinson and Ayres (1933), heating ZrO_2 hydrosols, observed decreases in viscosity, pH and "flocculation value". At the same time, light scattering was observed to increase.

Of these ageing experiments, the most significant are probably those by Thomas (1934) and Robinson and Ayres (1933), from which it may be concluded that (i) structural changes were occurring within the zirconia and (ii) the average particle size was increasing with time. Both of these ideas were revived later by Clearfield.

Early attempts to induce crystallinity in zirconia (Böhm and Niclassen, 1924) were only partially successful. Later, however, Clearfield (1964b) was able to produce both monoclinic and cubic modifications of hydrous zirconia by refluxing aqueous slurries of amorphous hydrous zirconia. Large decreases in pH were observed, and taken to signify the replacement of the anions originally present in the hydrous oxide by hydroxyl groups. Similar results were obtained when Clearfield refluxed aqueous solutions of zirconyl chloride. X-ray line broadening measurements suggested that there was an upper limit of about 120Å for /

/ for the crystallite size, and the close agreement between the interplanar spacings and those of the calcined oxides suggested that the actual composition of the crystalline hydrous zirconia was in fact close to $(ZrO_2)n$. The crystalline hydrous oxide particles still, however, contained a significant amount of coordinated water, and the retention of ion exchange properties (Amphlett, McDonald and Redman, 1958) indicated the presence of hydroxyl groups, the bulk of which was thought to be on the surface of the crystallites. The general formula for hydrous zirconia was given by Clearfield (1964a) as:-

$$\left[ZrO_b\ (OH)_{4-2B} \cdot XH_2O\right]_n$$

the value of 'b' being variable according to the conditions of preparation.

With the general composition of amorphous zirconia thus established, Clearfield (1964a) was able to postulate a mechanism whereby the crystallization from solution could take place. Lundgren (1959) had pointed out a structural similarity between the tetrameric complex in $ZrOCl_2 8H_2O$ (figure 1), and the spatial distribution of ZrO_2 chains in the fluorite lattice of cubic zirconium dioxide. This provided a basis for Clearfield's proposed mechanism of crystal growth, which was based on cross-linking of tetramers. Since monoclinic ZrO_2, the stable modification at room temperature may be regarded as a distorted fluorite lattice (Lundgren (1959), a relationship between monoclinic ZrO_2 and $ZrOCl_2 8H_2O$ could be established, via the tetrameric cation.

More recently, thermal analysis and Infra-red Spectroscopy have been used by Vivien, Livage and Mazieres (1970) to demonstrate that amorphous zirconia contained water molecules and residual hydroxyl groups. The general formula given for the "hydrated hydroxyoxide" was $ZrO_{2-x}(OH)_{2x}yH_2O$, which is seen to be the same as that proposed by Clearfield (1964a). The authors noted a correspondence between the Zr - O absorption bands of /

/ of the hydrated hydroxyoxides and those in the crystalline oxides. These results were subsequently supported by Broad-band N.M.R. studies (Vivien, Livage, Mazieres, Gradsztajn and Conard, 1970).

Although the conclusions of Vivien, Livage and Mazieres were in good agreement with those of Clearfield in that both agreed upon the composition of amorphous zirconia, the actual structures proposed for the material were different. Clearfield's proposed structure was based upon cross-linked tetramers, whilst that proposed by Livage, Mazieres, and Doi (1966, 1968 a, b), obtained from X-ray and neutron diffraction, was based upon the tetragonal phase of ZrO_2. Inter-atomic distances obtained from Fourier transforms compared favourably with those of tetragonal ZrO_2, and the proposed structure largely depended upon this.

CRYSTALLINE ZIRCONIUM DIOXIDES: Zirconium dioxide has been shown to exist as a number of different modifications by Cöhn (1935), Clark and Reynolds (1937) and Komissarova, Simanov and Vladimirova (1960). The most widely studied of these modifications is the stable, monoclinic phase which, besides occurring naturally as the mineral Baddeleyite, has been produced by the thermal dissociation of zirconyl salts, or by ignition of "zirconium hydroxide" at temperatures between 600 and 1000°C (Ruff, Ebert, 1929, Clark and Reynolds, 1937, Clabough and Gilchrist, 1952). The following lattice parameters have been reported:-

Table 1 /

/ Table 1

LATTICE PARAMETERS OF MONOCLINIC ZrO_2

SOURCE	a (Å)	b (Å)	c (Å)	B
Yardley (1926)	5.17	5.27	5.31	80°32'
Ruff & Ebert (1929)	5.184	5.276	5.319	80°48'
Cöhn & Tolksdorf (1931)	5.22	5.27	5.38	80°32'
Duwez, Odell & Brown (1952)	5.17	5.26	5.30	80°10'
Curtis, Davey & Johnson (1954)	5.20	5.25	5.38	80°2'
McCullough & Trueblood (1959)	5.17	5.23	5.34	80°45'
Adam & Rogers (1959)	5.14	5.21	5.31	80°36'
Komissarova, Simanov & Vladimirova (1960)	5.12	5.20	5.30	80°49'

Monoclinic ZrO_2, accepted as being the stable form between room temperature and 1000°C (Cöhn 1935), has been the subject of several X-ray crystal structure analyses. The first, by Naray-Szabo (1936) was based on the available X-ray data by Yardley (1926). This proposed structure required unsatisfactory packing arrangements and also involved some unreasonable bond lengths. McCullough and Trueblood (1959) were able to propose another structure, based on projection data, and again using natural baddeleyite. This structure, later confirmed and refined by Smith and Newkirk (1965) has an interesting feature in that each zirconium atom is surrounded by seven nearest neighbour oxygen atoms, rather a novel departure from the usual eight-fold coordination associated with Zr (IV), as pointed out by Gillespie (1961). Smith and Newkirk used synthetic single crystals, thereby overcoming the problem encountered by the earlier workers, of finding crystals which did /

/ did not exhibit twinning. Their analysis was based on the cell parameters given by Adam and Rogers (1959).

The high temperature, tetragonal form of ZrO_2 was first observed by Ruff and Ebert (1929) and is usually regarded as representing a distorted fluorite lattice. By igniting "zirconium hydroxide" at 500 - 600°C, a tetragonal form of ZrO_2 was obtained by Clark and Reynolds (1937), who regarded it as being identical to the high temperature tetragonal phase which could be produced from monoclinic ZrO_2 by a reversible change at 1100°C (Ruff and Ebert, 1929, Murray and Allison, 1954). The findings of Clark and Reynolds (1937) are contradictory to the claim made by Cöhn (1935), that monoclinic ZrO_2 was the stable phase up to 1000°C.

The following are accepted as being the lattice parameters of tetragonal ZrO_2.

Table 2

LATTICE PARAMETERS OF TETRAGONAL ZrO_2

SOURCE	TYPE	a (Å)	c (Å)
Ruff & Ebert (1929)	High Temp.	5.076	5.160
Clark & Reynolds (1937)	Low Temp.	5.074	5.160
Komissarova et al (1960)	Low Temp.	5.08	5.16

Regarding tetragonal ZrO_2 as a body centred lattice, rather than a face-centred lattice, as is commonly applied, Tuefer (1962) reported the /

/ the unit cell dimensions as being, a = 3.64, c = 5.27 Å, at 1250°C, and provided a crystal structure analysis on this basis.

A cubic form of ZrO_2 was reported by van Arkel (1924) to be stable at temperature greater than 1400°C. However, other workers (Ruff and Ebert, 1929, Cöhn and Tolksdorf, 1930, Passerin 1930, Duwez and Odell 1950) have suggested that this phase is only stable in the presence of othere oxides, such as those of Be, Mg, Ca, etc. More recently, this cubic phase is claimed to have been produced from monoclinic ZrO_2 and at 100°C, by the action of fast neutrons (Wittels and Schimil 1956). The lattice parameter, a, is reported by various authors as between 5.06 and 5.10 Å, the accepted value being 5.08 Å, as given by Duwez and Odell, (1950).

In the course of refluxing aqueous slurries of amorphous hydrous zirconia Clearfield (1964) noted a progressive transformation:-

amorphous ⟶ cubic + monoclinic ⟶ monoclinic hydrous zirconia

He also noted the very close similarity between the lattice spacings and those of the calcined oxides. The cubic hydrous zirconia has been questioned by Garvie (1965) who pointed out that when this phase was heated, some of the broad X-ray lines emerged as the characteristic tetragonal doublets. Thus the "cubic" phase was suggested to be in fact the tetragonal form, with the X-ray doublets masked by a line broadening effect. The occurrence of the metastable tetragonal ZrO_2 at relatively low temperatures was attributed by Garvie (1965) to a crystallite size effect.

A trigonal form was claimed by Cöhn and Tolksdorf (1930, 1935), for temperatures in excess of 1900°C, having parameters a = 3.59 and c = 5.99 Å. However, since later workers have failed to produce this modification, its existance has been disclaimed, as by Weber (1957).

/ -

CRYSTALLINE HYDRATES OF ZIRCONYL CHLORIDE: Numerous crystalline hydrates of zirconyl chloride have been described. The most easily prepared, and consequently the most widely studied is the octahydrate. The formula $ZrOCl_28H_2O$ was first assigned by Paykull (1873) to the crystalline solid obtained by dissolving zirconium hydroxide in hydrochloric acid and allowing the solution to evaporate slowly. This formula was confirmed by Venable and Baskerville (1898), who also prepared the hexa- and trihydrates . The octahydrate has been largely used as the starting material in the preparation of lower hydrates. Thus Venable (1894, 1898) prepared tri- and dihydrates, whilst Lange (1910) obtained the tetrahydrate. Using similar techniques Chauvenet (1912, 1917) produced compounds said to contain 6 and 3.5 molecules of water, as well as the anhydrous $ZrOCl_2$. Missenden (1922) also prepared anhydrous zirconyl chloride, as well as the monohydrate. Dehydration in dry air was used by Akhrap-Simonova (1938) to prepare $ZrOCl_22H_2O$, whilst heating $ZrOCl_28H_2O$ at 180 - 270°C formed the anhydrous salt. A series of hydrates containing 6, 4, 3 and 2 molecules of water was prepared by Schmid (1927).

Many of these results from various workers are contradictory in detail, a probable reason for this being that the analytical methods available to these early workers did not provide sufficiently accurate data upon which to base formulae. Furthermore, hafnium-free zirconium preparations were not readily obtainable and consequently there was some impurity always present.

The confusion led Komissarova, Plyuschev and Kremenskya (1960) to carry out an extensive investigation into the dehydration of $ZrOCl_28H_2O$, which was prepared from hafnium-free zirconium. By thermal dehydration they showed the existence of the tetra and trihydrates, and at temperatures at which further dehydration was induced, chlorine was lost also, so that the final product was ZrO_2. This was found at temperatures /

/ temperatures ranging from 140 to 500°C depending upon the physical technique being employed.

From solubility considerations, Goroschenko and Spasibenko (1962) suggested that two hydrates, the octa- and trihydrate were obtainable as equilibrium forms. Later (1967) from measurements of water vapour pressure above the crystals obtained by dehydration of the octahydrate over H_2SO_4, at 20°C, they proposed a series of hydrates having 7, 6.5, 6, 5.5, 4.5 and 4 molecules of water. Characterization of the hepta, hexa and tetrahydrates, as well as the octahydrate, has been carried out by the same workers (1969), using heating thermograms, and infrared spectroscopy. It appeared that all the hydrates thus studies contained crystallization and coordination water molecules, while, from the I.R. spectra, Goroschenko and Spasibenko concluded that only the tetrahydrate contained ZrO^{2+} ions. This was in general agreement with the X-ray study by Clearfield and Vaughan (1956) of the octahydrate, where the Zr (IV) ions were cyclic tetramers.

Much of the early chemical interest in zirconium has been in the polymerization associated with its hydrolysis. Many of the apparent contradictions in the data presented by various workers can be explained when the effect of ageing in the solutions is taken into account, bearing in mind also that different physical techniques often tend to give different results for a system. The processes whereby the salt zirconyl chloride may be transformed into amorphous, and then crystalline zirconia have been investigated and mechanisms accounting for these changes have been presented. Structural models for amorphous zirconia have been presented, from various sources. Much of the literature data on the crystalline phases of ZrO_2 is conflicting, and no reliable phase diagram is obtainable. A probable reason for this is the marked effect of small amounts of impurities upon the various phases.

Zirconyl /

/ Zirconyl Chloride itself has been studied widely and X-ray structural data for its most stable hydrate, $ZrOCl_2 8H_2O$, is available. Some recent Russian work involving thermogravimetry and infra-red spectroscopy, has produced what appears to be reasonable evidence for a whole range of hydrates.

Object of Present Work

The object of the present work was to investigate the hydrolysis of Zr (IV) in aqueous solution. In particular, evidence was to be sought in support of the tetrameric cations, as postulated by other workers. This would involve the examination of these and related species in the electron microscope, changing as little as possible their "solution" structure. The aims of the work may be broadly defined as follows:-

(a) to develop a technique for examining the polymeric species in as close a state as possible to that in solution.

(b) to devise a means of resolving particles in the 5 - 10 Å size range in the electron microscope.

(c) to correlate structural features observed with pH, and other physical data.

(d) to investigate the transition of amorphous to crystalline zirconia, as an ageing effect.

EXPERIMENTAL

EXPERIMENTAL

ELECTRON MICROSCOPY

INTRODUCTION 19
IMAGE FORMATION 21
CONTRAST 25
FACTORS AFFECTING INFORMATION
RETRIEVAL 32
RESOLUTION 37
ELECTRON DIFFRACTION 38
SPECIMEN SUPPORT METHODS 43
REGULAR ATTAINMENT OF
OPTIMUM PERFORMANCE 44
IMAGE RECORDING 45
X-RAY POWDER PHOTOGRAPHY 47
pH MEASUREMENT 47
NUCLEAR MAGNETIC RESONANCE 47
SURFACE AREA DETERMINATION 50

ELECTRON MICROSCOPY

INTRODUCTION: The ability of a magnetic lens to focus an electron beam was first demonstrated by Busch (1926) and a few years later Knoll and Ruska (1932) constructed the first electron microscope, a commercial model becoming available in 1938 (von Borries and Ruska). This instrument was capable of a far higher resolution than light microscopes by virtue of the very short wavelength of an electron beam and hopes were high that resolution of sub-atomic dimensions would be achieved.

In an electron microscope the electron beam is produced by a heated tungsten filament. The beam,accelerated by a potential usually between 40 and 100 kilovolts, is collimated and focused on the specimem by a condenser lens system. The electron image of the specimen is then magnified, usually in three stages and a range of magnifications from 200x up to 500,000x is available in modern instruments.

The theories of lens design and electron optics have been extensively reviewed (Zworykin, Morton, Ramberg, Hillier and Vance, 1945, Cosslett, 1951, Hall, 1953, Hirsch, Howie, Nicholson, Pashley and Whelan, 1965) and various aspects of modern instruments have been described.

Although modern high-performance instruments use electro-magnetic lenses, other systems have been used from time to time, mainly on smaller microscopes. The Hitachi 8S and Siemens Elmiskop 51 both use permanent magnet lenses, whilst electrostatic lenses were used in some early instruments although performance was poorer than for electromagnetic lenses /

FIGURE 3

Ray diagrams in the electron microscope showing

a) transmission microscopy
b) electron diffraction

(after Hirsch, Howie, Nicholson, Pashley and Whelan, 1965)

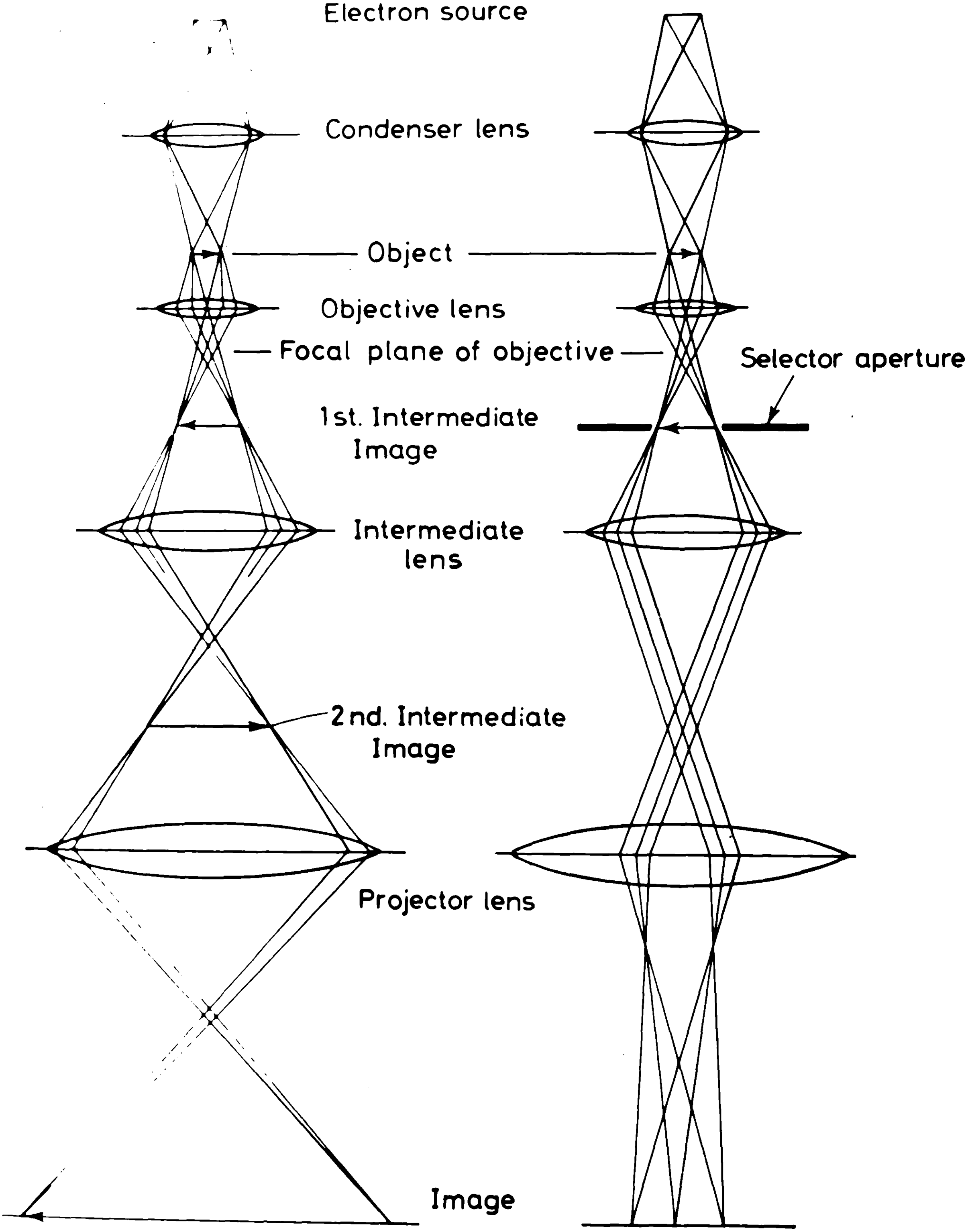
Electron source
Condenser lens
Object
Objective lens
Focal plane of objective
Selector aperture
1st. Intermediate Image
Intermediate lens
2nd. Intermediate Image
Projector lens
Image

Microscopy
(a)

Diffraction
(b)

/ lenses (Grivet, 1951). More recently, Fernández-Morán (1966) has constructed liquid helium-cooled super-conducting lenses, and has claimed a marked improvement in resolution.

IMAGE FORMATION:

(i) Electron Optical System: The electron optical system of the microscope is shown schematically in figure 3, two modes of operation, transmission and microscopy and electron diffraction being shown.

The illuminating system, shown in figure 3 as a single lens, actually consists of two lenses. Two methods of illuminating the specimen may be employed, using either single or double condenser lenses, as shown in figure 4. The single condenser projects an image of the beam cross-over near the electron source, onto the specimen, giving a minimum spot diameter of about 60 . By using the double condenser arrangement it is possible to restrict the illuminated area to the field of view. In this way problems arising from overheating, charging and contamination of the specimen can be partially avoided. The first condenser, a strong lens, demagnifies the beam source by a factor of up to 100, the second condenser projecting this image onto the specimen, with approximately a two-fold magnification. In this way, a spot diameter down to 2 can be obtained.

Image contrast is formed by the objective lens and it is the quality of this lens which largely determines the ultimate performance of the microscope. Inaccuracies in the manufacture of the soft iron polepiece, and inhomogeneities in its composition are among the limiting factors.

In light optical systems, compensation of lens defects is effected by the use of concave as well as convex lenses. In electron optics, however, equivalence is not possible, because magnetic lenses are all convergent, so that aberration compensation cannot be achieved in this way.

The /

FIGURE 4.

Single and double condenser illumination in the Siemens Elmiskop 1 and 1A.

a) Single Condenser
b) Double Condenser

(after Hirsch, Howie, Nicholson, Pashley and Whelan, 1965)

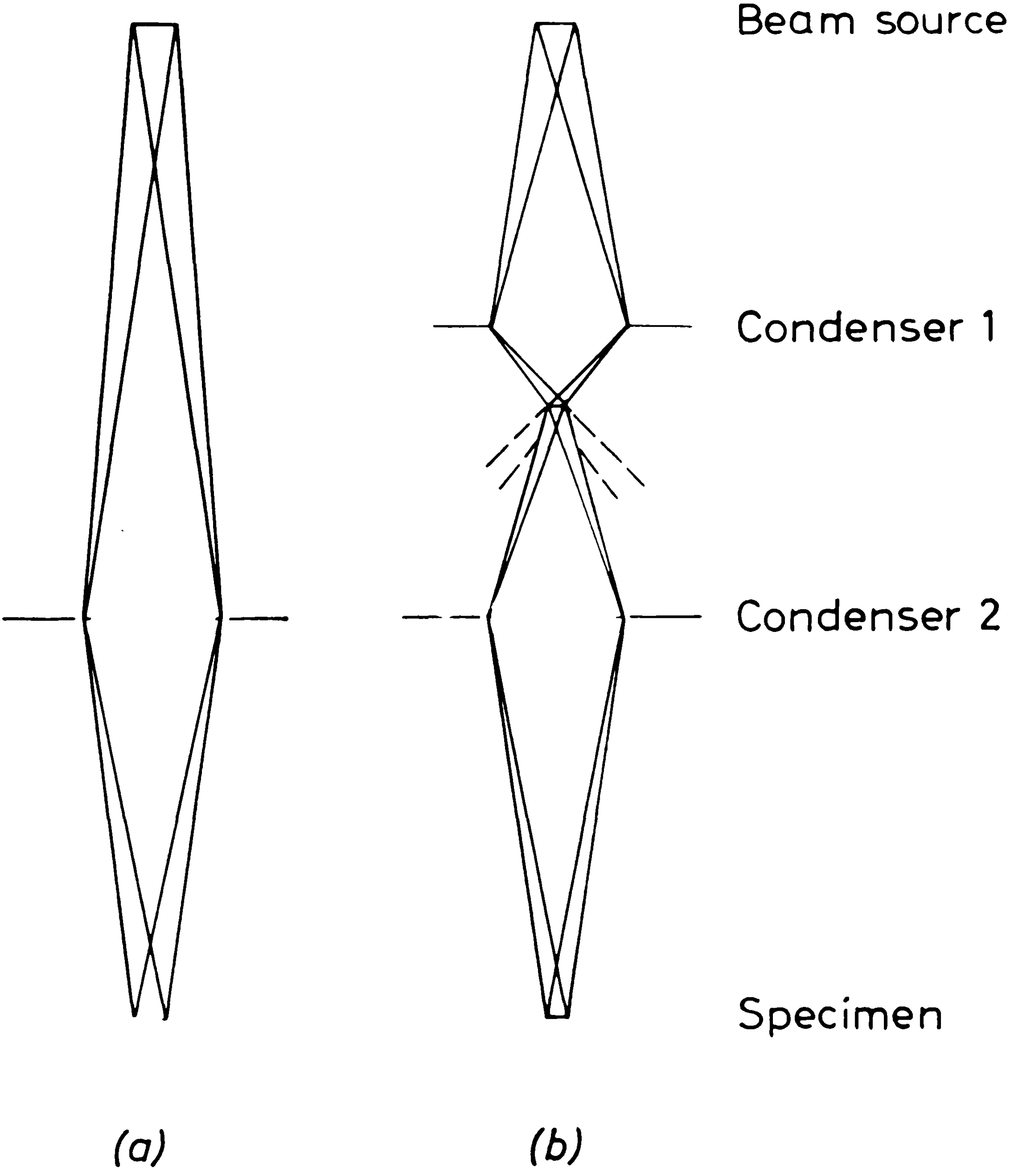
Beam source
Condenser 1
Condenser 2
Specimen
(a)
(b)

/ The other lenses in the magnification system, the intermediate and projector lenses, are less important in terms of performance than the objective lens, because they simply magnify the image, and its aberrations, formed by the objective lens. Any short-comings in the performance of intermediate and projector lenses will then be negligible by comparison.

(ii) Information content of Electron Beam: An 80 KV electron beam has a wavelength of 0.042Å and electron waves scattered by interaction with the specimen will carry information about structural features greater than this in size. This led to the early hopes of resolution well below 1Å. However point resolution as discussed later is at present limited to about 3Å, although lattice images below 1Å, have recently been obtained by Yada (1969)

The problem of attaining meaningful resolution is two-fold:-

(a) How may the information content in the scattered beams be recovered?

(b) Is there a meaningful way in which this information can be interpreted?

There are also two factors limiting the retrieval and interpretation of the information.

(a) The form in which the information is carried. The information will be represented by perturbations in the electron waves.

(b) Aberrations. Defects in the electron optical system will also give rise to perturbations in the electron waves.

If the perturbations in the electron beams arising from structural features in the specimen are significantly greater than those arising from /

/ from aberrations, then meaningful resolution may result, although the exact interpretation of it will be more difficult.

(iii) Electron Scattering: Before discussing the various approaches by which these problems are tackled, it is necessary to summarise the salient features of electron scattering. Two distinct types of scattering affect an electron beam when it interacts with the specimen.

(a) Inelastic Scattering: (a) When electrons interact with orbital electrons in the specimen they lose energy and are inelastically scattered. Inelastically scattered waves are incoherent and do not contribute towards meaningful image contrast, although some contrast effects have been in fact observed, using only inelastically scattered electrons. (Kamiya and Uyeda, 1961). Inelastic collisions of this nature are responsible for scattering through angles of between a 10^{-4} and 10^{-2} radians and its effect is observed in crystalline specimens as diffuseness of Bragg spots in the diffraction pattern of a thick crystal.

(b) In addition to single inelastic collisions, the Coulombic interaction between a fast electron and the delocalized electrons of a crystal can give rise to collective oscillations of the whole system of conduction electrons. These oscillations are known as plasmons (Pines, 1956, 1963). The effect of these may be neglected in most work.

In addition, inelastic scattering will arise from the thermal vibration of the atoms in the specimen. This scattering effect, however, is also of little importance in most studies.

(b) Elastic Scattering: Electrons which interact with nuclei in the specimen do not lose energy being elastically scattered. The scattered waves are cohherent with respect to the primary beam. In a crystalline specimen, the angles through which electrons are elastically scattered are determined by the Bragg Law, relating the crystal lattice geometry, and /

/ and the wavelength of the electrons, as shown in the equation:-

$\lambda = 2d_{hkl} \sin \theta$, λ being the electron beam wavelength, θ the angle of diffraction, about 10^{-2} radians, d_{hkl} is the interplanar spacing for (hkl) planes.

CONTRAST FORMATION:

(i) a. Thickness Contrast: A thick specimen will give rise to much scattering of the electron beam and, if the scattered electrons are then prevented from contributing to the final image by the insertion of a limiting aperture in the back focal plane of the objective lens, the thick parts of the specimen will be imaged as dark areas. A similar situation arises with specimens containing heavy atoms and to this type of contrast, the term "Mass-Thickness" Contrast may be applied.

(i) b. Diffraction Contrast: In crystalline specimens more than 100Å in thickness contrast is obtained by removal of Bragg diffracted beams from the image-forming electrons, also by the insertion of a limiting objective aperture. In this way areas of the specimen which are in a strongly diffracting position will be imaged as dark areas, as in the case of buckling contours often observed in thin crystals.

Kinematical Theory: For thin specimens where the electrons interact only once with the specimen, a mathematical treatment has been extensively developed to allow calculation of the intensity of the diffracted beams. Known as the Kinematical Theory, it accounts, with reasonable success, for contrast variations in crystalline specimens, arising from dislocations, variations in thickness and other features (Whelan, 1959, Hirsch, Howie, Nicholson, Pashley and Whelan, 1965). By calculating the total scattered Intensity, and knowing the size of the limiting objective aperture the total intensity of the remaining image-forming rays /

/ rays can thus be found. It must be noted, however, that in this method the information content of the scattered electron waves is not recovered. However, the detailed knowledge, albeit approximate, provided by the Kinematical Theory, allows one to know what is being removed from the primary beam and, although this beam itself carries no structural information, the knowledge of the total information loss, along with the contrast features observed allows for reasonably accurate interpretation of these contrast features to be made.

Dynamical Theory: In thick crystals, the Kinematical Theory has its shortcomings and the Dynamical Theory has been developed for electron diffraction in thick crystals. This theory takes into consideration the possibility of the diffracted wave being itself scattered by atoms in the crystal. The interaction of primary and scattered waves is also taken into account.

(ii) Phase Contrast: Contrast which arises from interference between a transmitted wave of amplitude T and a scattered one of amplitude D, of phase ($\frac{\pi}{2} + \chi$), relative to the transmitted wave, is due to the combination of the two waves:-

$\psi = T + iDe^{i\chi}$, χ being the phase difference between the two waves.

The intensity of this wave is given by

$|\psi|^2 = 1 - 2TD \sin\chi$, the condition for maximum contrast being as follows:-

$$G_{max} = 4TD, \text{ if } \sin\chi = 1$$

This contrast is known as phase contrast, since it is dependent upon the phase difference introduced in the scattered wave by the object, and by the objective lens. A correct interpretation of phase contrast requires /

/ requires an understanding of the effect of this phase difference, χ , and an ability to control it. This contrast is dominant in the 5 - 15Å size range in specimens less than 100Å thick. (Lenz and Scheffels 1958, Thon 1966)

The two factors which are important in determining the contrast are the instrumental phase χ , and the Fresnel transform, for an object of finite thickness. The Fresnel transform is the vertical phase summation in the object and is analogous to the Fraunhofer structure factor in crystallography.

In a 3-dimensional solid object, if the atoms are randomly disposed, the image will be a random superposition of Airey discs, with the appearance of random noise. All solids, however, possess short range atomic order, so that the intensity distribution in the image ought to represent the regions of short-range order in the object. If the specimen thickness is comparable with the extent of these ordered regions a reasonable interpretation of the image should be possible, based on the Fresnel transform at a given value of defocus. The contrast G_{12} between two points is given by:-

$$G_{12} = \frac{-4\pi}{\lambda} \int_{0}^{\beta_{obj}} (F_1 - F_2) \sin \chi \beta \, d\beta \quad \text{- - - -} \quad (1)$$

$(F_1 - F_2)$ being the difference between the two real parts of the two Fresnel transforms.

The contrast thus depends on $\sin \chi$, and also on $(F_1 - F_2)$ and the interpretation of phase contrast becomes the problem of attempting to deduce $(F_1 - F_2)$ from the above equation, knowing the behaviour of sin for the particular instrument. Quantitative determination of the behaviour of $\sin \chi$ cannot at present be determined and the following phase expression is used to give a value of χ :-

/ -

$$\chi = \frac{|K|}{2}\Delta L_o\beta^2 - \frac{|K|}{4} C_s\beta^4 + \chi_{ab} + \chi(t) \cdots\cdots (2)$$

Where $|K|$ is the wave vector for the scattered beam, ΔL_o the defocus value, which is the controllable term and C_S the spherical aberration coefficient. The term χ ab represents the effect of astigmatism, which may be minimized by careful compensation. χ (t) describes the effect of lens instabilities and also stray fields.

For maximum phase contrast it can be shown that:-

$$\frac{|K|}{2}\Delta L_c\beta^2 - \frac{|K|}{4} C_s\beta^4 = (2l-1)\frac{\pi}{2} \cdots\cdot (3)$$, l being an integer.

For small angles, the relationship $\beta \doteq \frac{\lambda}{a}$ can be applied as the relationship between the Bragg angle β and the spacing 'a' in the object. In equation (3), the value of defocus ΔL_o to optimise the contrast for a given value of 'a' is determined by an isophase diagram as shown in figure 5. Thon (1966) has carried out extensive experimental studies of this relationship, measuring the dominant spacings in the image as a function of ΔL_o, using a light diffractometer (Hansen and Morgenstein, 1965). The agreement between his experimental results and the theoretical treatment was good and it was concluded by Heidenreich, (1967) that the transform of a phase contrast image was capable of yielding very important information.

Interpretation of phase contrast detail thus requires a knowledge of defocus and of the Fresnel transform. The image point intensity distribution is a phase map in which points of equal intensity are points of equivalent phase amplitude. This factor would need to be taken into account for valid interpretation of high resolution images. The variation of χ with ΔL_c shows why a true equivalence cannot be made for micrographs in a through-focal series, and without a knowlege of ΔL_c and the Fresnel transform, any interpretations made of image phase contrast must be tentative and at the present state of phase contrast theory and instrumental design this is all that is possible.

Recently /

FIGURE 5

Iso-phase lines for maximum phase contrast of spacing "a" in an object as a function of ΔL_o, the defocus.

(After Heidenreich, 1967)

/ Recently, attempts have been made by Fernández-Morán (1960) to achieve high resolution phase contrast by the use of objective phase plates of composite single crystal films with adjustable electric fields, or ferromagnetic thin-film apertures, thus permitting phase shift control. He noted a marked improvement in resolution. Thon et al (1968) made zonal correction plates, following suggestions by Hoppe (1961, 1963, 1967) and Lenz (1963) that such plates, in the objective lens, would improve resolution and phase contrast in the image by removing certain phases. The exact significance of their results is however not clear at present, although it appeared that the resolution limit using a conventional circular aperture could be surpassed. Other studies of phase contrast images have been carried out by Locquin and Bessis (1948), Locquin (1955), Menter (1956), Lenz and Scheffels (1958), Heidenreich (1965) and van Donsten and Premsela (1966), and others.

(iii) Electron Scattering Cross-Sections: For elastically scattered electrons, the total elastic scattering cross-section, Qel, may be represented by the following:-

$$\text{Qel} = \int_{\alpha=0}^{2\pi}\int_{\beta=0}^{\pi} |\psi_g|^2 \sin\beta \, d\beta \, d\alpha$$

$$= \int_{\alpha=0}^{2\pi}\int_{\beta=0}^{\beta_{obj}} |\psi_g|^2 \sin\beta \, d\beta \, d\alpha + \int_{\alpha=0}^{2\pi}\int_{\beta=\beta_{obj}}^{\pi} |\psi_g|^2 \sin\beta \, d\beta \, d\alpha$$

Where ψ_g = amplitude of scattered wave, β the scattering angle, and α the angle variable about the optic axis. $|\psi_g(\alpha,\beta)|^2$ is the corresponding intensity distribution at the back focal plane of the objective, and this is imaged as an electron diffraction pattern when the microscope is operated in the selected area diffraction mode.

For phase contrast the cross-section is given by the first of the two integrals, arising from that portion of the diffraction pattern passing through the objective aperture, whereas for diffraction contrast, the cross-section is determined by that part of the diffraction pattern which falls /

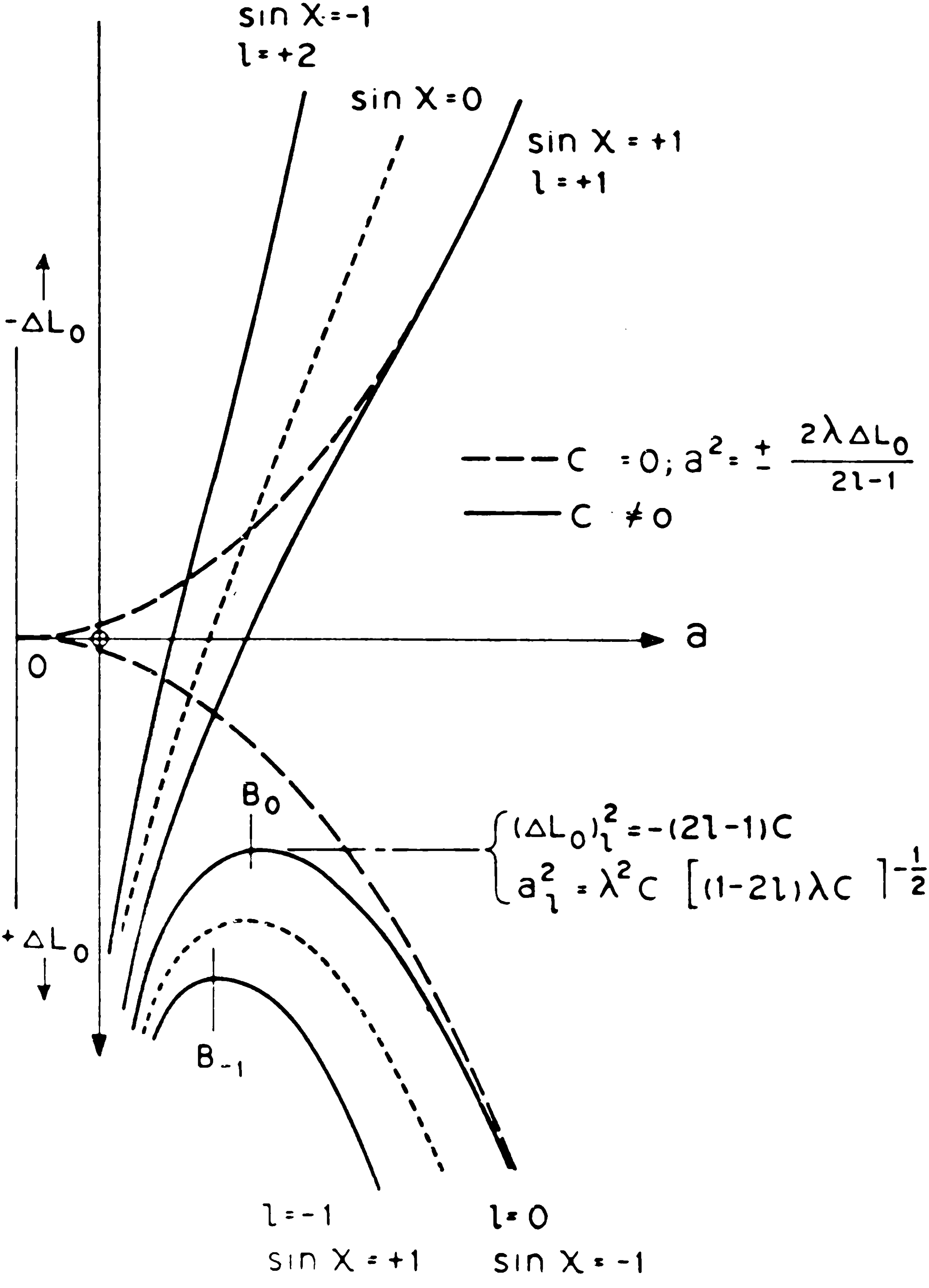
$\sin X = -1$
$l = +2$
$\sin X = 0$
$\sin X = +1$
$l = +1$
$-\Delta L_0$
$C = 0;\ a^2 = \pm \frac{2\lambda \Delta L_0}{2l-1}$
$C \neq 0$
a
0
B_0
$\begin{cases} (\Delta L_0)_l^2 = -(2l-1)C \\ a_l^2 = \lambda^2 C \left[(1-2l)\lambda C\right]^{-\frac{1}{2}} \end{cases}$
$+\Delta L_0$
B_{-1}
$l = -1$
$\sin X = +1$
$l = 0$
$\sin X = -1$

/ falls outside the limits of the aperture.

A similar treatment may be applied in the case of inelastically scattered electrons. Since inelastic scattering tends towards small angles, its cross section within the objective aperture will be large, compared with that outside the aperture and, since inelastically scattered electrons are not coherent, phase contrast is not enhanced by their inclusion.

It has been mentioned by Crewe (1970) that the theory of elastic scattering indicates that elastically scattered electrons are proportional to the thickness of the specimen and to its atomic number to the 4/3 power. Inelastically scattered electrons are proportional to the thickness of the specimen, and the atomic number to the 1/3 power. From this it can be seen that the ratio of elastic to inelastic scattering cross-sections for a given element will be proportional to its atomic number. Thus light elements, such as carbon, have an inelastic cross-section several times greater than the elastic cross-section, as is shown in figure 6 which applies to 50 KV electrons (Lenz, 1954).

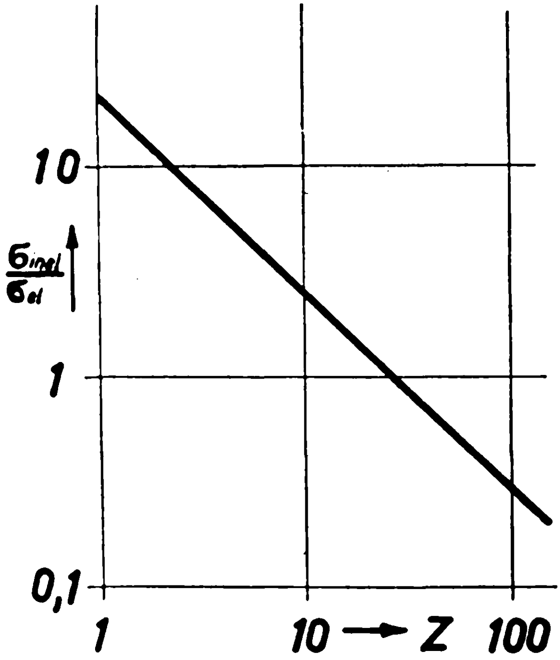

Figure 6 . Variation of ratio of inelastic to elastic scattering cross-sections with atomic number. (after Lenz, 1954)

Specimens consisting of such elements are therefore not well suited for high resolution phase contrast microscopy, because of the large contribution from small-angle, inelastic scattering. In particular, carbonaceous specimens, which include the whole range of biological materials, are really unsuitable for good phase contrast. A further disadvantage lies in the dissipation of energy into the specimen as a result of inelastic scattering. This is particularly damaging to delicate organic materials, and also brings about randomization of thin carbon films. (Dowell, Farrant and Williams, 1966). Specimens containing heavy elements, provided they are sufficiently thin to allow good penetration, are more suitable for phase contrast, in that there will be a higher proportion of elastically scattered electrons.

FACTORS LIMITING RETRIEVAL OF INFORMATION:

Despite the efforts to improve the resolution attainable in a modern microscope, there are a number of factors which hinder total retrieval of the information content of the scattered beams. Among these are the various aberrations which affect the electron optical system, especially the objective lens, whose performance is most critical.

(i) Spherical Aberration: This is the most severe effect and results in peripheral rays passing through the objective lens being brought to a focus before those closer to the axis, as shown in figure 7 . Thus a point in the object is imaged as a disc by the objective lens.

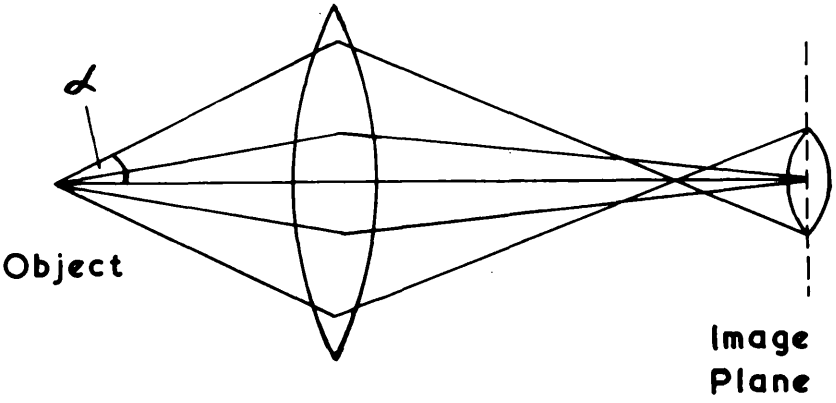

Figure 7. Schematic representation of spherical Aberration.

This effect is overcome to some extent by the insertion of a limiting aperture in the back focal plane of the objective lens, in order to remove the most widely scattered waves. This procedure is used in the production of diffraction contrast images. However as was noted earlier there is an information loss due to the removal of these scattered electrons and a compromise must be sought with regard to the optimum size of the objective aperture. This compromise is expressed in the equation:

$$\delta_{min} = B\lambda^{\frac{3}{4}} C_s^{\frac{1}{4}}$$

δ min being the minimum size of a resolvable point object. B is a constant, ≑ unity.

The optimum size of the objective aperture, α_{opt} , is then given by:

$$\alpha_{opt} = A\lambda^{\frac{1}{4}} C_s^{-\frac{1}{4}}$$

A is a constant, ≑ unity.

In practice, α_{opt} , the angle subtended at the specimen by the objective aperture, is about 6×10^{-3} radians, corresponding to an aperture diameter of approximately 40μ , and apertures of 30 and 50μ diameter are used in conventional transmission microscopy.

Where phase contrast is required, larger objective apertures up to 200 in diamater are used, and in some cases they have been removed completely (Heidenreich, Hess and Bann, 1968), although the attendant increase in information is normally offset to some extent by the increase in Spherical Aberration. However, since

$C_s = cf$, f being the objective focal length,
c being ≑ unity,

it can be seen that a reduction in focal length will reduce the Spherical Aberration coefficient C_s. Thus Heidenreich et al (1968) and Fernández-Morán (1966) were able to reduce the Spherical Aberration effect /

/ effect by reducing objective lens focal lengths (from 2.8 mm to 2.1 and 1.8 mm respectively).

Short focal length objective lenses are now an important feature in current high resolution microscopes. The A.E.I., E.M.8 electron microscope features an objective lens of focal length 1.1 mm with a guaranteed point resolution of 3Å.

Dowell (1962) was able to reduce Spherical Aberration in lattice images by tilting the illumination at the Bragg angle, with respect to the optic axis. Using this technique, lattice images down to 0.88Å, the (200) planes in Ni, have recently been recorded by Yada and Hibi, (1969). This method, however, is applicable only to lattice fringes and is not a good criterion of resolving power.

(ii) Chromatic Aberration: Chromatic Aberration arises from the energy spread in the electrons passing through the objective lens, as a result of which the electrons of lower energy are brought to a focus before those of higher energy, forming a disc of confusion at the image plane. This spread in energy may be due to fluctuations in power supplies to the lenses and in the high tension. In modern instruments, however, such variations are kept within tolerable limits. The other, more serious source of chromatic aberration is the effect of different path lengths taken by electrons through the specimen, and an important requirement for high resolution is that the specimen be sufficiently thin for this effect to be insignificant. Cosslett (1957) has shown that chromatic aberration will limit resolution of points in a graphite to approximately one tenth of the specimen thickness, at 100 KV.

(iii) Astigmatism: A third effect, important in high resolution electron microscopy is astigmatism, resulting from assymetry in the objective lens field, produced in turn by inhomogeneities in the soft iron polepiece, or by inaccuracies in its manufacture. The lens has effectively /

/ effectively different focal lengths for paraxial rays in the two principal planes of asymmetry. In addition to inherent astigmatism there is induced astigmatism due to contamination within the microscope column, particularly on the objective aperture. Charge build-up on the contamination produces distorting fields. Careful cleaning of surfaces in the microscope which are exposed to the electron beam, particularly the apertures, must be carried out in order to minimize the induced astimatism. Correction, which is achieved by using a device which produces an elliptical compensating field, may be performed using the fringe test described by Haine and Mulvey, (1954). A particular source of induced astigmatism arises from contamination of the objective aperture. Devices for heating objective apertures in situ, to remove contamination, have occasionally been described, as in the current Ikstra Lem 4C. However, such devices have not been notably successful. Perhaps the most important advance in this aspect is the production of thin foil apertures which are virtually contamination-free.

(iv) Coherence: The coherence of the electron beam impinging upon the specimen is an important factor in high resolution. The coherence of the illumination is improved by the use of a small condenser aperture, resulting in much clearer Fresnel fringes. This is especially useful in astigmatism correction. However, there is a consequent illumination loss and condenser apertures normally used are either 100 or 200 in diamater. The use of pointed filaments was first demonstrated by Hibi (1954), and a marked improvement in beam coherence was shown. Fernández-Morán (1966) has developed pointed cathodes using single-crystal tungsten tips, whereas commercially available pointed filaments are generally ground to a point.

By using these filaments, a much higher current density is obtainable, and consequently a smaller condenser aperture may be used.

With instrumental conditions carefully chosen and adjusted to give optimum performance, it is not always possible to achieve the best resolution /

/ resolution of which the microscope is then capable, in that the specimen itself often imposes limits on the resolution. Beside the thickness considerations mentioned earlier, there are a number of ways in which the specimen is affected by the electron beam.

(v) Contamination: This was first noted by Watson (1947) and was for a long time a major hindrance in high resolution microscopy, a deposit of amorphous material building up on the specimen, under the action of the electron beam. Fine detail was thus obscured, This deposit was shown by Hillier (1948) and König (1951) to be amorphous, and carbonaceous in composition and it was thought to be a hydrocarbon polymer which was subsequently carbonised by further electron bombardment. Elegant studies by Ennos (1953, 1954) and Heide (1958, 1963) have furnished much information regarding the nature of contamination and the processes involved in its formation. In the light of their findings, various devices for reducing contamination rates, which may exceed 10Å per minute, have been constructed (Schott and Leisegang, 1956, Heide, 1958, 1960, 1964). Most modern electron microscopes are equipped with anti-contamination devices, which consist of liquid nitrogen-cooled jackets which surround the specimen, and on which the organic vapours which lead to most contamination will preferentially condense. By means of such devices contamination rates as low as 0.1Å per minute are possible and, except in cases where the specimen must undergo prolonged beam exposure, contamination no longer poses a serious problem. Yada and Hibi (1966) noticed that a contamination layer could actually be removed from a specimen, under the intense electrom beam irradiation produced by a pointed filament.

(vi) Specimen Stability: The stability of the specimen is another important factor in electron microscopy. Many inorganic compounds, particularly hydrates, will be unstable in the vacuum under which they are examined. Ionic salts, particularly halides, are known to break down to form oxides, etc. under intense beam irradiation which is a more serious effect, producing physical as well as chemical changes. Delicate /

/ Delicate organic specimens deteriorate rapidly in the electron beam, as a result of polymerization and cross-linking. The problem of beam damage may now be largely avoided by the use of an image intensifier which will allow a much lower electrom beam intensity to be employed.

RESOLUTION:

Resolution was discussed by Cosslett (1951) in terms of the distance between the centres of two separate points in the image, and the resolving power of a microscope is usually taken to be the smallest value for this distance which can be measured in at least two successive micrographs (von Borries, 1944; Ruska, 1954) the reason for this being that electron noise can result in contrast effects which, in a single micrograph, may be regarded as significant structure. Dowell, Farrant and Williams (1966) however pointed out that a resolving power of 3Å by this criterion was by no means certain, since in pairs of micrographs having the required correspondence of points, there were many more points which did not correspond at all. This was attributed to structural changes occurring in the specimen and they concluded that the traditional test specimens which consisted of platinum particles on a carbon film, were no suitable criteria for unambiguous resolution of 3Å detail.

Another criterion of resolving power, suggested by Haine (1961) is based on the width of Fresnel fringes around a hole in a thin carbon film. This was estimated to be suitable for resolution up to 5Å, above which the granularity of the film complicated the evaluation (Heidenreich, Hess and Bann, 1968).

More recently , lattice fringe spacings have been quoted as an estimate of resolving power, particularly since crystal lattices with spacings less than 2Å have been resolved.

Thon /

/ Thon (1964) has pointed out that lattice image formation and the resolution of points are achieved by two quite distinct mechanisms, and point resolution was shown to be a much more exacting criterion of instrument (and operator) performance.

Finally, an attempt was made by Kikutchi (1967) to show that 5Å point resolution by phase contrast, required only a single micrograph. The argument was based on considerations of electron noise and specimen damage occurring between the two exposures normally taken. Most high resolution studies, however, continue to use two more micrographs for comparison, since the mechanism of phase contrast image formation has not yet been fully evaluated.

Von Borries and Kausche (1940) derived an expression relating the diameter d' of a polygonal platelet with n sides to the resolving power, δ , of the microscope. For resolution of the shape of the polygon, the following relationship was found:-

$$d' = 2\,\delta\left(1 + \cos\frac{\pi}{n}\right)\sqrt{\frac{n}{\pi}\cot\frac{\pi}{n}}$$

, and a graphical representation of this is shown in figure 8 .

Thus for a four-sided platelet of diameter 10Å to be resolved as such, a resolving power better than 10Å by a factor of 3.7 would be required, i.e. a resolving power of 2.7Å.

By comparison, modern high-performance microscopes guarantee a point-to-point power of 3Å (J.E.O.L.Co. - J.E.M. 100B; A.E.I. - E.M.8).

ELECTRON DIFFRACTION:

Crystalline specimens will, as has already been indicated, diffract an electron beam, in accordance with the Bragg law. The diffracted beams, along with the undeviated beam are brought to a focus at the back focal plane of the objective lens, as shown in figure 3 .

In /

FIGURE 8

Ratio of least diameter of a polygon permitting recognition of shape, to the limit of resolution, as a function of the number of sides of the polygon.

(After von Borries and Kausche, 1940)

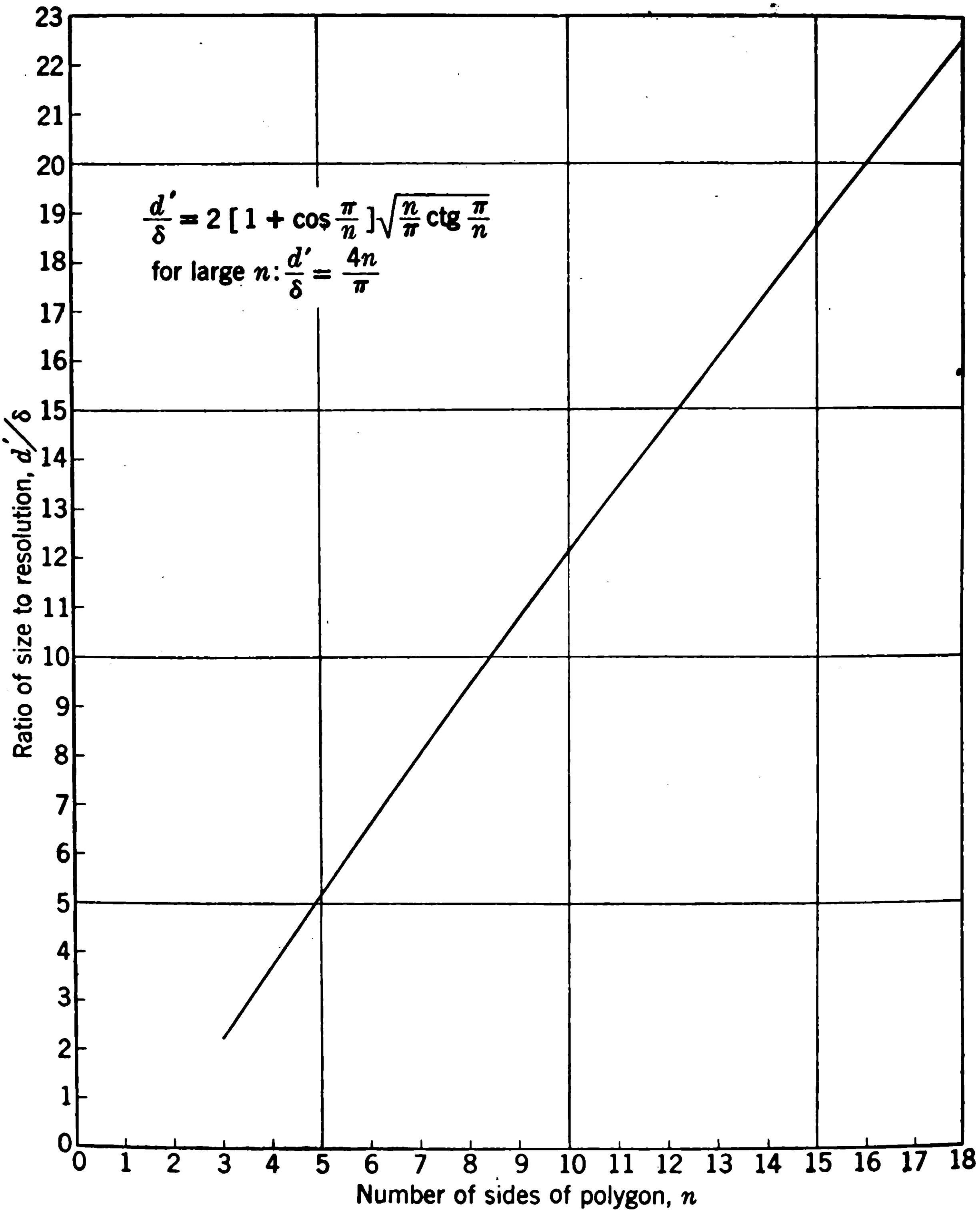
$\frac{d'}{\delta} = 2\left[1 + \cos\frac{\pi}{n}\right]\sqrt{\frac{n}{\pi}\,\mathrm{ctg}\,\frac{\pi}{n}}$
for large n: $\frac{d'}{\delta} = \frac{4n}{\pi}$
Ratio of size to resolution, d'/δ
0
1
2
3
4
5
6
7
8
9
10
11
12
13
14
15
16
17
18
19
20
21
22
23
Number of sides of polygon, n
0
1
2
3
4
5
6
7
8
9
10
11
12
13
14
15
16
17
18

/ In normal transmission microscopy, the intermediate and projector lens are focussed upon the first intermediate image plane, so that the final image is actually a magnified projection of this plane. For electron diffraction, however, the focussed array of diffracted beams at the back focal plane of the objective lens is imaged instead.

Selected Area Diffraction: This technique, developed by Le Poole (1947) enables diffraction patterns to be obtained from small areas of the specimen, so that a correlation between features observed in the specimen and its crystallography may be made. For this technique the intermediate lens is reduced in strength so that the back focal plane of the objective is magnified and projected onto the final screen. By insertion of a selector aperture in the first intermediate image plane, the area of the specimen giving rise to a particular diffraction pattern can be correlated almost exactly. The accuracy of selected area diffraction has been discussed by Agar (1960), Phillips (1960) and Rieke (1961) and Spherical Aberration was shown to be one of the major sources of error in the selected area.

Inter-planar spacings are derived from a diffraction pattern as follows:-

It may be shown that

$\frac{D/2}{L} = \tan 2\theta$, D being the diameter of a pair of diffraction spots, or of a "polycrystalline" ring, L being the effective camera length.

If θ is small, then $\tan 2\theta \doteqdot 2\sin\theta \doteqdot 2\theta$

$$\begin{aligned} \text{and } D &= 2L \cdot 2\theta \\ &= 4L \cdot \frac{\lambda}{2d}, \end{aligned}$$ from the Bragg relationship.

Therefore, $\frac{D.d}{2} = L =$ "Camera Constant", K.

The /

/ The camera constant may be found by calibration with a sample, of known lattice parameters, which gives a sharp ring pattern. An evaporated film of Thallous Chloride is often used for this purpose.

The accuracy of the camera constant is governed by small instrumental variations, errors in procedure, and errors in measurement, and can be as good as 0.1 per cent.

It has been noted by Andrews, Dyson and Keown (1967) that the camera constant actually varies with the diffraction ring diameter, the relationship being approximately linear. This variation is due to the decreasing validity of the expression.

$$\tan 2\theta \doteqdot 2\sin\theta \doteqdot 2\theta$$

as the value of θ increases. Thus, as the ring diameter increases, the camera "constant" increases, a typical example of this effect being shown in figure 9 , the material used being Thallous Chloride.

Where $D = 5$ cm. and $L = 40$ cm., the correction to the interplanar spacing is about 0.15 per cent, slightly larger than the variation due to random errors.

FIGURE 9

Variation of camera constant with ring diameter.

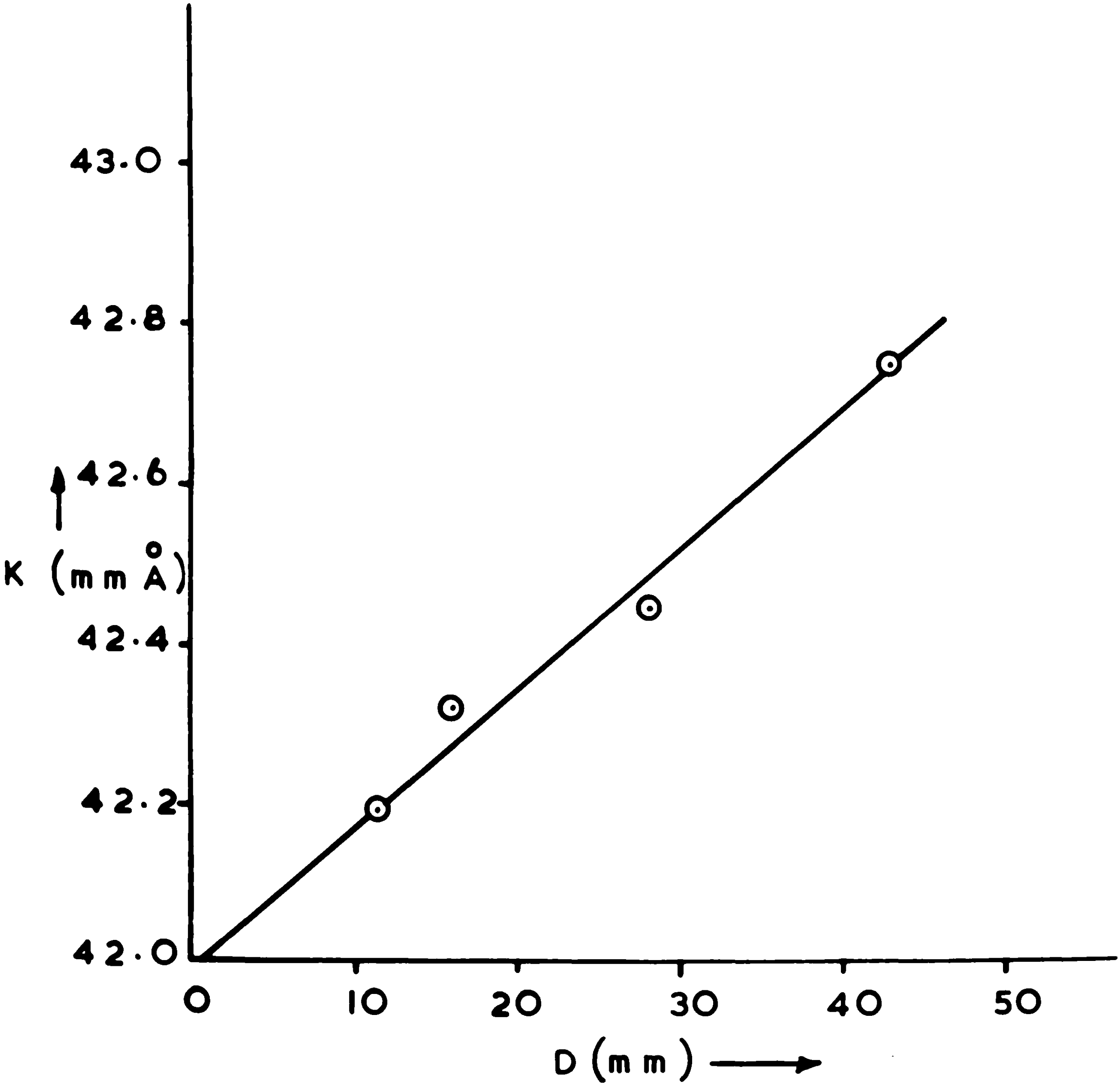
43·0
42·8
42·6
42·4
42·2
42·0
K (mm Å)
0
10
20
30
40
50
D (mm)

SPECIMEN SUPPORT TECHNIQUES: Conventional electron microscope specimen mounts consist of either copper grids, or perforated Platinum-Iridium discs. They are usually coated with a thin film of carbon prepared by the evaporation method described by Bradley (1954). Such films are useful for supporting specimens at medium magnifications. At high magnification, however, the structure of the carbon film itself can affect the quality of the image. It has been suggested by Boiko, Palatnik and Dervyanchenko (1968) that carbon films consist of particles about 12Å in diamater, which is certainly consistent with observed results, although the dependence of image granularity on objective lens focussing (van Dorsten and Premsela, 1966) makes accurate measurement difficult. Furthermore, the evaporation conditions will control the grain size of the carbon film.

Various methods of avoiding background structure in high resolution images have been developed, the most widely employed being the use of perforated support films, generally of nitrocellulose or formvar, and reinforced with carbon. This technique was used by Bassett, Menter and Pashley (1956) to resolve the (020) lattice image in a MoO_3 crystal with a spacing of 6.93 Å. The crystal was suspended over a hole in the support film and thus photographed.

The use of perforated films offers a further advantage in that astigmatism checks may be carried out with the same specimen. It is found, however, that when a drop of a colloidal sample is allowed to evaporate on such a mount, the surface tension effects tend to draw most of the particles around the edges of the holes, with the result that very few of the particles actually project across them.

Thin clearage flakes of graphite, less than 10 Å thick, have been used by Fernández-Morán (1966) as supports, since they have a finer and more regular substructure than carbon films. He also used thin mica flakes with regular 100 Å holes, produced by fission tracks. The use of asbestos fibres as a "filter" to collect air-borne particles was /

/ was mentioned by Hall (1953) and various other techniques using fibres as supports have been reported, although high-resolution work was only carried out in a few of these reports (e.g. Fernández-Morán 1966).

In the present study, carbon and silica films were used as support substrates for low and medium resolution microscopy and electron diffraction. For high resolution it was found that fibres of chrysotile offered the best specimen support, in that background-free micrographs of colloidal material could be obtained. A detailed study of chrysotile was carried out and the results presented in Part 2 of this thesis.

REGULAR ATTAINMENT OF OPTIMUM PERFORMANCE: The Siemens Elmiskop IA used in the present study has a guaranteed point resolving power of 8Å. The tetrameric Zr (IV) species already mentioned, $[Zr(OH)_2 \cdot 4H_2O]_4^{8+}$ has length and width both equal to approximately 9Å, the distance between nearest Zirconium atoms being 3.50Å (Clearfield 1969). For resolution of this tetramer to be a reasonable proposition, the guaranteed resolving power of the microscope would have to be attained, and surpassed if possible. Furthermore, a suitable way of preparing a specimen would have to be developed. The actual shape of the tetramer would not be distinguishable, however, since this would require a point to point resolving power of 2Å, well beyond the capabilities of the instrument.

The instrumental performance was improved in the following ways:-

(i) Use of pointed filaments: Use of pointed filaments gave a marked improvement in beam coherence, evidenced by the increased number of Fresnel fringes which were resolved. The higher illumination intensity allowed the use of smaller condenser apertures, 50 or 100 in diameter with a further improvement in coherence, and consequently in the final image quality.

(ii) /

(ii) Use of thin-foil apertures: The use of such apertures as a means of lowering induced astigmatism has been noted. 50 diameter apertures are available commercially and in the initial stages of the work, these were used in the objective lens system. Later, thin silver apertures of various diameters were made, after the method described by Stabenow (1968). A conventional Pt / Ir aperture was first coated with a layer of sodium metaphosphate, onto which a thin film of silver was then evaporated. The silver foil thus formed was floated off in distilled water and collected upon a support ring usually a widened aperture. When the assembly was dry the foil was fixed in position by conducting adhesive and transferred to the microscope.

By using such apertures in both the condenser and objective lenses, it was possible to operate the microscope for a period of several days, without re-correcting the objective stigmator setting.

(iii) Phase contrast: This was improved by the use of a 200 diameter (thin foil) objective aperture, which allowed a greater number of scattered rays to contribute to the final image. It was decided not to use the technique of Heidenreich et al (1968) of completely removing the objective aperture, because in the instrument used, there was no facility for using a short focal length objective polepiece, and consequently there could be no spherical aberration improvement.

By operation of the microscope under the conditions described above, with an accelerating voltage of 80 KV, and an instrumental magnification of 160,000X it was possible to achieve a point to point resolution of about 5Å, which was adequate for the requirements of the study.

IMAGE RECORDING:

Electron microscope images are, in the Elmiskop 1A, recorded on photographic plates situated below the final screen. In this work, Ilford Special Lantern Contrasty plates were used, and proved adequate

for /

/ for the high resolution studies, as well as for the more routine work. The newer Electron Image Plates were also used in a series of tests, but the increase in quality was not sufficient to warrant their exclusive use.

X-RAY POWDER PHOTOGRAPHY:

Specimens for examination were prepared by drying and powdering the material in an agate manner. The powder was mixed with "Durofix" adhesive, rubbed into a paste, and rolled between glass slides to form a small tube approximately 0.2 mm. in diameter. When dry this tube could then be mounted in an X-ray camera in the usual manner. Use of a copper target and nickel filter gave Cu K_{α} radiation, with a wavelength of 1.542Å. The generator was run at 35 Kilovolts and 15 microamps, for periods of time between 5 and 7 hours.

pH MEASUREMENT:

As soon as samples were removed from the refluxing solution, they were cooled rapidly in order to retard further hydrolysis. An E.I.L. model 23A/pH meter was used in conjunction with a digital voltmeter and it was thus possible to measure pH to within 0.01 unit. A combination glass-colomel electrode was used, and the calibration of the meter was checked frequently, using standard buffer solutions of 4.00 and 1.00, made by the methods described by Robinson and Stokes (1959).

NUCLEAR MAGNETIC RESONANCE:

High resolution N.M.R. spectroscopy may be used as a means of studying exchange reactions in an equilibrium system.

A typical example would be two molecules, HA and H*B, participating in the equilibrium reaction:-

$$HA + H^*B \rightleftharpoons H^*A + HB$$

If there was no exchange and if the protons bound to A were chemically different from those bound to B, two separated proton resonance frequencies /

/ frequencies would be detectable, provided their chemical shifts ν_A and ν_B were sufficiently far apart. When exchange does occur, the spectrum would be determined by two parameters τ and σ, respectively the average lifetime of the proton in each environment and the frequency separation (in cycles per second) between the two signals in the absence of exchange.

If τ is much larger than $\frac{1}{\sigma}$, i.e. $\tau \rightarrow \infty$, two separate signals are observed, the exchange being very slow. When the rate of exchange increases a line broadening of the two signals is observed, whilst for τ values smaller than $\frac{1}{\sigma}$, the two signals collapse into a single, broad peak. Finally, when exchange is very fast an averaged, sharp signal is observed. The theory of signal shape has been developed by Pople, Schneider and Bernstein (1959) and the effect of different exchange rates demonstrated by Van der Berghe, Van der Kelen and Eekhaut (1967).

A similar situation arises in the case of protons attached to molecules which are in different environments, although they are chemically similar. For example if proton exchange between bulk water and water which was in some way restricted, was sufficiently slow, two separate proton signals would be observed, provided ν_A and ν_B were sufficiently well separated.

Parallel to these cases of proton exchange, but quite distinct, is the exchange of molecules between two environments. Here the protons remain attached to the molecules concerned and the splitting of signals will be determined by factors similar to those already mentioned.

In the present work, high-resolution spectra were recorded on a VARIAN T.60 N.M.R. spectrometer. The samples were aqueous suspensions of hydrous /

/ hydrous zirconia, prepared by refluxing zirconyl chloride solutions. To each sample a drop of dioxan was added, as a calibrant for the chemical shift of the proton signals.

COLLOID PREPARATION:

Amorphous zirconia has been prepared by precipitation from Zr (IV) solutions by base. When fresh, this zirconia is partially soluble in hot water. However, irreversible changes are brought about by ageing, the effect being that the zirconia becomes insoluble. Finally, it is possible to induce crystallization by further ageing, usually by refluxing. Zirconia may also be obtained by refluxing zirconyl chloride solutions and in the present work, this latter method was preferred, most of the samples studied being prepared by refluxing 100 ml. solutions of zirconyl chloride. This method offered an advantage over ammonia-precipitation, since there was an opportunity to examine the hydrolysis products at various stages in their formation.

MATERIAL USED:

The zirconyl chloride was obtained as the octahydrate, $ZrOCl_2 8H_2O$. Spectrascopically pure material was obtained from Johnson-Matthey, Ltd. A list of quoted impurity levels is given in Table 3 .

Table 3 .

IMPURITY CONTENT IN "SPECPURE" $ZrOCl_2 8H_2O$

Impurity	Concentration (p.p.m.)
Na	5
Fe	3
Al	2
Mg	$\leq$ 1
Hf	$\leq$ 200

/ Any other impurities present were below the limits of detection.

SURFACE AREA DETERMINATION

This was carried out using a standard Perkin-Elmer-Shell Sorptometer. The sample used was monoclinic zirconia, obtained by prolonged reflux of zirconyl chloride. The crystallites were air-dried at 60°C, and subsequently degassed for one hour in flowing helium at 120°C.

RESULTS

RESULTS

ZIRCONYL CHLORIDE

(i) X-RAY POWDER DIFFRACTION ... 53
(ii) ELECTRON DIFFRACTION 57
CONCLUSIONS 68

ZIRCONIA

LOW RESOLUTION AND ELECTRON DIFFRACTION 69
CONCLUSIONS 100
HIGH RESOLUTION 102
NUCLEAR MAGNETIC RESONANCE 119
SURFACE AREA 121

ZIRCONYL CHLORIDE:

(i) X-Ray Powder Diffraction: Spectroscopically pure zirconyl chloride was examined by X-ray powder photography; the spacings measured are recorded in Table 4, along with literature values for $ZrOCl_2 8H_2O$ (Hanawalt, Rinn and Frevel, 1938) and $ZrOCl_2 3H_2O$ (Goroschenko and Spasibenko, 1962). Also recorded in Table 4 are the spacings obtained from the crystalline solid obtained from a slow evaporation of an aqueous solution of zirconyl chloride. It can be seen that, for spacings below 8Å, there is close agreement between those for "Spec-Pure" $ZrOCl_2 8H_2O$, the solid obtained by evaporation, and literature values quoted for $ZrOCl_2 8H_2O$. In addition, there is good agreement between some of the observed spacings and those of $ZrOCl_2 3H_2O$. The evaporite solid, however gave numerous lines which are unaccounted for by either the octa- or the tri-hydrates and it is proposed that these spacings are due to the presence of other hydrates not characterized in the literature. In both the "Spec-Pure" and the evaporated samples, a line corresponding to a spacing of 8.42 - 8.45Å was observed, corresponding to neither of the two sets of literature values quoted. This line was attributed to the presence of another hydrate, or, alternatively, to the presence of hydrolyzed material.

One difficulty encountered in the preparation of finely powdered samples for this study was that, when zirconyl chloride crystals were ground between glass slides or in an agate mortar, they became almost sticky in texture. It is believed that absorption of moisture from the atmosphere was taking place, probably leading to the formation of a whole range of hydrates. This would account for the extra spacings observed.

The lines corresponding to the two highest spacings, 10.6 and 12.8Å, were very poorly defined in both powder photographs,

the resulting difficulty in their measurement leading to

the /

Table 4.

"Spec-Pure" Zirconyl Chloride	Evaporated from Solution	$ZrOCl_2.8H_2O$.*	$ZrOCl_2.3H_2O$.**
d (Å)	d (Å)	d (Å)	d (Å)
11.78	12.62	12.8	-
10.05	10.20	10.6	-
8.42	8.45	-	-
	7.9	7.9	7.55
	6.86	6.9	6.89
6.51		-	-
	6.23	-	-
	5.14	-	-
4.93	4.74	4.80	-
4.25	4.15	4.12	4.14
	4.02	-	3.97
	3.80	3.82	3.80
	3.66	-	-
3.61	3.58	3.60	3.58
3.37	3.43	-	-
	3.30	-	-
3.26	3.23	3.24	3.23
3.20	3.13	-	3.14
	3.00	-	-
2.85	2.92	2.96	-
2.74	2.72	2.74	2.72
	2.66	-	2.64
	2.58	-	-
	2.53	-	-
	2.43	-	2.38
2.24	2.22	2.22	-
2.14	2.15	2.15	2.15
2.07	2.07	2.07	2.07
1.84	1.81	1.81	1.81
1.72	1.71	1.71	1.71

* Hanawalt, Rinn and Flever (1938)

** Goroschenko and Spasibenko (1962)

PLATE 1

Crystals of zirconyl chloride,
from a drop of aqueous solution.
Magnification: 100,000X

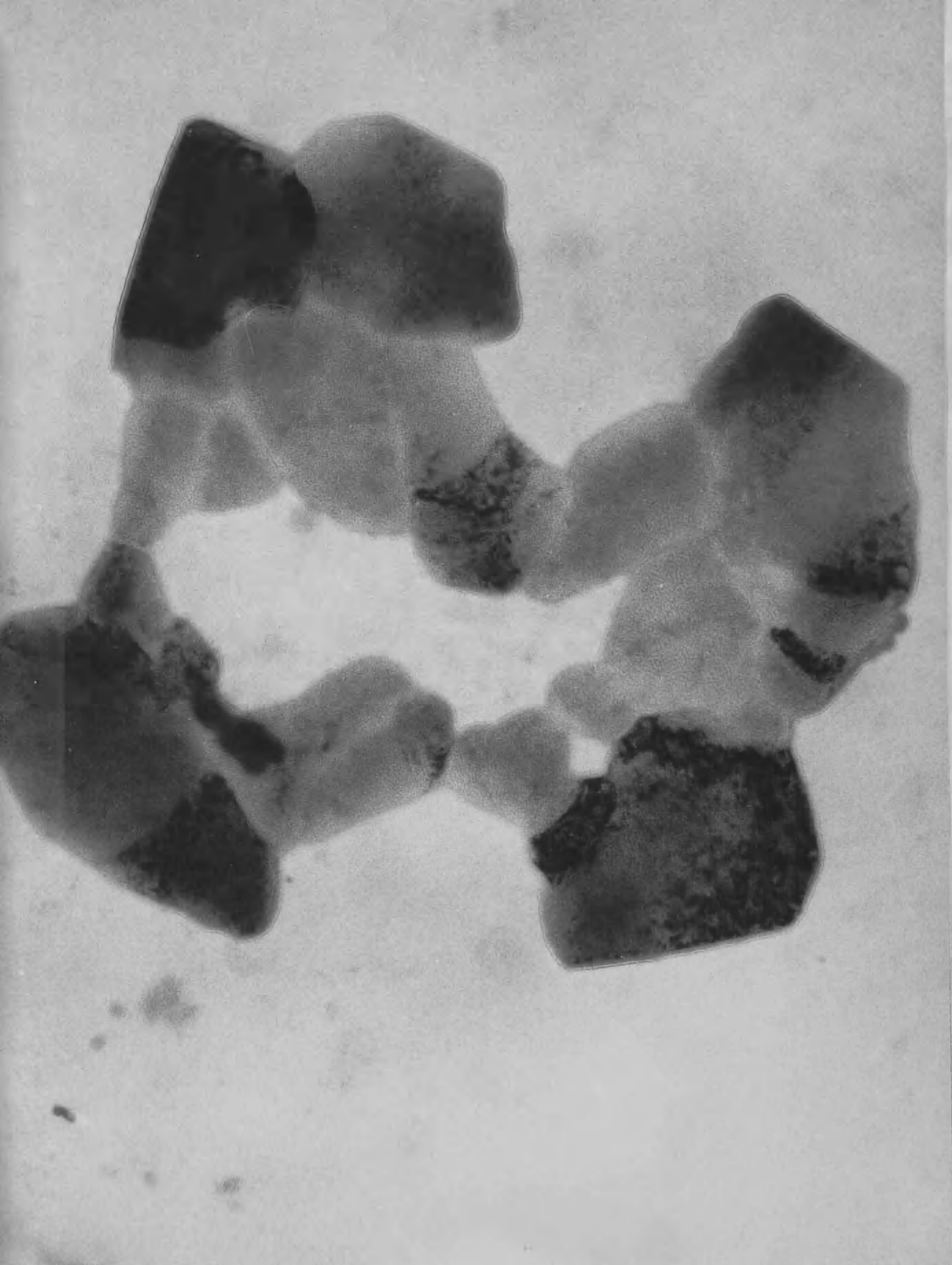

PLATE 2

Selected Area Electron Diffraction pattern corresponding to the group of crystallites in Plate 1.

/ the inaccuracy.

It is concluded that zirconyl chloride may be recrystallized from an aqueous solution, as a series of hydrates, without undergoing irreversible hydrolysis.

(ii) Electron Diffraction: Electton Diffraction studies of zirconyl chloride yielded a wide range of results, the actual preparation techniques determining the products as follows:-

(a) An aqueous solution of $ZrOCl_2 8H_2O$ was evaporated on to a Silica coated Pt/Ir mount, the crystallites thus obtained being shown typically in Plate 1. From the electron diffraction pattern of this group of crystallites (Plate 2), the following spacings, given in Table 5, were obtained. "-" denotes disagreement, a blank space implies that no value is available.

Table 5.

d (Measured)	d ($ZrOCl_2 8H_2O$)	d ($ZrOCl_2 3H_2O$)
3.24 Å	3.24	3.23
2.77	2.74	2.72
1.97	2.00	(1.99
		(1.95
1.62	1.62	1.62
1.38		1.42
1.24		1.21

Within the accuracy of this method it is clear that the two hydrates cannot be unambiguously identified from the small number of spacings available.

The /

PLATE 3

Zirconyl chloride crystals, as shown in Plate 1, after three days' exposure to the atmosphere.

Magnification: 100,000X

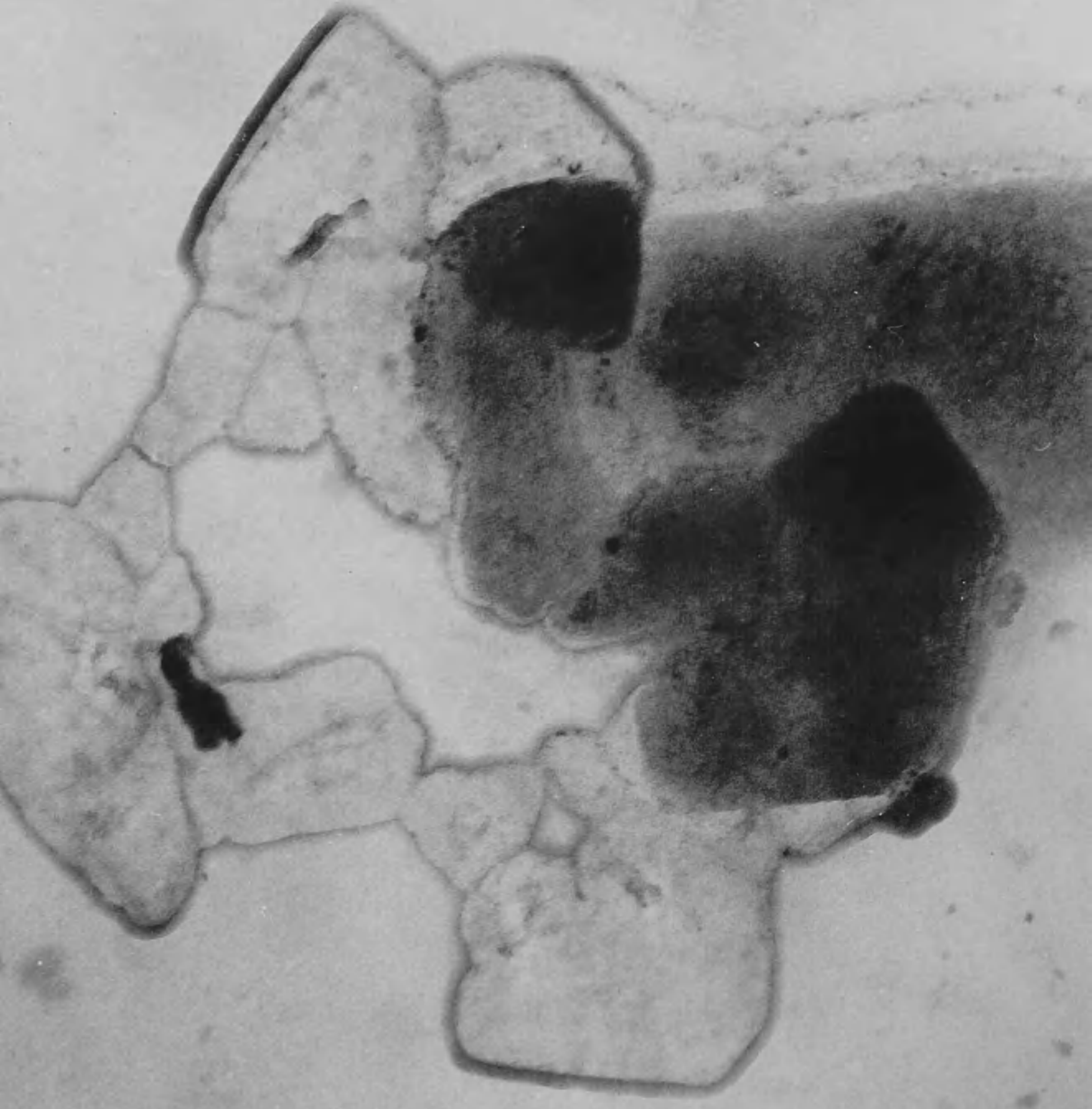

PLATE 4

Selected Area Diffraction
for the group of crystallites
shown in Plate 3.

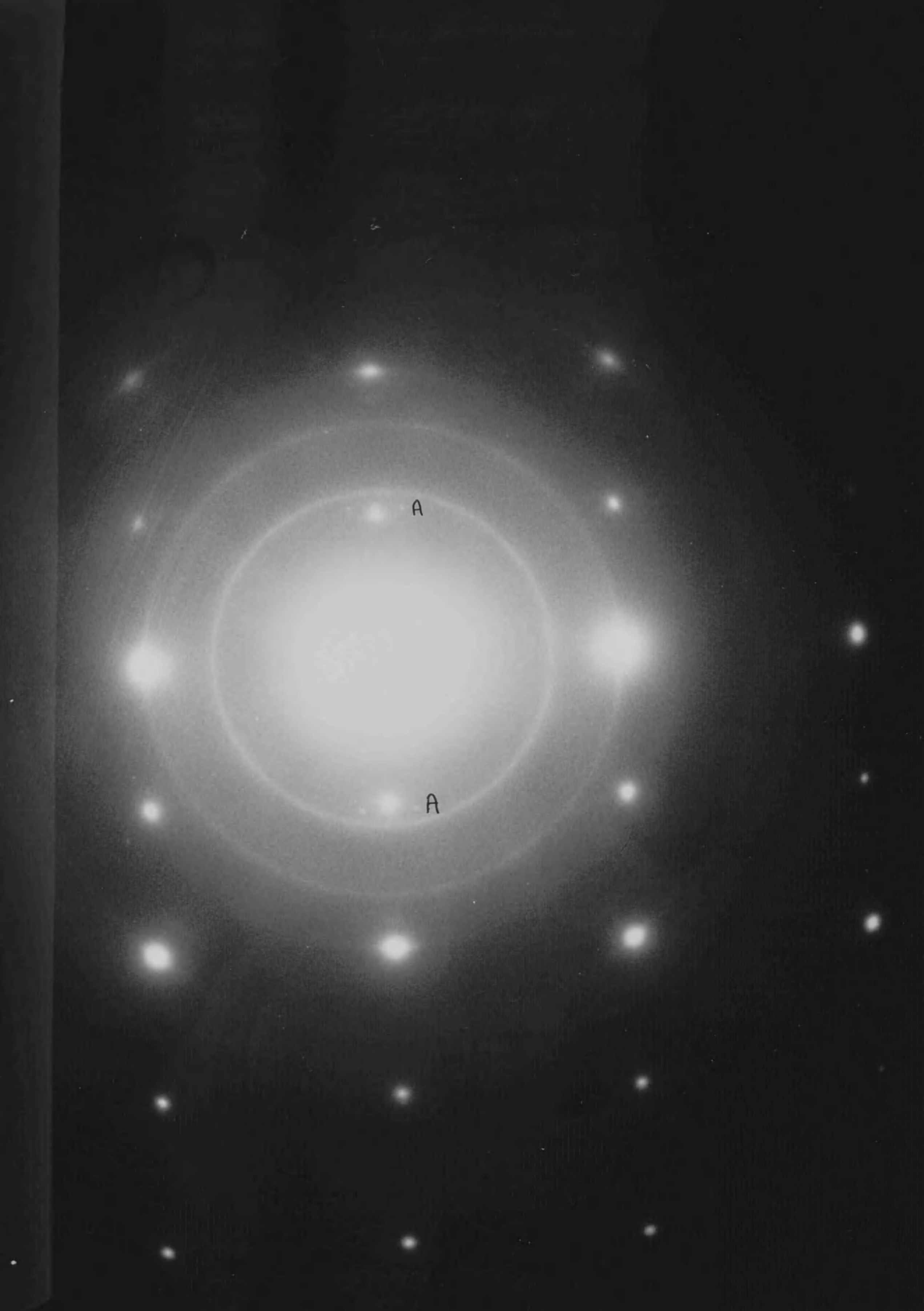
A
A

/ The specimen was exposed to the atmosphere for three days and then re-examined in the microscope. A marked change in the morphology of the crystallites was observed, as is shown in Plate 3., which shows the same as Plate 1 after exposure to the atmosphere. The dark rim round the specimen is due to contamination, the specimen having been exposed to the electron beam for several minutes.

The electron diffraction pattern of the specimen was also completely changed, as is shown in Plate 4. The single crystal spot pattern, along with a number of rings, gave the following spacings.

Table 6 .

d (Measured)	d ($ZrOCl_2 8H_2O$)	d ($ZrOCl_2 3H_2O$)
3.21 (Å)	3.24	3.23
3.05	2.96	-
2.78	2.74	2.72
1.97	2.00	1.99
1.76	-	1.78
1.68	1.71	1.69
1.25		1.21
0.94		
0.84		

Again, it is not possible to make a definite statement about the particular hydrate present; although there is certainly closest agreement between the observed spacings and those of the tri-hydrate, the limits of the experimental accuracy would also accomodate the octahydrate.

Extensive recrystallization has taken place, producing mainly a single crystal, /

PLATE 5

Group of zirconyl chloride
crystallites, as in Plate
3, heated to 350°C.
Magnification: 100,000X

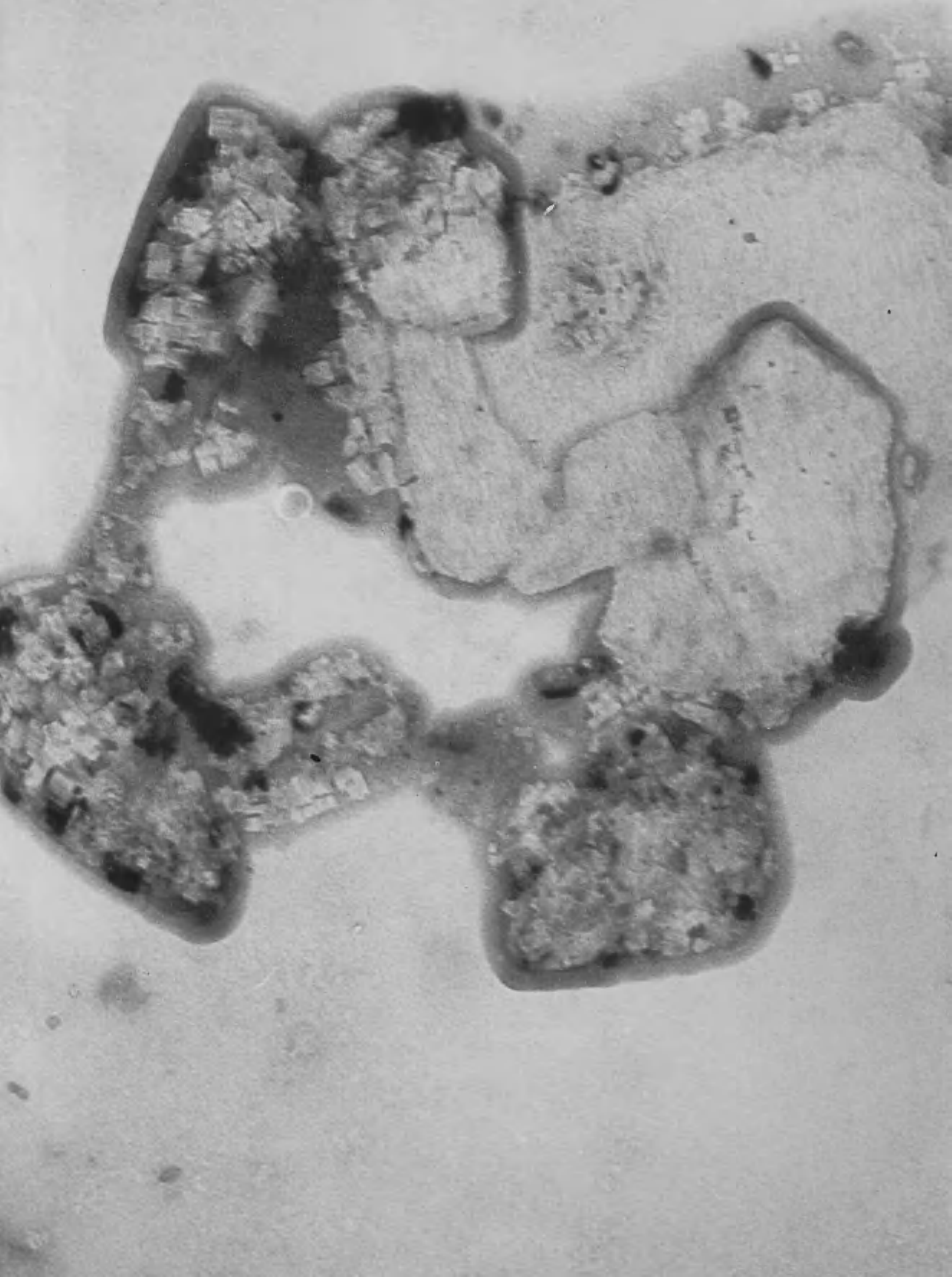

/ crystal, with a polycrystalline material also present, as shown by the two well-defined rings in Plate 4, corresponding to 2.78 and 1.97Å. The spots shown at 'A', corresponding to 3.05Å, are probably due to a double diffraction effect, and this would account for the lack of agreement between this spacing and the literature values.

Another fresh specimen prepared in the same way as before gave single crystals of zirconyl chloride, with the following electron diffraction spacings, shown in Table 7 .

Table 7 .

d (Measured)	d ($ZrOCl_27H_2O$)*	d ($ZrOCl_26H_2O$)*
2.69 (Å)	2.71	2.70
1.90	1.89	1.90
1.34	1.33	1.33
1.20	1.19	1.20
0.89		
0.84		

* Spasibenko and Goroschenko (1969)

There is very good agreement between the observed spacings and those of the hepta- and hexahydrates recorded by the Russian authors. It must be pointed out, however, that, for these two hydrates, Spasibenko and Goroschenko recorded a large number of spacings and it is of dubious validity to identify the crystals in this sample on the basis of the single crystal diffraction pattern which allow the measurement of only a small number of spacings.

However, as has been already pointed out, the agreement is excellent.

When /

/ When specimens were heated in the electron microscope to 350°C, the crystals decomposed rapidly, as Plate 5 illustrates, the area shown being the same as that shown in Plates 3 and 1. The decomposition was evidenced in the loss of diffraction patterns at this temperature. Heating at 400°C brought about extensive crystallization, as shown in Plate 6.

The polycrystalline electron diffraction pattern in Plate 7 characteristic of cubic crystals, gave the following spacings:-

Table 8 .

d (measured) Å	d (cubic ZrO_2)*	d (tetragonal ZrO_2)**
2.98	2.92	2.94
2.55	2.53	2.58 2.54
2.11	-	-
1.80	1.80	1.80
1.54	1.53	1.55 1.53
1.48	1.46	1.47
1.27	1.27	1.29 1.27
1.17	1.16	
1.13	1.13	
1.04	1.03	
0.98	0.98	
0.89	0.90	
0.86	0.86	
0.80	0.80	

* Duwez and Odell (1950)

** Komissarova, Simanov and Vladimirova (1960)

PLATE 6

Polycrystalline film of
zirconium dioxide, formed
by heating zirconyl chloride
to 400°C.
Magnification: 100,000X

PLATE 7

Polycrystalline diffraction
pattern obtained from the
ZrO_2 film at 450°C.
Magnification: 100,000X

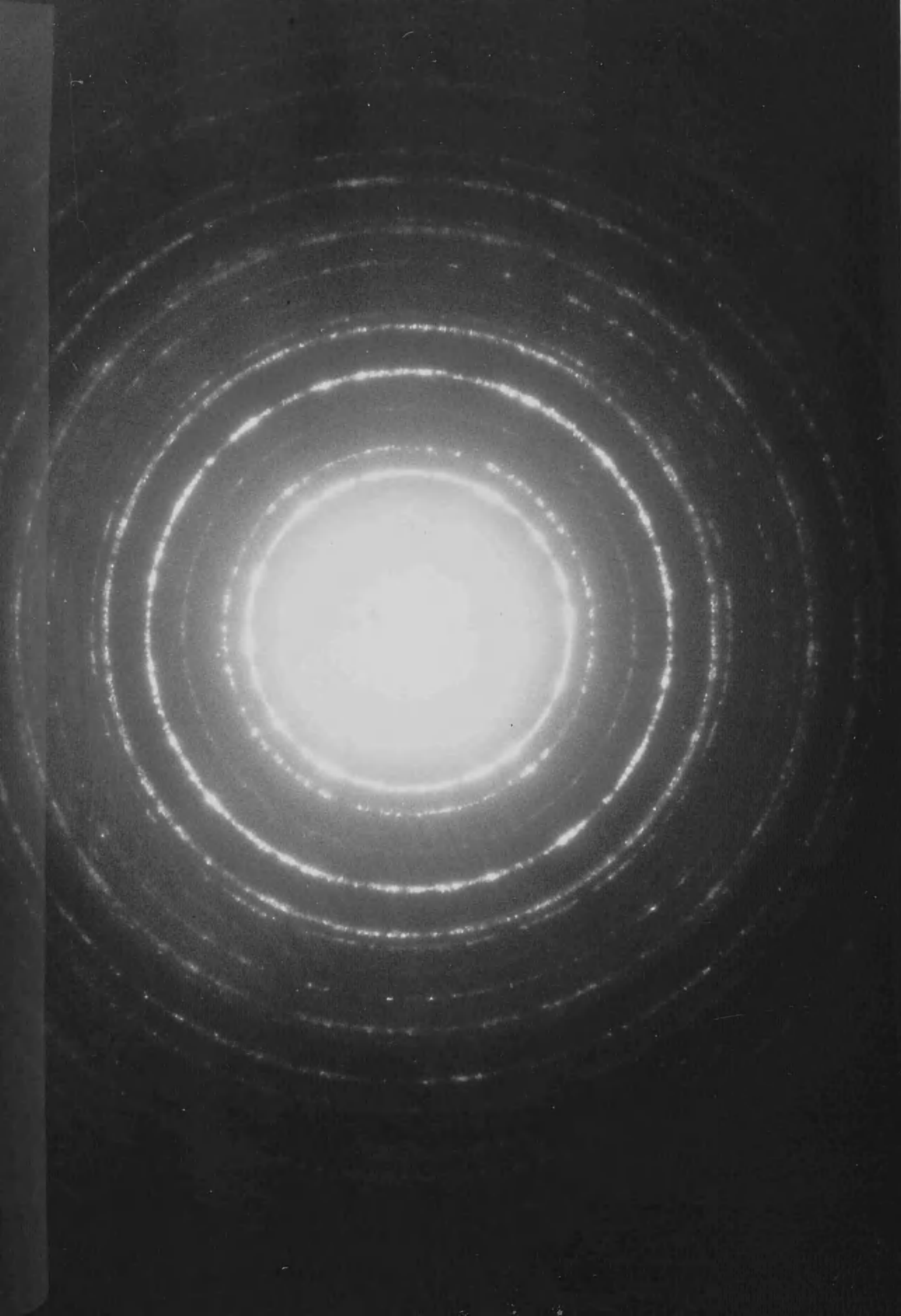

/ It is evident from the close agreement between observed and literature values that the crystalline film formed is zirconium dioxide, probably the cubic modification, which would be stabilized by the presence of the silica film. The possibility of its being tetragonal ZrO_2 cannot, however, be discounted, since the only distinguishing spacings are the closely spaced doublets, which would be difficult to resolve clearly by electron diffraction. Line broadening was mentioned earlier as a complication in X-ray studies of this material (Garvie 1965).

(b) Crystals of "Spec-Pure" $ZrOCl_28H_2O$, ground between glass slides, were picked up on a carbon coated copper grid and examined immediately in the microscope. Although most of the crystals were too thick to allow sufficient beam penetration, some were thin enough to give single crystal diffraction patterns.

The following values in Table 9 were obtained from a number of crystals:-

Table 9 .

a) b)

d (measured)	d ($ZrOCl_27H_2O$)*	d (measured)	d ($ZrOCl_26H_2O$)*
6.08 Å	6.00	3.50	3.53
4.36	4.38	3.20	3.18
3.04	3.03	2.92	2.97
2.76	2.71	2.13	2.14
2.03	2.03	1.88	1.90
1.94	1.92	1.74	1.77
1.19	1.19		

* Spasibenko and Goroschenko (1969)

/ -

/-

c)

d (measured)	d ($ZrOCl_2 4H_2O$)*
6.25 (Å)	-
4.28	4.29
3.96	3.97
3.11	3.09
2.38	2.36
2.14	2.14
1.95	2.02
1.74	1.72

* Spasibenko and Goroschenko (1969)

There is again very close agreement between the measured spacings and those quoted for $ZrOCl_2(7, 6, 4)H_2O$. Within the limits of this technique, namely the accuracy and the small number of spacings measured it appears likely that these three hydrates are in fact present.

(c) Dispersion in Cyclohexane: Dry, distilled cyclohexane was used as a suspending medium in which crystals of "Spec-Pure" zirconyl chloride were ultra-sonically dispersed. A drop of this suspension was evaporated on a carbon film and examined in the electron microscope. Several diffraction patterns were observed, although the crystals giving rise to them were extremely unstable in the electron beam, the patterns fading very rapidly. However, some of these patterns were recorded, and the spacings are given in Table 10.

Table 10.

/ -

/ -

a) d (measured)	b) d (measured)
4.24 (Å)	4.58
3.78	2.64
2.97	1.73
2.48	1.53
2.25	1.32
2.10	1.27
2.10	0.99

These spacings were not accounted for by the series of hydrates already discussed and it is thought that they represent either less stable hydrates, or else complexes formed by interaction of the zirconyl chloride and cyclohexane.

It is concluded from this study of zirconyl chloride that:-

(i) In the electron microscope the octahydrate is partially dehydrated to give a whole range of lower hydrates, although positive identification of these is ambiguous because of the small number of d-spacings available for comparison with literature data.

(ii) Zirconyl Chloride is decomposed by heating at 350°C, forming ZrO_2 in the cubic or tetragonal phase.

Thus the behavious of zirconyl chloride octahydrate in the electron microscope was established in terms of dehydration and thermal breakdown to ZrO_2.

LOW RESOLUTION ELECTRON MICROSCOPY AND DIFFRACTION

ZIRCONIA

A. Precipitation by Ammonia

(i) Amorphous zirconia. This was precipitated from an aqueous solution of zirconyl chloride by ammonia. To 50 ml. of 2 M zirconyl chloride 100 ml. of M ammonia was added. The pH of the solution rose from 0.21 to 1.63, while a flocculent white precipitate formed. Plate 8 shows an example of this material, which gave only broad, extremely diffuse rings in its electron diffraction pattern. When this gelatinous precipitate was refluxed, there was a pronounced initial drop in pH, occurring within the first hour of reflux, as shown in figure 10.

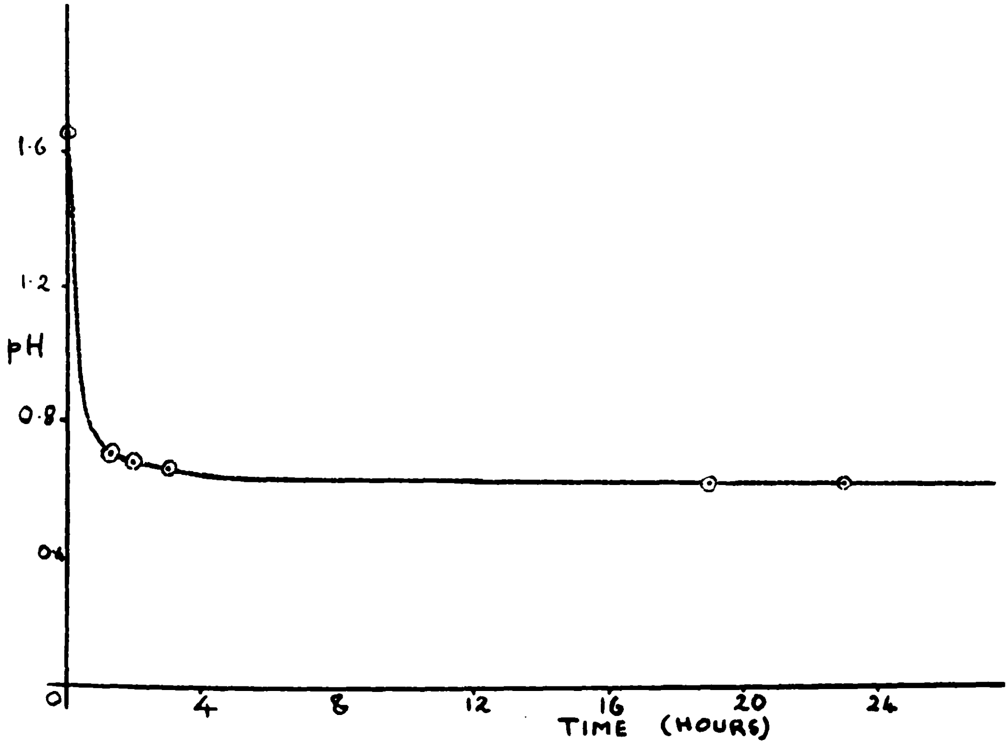

Figure 10. Variation of pH with time of reflux of amorphous zirconia. Most of the precipitate redissolved during this time, only a faint opalescence remaining.

(ii) /

PLATE 8

Amorphous zirconia, pre-
cipitated from zirconyl
chloride solution by
addition of ammonia.
Magnification: 100,100X

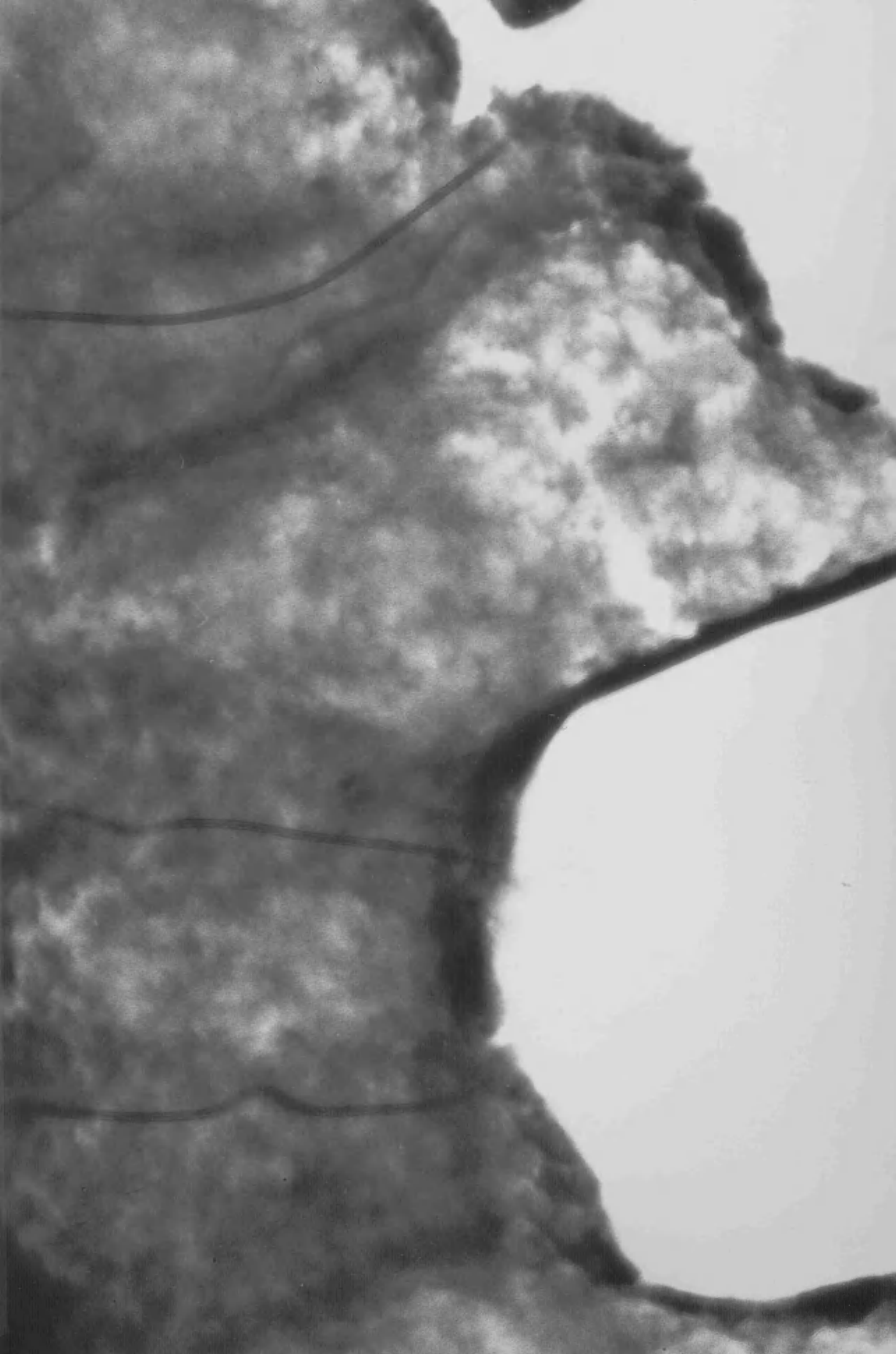

PLATE 9

Monoclinic zirconia, formed
by prolonged reflux of
amorphous zirconia suspension.
Magnification: 100,000X

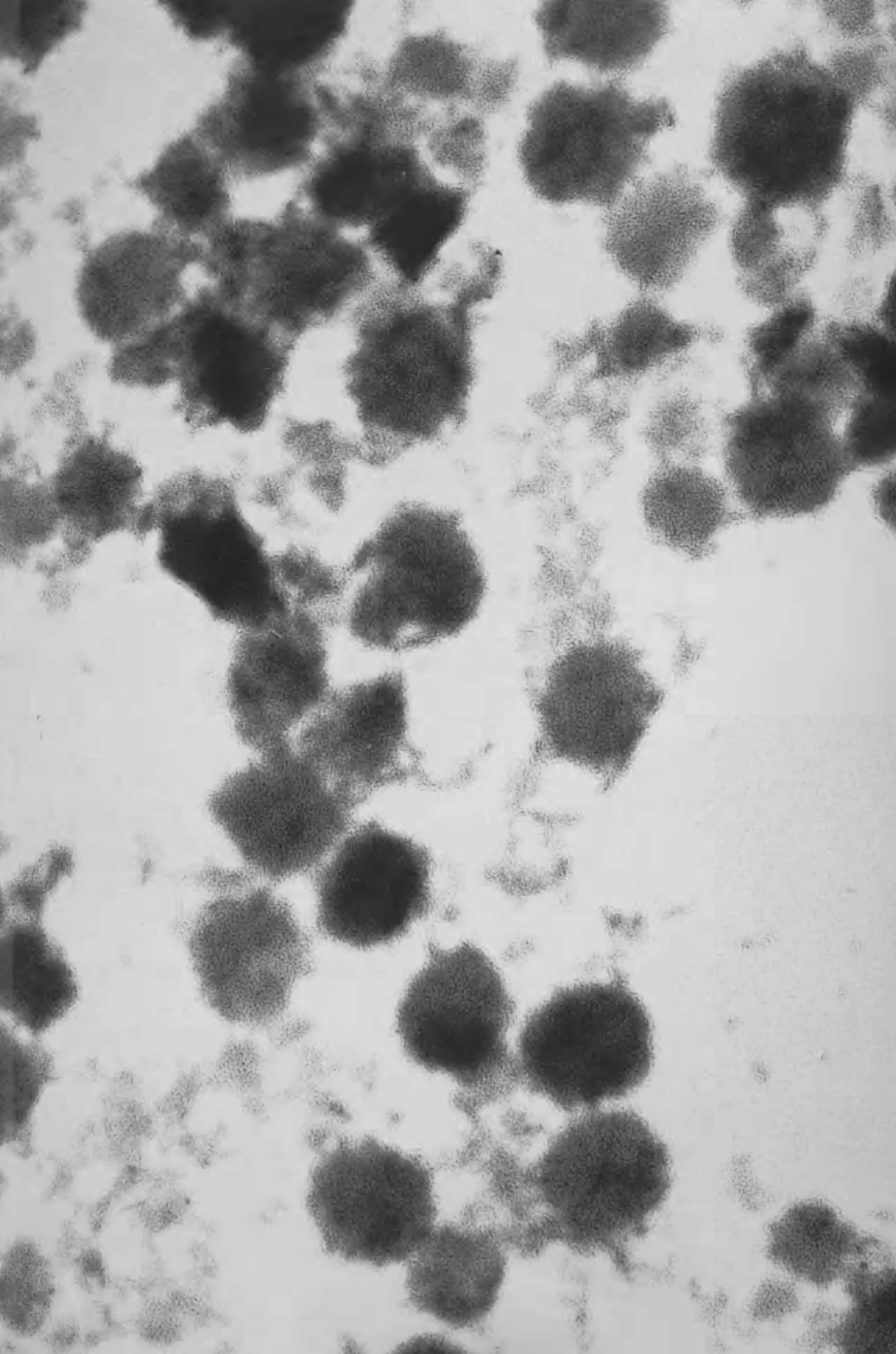

(ii) Monoclinic zirconia. Prolonged reflux resulted in further precipitation, the suspension becoming milky, and faintly pink. The precipitate now consisted of rounded particles, together with smaller aggregates of amorphous material. A typical distribution of particles is shown in Plate 9. The polycrystalline electron diffraction pattern for this sample gave the following spacings, as in Table 11.

Table 11.

d (measured)	d (monoclinic ZrO_2) *
5.05 Å	5.04
3.65	3.63
3.16	3.16
2.79	2.83
2.60	2.62
2.50	2.54
2.17	2.18
1.98	1.99
1.81	1.82
1.66	1.66

* A.S.T.M., 13 - 307 (G.E.C., A.N.P. Dept., Ohio)

Comparison of the measured spacings and those quoted for monoclinic zirconium oxide indicates that the particles consist of monoclinic zirconia.

The irregularly shaped crystallites had a narrow size distribution, as figure 11 illustrates, the average diameter being 1100 Å. This is larger than the average particle size proposed by Clearfield (1964b) for zirconia prepared in a similar manner. However, his predictions were based on X-ray line broadening measurements and a strict comparison is /

PLATE 10

Crystalline zirconia, formed by heating amorphous zirconia shown in Plate 8, to 550°C.
Magnification: 100,000X

PLATE 11

Electron Diffraction pattern of crystalline zirconia as shown in Plate 10.

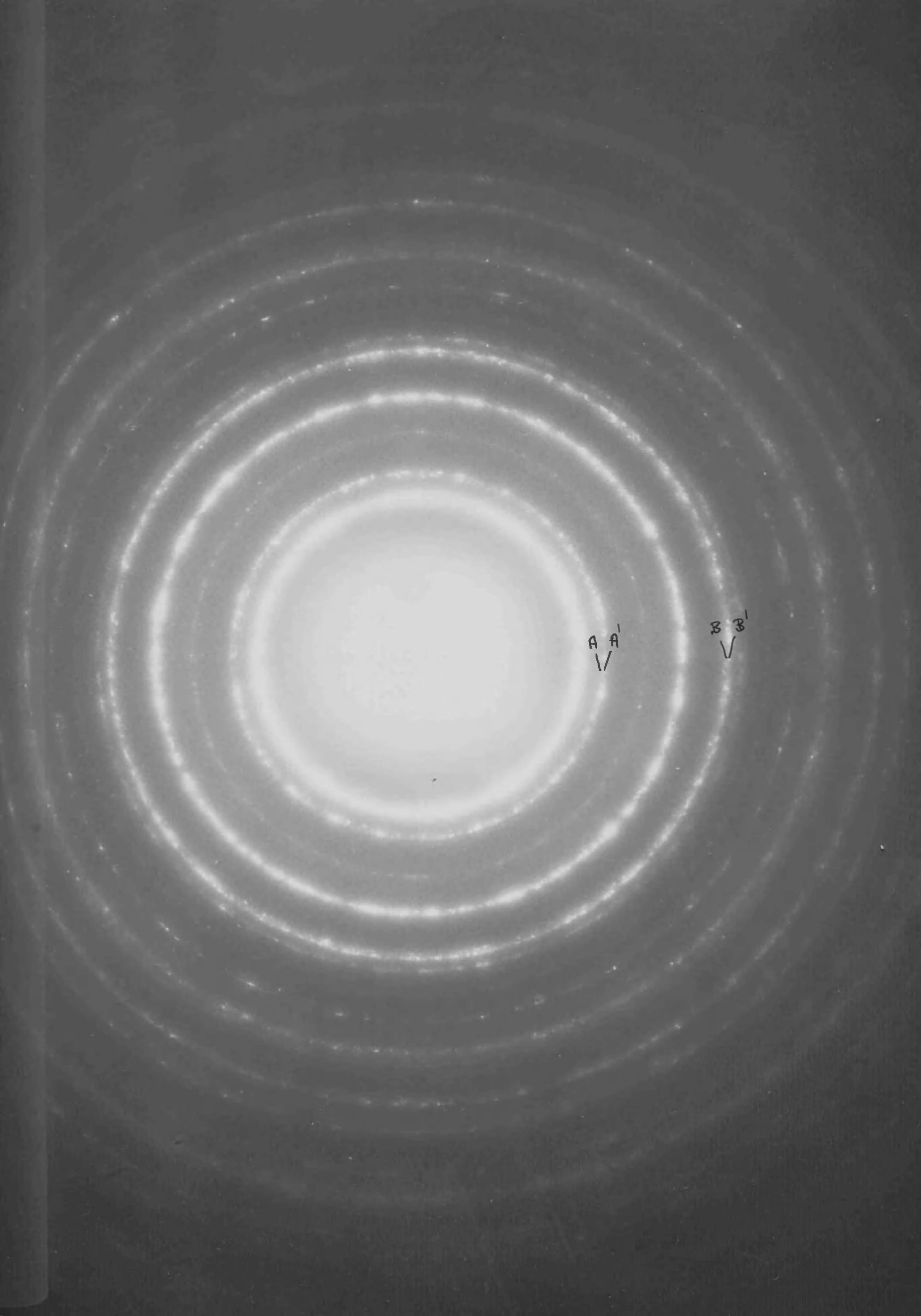
A A'
B B'

/ is not quite valid. The presence of amorphous zirconia, as revealed by electron microscopy, would contribute towards a line broadening effect, thus leading to a lower "average size" than would be normally true for the crystalline particles.

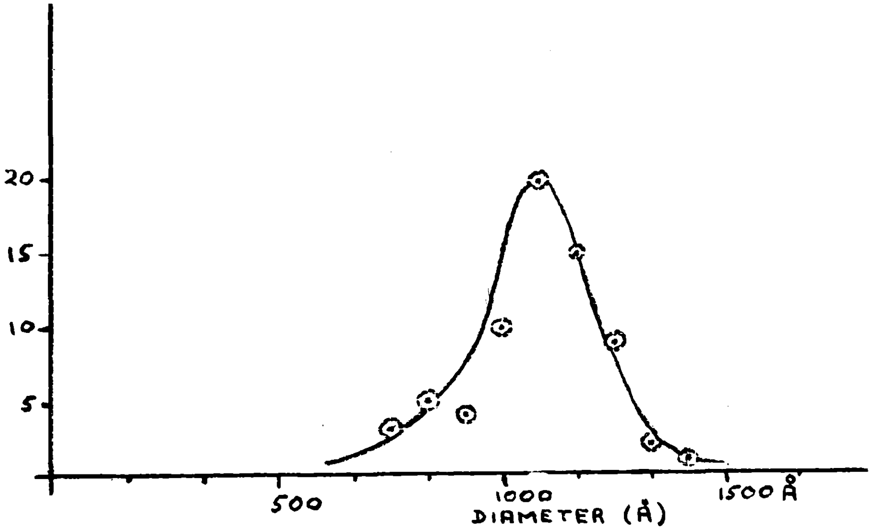

Figure 11. Particle size distribution for monoclinic zirconia particles.

(iii) Tetragonal zirconia. A sample of the amorphous zirconia precipitated by ammonia was heated in the electron microscope, use the object heating device as manufactured by Siemens. Plate 10 shows the same area as Plate 8, after heating to 550°C. At this temperature crystallization occurred, as indicated by the electron diffraction pattern, Plate 11, for the same area. It can be seen that two sets of closely spaced doublets are just resolved (A A' and B B' in Plate 11). By careful measurement of an enlargement of the plate, the following spacings were obtained, as presented in Table 12.

Table 12.

/ -

Table 12.

d (measured)	d (cubic ZrO_2) *	d (tetragonal ZrO_2) **
2.94 Å	2.92	2.95
2.59	-	2.58
2.54	2.53	2.54
2.09	-	-
1.80	1.80	1.80
1.54	-	1.55
1.53	1.53	1.53
1.47	1.46	1.47
1.36	-	-
1.25	1.27	1.27
1.15	1.16	1.16 (calc.)

* Duwez and Odell (1950)

** Komissarova et al (1960)

The agreement between the spacings measured and those of both cubic and tetragonal ZrO_2 is excellent. The two lines corresponding to 2.59 and 1.54 Å are, however, taken as evidence that the phase present is in fact tetragonal zirconia, since they correspond to the (002) and (113) spacings which in the cubic phase would coincide with the (200) and (311), with values of 2.53 and 1.53 respectively. The measured spacings for which no agreement was found, namely 2.09 and 1.36 Å will be discussed later.

B. Precipitation by Reflux of Zirconyl Chloride.

Hydrous zirconia was also prepared by refluxing zirconyl chloride solutions, the hydrolysis being followed by pH measurements. As the reflux proceeded an initial sharp drop in the pH was noted, this being followed by a gradual levelling off in the pH curve, as shown in figure 12.

PLATE 12

Crystals of zirconyl chloride,
from an aqueous solution
refluxed for one hour.
Magnification: 100,000X

/ -

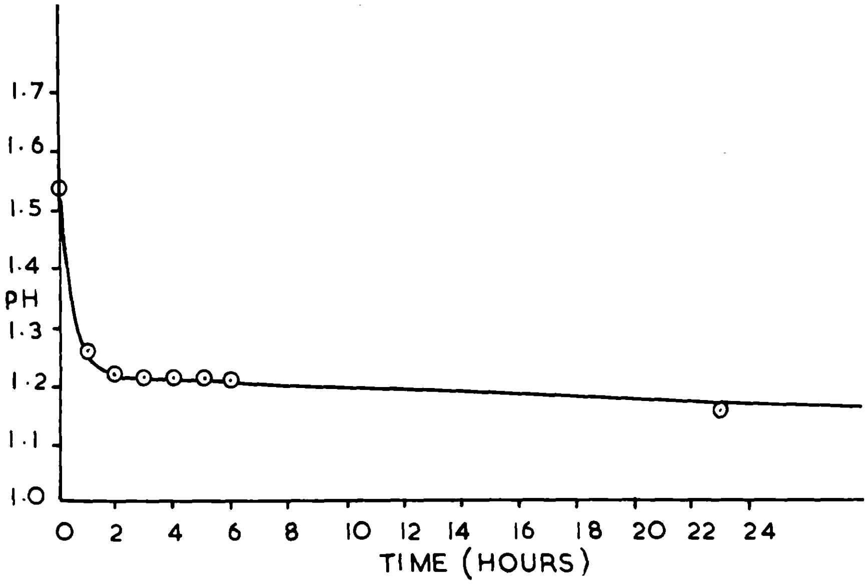

Figure 12. Variation of pH with time of reflux of 0.055 M zirconyl chloride solution.

Samples were withdrawn at various stages in the hydrolysis and the colloidal material examined in the microscope by allowing a diluted drop of the suspension to evaporate on a specimen mount. Silica films were usually employed as substrates. The results obtained for the hydrolysis of a 0.055 M solution are as follows:-

(i) Zirconyl chloride hydrates. A fresh solution gave a range of crystalline materials, which have been described previously. They were concluded to be various hydrates of zirconyl chloride.

After one hour of reflux, the deposit was still mainly crystalline, as shown in Plate 12. Single crystal diffraction patterns for these crystals gave the following spacings:-

Table 13. / -

PLATE 13

Amorphous zirconia, after six hours' reflux of zirconyl chloride solution.
Magnification: 100,000X

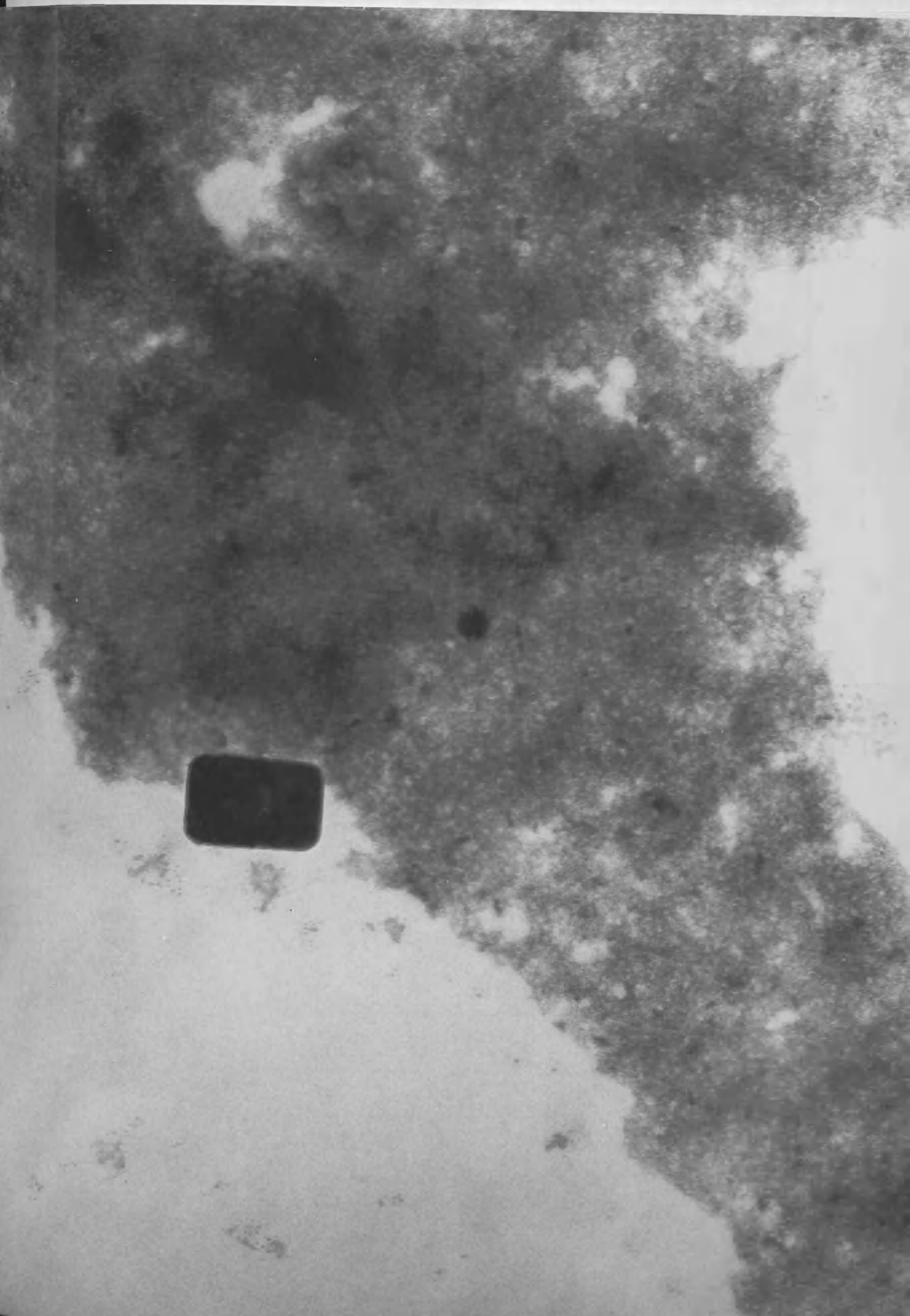

Table 13.

	d ($ZrOCl_2nH_2O$)				
d (measured) Å	n = 8	7	6	4	3
3.14 Å	-	3.08	3.11	3.09	3.14
1.92	1.91	1.92	1.90	1.84	1.95
1.60	1.62	1.63	1.61	1.61	1.62
1.56	1.57	1.57	1.55	1.56	-
1.23	-	1.24	1.26	1.25	1.21
1.20	-	1.09	1.09	1.09	-
1.06	-	1.07	1.04	1.07	-
0.91					

It is clear from this table that it is not possible to identify these crystals with certainty, although there is a strong suggestion that they are hydrates of zirconyl chloride.

(ii) Amorphous zirconia. After six hours reflux, a preponderance of amorphous material was observed, along with a few single crystals, as shown in Plate 13. The single crystal shown here, along with other single crystals, gave the following set of spacings, measured from the electron diffraction patterns, which were identical.

Table 14.

	$ZrOCl_2nH_2O$			
d (measured)	n = 8	7	6	4
2.79	2.74	2.83	2.70	2.75
1.97	2.00	1.99	2.04	2.02
1.40	1.42	1.41	1.41	1.41
1.25		1.24	1.26	1.25
0.94				

Table 15.

	$ZrOCl_2nH_2O$	
d (measured)	n = 7	6
1.97 Å	1.99	2.04
1.68	1.66	1.68
1.24	1.24	1.26
0.98	0.99	0.99
0.94		
0.84		

As may be seen from these spacings, it seems likely that hydrates of zirconyl chloride were still present, although it is again not possible to identify any with certainty. The fact that zirconyl chloride remains after six hours of reflux would indicate that the initial fast hydrolysis is not irreversible. This is similar to the case of ammonia addition, although the two forms of amorphous zirconia (Plates 8 and 13) are not themselves identical, since the flocculent mass produced by ammonia redissolved, whereas the opalescence present after six hours reflux of zirconyl chloride solution became more intense on continued refluxing.

The opalescence which was becoming evident after about six hours was evidence of particle growth and increased gradually until the suspension was milky. At about this stage small, dense particles were becoming visible in the electron microscope, quite distinct in appearance from both the amorphous zirconia and the crystalline hydrates observed earlier.

(iii) Monoclinic zirconia. A sample refluxed for 25 hours had a pH of 1.16 and a specimen examined in the microscope showed little evidence of amorphous material. The deposit consisted of small particles, similar in appearance to those observed after twelve hours. A typical dispersion /

PLATE 14

Monoclinic zirconia, after 25 hours' reflux of zirconyl chloride solution.

Magnification: 400,000X

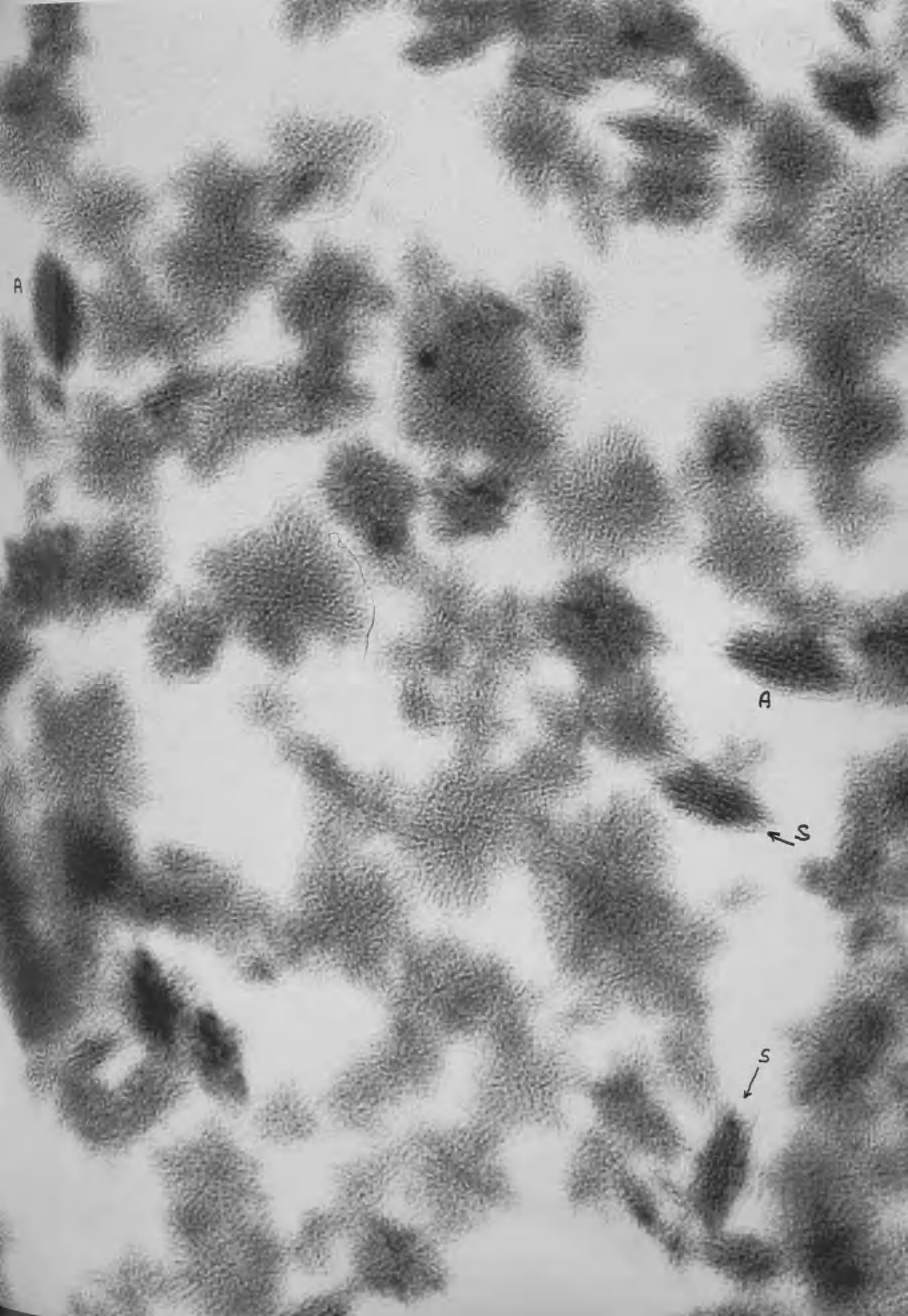
A
A
S
S

PLATE 15

Electron Diffraction pattern corresponding to crystallites shown in Plate 14.

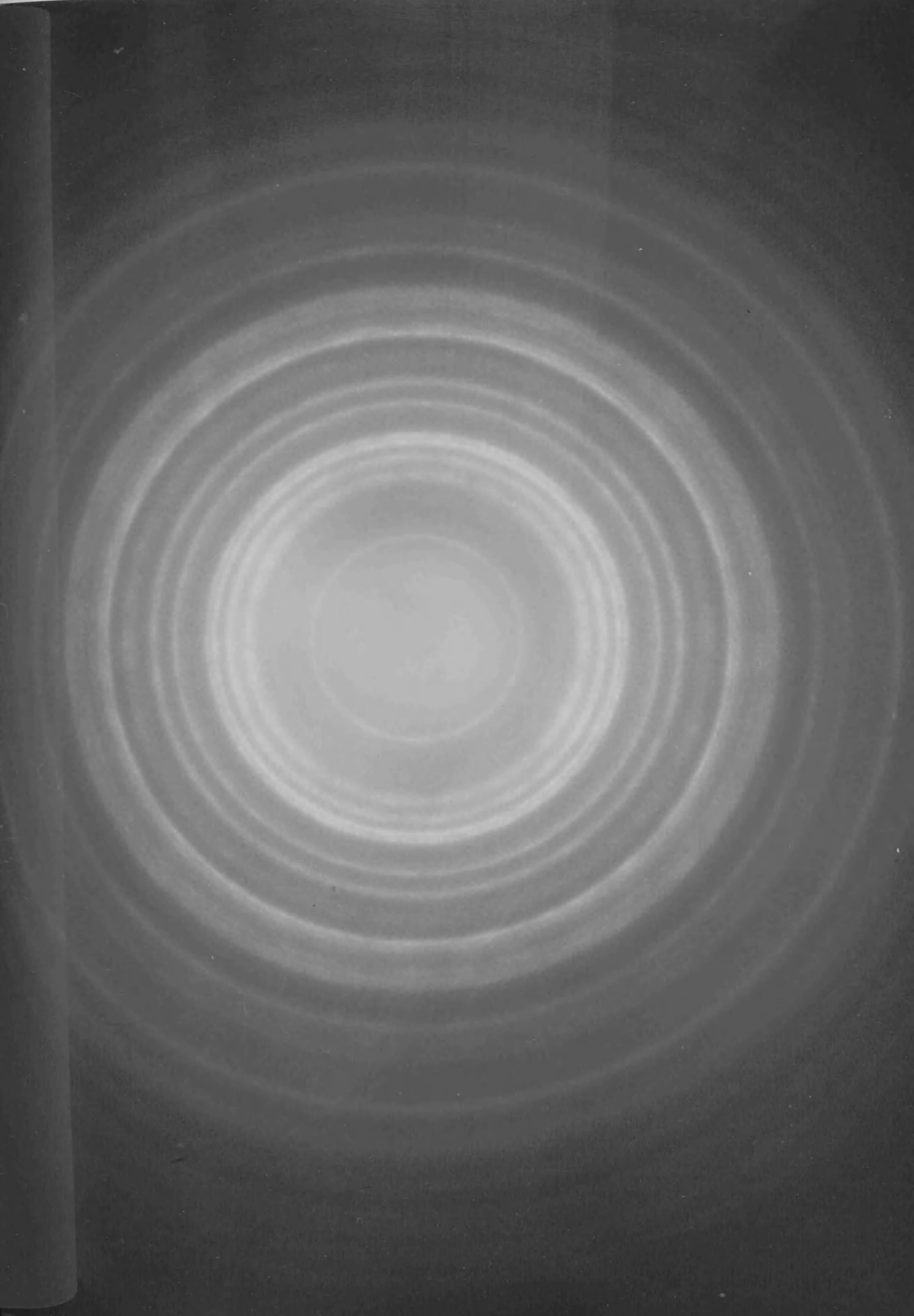

/ dispersion of these crystallites is shown in Plate 14. The electron diffraction pattern for this sample is shown in Plate 15. In the measurement of this pattern, the variation of camera constant with ring diameter was taken into account, in order to increase the accuracy over a wide range of spacings. The relationship between camera constant and ring diameter was shown in Figure 9. The spacings measured from Plate 15 are recorded in Table 16, together with those derived from an X-ray powder photograph for an air-dried sample of the solid.

Table 16.

Electron Diffraction d	X-ray Diffraction	Monoclinic ZrO_2
5.05 Å	5.04	5.04
3.67	3.67	3.69
3.16	3.17	3.16
2.82	2.83	2.83
2.63	2.62	2.62
2.55	2.53	2.54
2.22	-	2.21
-	2.18	2.18
2.02	2.00	2.01
1.85	1.85	1.84
-	1.81	1.82
1.72		1.69
1.68		1.66
1.57		1.58
1.49		1.51

Comparison of the measured spacings with literature values established the identity of the crystalline particles as monoclinic zirconia.

From /

From these results it can be seen that there is a slight improvement in the accuracy when camera constant variation is considered, although it is almost cancelled out by other random errors.

The crystallites of monoclinic zirconia were observed as two apparently distinct types:-

a) extremely uniform, lozenge-shaped crystals, as shown at 'A' in Plate 14. These crystallites were known as "pods".

b) less regulary shaped crystals, usually roughly square in outline. Because of their spiky appearance, these were called "stars".

Particle Dimensions. A striking feature of the "pods" was their narrow size distribution. Figure 13 shows the length distribution, measured along the main axes.. The average length was found to be 670 Å, the diameter being 280 Å.

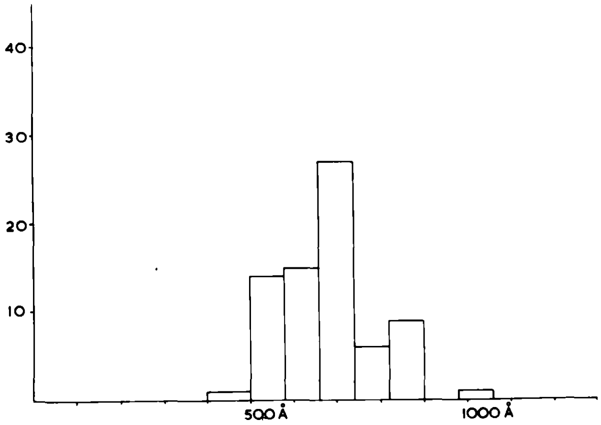

Figure 13. Block histogram for length of monoclinic zirconia "pods".

The /

PLATE 16

Crystallites of monoclinic zirconia, after prolonged reflux of 0.5 M zirconyl chloride solution.

Magnification: 400,000X

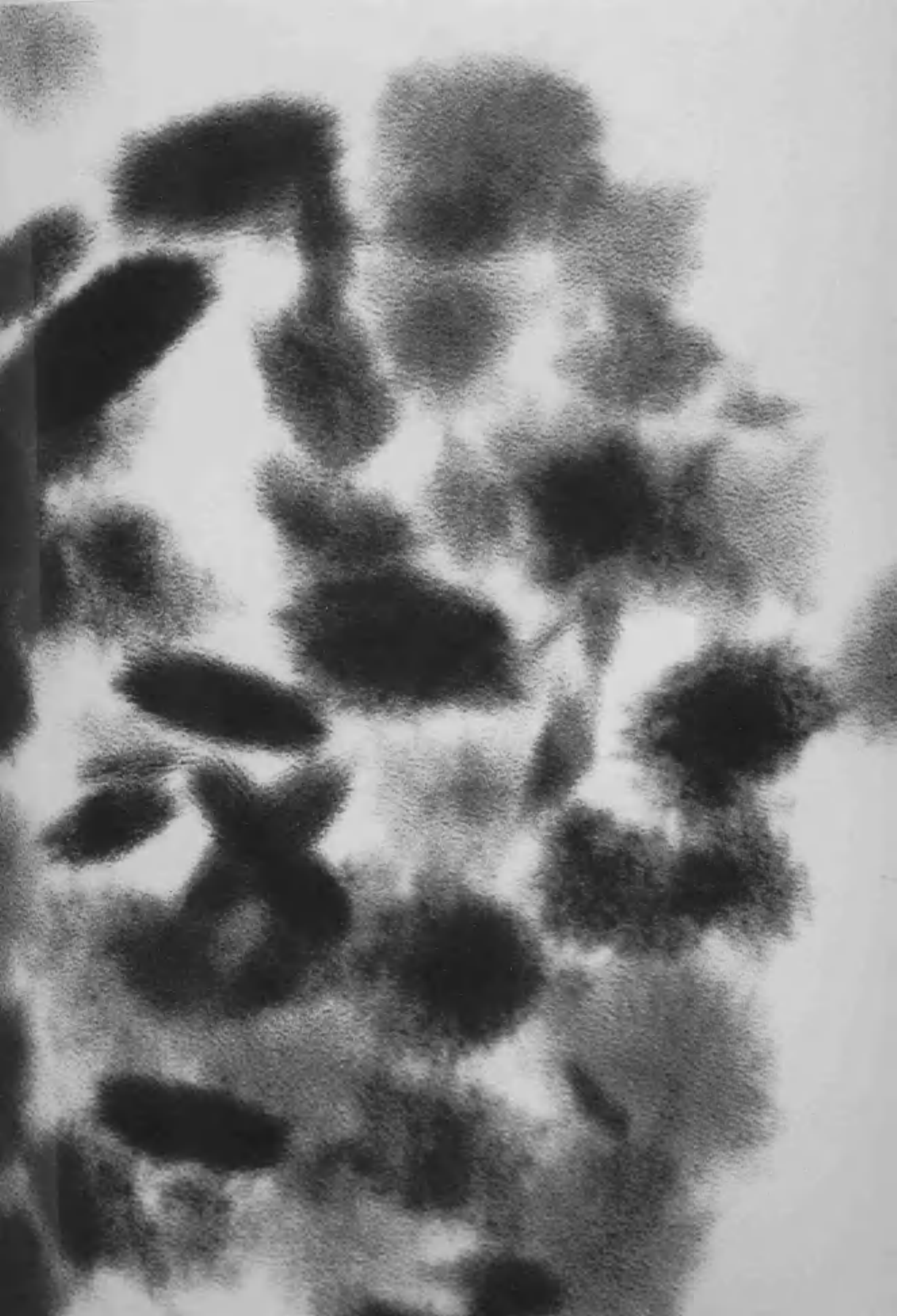

PLATE 17

The same area as Plate 16, with objective lens under-focussed.

Magnification: 400,000X

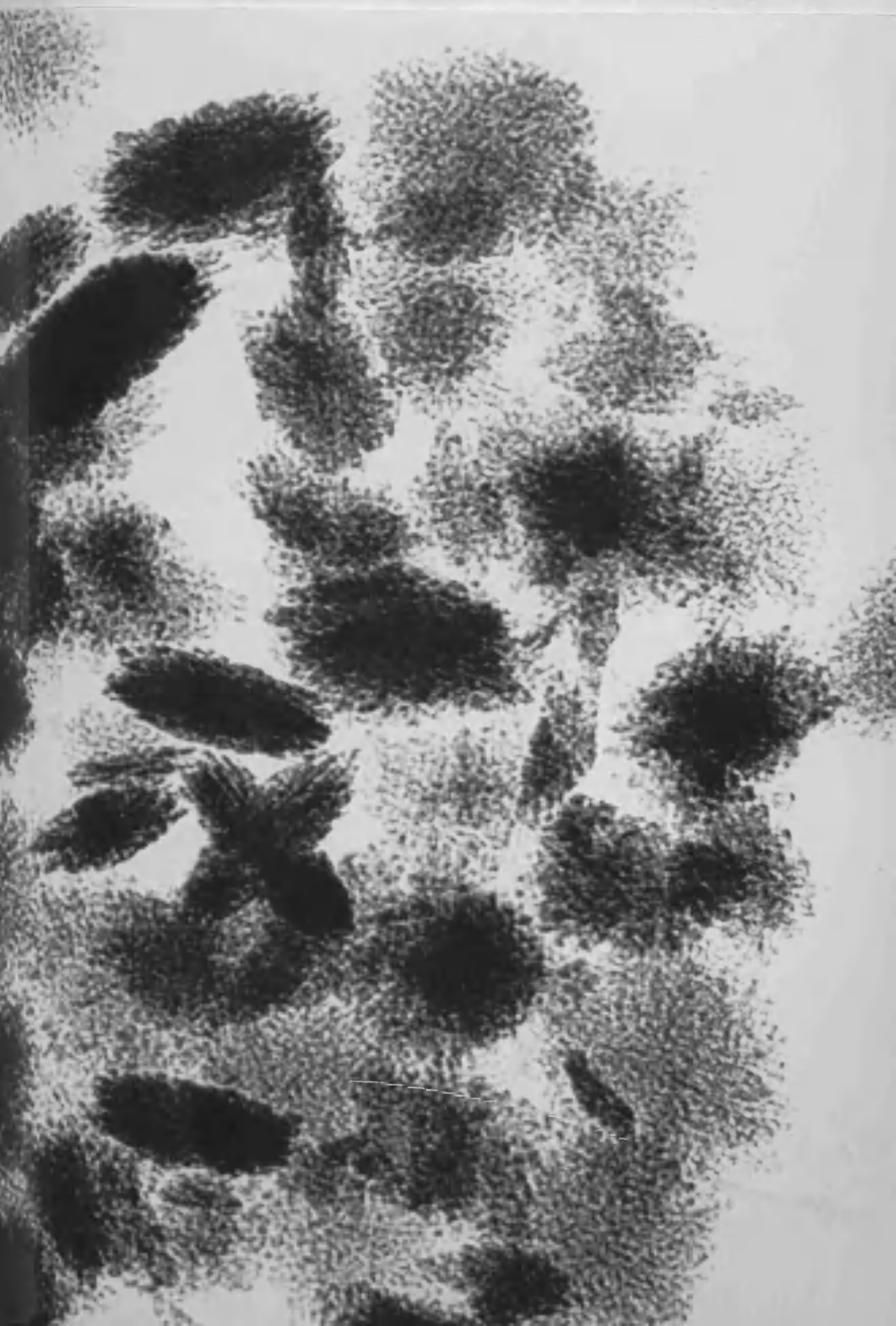

The average particle size for the "stars" was approximately 600 Å.

Striations. The "pods" all possessed prominent striations along their lengths, with a repeat distance of approximately 30 Å, as shown at 'S' in Plate 14. Although the contrast of these fringes was to some extent dependent on the focussing of the objective lens, as Plates 16 and 17 illustrate, they did remain visible at or near exact focus. From this it was concluded that the fringes represented structural features within the crystallites, and were not artifacts. Similar striations, although less prominent, were detectable on most of the "stars". In these cases, the striations were orientated along the diagonals of the "squares", as shown at "D" in Plate 17.

Electron Diffraction. By using a 5 μ selector aperture and double condenser illumination it was possible to obtain selected area diffraction patterns from single, isolated crystallites. A diffraction pattern obtained for a "star" is shown in Plate 18. Similar patterns were obtained for all the single "stars" observed. From a knowledge of d-spacings and corresponding (h k l) values it was possible to index the spot pattern as shown in the Plate. A consistent set of indices is obtained by inserting (h k l) values of 102, 100 and 002 to the points P_1, P_2 and P_3 respectively. Taking these points as lying in the (u v w) reciprocal lattice plane, it follows that:-

$$h_1 u + k_1 v + l_1 w = o \text{ and } h_2 u + k_2 v + l_2 w = o$$

from which it follows that:-

$$(u\ v\ w) = (k_1 l_2 - l_1 k_2,\ l_1 h_2 - h_1 l_2,\ h_1 k_2 - k_1 h_2)$$

Inserting (102) for $(h_1\ k_1\ l_1)$ and (100) for $(h_2 k_2 l_2)$ it was found that (u v w) = (020).

Thus /

PLATE 18

Selected Area Electron Diffraction pattern for monoclinic zirconia "star".

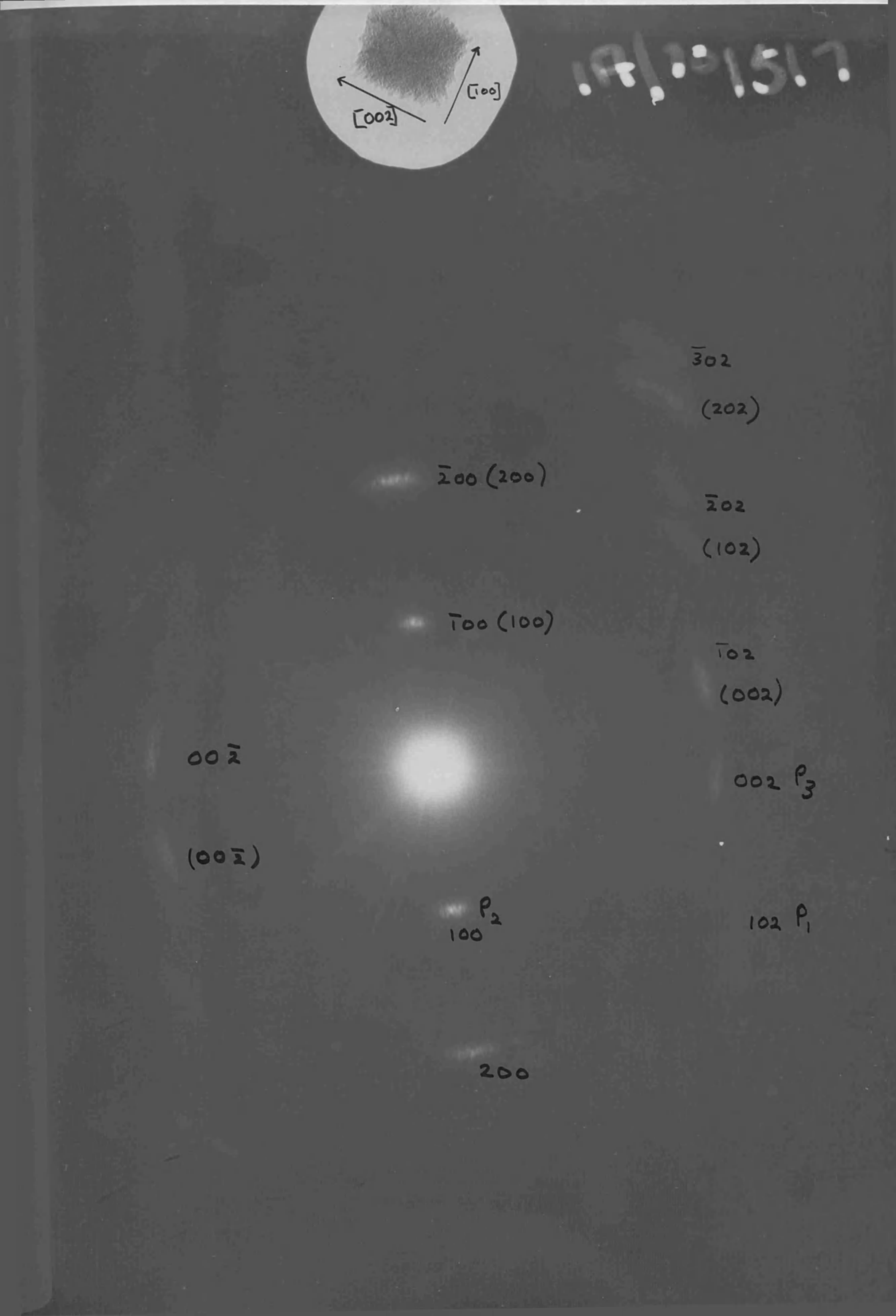

1A|101517
[002]
[100]
$\bar{3}02$
(202)
$\bar{2}00$ (200)
$\bar{2}02$
(102)
$\bar{1}00$ (100)
$\bar{1}02$
(002)
$00\bar{2}$
002 P_3
$(00\bar{2})$
P_2
100
102 P_1
200

Thus the reciprocal lattice plane (as in Plate 18) was shown to be (020), with the b-axis parallel to the electron beam.

Examination of the diffraction pattern shows a mirror plane, as denoted by AB in Plate 18. This indicates that the pattern is in fact symmetrical in the [100] direction. The (020) reciprocal lattice for a monoclinic crystal would not possess such symmetry, unless twinning were present. With $\beta = 80^{\circ}$ approximately, twinning on (100) is thus indicated, with a twinning angle of about 10°. Miller Indices corresponding to the twin component are enclosed in brackets in Plate 18.

The transmission image of the crystal may be related directly to its diffraction pattern if lens rotation of the image is taken into consideration. The angle may be measured by superimposing a selected area transmission image and the corresponding diffraction pattern upon the same plate. If a crystal with well-defined, crystallographic boundaries is chosen it will be possible to correlate the reciprocal lattice with the crystal faces. Plate 19 shows a crystal of molybdenum trioxide, with the corresponding diffraction pattern. In order to allign the [100] direction, which is normal to the long axis of the crystal, with the corresponding direction in the reciprocal lattice the crystal image must be rotated through 26° in a counter-clockwise direction. Thus the image is rotated through this angle when passing from selected area "transmission" to "diffraction". In addition, the image is inverted by the objective lens, relative to the diffraction pattern. A similar value for lens rotation was obtained using a single crystal chrysatile filament, and alligning the [001] directions. These effects are discussed by Hirsch et al. (1965).

Taking these effects into consideration it is seen that an image rotation of 206° is effective in alligning the image and its diffraction pattern, although usually the inversion of the image is ignored and the rotation of 26° only is applied.

In /

PLATE 19

Superimposition of MoO_3 crystal and its selected area diffraction.

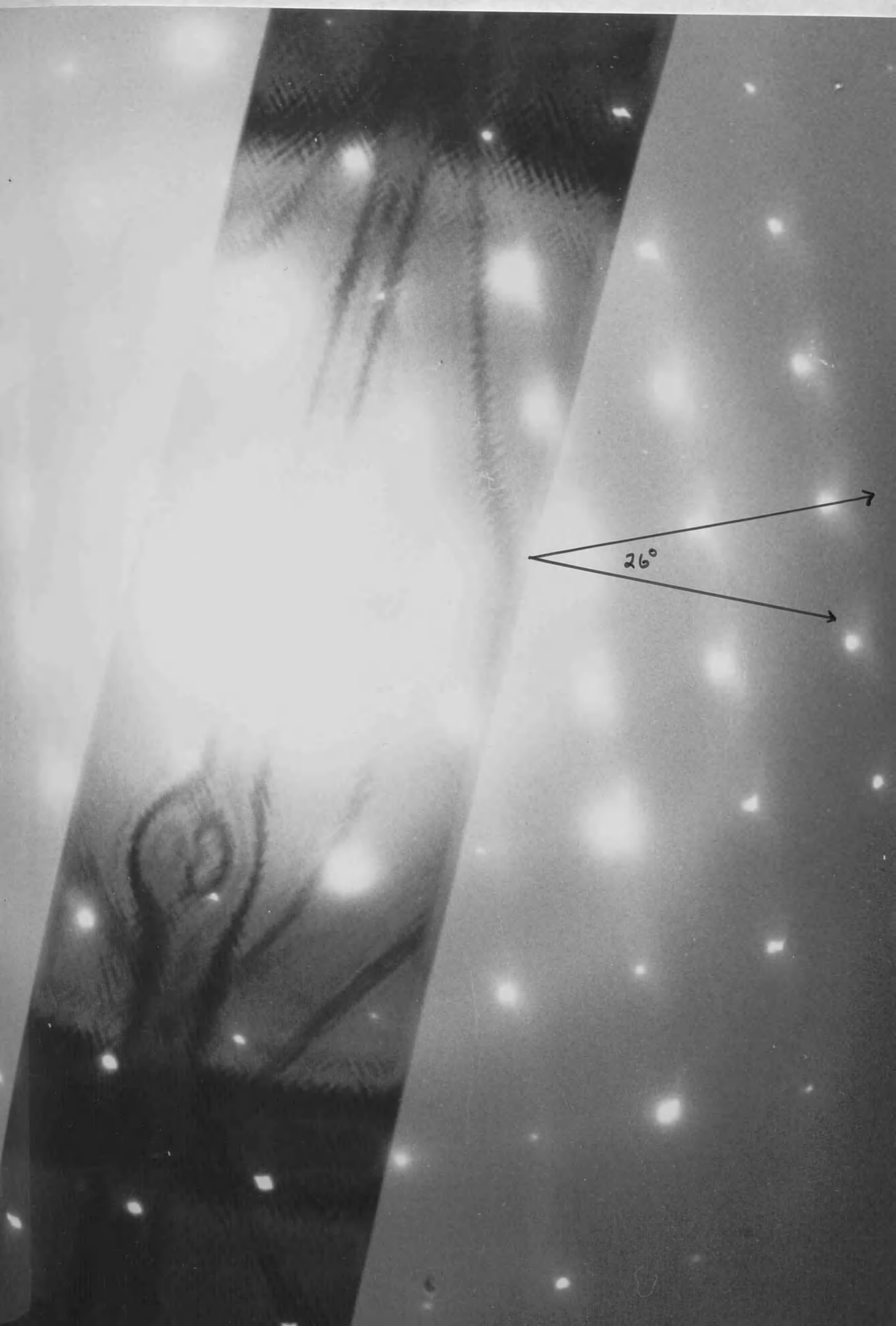
26°

PLATE 20

Selected Area Electron Diffraction pattern for monoclinic zirconia "pod".

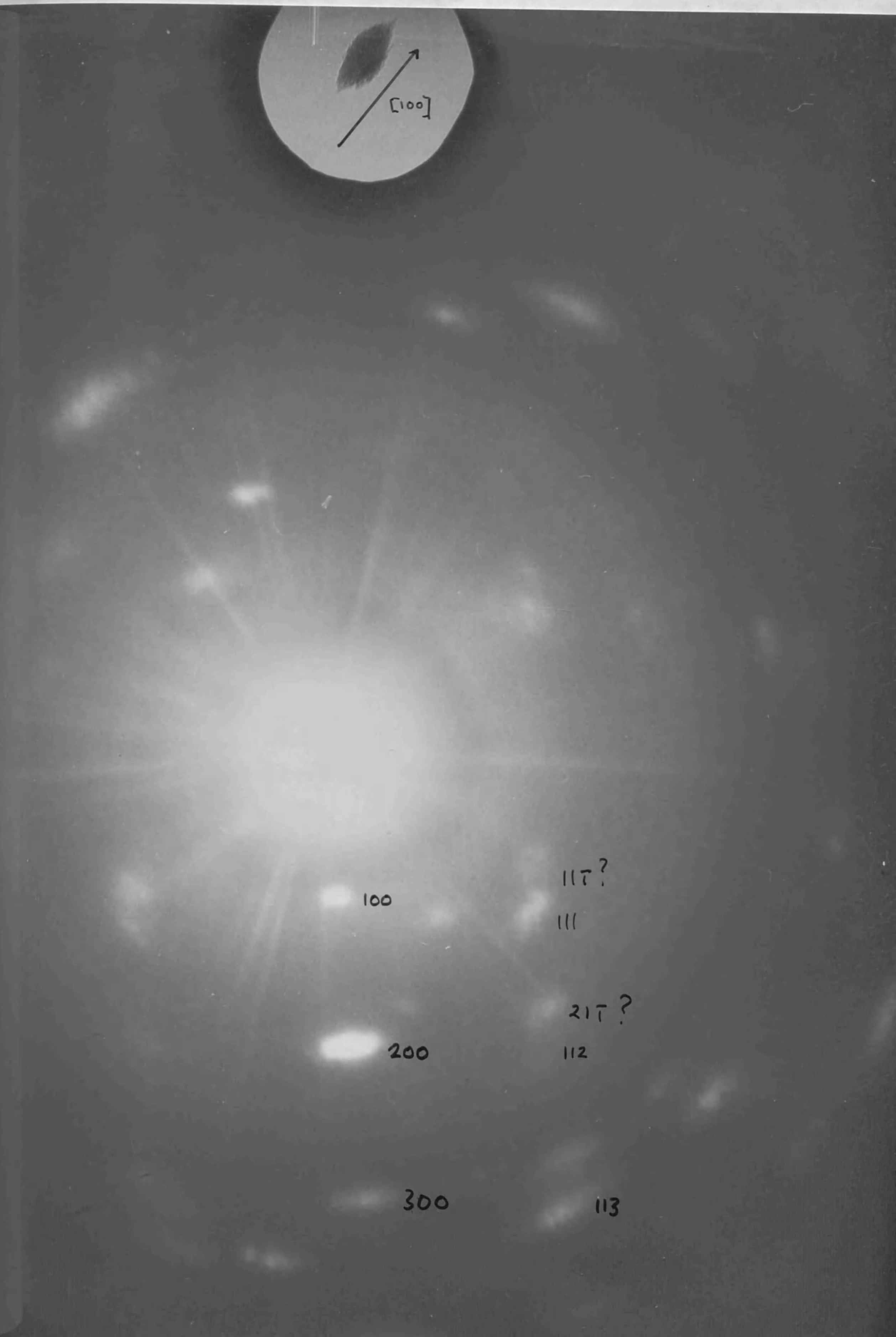
[100]
$11\bar{1}$?
100
111
$21\bar{1}$?
200
112
300
113

In plate 18 the [100] and [002] directions are shown beside the image of the crystal. The twinning already mentioned takes place in the [100] direction and thus there is no obvious correlation between it and the striations.

There was a marked diffuseness in the diffraction spots, and arcing of up to 10° was observed. This suggested that the "stars" actually consisted of well-orientated bundles of smaller crystallites. Since ultra-sonic bombardment failed to disperse these supposed "subcrystals" it is believed that a fairly rigid matrix exists, with apparently more than weak electrostatic attraction prevailing between the components.

Although isolated "stars" occurred frequently on any given specimen grid, it was a noteable feature that the majority of the "pods" observed were in contact with other particles. However, single-crystal diffraction patterns of isolated "pods" were obtained, one such pattern being shown in Plate 20. The indexing shown is extremely tentative although it appears that the b-axis is in fact inclined to the electron beam rather than parallel to it. Although no two patterns were alike, it was observed that 'a' and 'c' reflections did not occur together on any one pattern. Furthermore, where 'a' reflections were present there was evidence for twinning on (100). It was thus concluded that so-called "pods" arose from particular orientations of the "star" structures, the plate-like stars being oriented more or less perpendicular to the support film, lying on either their (100) or (002) faces. The confused diffraction patterns would then arise from the tilting of the crystals with respect to the electron beam.

In all observed cases, the "pods" appeared more electron-dense than the "stars", implying a greater thickness, the direction of the electron beam. This lends support to the concept that the "pods" may be stars which are lying end-on.

Twinning /

Twinning, both in natural baddeleyite and in synthetic ZrO_2 has been long known and several authors have discussed it in detail. As in the present study of monoclinic hydrous zirconia, the twinning is nearly always on the (100), to the extent that very few untwinned crystals are found.

The size distribution of the "stars" (and "pods") was not changed by prolonged reflux of several months. Furthermore, variations in concentration of the initial zirconyl chloride solution (from 0.05 M to 0.5 M) did not in any way alter the dimension or appearance of the final crystalline hydrous zirconia and it is concluded that the size range described here must apply to the terminal stages of crystal growth, over a wide range of concentration.

(iv) Tetragonal zirconia. Amorphous zirconia, prepared by refluxing a 0.5 M solution of zirconyl chloride, was mounted on a Silica film and examined in the electron microscope. A typical sample from a solution refluxed for two hours, is shown in Plate 21. At 320°C there was evidence of decomposition occurring in the small crystallites present. The amorphous zirconia did not, however, crystallize until the temperature was raised to 730°C, when there was evidence of extensive crystallization taking place, the area corresponding to Plate 21 being shown in Plate 22. The polycrystalline electron diffraction pattern as shown in Plate 23 consisted of smooth rings. These were calibrated against thallous chloride, and again the variation of camera constant was taken into account, in an attempt to resolve whether cubic, or tetragonal zirconia was in fact present. The spacings measured are compared with literature values for both the cubic and tetragonal phases of ZrO_2.

Table 17.

/ -

PLATE 21

Amorphous zirconia obtained
by refluxing a zirconyl
chloride solution for two hours.
Magnification: 100,000X

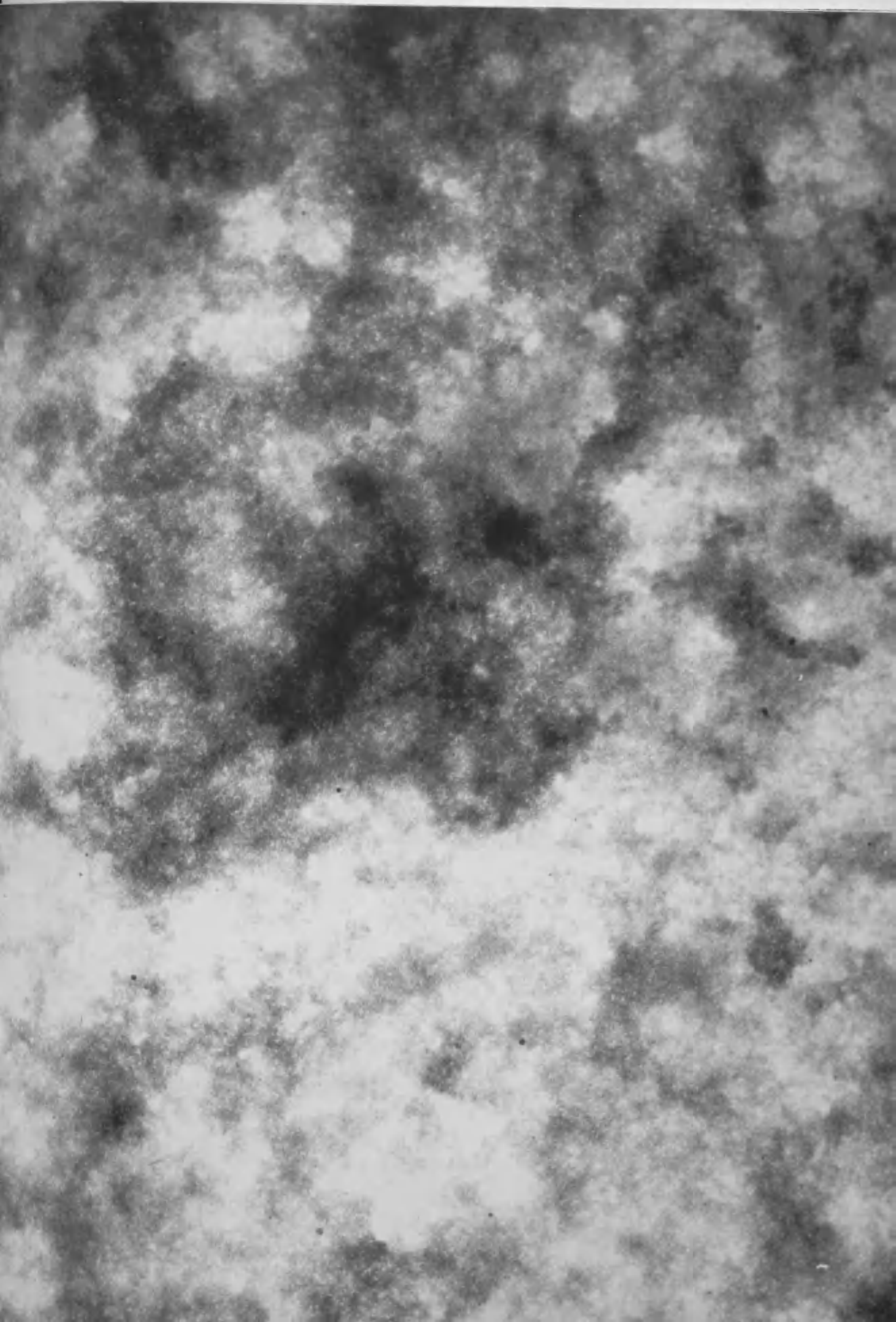

PLATE 22

Area corresponding to that shown in Plate 18, after heating to 730°C.
Magnification: 100,000X

PLATE 23

Electron Diffraction pattern
for crystalline zirconia at
730°C, as shown in Plate 19.

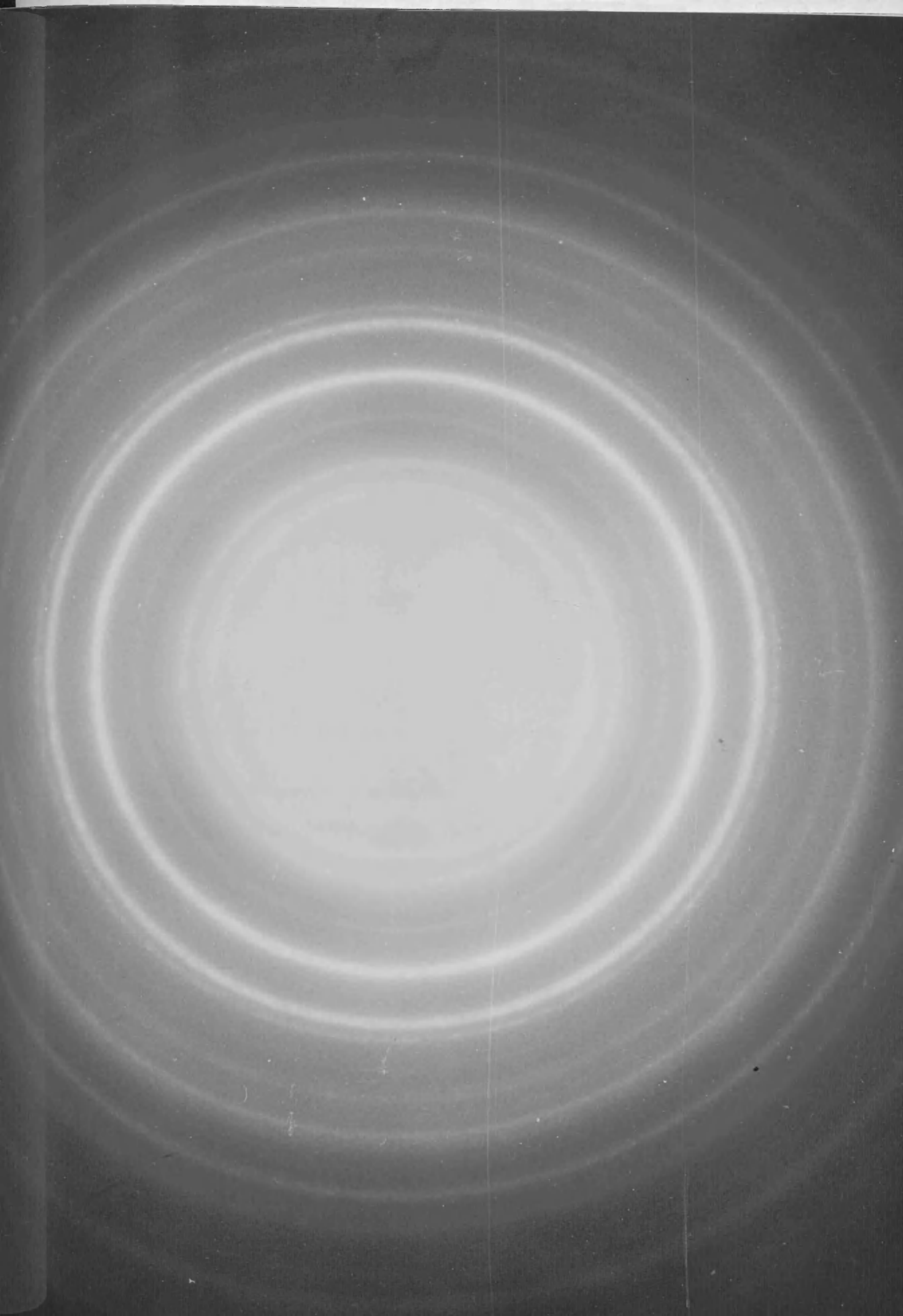

/ -

d (measured)	d (cubic ZrO_2)	d (tetragonal ZrO_2)
2.91 Å	2.92	2.95
2.55	2.53	2.58
		2.54
2.09	-	-
1.80	1.80	1.80
1.54	1.53	1.55
		1.53
1.47	1.46	1.47
1.36	-	-
1.29		1.29
1.26	1.27	1.27
1.22	-	-
1.17	1.16	1.16
1.04	1.03	1.04

(Calculated)

There is close agreement between the measured spacings and those of the cubic and tetragonal phases. Two rings, corresponding to the (004) and (400) reflections of the tetragonal phase, are only just resolved and this is taken as evidence for tetragonal zirconia being the phase present. The two other sets of doublets, corresponding to the (002), (200) and (113), (311) reflections are presumably masked by the width of the electron diffraction rings themselves.

Three of the spacings measured did not correspond to any of the ZrO_2 spacings listed. These spacings correspond to zirconium orthosilicate, which is the mineral Zircon, as shown in Table 18.

Table 18.

/ -

/ -

d (measured)	d ($ZrSiO_4$) *
2.09 Å	2.07
1.36	1.36
1.22	1.25 1.19

* N.B.S. Circular (1955)

By combining tables 17 and 18 it may be seen than many of the observed spacings which have been ascribed to tetragonal (or cubic) ZrO_2 also agree with those of $ZrSiO_4$, as shown below:-

Table 19.

d (measured)	d ($ZrSiO_4$)	d (tetragonal ZrO_2)
2.91 Å	-	2.95
2.55	2.52	2.58 2.54
2.09	2.07	-
1.80	-	1.80
1.54	1.55	1.55 1.53
1.47	1.48	1.47
1.36	1.36	-
1.29	1.29	1.29
1.26	1.26	1.27
1.22	1.25 1.19	-
1.17	1.17	1.16
1.04	1.04	1.04

From this it is concluded that the mineral Zircon is formed, by the thermally induced interaction of the zirconia with the silica support film. This also explains the "extra" lines mentioned earlier.

Attack of silica has been noted by other workers, particularly in experiments involving thermal ageing of oxides or hydroxides in silica vessels. Thus thorium silicate was made by Prasad, Beasley and Milligan (1967) and Bermann (1955) while Marshall, Gill and Slusher (1957, 1963) prepared a hydrate of uranium silicate. It has also been found by Baird (1970) that hot solutions of magnesium hydroxide react with silica flasks forming the clay mineral Hectcrite. In the present study, however, no attack of silica flasks by refluxing zirconia was detected.

The main points emerging from this section are the following:-

(i) Amorphous zirconia is formed by ammonia precipitation, and also by refluxing zirconyl chloride solutions. The two compounds thus prepared appear to be different.

(ii) By heating amorphous zirconia prepared either by precipitation or by reflux, the tetragonal phase is formed. This transformation was observed in the electron microscope.

(iii) Monoclinic zirconia is formed by refluxing amorphous zirconia, or zirconyl chloride solutions. The crystallites are well-defined and possess narrow size distributions, particularly for the material formed by reflux of zirconyl chloride. The crystal growth terminates in a relatively short time, with a particle size of approximately 650 - 700 Å regardless of concentration.

(iv) /

(iv) Zirconia reacts with a silica support film when heated, forming Zircon.

ZIRCONIA: HIGH RESOLUTION

In the high resolution study of zirconia, chrysotile asbestos filaments were used as a supporting mesh for the colloid particles, the numerous advantages in their use being discussed in Part 2 of this thesis. However, it was found that a drop of colloid, when evaporated on to a chrysotile network, produced an extremely thick deposit in some areas, and no deposit in others. Furthermore, the variety of artifacts due to drying down of the colloid, as mentioned earlier, made this preparation technique unsuitable for the system under investigation. It was found that a glass atomiser could produce a fairly even deposit on a carbon film, a gold hydrosol being used in preliminary tests. Droplets as small as a few microns across were produced in this way, and the use of the atomiser was considered an additional advantage in that evaporation was extremely rapid for such small droplets. In this way drying-down artifacts were minimized, and by using the spray in conjunction with a chrysotile network, it was possible to obtain specimens in which the colloidal material was suspended evenly between the fibres.

Refluxing a 0.055 M zirconyl chloride solution yielded the following results, the specimens being prepared using the spray technique described above. The chrysotile fibres were obtained from Valmalenco.

a) Fresh solution: A freshly prepared solution gave no observable deposit when sprayed on to the fibres. From this it was concluded that there had been no extensive polymerization beyond the tetramer $\left[Zr\,(OH)_2 4H_2O \right]_4^{8+}$. The pH of the solution was however, 1.54, implying that hydrolysis had in fact gone beyond this stage.

b) Two hour reflux: A sample prepared as before showed extensive areas of thin, coherent films suspended between chrysotile fibres, as shown in Plate 24. Structural features may be compared with the same area, photographed under slightly different focussing conditions, in Plates 25 and 26, which form a focal series. These films showed reproducible features in the 7 - 10 Å size range and, although no shapes /

PLATE 24

Zirconia, obtained by two hour
reflux of zirconyl chloride:
suspended between chrysotile fibres.
Magnification: 2,000,000X

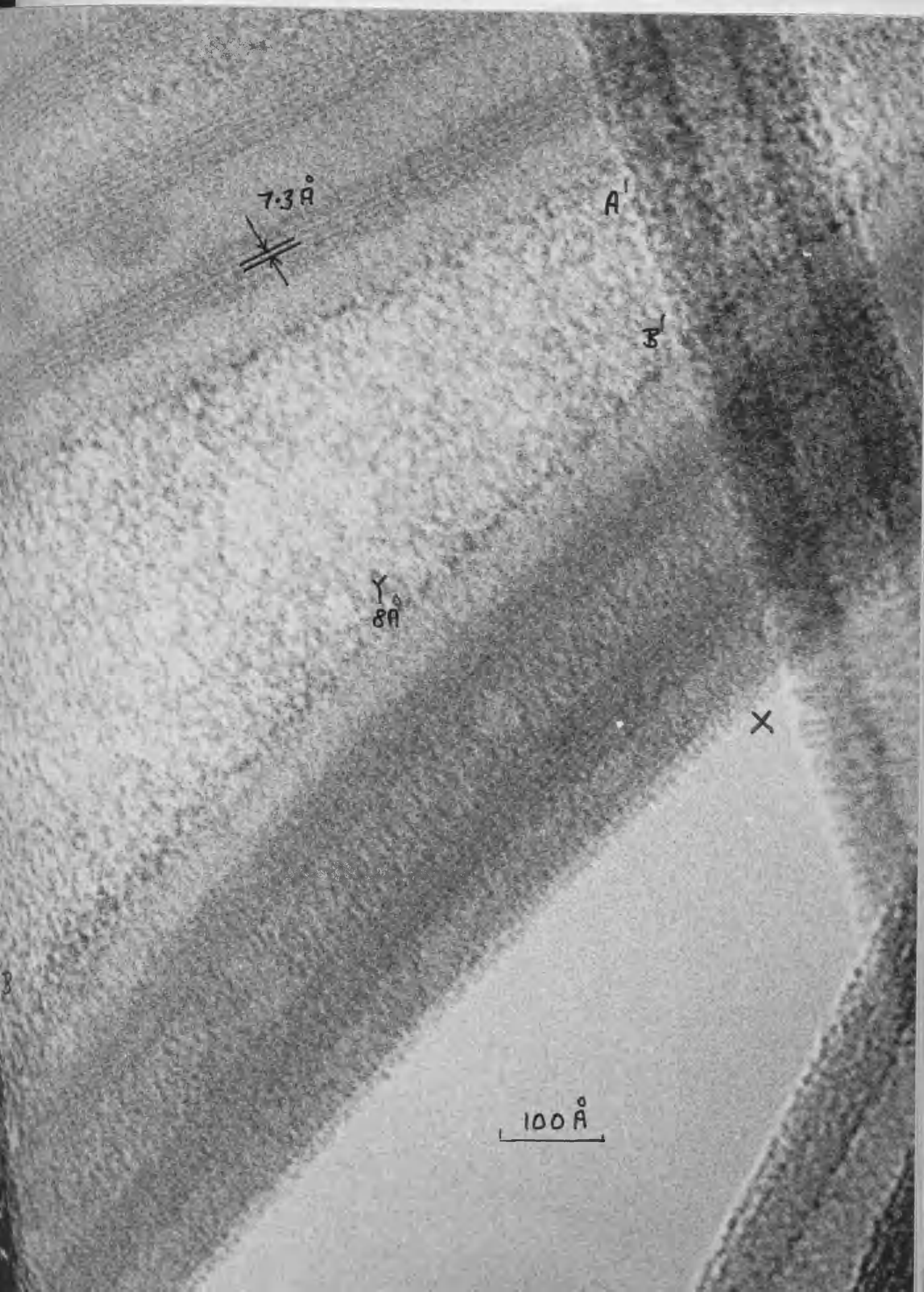
7·3 Å
A'
B'
Y
8Å
X
B
100 Å

PLATE 25

The same area as that shown in Plate 24, taken with objective lens underfocussed.
Magnification: 2,000,000X

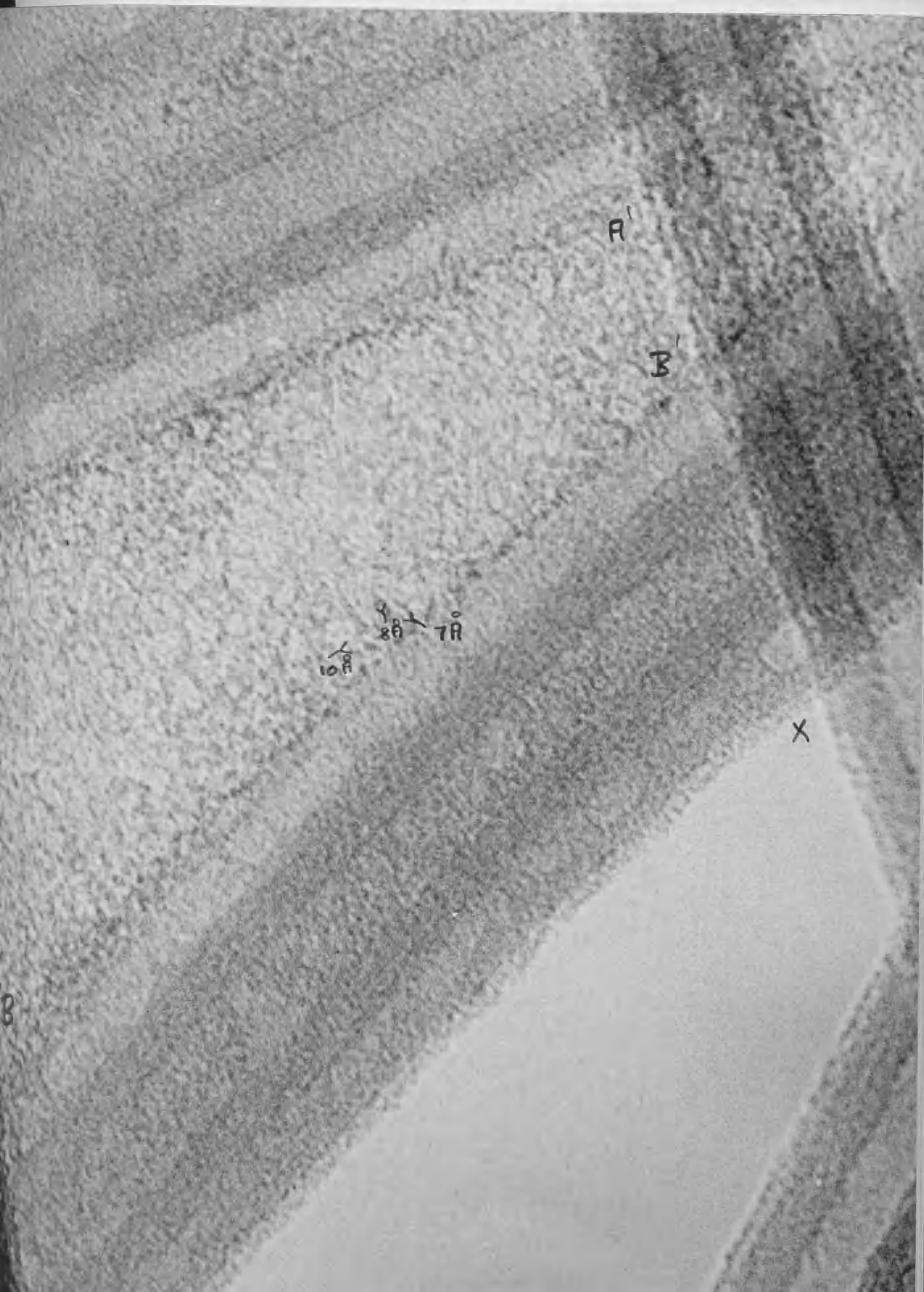
A'
B'
8Å
7Å
10Å
X
B

PLATE 26

The same area as shown in previous two plates, with different focus.

Magnification: 2,000,000X

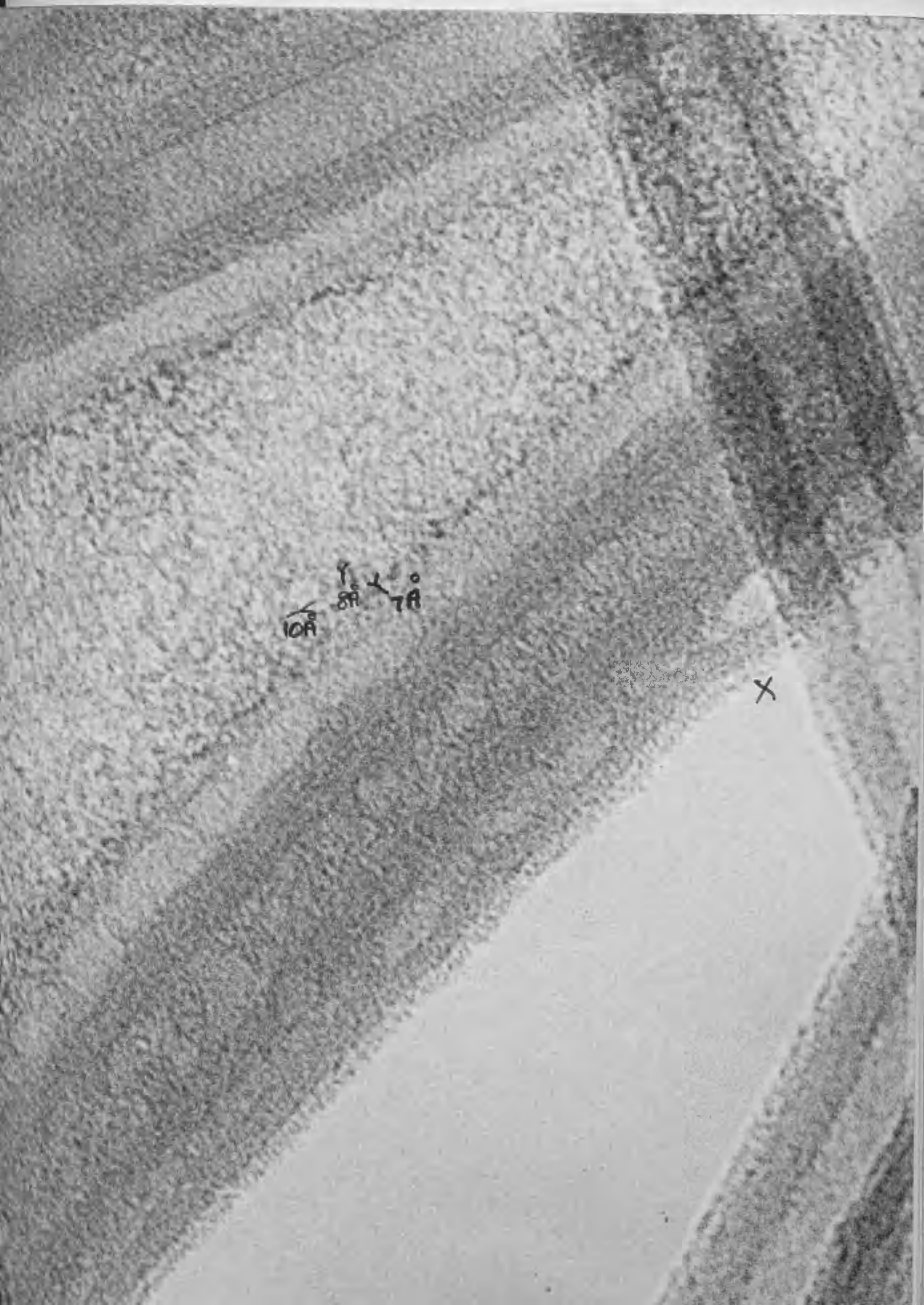
10Å
8Å
7Å
X

PLATE 27

Amorphous zirconia, after
four hours reflux, suspended
between chrysotile fibres.
Magnification: 2,000,000X

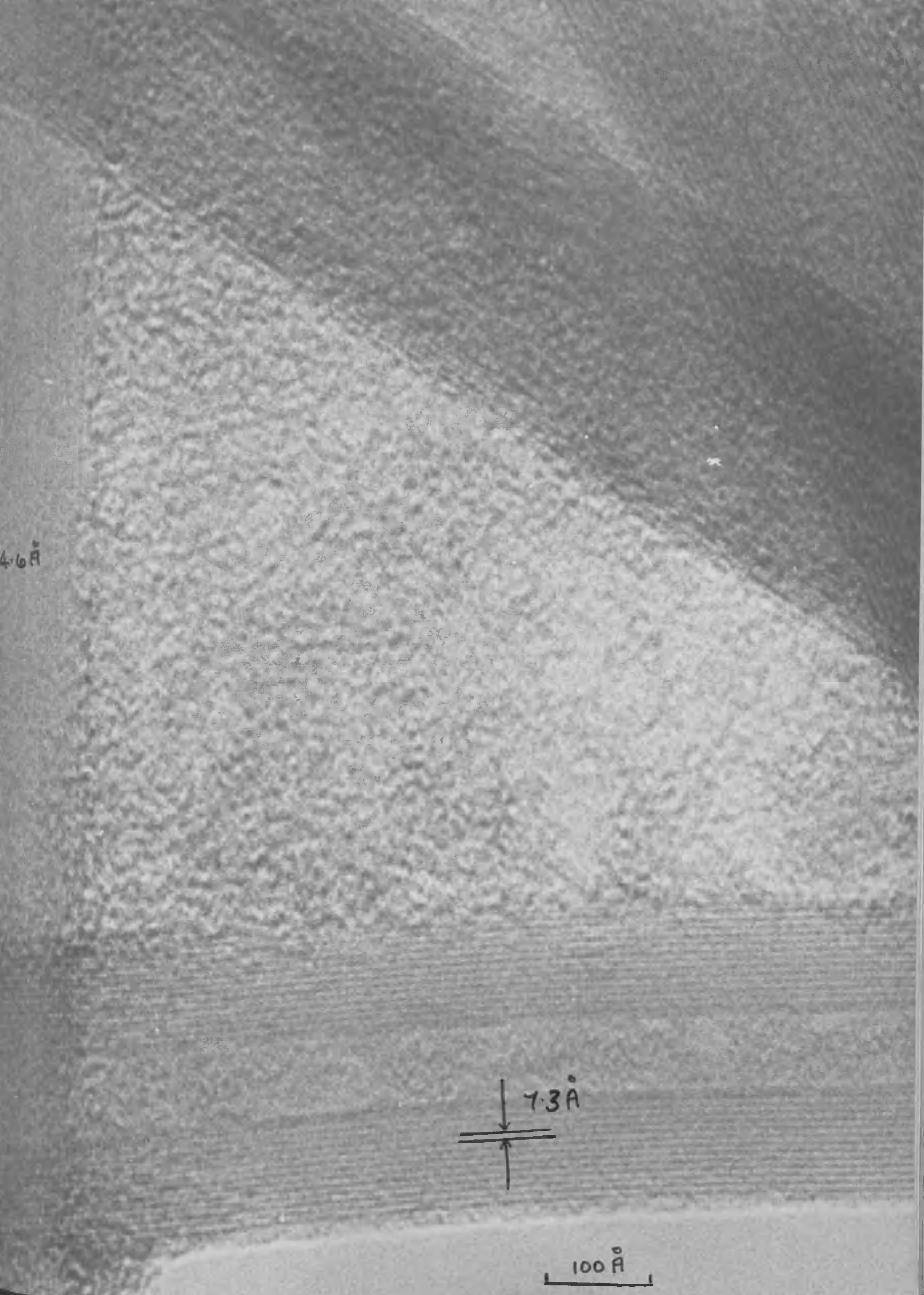
4·6Å
7·3Å
100 Å

PLATE 28

Same area of amorphous zirconia, with focussing altered.
Magnification: 2,000,000X

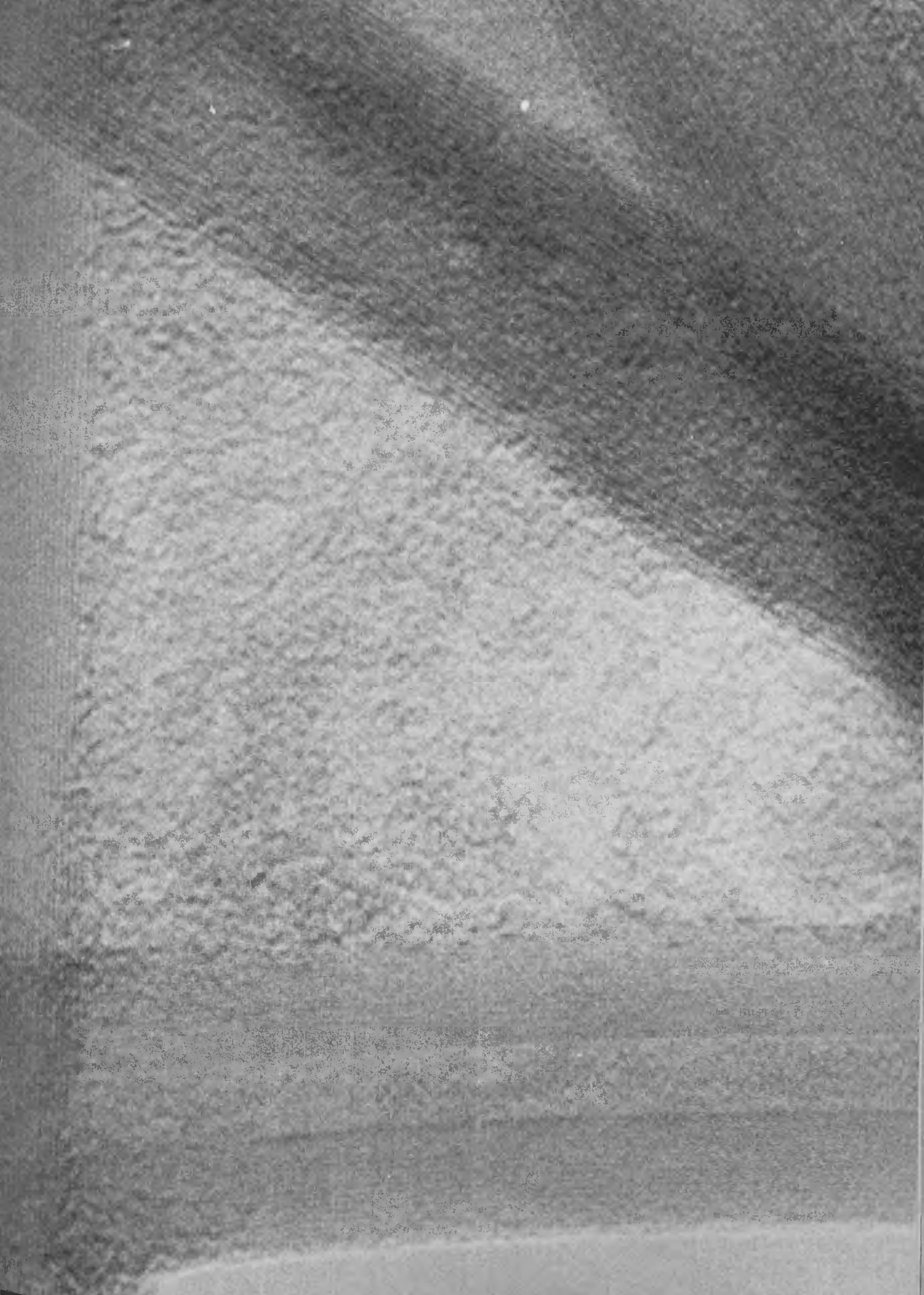

/ shapes could be distinguished, the dimensions of these structural units, based on the separation between adjacent centres, were consistent with those of the cyclic tetramer already mentioned. Since a 50 thin-foil objective aperture was used, phase contrast effects are not greatly enhanced, although well-defined fringe profiles corresponding to the (001) lattice planes in the chrysotile fibres, are visible and may be used as an internal calibration for accurate measurements. A concentration of dense particles is seen along the edges of the chrysotile fibres in contact with the zirconia film, at AA' and BB' in Plate 24. Since the outer layer of the cylindrical lattice is composed entirely of hydroxyl groups, there will be a high attraction towards positively charged species. Thus it is reasonable to suggest that these dense particles, approximately 8 - 10 Å in size, are positively charged, and are probably tetramers, or aggregates. The pH of the solution had dropped to 1.22, indicating that further hydrolysis had taken place.

c) Four hour reflux: The appearance of the sheets of zirconia, as shown in Plates 27 and 28, is similar to that observed after two hours and, since the pH was virtually unchanged (1.21) it was evident that little further hydrolysis had taken place. There was less evidence of any concentration of the zirconia along the outer edges of the supporting fibres. This could be interpreted in terms of increased cross-linking, resulting in the small aggregates, or tetramers becoming included in larger sheets.

d) 8½ hour reflux: After six hours the solution showed signs of opalescence, which after 8½ hours was quite distinct. This was taken to indicate growth of particles in the solution. A specimen examined in the microscope showed amorphous films suspended between chrysotile fibres. In specific areas of the sheets a pronounced darkening of the sheets was evident, as at 'A' in Plates 29 and 30. This was taken to represent an increase in the thickness of the film in these regions. In the other parts of the films, structural features /

PLATE 29

Amorphous zirconia after 8½
hours reflux, showing darkening
in specific areas, as at 'A'.
Magnification: 2,000,000X

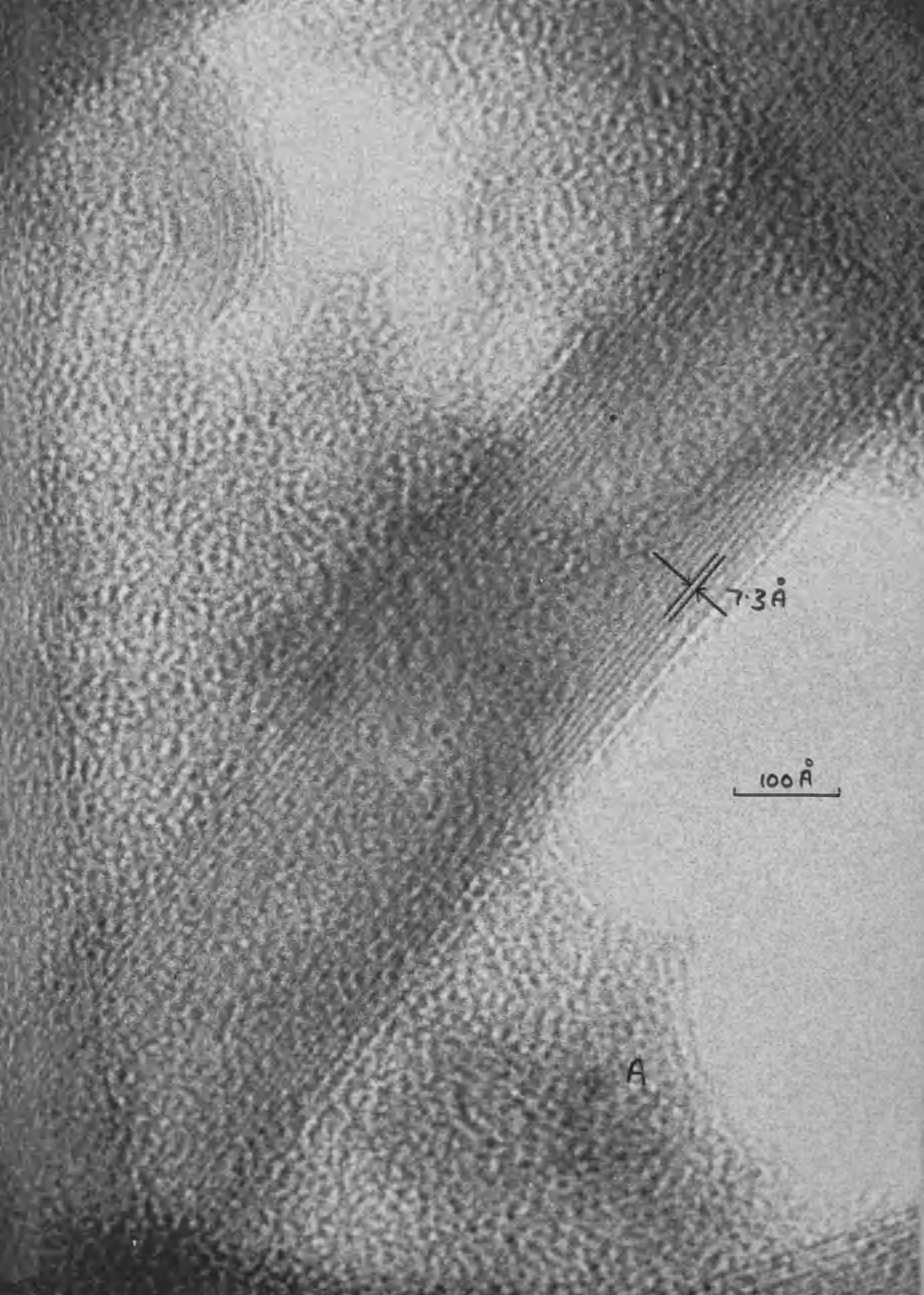
7·3Å
100Å
A

PLATE 30

Amorphous zirconia, as shown
in Plate 29, with the objective
lens overfocussed.
Magnification: 2,000,000X

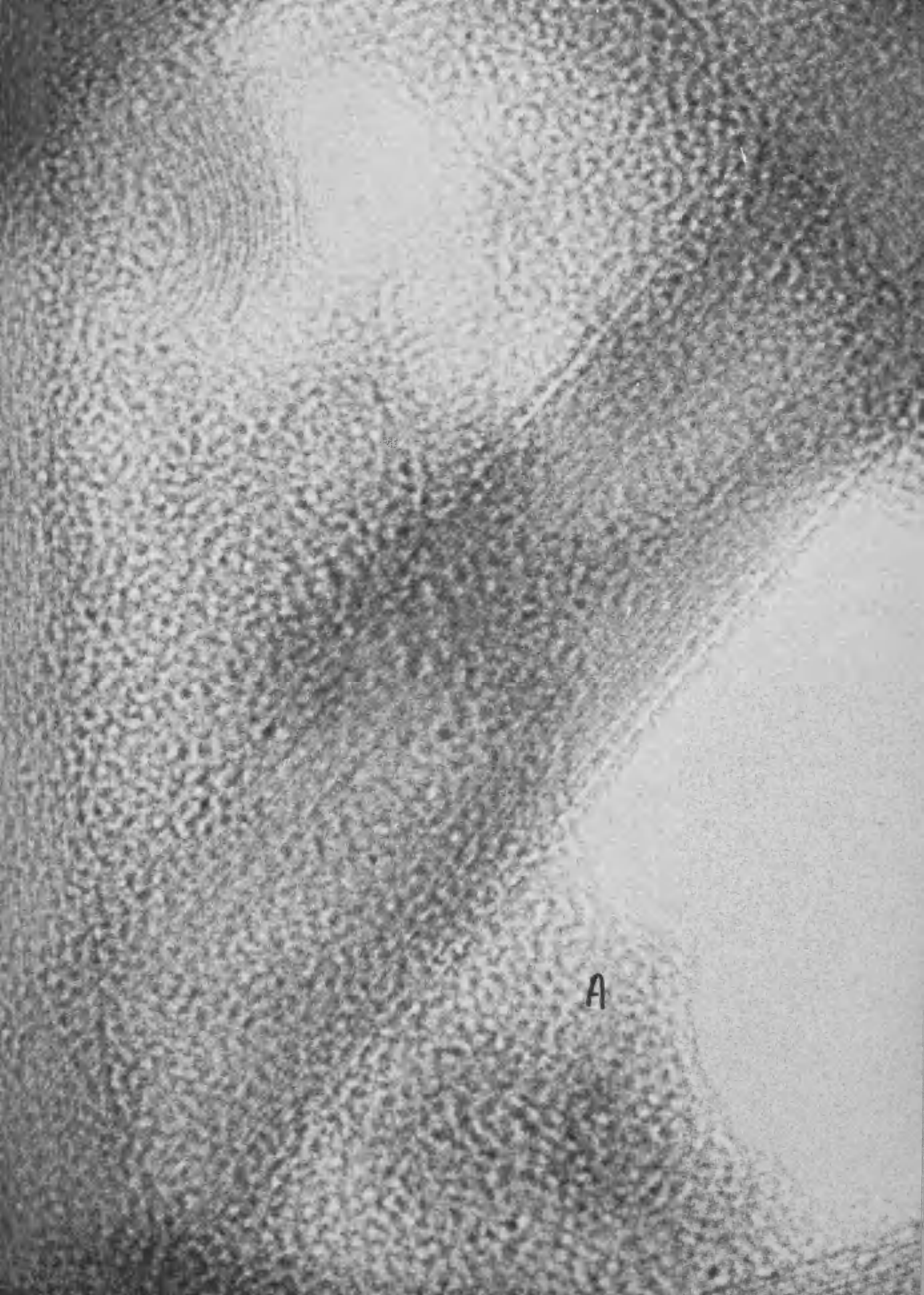
A

/ features similar to those observed in earlier samples, were present. The pH at this time was 1.21, indicating that the hydrolysis was extremely slow.

e) 16 hour reflux: After 16 hours the solution had become milky, and further particle growth had obviously taken place. Distinct crystallites were observed in a matrix of amorphous material, as at "X" in Plate 31. These dense particles were shown already to be monoclinic zirconia, and after 16 hours their shapes were becoming fairly well defined.

f) 25 hour reflux: By 25 hours the crystallites were recognisable as being the same as those observed earlier under low resolution. There was now little trace of the amorphous zirconia and it was concluded that the transformation into crystalline zirconia was more or less complete. A typical "star" is shown at "S" in Plate 32, the irregular outline being clearly distinguishable. A "pod", or a "star" which is parallel to the beam, is shown between two chrysatile fibres in Plate 33, where the contrast of the broad striations is enhanced by a degree of under-focus. The width of the striations, about 30 Å, may in this micrograph be compared with the fringe profile corresponding to the (001) lattice planes of chrysotile, with the 7.3 Å spacing.

On several of the crystallites fringe patterns were resolved, with a spacing of approximately 5 Å. By internal calibration of these fringes against those of the chrysotile lattice images it was possible to measure these spacings with reasonable accuracy. Thus the fringes at 'A' in Plate 34 were shown to have an average spacing of 4.9 Å. These striations were reproducible in successive plates in a focal series, as Plate 35 illustrates. In Plate 32, the fringes at 'B' had an average spacing of 5.06 Å, while those at 'C' in Plate 36 were shown to be 5.02 Å apart.

It was not possible to correlate these fringe patterns with the edges of the crystals, in that the edges were in most cases obscured by other /

PLATE 31

Growth of crystalline zirconia
in a matrix of amorphous zirconia,
after 16 hour reflux.
Magnification: 2,000,000X

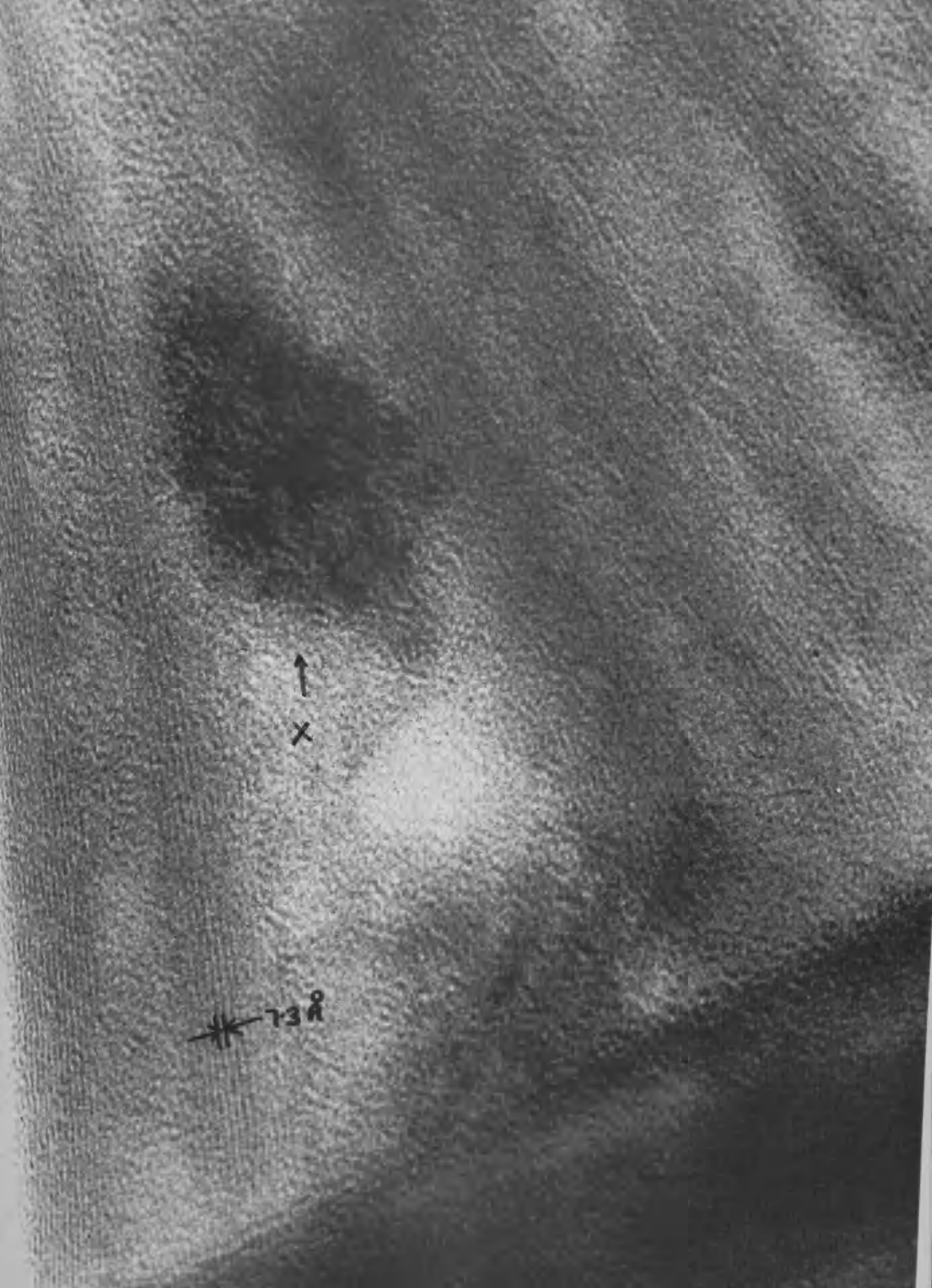
×
7·3 Å

PLATE 32

Crystallites of monoclinic zirconia on chrysotile, after crystal growth has ceased. This was found after 25 hours of reflux. Note striations of 5.06 Å, at "B".

Magnification: 1,600,000X

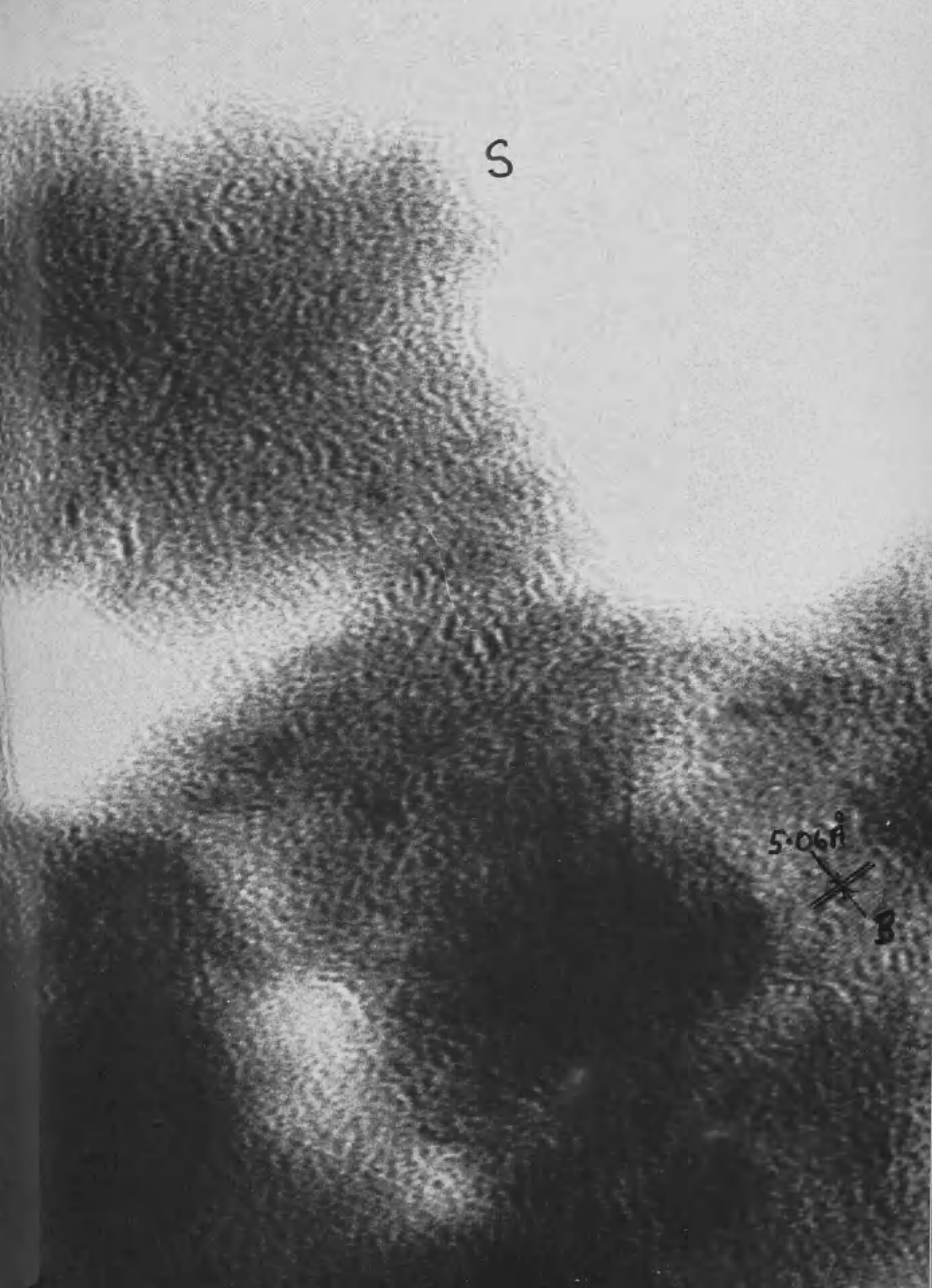
S
5·06Å
B

PLATE 33

Monoclinic zirconia. In this micrograph a "pod" is held between two chrysotile fibres.
Magnification: 2,240,000X

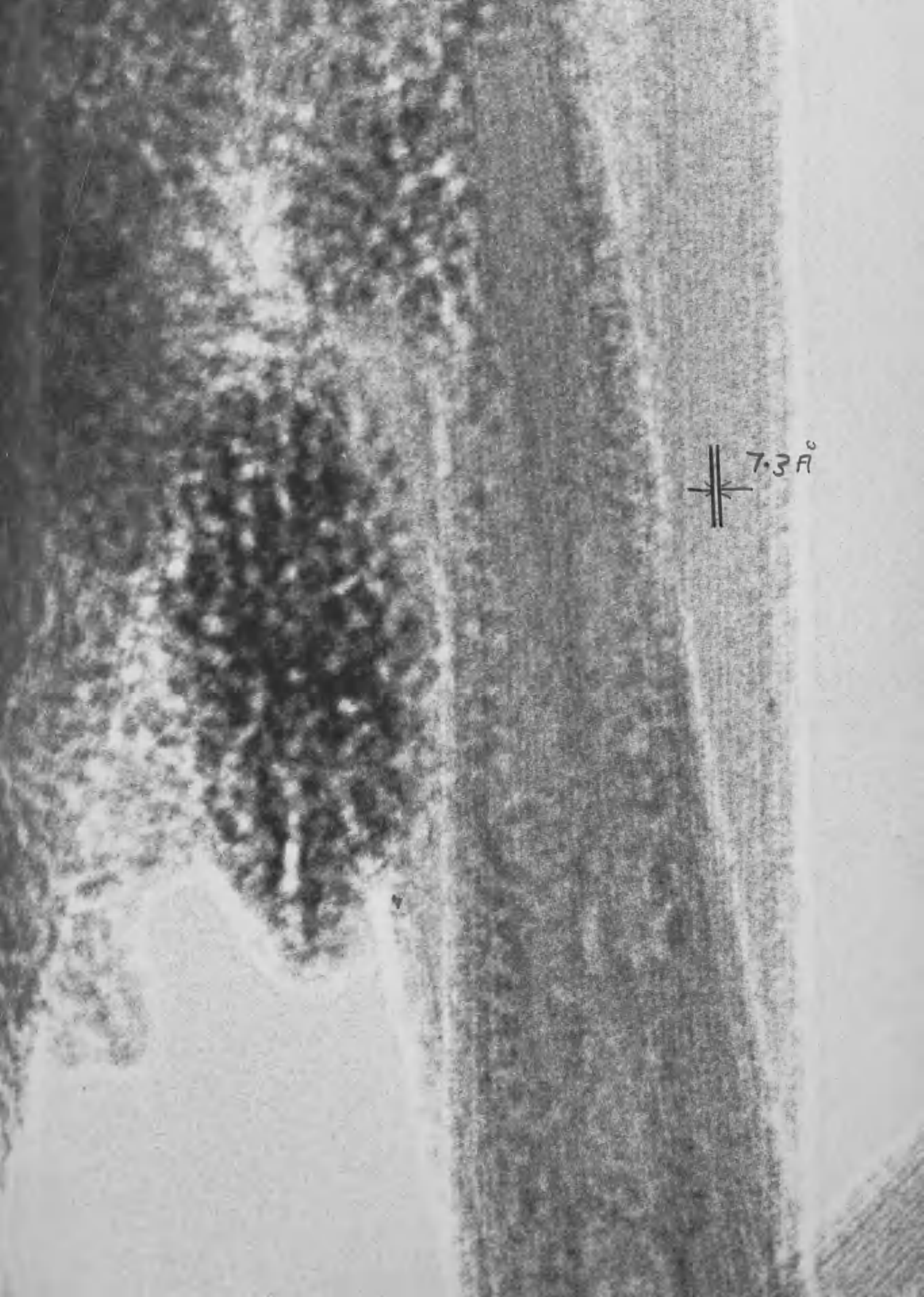
7·3 Å

PLATE 34

Flake of monoclinic zirconia,
on chrysotile, showing 4.9 Å
striations at "A".
Magnification: 2,640,000X

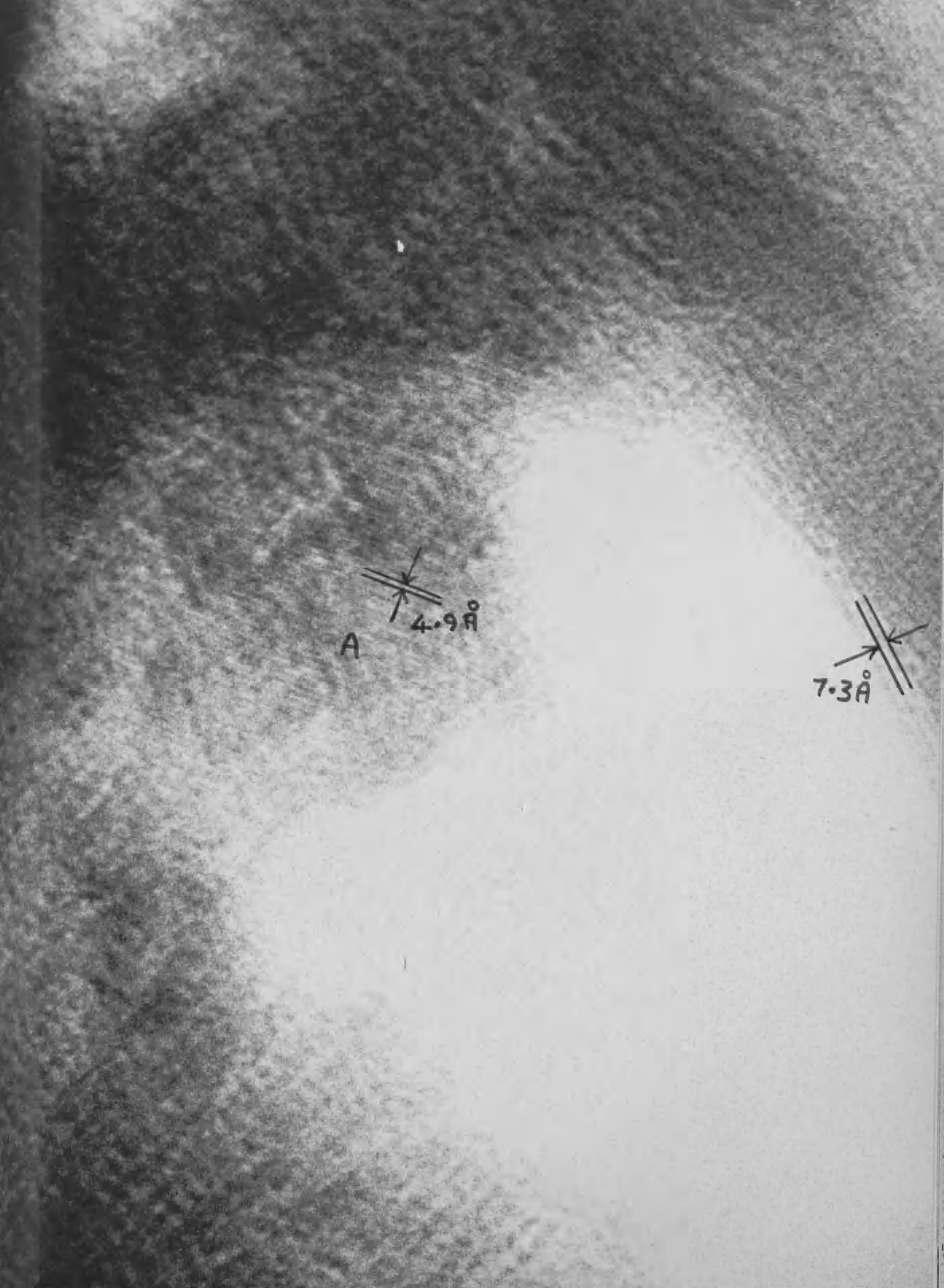
4·9Å
A
7·3Å

PLATE 35

The same area as shown in
Plate 35, under different
focus conditions.
Magnification: 2,640,000X

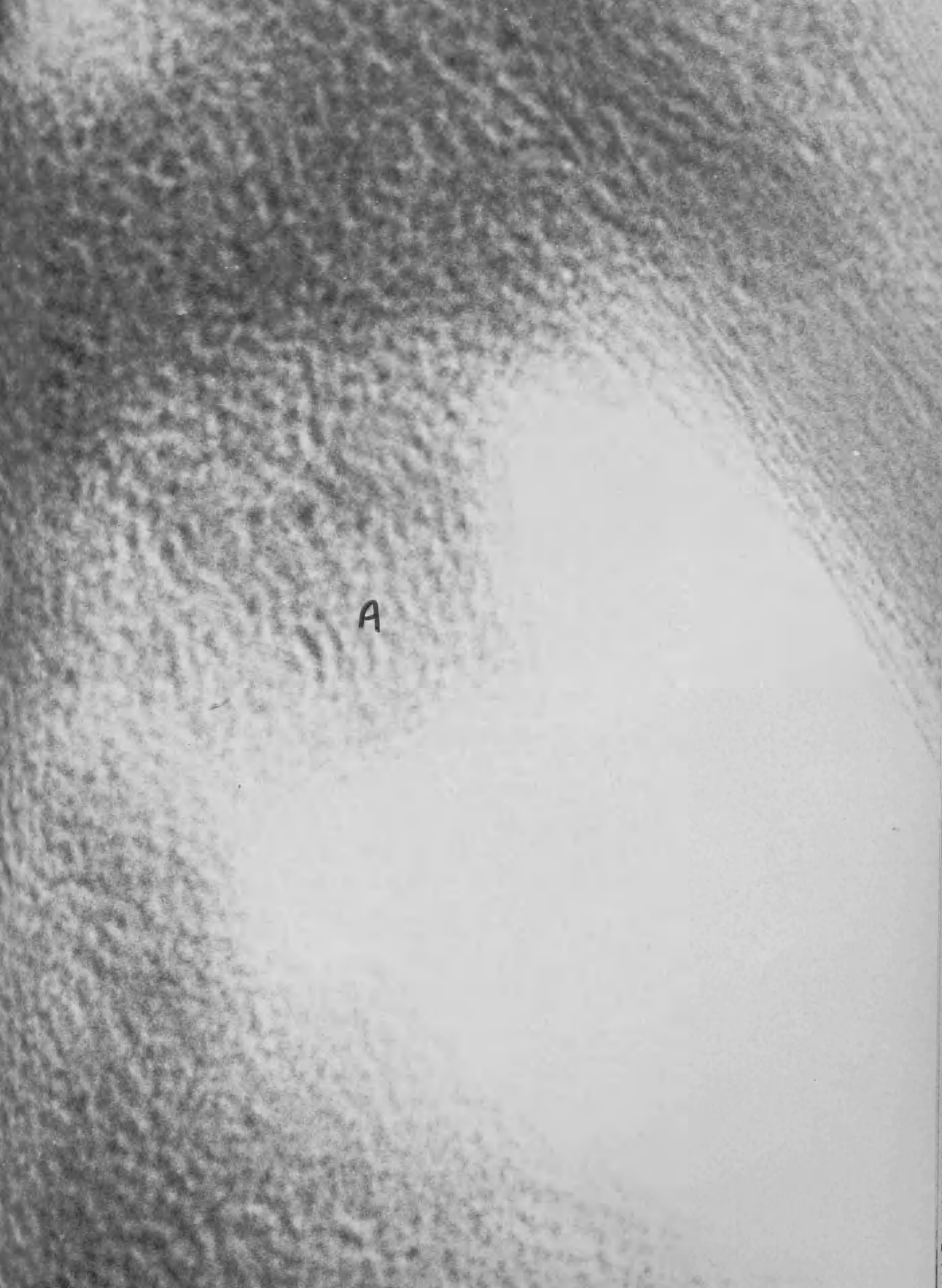
A

PLATE 36

Flakes of monoclinic zirconia,
supported by chrysotile fibres,
showing 5.02 Å striations at "C".
Magnification: 2,640,000X

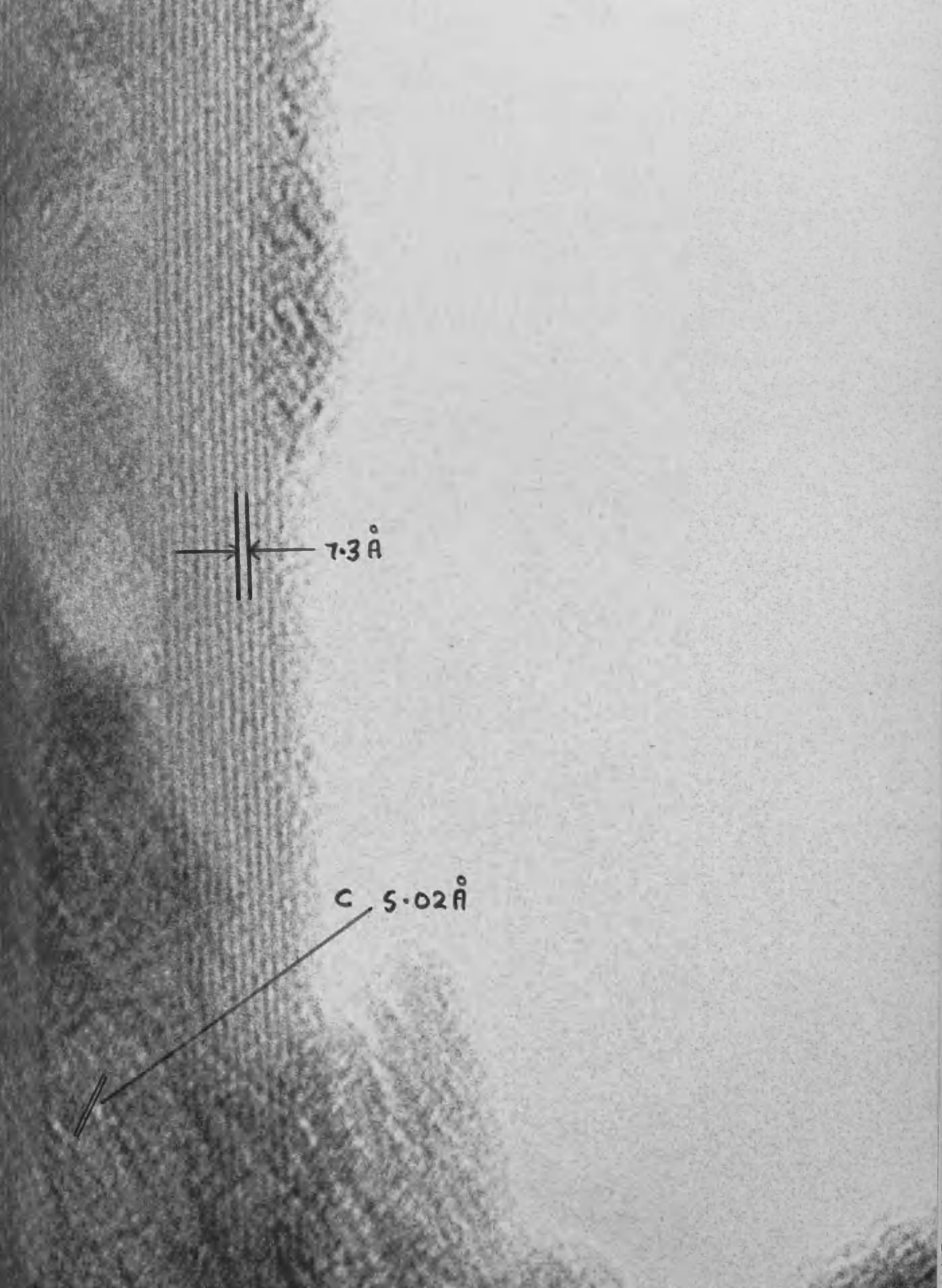
7·3 Å
c 5·02 Å

/ other crystals. Nevertheless, they correspond closely with the (100) d-spacing of monoclinic zirconia, which has the value 5.04 Å.

Prolonged reflux for periods of up to several months produced no further crystal growth and it was assumed that most, if not all, of the hydrolysis and oxolation had taken place within the first 25 hours, although the pH was 1.15 and not 1.00 as would have been appropriate for 0.055 M zirconyl chloride undergoing complete hydrolysis. If such a discrepancy is significant it is likely that there are residual water and hydroxyl molecules attached to the zirconia, as is the case with amorphous zirconia, with its ion exchange properties.

RESULTS

Nuclear Magnetic Resonance

Proton resonance signals were measured for colloid samples at various stages during the hydrolysis, and for various concentrations of Zr (IV). It was observed that the signals showed increasing broadening with time of reflux, until a constant value was attained. This maximum broadening varied directly with the concentration of Zr (IV). Figure 14 shows a resonance signal measured on distilled water. It can be seen that the signal from a fresh 0.05 M zirconyl chloride is very similar in appearance to this (figure 15). After prolonged reflux, the signal from the solution is slightly broader, as shown in figure 16. For comparison, a signal obtained from a 0.25 M solution after prolonged reflux, is shown in figure 17.

The results are summarized graphically in figure 18 where, for broad signals, the signal width at half the peak heigh, W ($\frac{1}{2}$), is plotted against the concentration of Zr (IV), and in figure 19 where W ($\frac{1}{2}$) is plotted against time of reflux, for constant Zr (IV) concentration.

As has already been discussed, signal broadening will occur when two "different" protons or molecules undergo exchange which is sufficiently slow not to be averaged out by the instrument, (but not so slow as to give rise to two separate signals). In the case of hydrous zirconia, the very marked broadening is consistent with the following:-

(a) Exchange between bulk water and water "trapped" in pores in the zirconia.

(b) Exchange between bulk water and water of solvation of Zr (IV).

(c) Exchange between bulk water and water held on other active sites on the zirconia.

(d) / -

(d) Proton exchange between bulk water and -OH sites on the surface. This may occur as follows:-

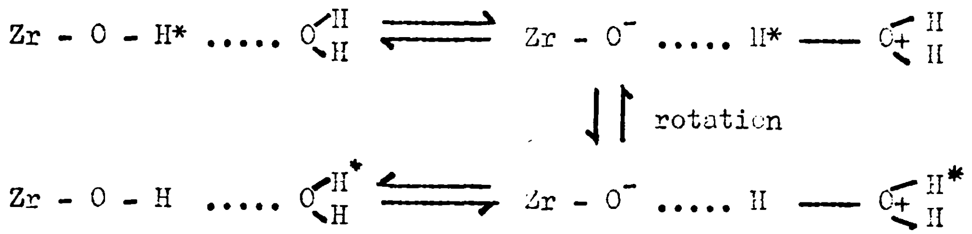

$$\begin{array}{ccc} \mathrm{Zr-O-H^{*}\cdots\cdots O<^{H}_{H}} & \rightleftharpoons & \mathrm{Zr-O^{-}\cdots\cdots H^{*}-\overset{+}{O}<^{H}_{H}} \\ & & \downarrow\uparrow\ \text{rotation} \\ \mathrm{Zr-O-H\cdots\cdots O<^{H^{*}}_{H}} & \rightleftharpoons & \mathrm{Zr-O^{-}\cdots\cdots H-\overset{+}{O}<^{H^{*}}_{H}} \end{array}$$

In highly acidic conditions this exchange will be extremely fast between bulk water and surface OH sites, and will result in a single sharp signal.

(e) Exchange between water in pores and OH sites. This may be sufficiently slow to give rise to some broadening of the proton signal.

(f) other proton exchange in the system.

Most of these explanations favour a porous material rather than "solid" particles.

A sample of the monoclinic zirconia was air-dried at 60°C and the dry powder examined by high resolution N.M.R. Had there been water present which was not tightly bound, it is possible that a resonance signal would have been observed. The absence of any signal merely showed that any water still present was quite rigidly bound to the zirconia, probably as coordination water.

An Infra-red spectrum of this solid confirmed the presence of water, two well defined, but broad peaks being visible, at 1620 and 3350 cm^{-1}. In the Infra-red spectrum of precipitated amorphous zirconia, absorption bands at 1620 and 3410 cm^{-1} were attributed respectively to H - O - H deformation and O - H stretching modes by Vivien et al (1970). From this and thermogravimetric evidence they concluded that the zirconia was a "hydrated hydroxy oxide", and it would appear from the I.R. /

/ I.R. spectrum of crystalline zirconia that the two materials are similar in constitution.

SURFACE AREA MEASUREMENT

Using the Sorptometer, a surface area of 143 m^2g^{-1} was found for monoclinic zirconia. This is comparable with surface areas of typical silica-alumina catalysts. Wu and Hall (1967) for instance quote the surface area of the commercial "Aerocat" as 433 m^2g^{-1}. Hightower, Gerberich and Hall (1967) measured the surface area of "fluorided alumina", in which some hydroxyls were replaced by F^- ions, as 143 m^2g^{-1}. AlF_3 on the other hand had a surface area of 6.3 m^2g^{-1}. Thus the surface area of the monoclinic zirconia is of the same order of magnitude as typical high-area catalysts supports. This could be due to either

(i) an extremely small particle size or

(ii) a porous structure for the zirconia.

It will be demonstrated in the following section that the observed particle sizes in crystalline zirconia are not consistent with such a high surface area unless the structure is porous.

FIGURE 14

Proton resonance signal obtained from distilled water.

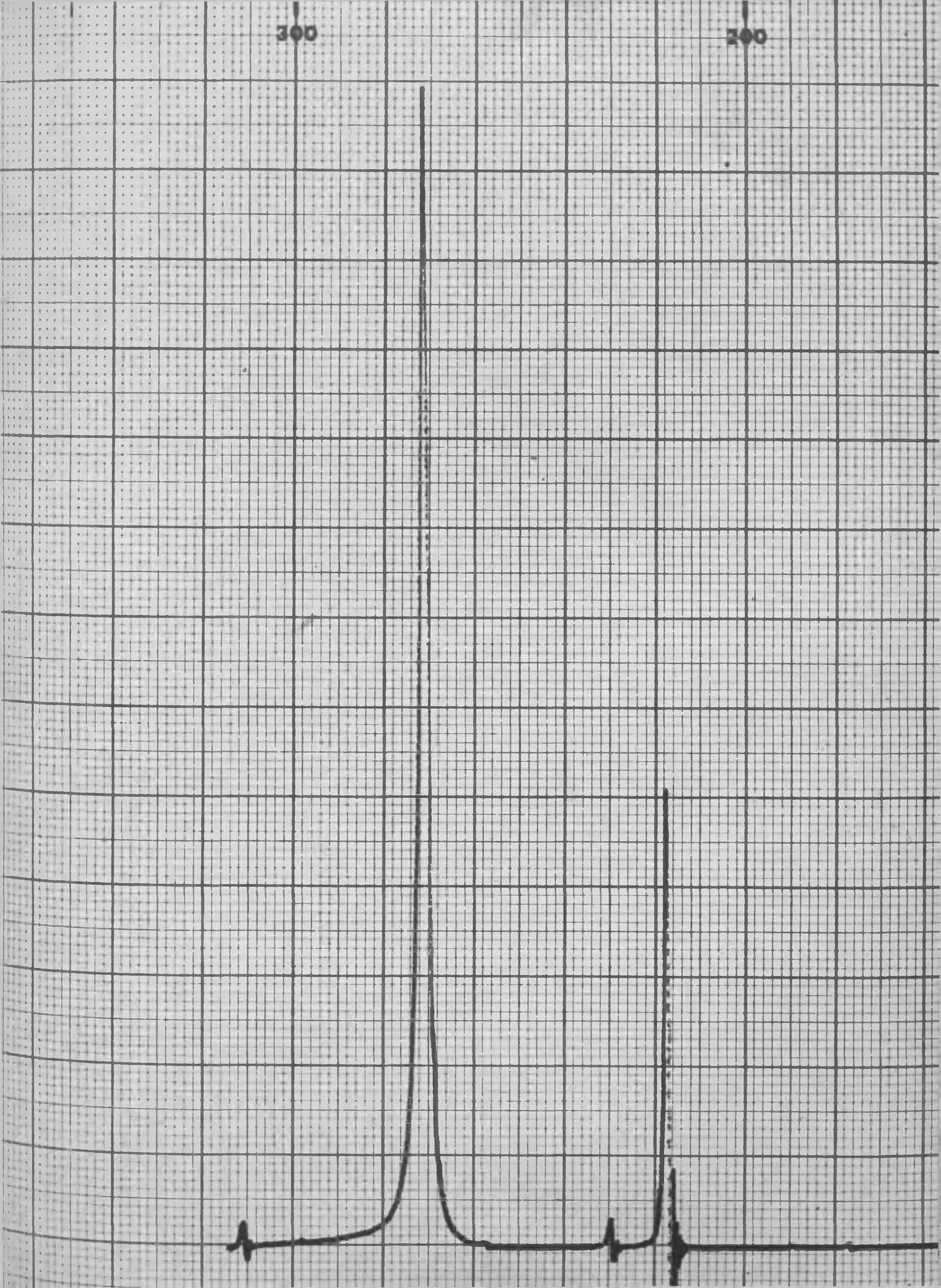
300
200

FIGURE 15

Proton resonance from fresh
0.05 M zirconyl chloride
solution.

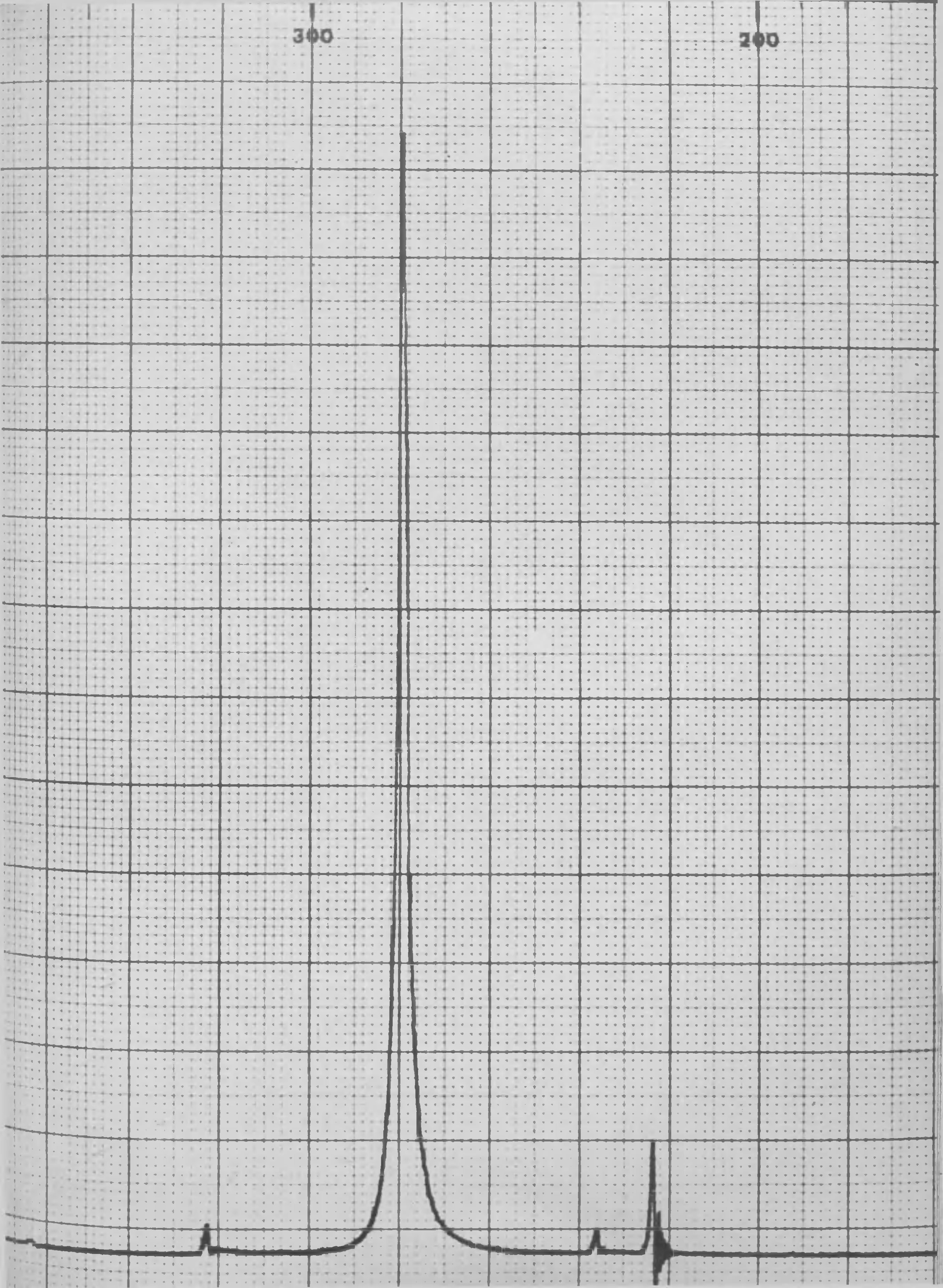
300
200

FIGURE 16

Proton resonance signal after prolonged reflux of 0.05 M zirconyl chloride.

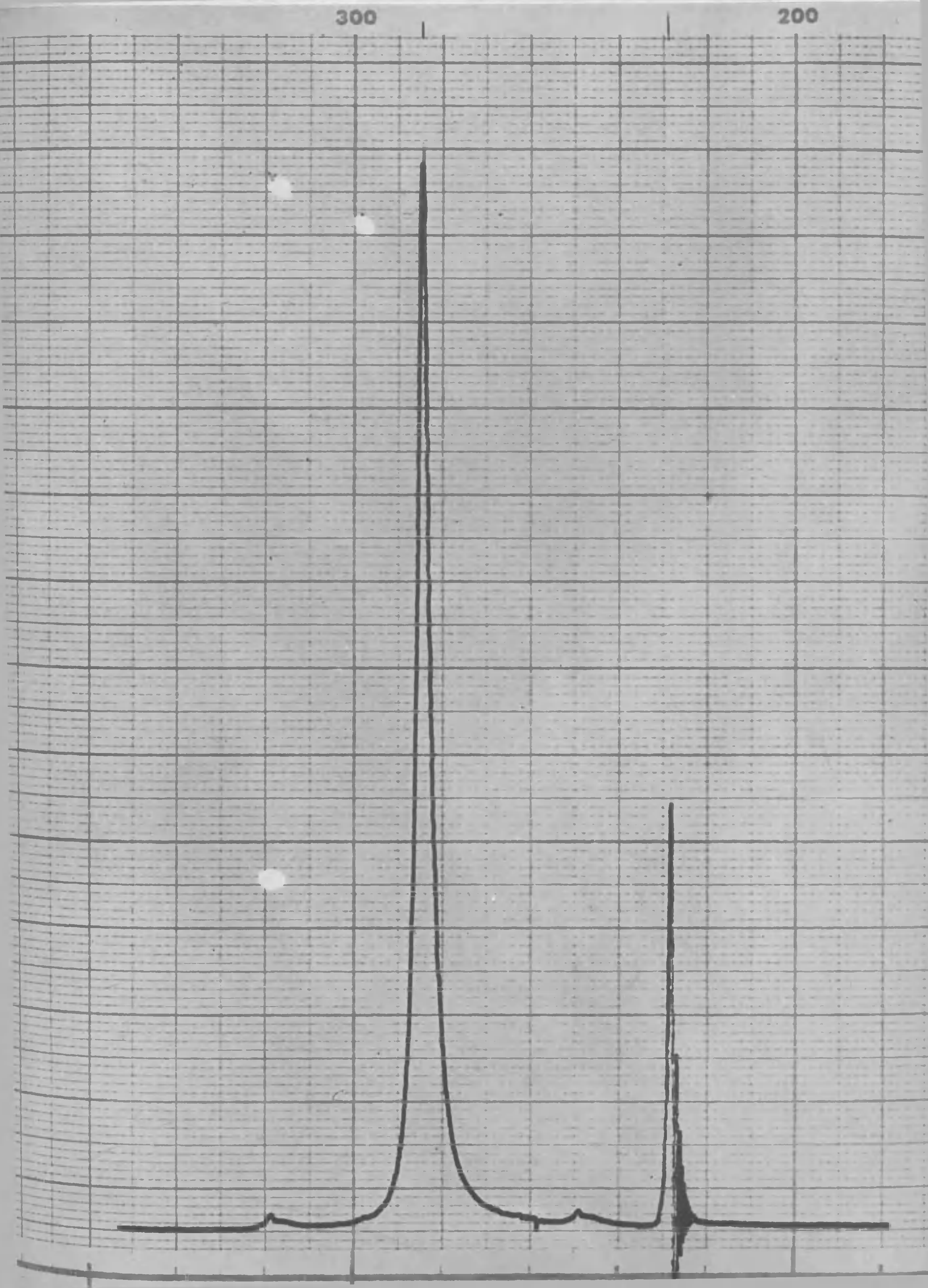
300
200

FIGURE 17

Proton resonance signal after prolonged reflux of 0.25 M zirconyl chloride.

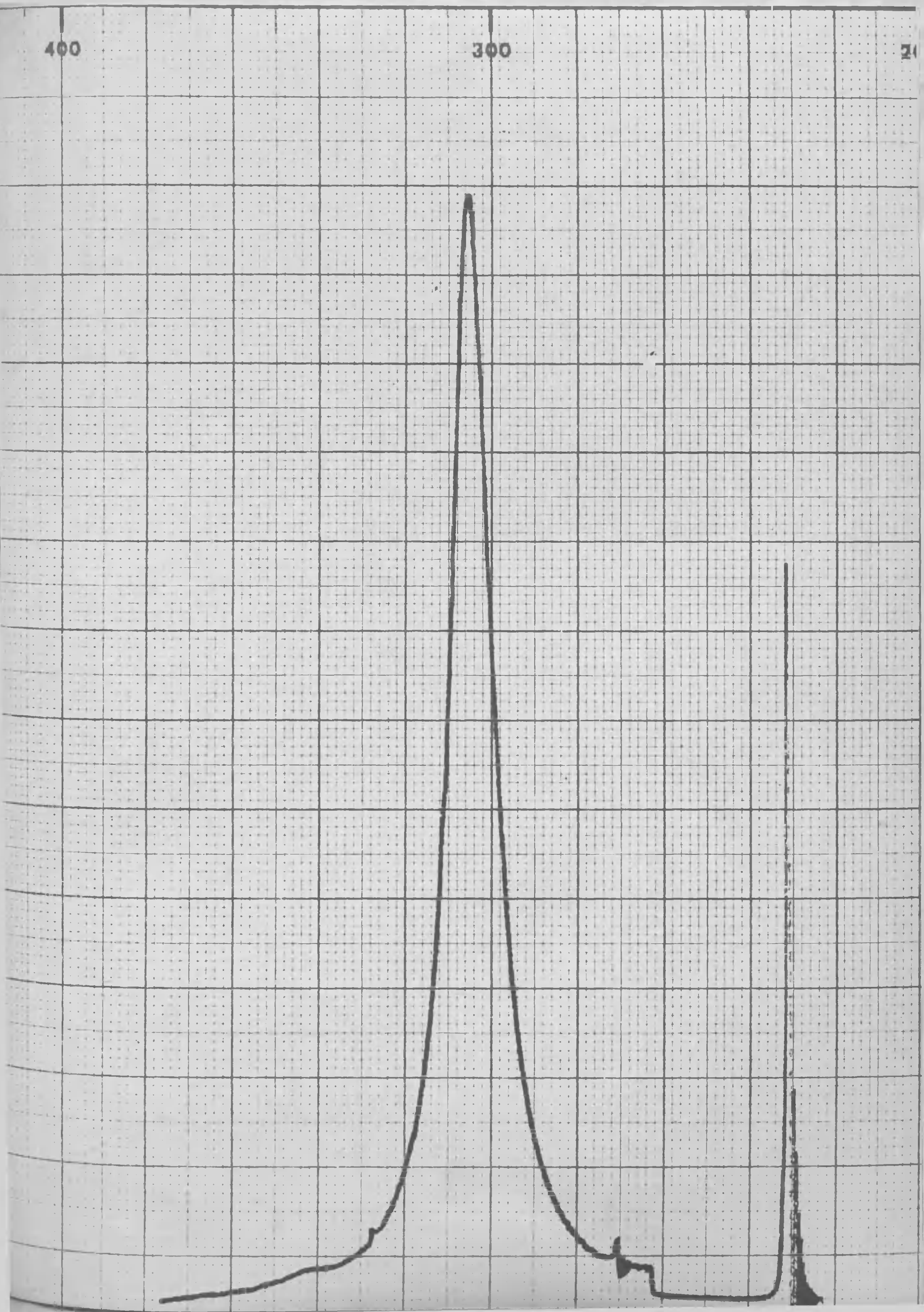
400
300
2

FIGURE 18

Variation of signal width with concentration of Zr (IV).

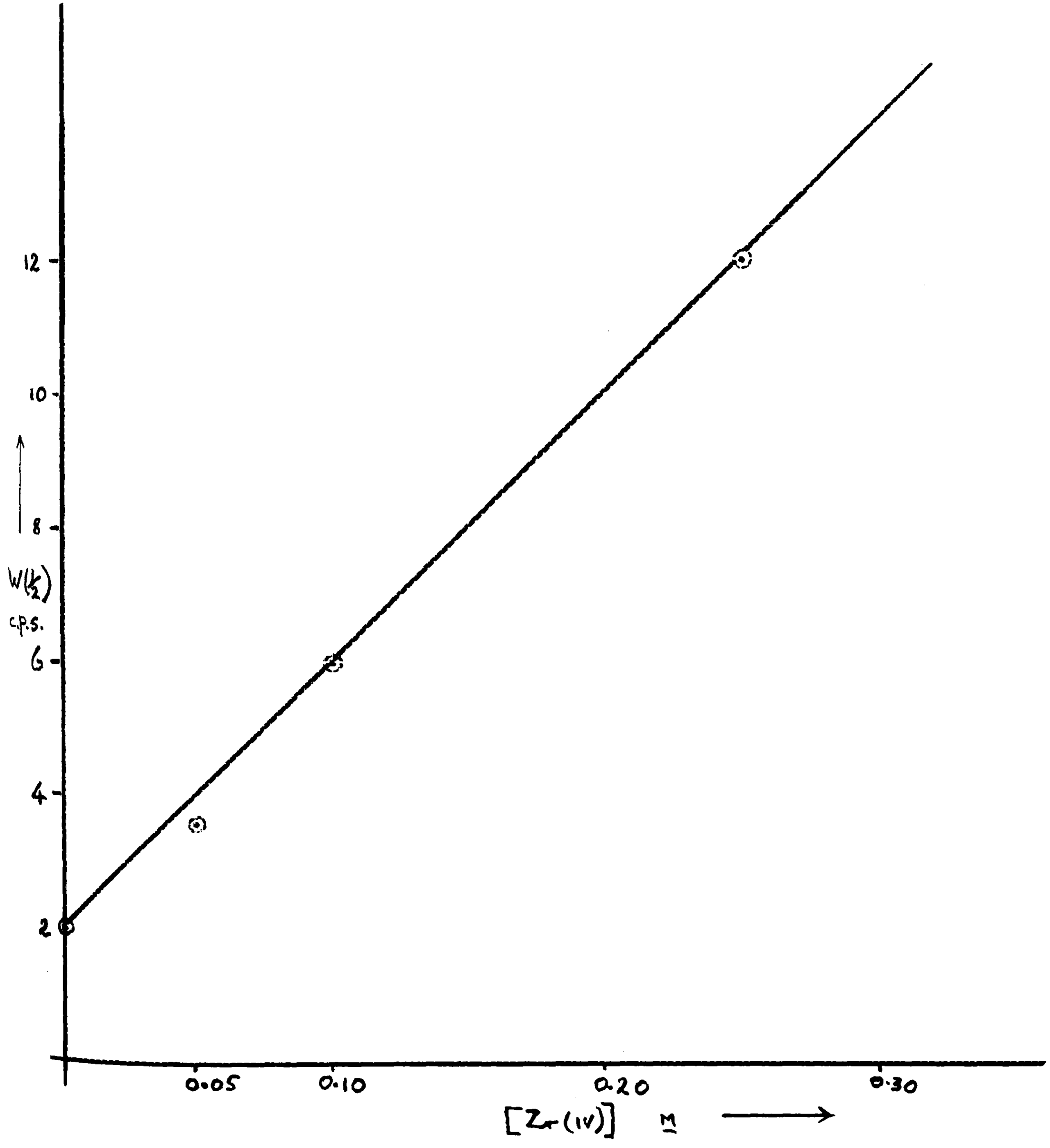
12
10
8
W(½) c.p.s.
6
4
2
0.05
0.10
0.20
0.30
[Zr(IV)] M

FIGURE 19

Variation of signal width with time of reflux.

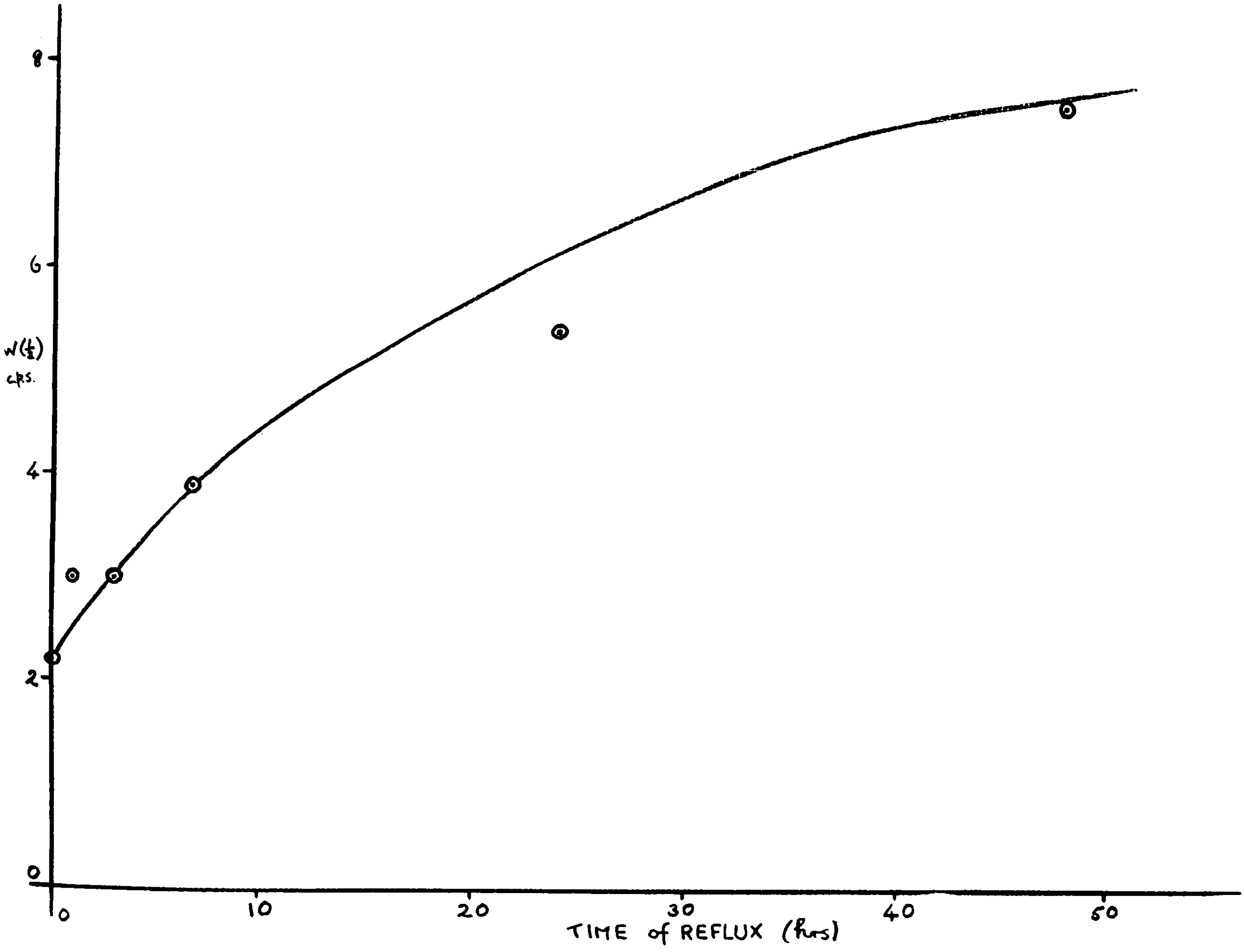
8
6
4
2
0
w(½) c.p.s.
0
10
20
30
40
50
TIME of REFLUX (hrs)

DISCUSSION

DISCUSSION

A. HYDROLYSIS AND

POLYMERIZATION 130

B. HYDROUS OXIDES

β-FeOOH AND HYDRATED OXO-HYDROXIDES 143
STRUCTURE OF MONOCLINIC HYDROUS ZIRCONIA 146

C. FUTURE STUDIES 150

DISCUSSION

A. Hydrolysis and polymerization

Various mechanisms have been devised to account for the formation of amorphous zirconia, and a number of models have been proposed for its structure.

Two of the mechanisms, are closely related in that they both involve the condensation of polynuclear cations, probably tetramers, with the result that the structure models arising via these mechanisms are similar. A third proposed model, however, invokes a different concept, the structure of zirconia being related to the lattice geometry of ZrO_2 in quite a different way.

In this section these theories are discussed, and evaluated in the light of the high resolution electron micrographs obtained in the present work.

A scheme has been proposed by Clearfield (1964) for the hydrolysis and polymerization occurring in an aqueous zirconyl chloride solution under reflux. Based upon the reasonable assumption that a tetrameric cation was present in fresh solutions (Muha and Vaughan, 1960), the scheme was as follows:-

$$\underset{\text{I}}{\left[Zr\,(OH)_2 \cdot 4H_2O\right]_4^{8+}} \longrightarrow \underset{\text{II}}{\left[Zr\,(OH)_{2+n}\,(4-n)H_2O\right]_4^{(8-4n)+}}$$

$$+\ 4nH^+ \longrightarrow \underset{\text{III}}{\left[Zr(OH)_4 . 2H_2O\right]_4} + 8H^+ \longrightarrow$$

$$\underset{\text{IV}}{4ZrO_2 . xH_2O} + (4-x)H_2O + 8H^+$$

/-

A 0.055 M solution had a pH of 1.54 which was lower than would be expected if the initial zirconyl complex was as given by 'I' above.

Further hydrolysis was informed, and a value of 0.6 for n, representing the degree of hydrolysis, was obtained from a consideration of the pH of the solution. This hydrolysis probably resulted in short-range cross-linking of tetramers, via hydroxyl bridges, and the average composition for the species in solution at this stage, $\left[Zr_4O_{10}.14H_2O\right]^{(5.6)+}$, implied that the aggregates probably consisted of two tetramers, linked together by a double hydroxyl bridge. The sample sprayed onto chrysotile fibres at this stage showed no visible deposit and it was thought that the dispersion of the material over the fibres resulted in extremely small aggregates of tetramers, or else small crystallites, none of which was large enough to be visible in the electron microscope. Evaporation of a droplet of the solution on a silica film, however, produced a series of crystalline compounds which were shown to be hydrates of zirconyl chloride. Thus the hydrolysis which takes place in a fresh aqueous solution and is largely olation was shown to be reversible, up to this stage.

Refluxing the solution for two hours brought about the marked changes in pH and in the morphology of the colloidal suspension. In the micrographs presented, there were structural features in the 6 - 10 Å size range. The tetramer proposed by Clearfield and Vaughan (1956) and Muha and Vaughan (1960) has, according to Clearfield, an overall length of 8.98 Å, and a thickness of 5.82 Å, the features observed are consistent with these dimensions and it is possible that this tetrameric species $\left[Zr\ (OH)_2 4H_2O\right]_4^{8+}$ is resolved in these micrographs. The pH of the colloid was 1.22 suggesting a value of about unity for 'n' in formula II and thus the average composition of the zirconyl complex was at this stage $\left[Zr\ (OH)_3.3H_2O\right]_4^{4+}$. This general formula could include a range of possible structures, from groups of two tetramers, bound by four hydroxyl bridges, with the formula $\left[Zr\ (OH)_3.3H_2O\right]_8^{8+}$, to /

/ to randomly linked sheets of tetramers with the overall composition $\left[Zr\,(OH)_3.3H_2O\right]_n^{4n+}$. In each case the charge is balanced by Cl^- anions in the matrix, along with other free OH^- ions. The dense particles concentrated along AA' and BB' in Plate 24, attracted to the outer hydroxyl layer of the chrysotile fibre, would support the former suggestion, whilst the thin coherent sheets suspended between the fibres, with 6 - 10 Å structural detail are consistent with sheets of linked tetramers, as shown schematically in figure 20. No information as to the thickness of the sheets observed could be obtained from the micrographs, although the extremely low contrast in some areas did suggest a very thin layer, possibly around 10 Å in thickness or les. It is proposed that at this stage in the hydrolysis, both small aggregates of closely bound tetramers, and more extensive randomly-linked sheets were present in the colloid.

As the reflux continued the observable changes were slower and after four hours, the general appearance of the colloidal particles was similar to that observed earlier. The pH of 1.21 indicated that little further hydrolysis had taken place. There was little evidence of the dense particles observed on the outer edges of chrysotile fibres, as was noted for the "two hour" sample. While this effect could easily have been due to local surface tension effects in the specimen preparation, it is also possible that further reflux was resulting in the formation of more ordered sheets of tetramers, involving both the randomly linked sheets and the smaller aggregates.

As the refluxing solutions became opalescent due to an increase in the size of the particles in suspension, well-defined areas were observed in the zirconia sheets which appeared thicker than the surrounding film, as at 'A' in Plate 29. The outline of these areas became more distinct, and the contrast between their appearance and that of the surrounding, thinner sheets, became more marked, as at 'X' in Plate , and it was shown that these thick regions became crystalline zirconia. In view of the fact that crystalline zirconia was formed, at the expense of the amorphous sheets, the following scheme may be proposed:-

/-

FIGURE 20

Randomly-linked sheet of tetramer units.

After Clearfield 1964.

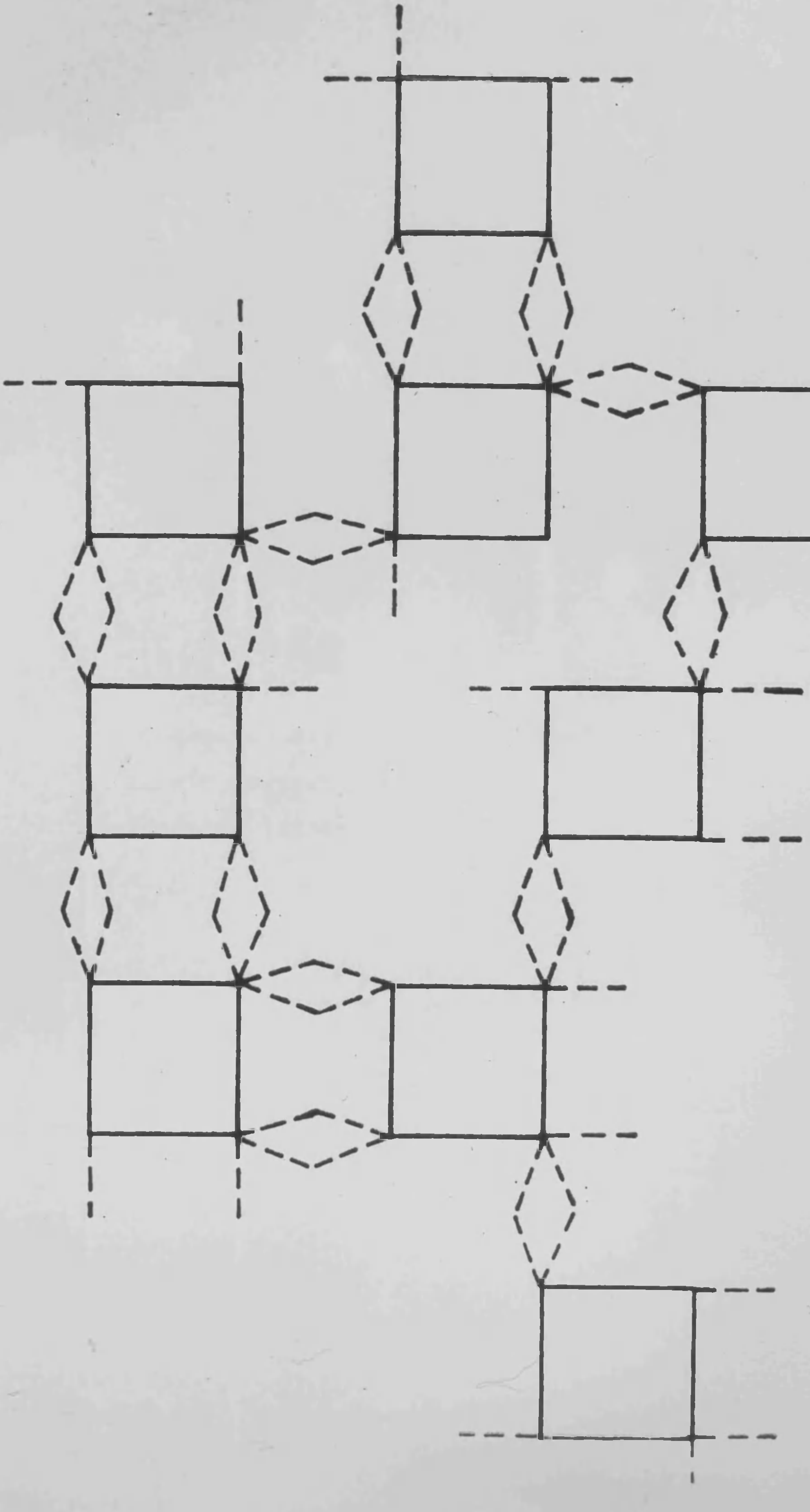

FIGURE 21

Tetramers belonging to adjacent sheets, superimposed on a fluorite lattice.

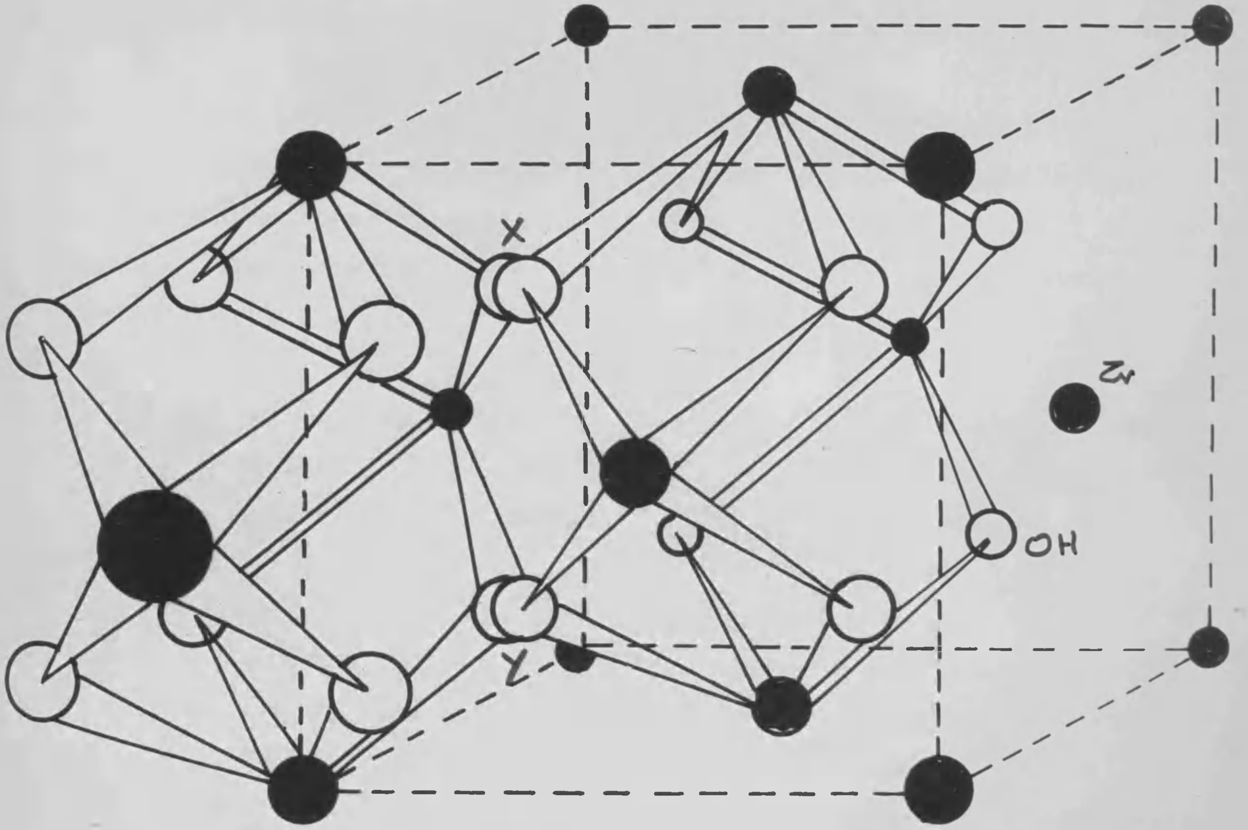
X
Zr
OH
Y

/ If tetramers belonging to two successive, parallel sheets are allowed to overlap in the manner shown in figure 21, it can readily be seen that the Zr atoms and hydroxyl groups are in the positions occupied by the components of a normal fluorite lattice. If oxolation, the formation of oxo-bridges at the expense of hydroxyl bridges, takes place at specific sites in the lattice, such as "X" and "Y" in figure 21, elimination of water will result in the formation of $\mathrm{Zr}{<}\genfrac{}{}{0pt}{}{\mathrm{O}}{\mathrm{O}}{>}\mathrm{Zr}$ bridges between the tetramer sheets. However, since the process takes place at the expense of the hydroxyl bridges (the only bonds within the sheets themselves) the sheets are weakened. Continued oxolation will result in increased cross-linking between the tetramer sheets, and an increased tendency towards fragmentation of the sheets themselves.

Since both olation (formation of hydroxyl bridges on hydrolysis) and oxolation are brought about by refluxing, there is likely to be some optimum lateral dimension for the tetramer layers, controlled by the relative rates of the two processes. The monoclinic crystallites (Plate) did in fact occur within a narrow size distribution, as shown in figure .

A cubic ZrO_2 unit cell, illustrating ZrO_2 chains is shown in figure 22, and the spatial relationship between these chains and the cyclic tetramers of $ZrOCl_2 8H_2O$ as in figure 1, may be seen. A (100) projection of ZrO_8 groups in cubic ZrO_2 is shown in figure 23.

A projection of the tetragonal phase, usually regarded as a distortion of the cubic phase, is shown in figure 24. It can be seen that there is no change in the bonding configuration between these two phases. Since the existence of cubic ZrO_2 as a stable phase of pure, stoichiometric ZrO_2 has been questioned (Weber, 1962; Garvie, 1965) it seems unlikely that the cubic phase is involved in the crystallization of zirconia in solution, as has been suggested by Clearfield. The tetragonal phase, metastable at room temperature, is more probably produced in cross-linking of tetramer sheets. Its occurrence at ambient temperatures has been attributed to a crystallite size effect by Garvie, and if this is the case, the tetragonal crystallites will undergo the transformation to the monoclinic phase if their size exceeds /

FIGURE 22

ZrO_2 chains in cubic ZrO_2.

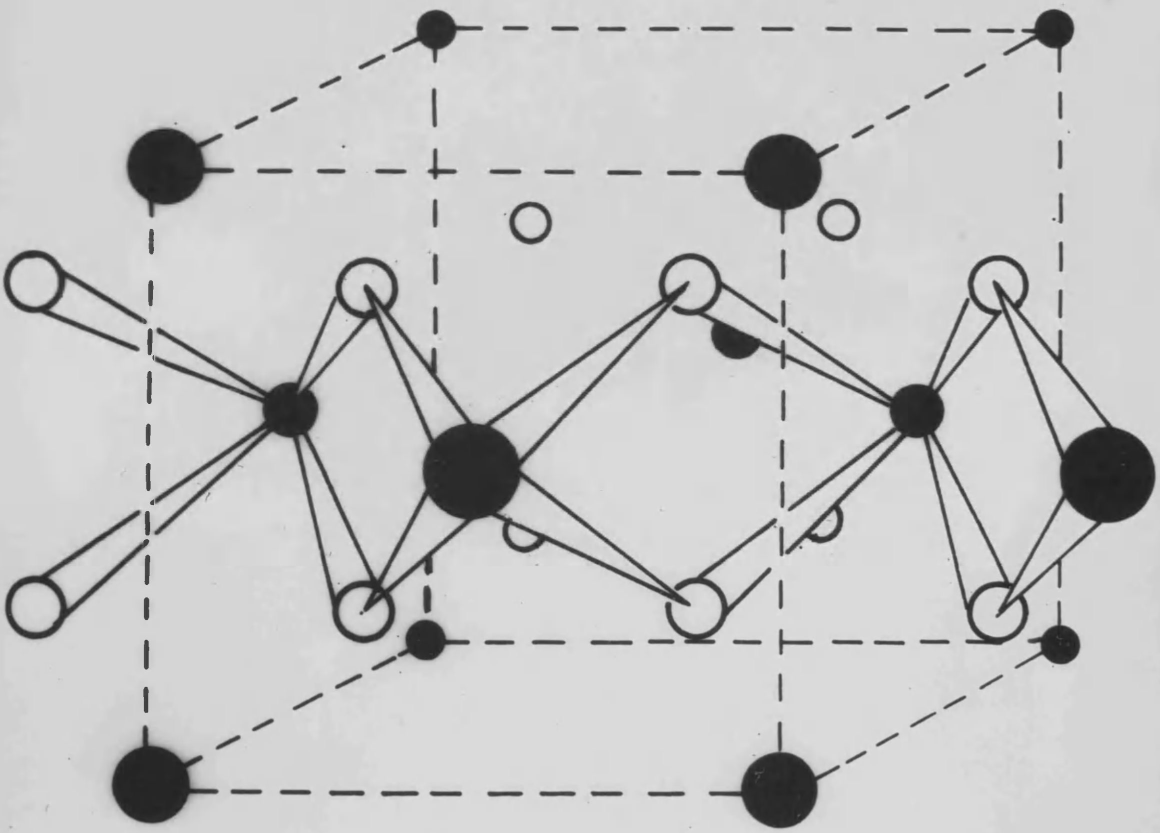

FIGURE 23

(100) projection of ZrO_8 groups in cubic ZrO_2.

After Smith and Newkirk (1965).

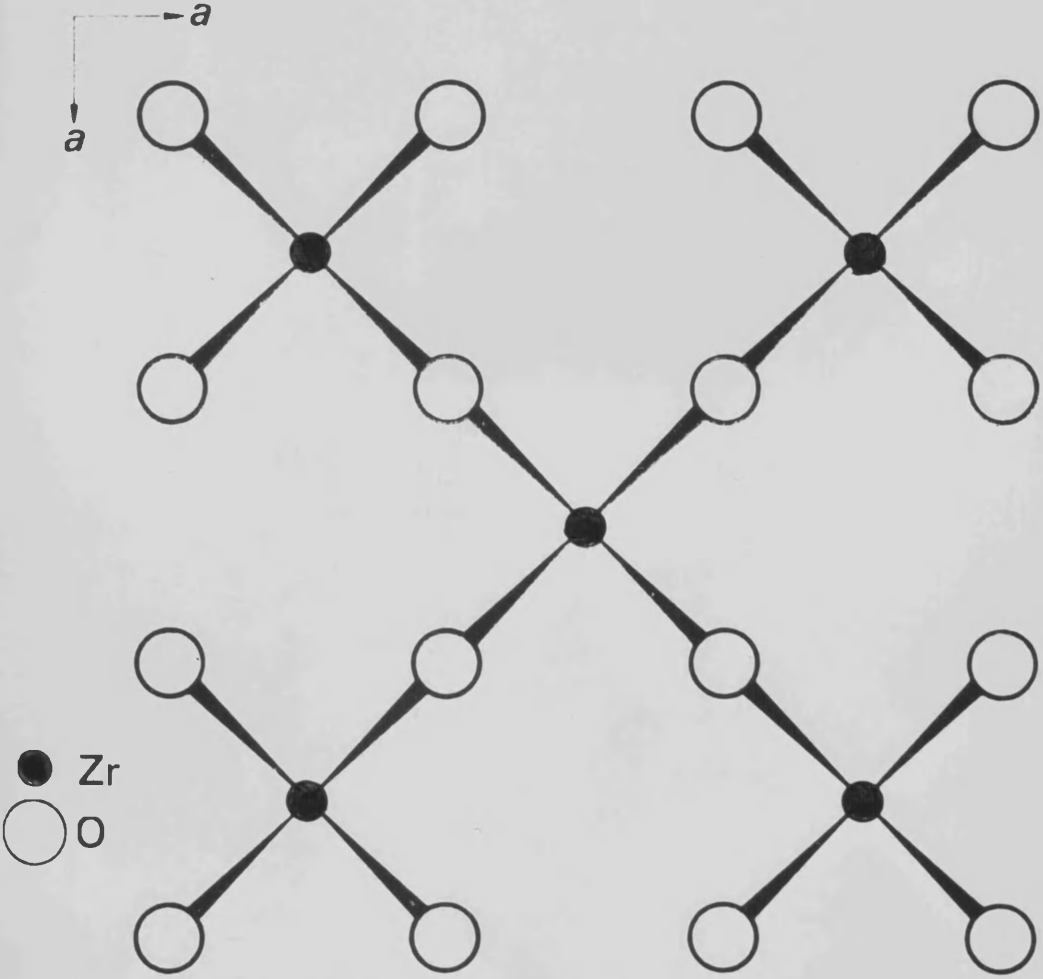
a
a
Zr
O

FIGURE 24

(110) projection of ZrO_8 groups in tetragonal ZrO_2.

After Smith and Newkirk (1965).

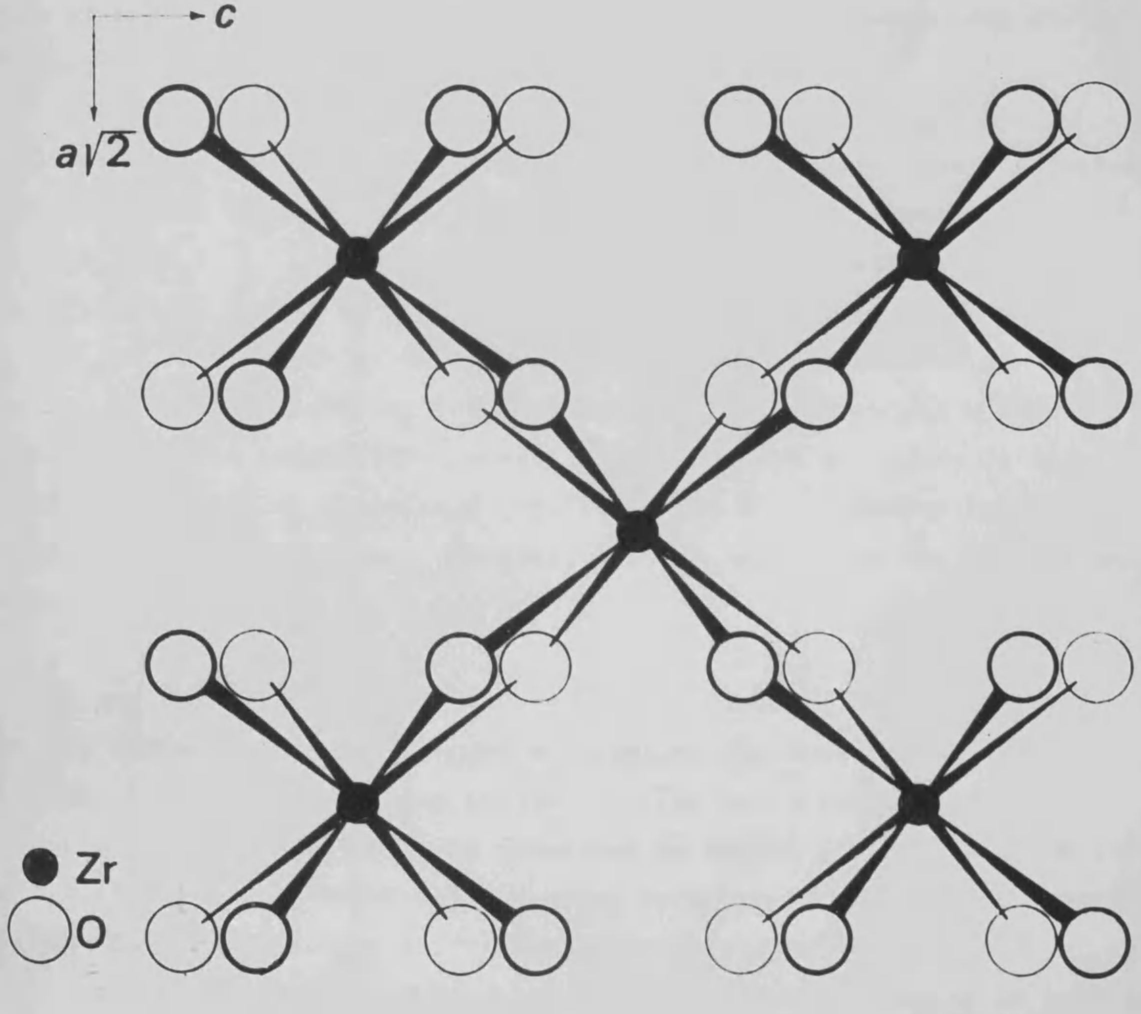
c
a√2
Zr
O

/ exceeds the critical size. Whereas in both the tetragonal and "cubic" phases, as well as in $ZrOCl_2 8H_2O$, the coordination of oxygen around the Zr atom was eight-fold, in monoclinic ZrO_2 each Zr atom is surrounded by seven oxygen atoms, as shown in the (100) projection in figure 25. Obviously there is a change in the bonding configuration in the tetragonal → monoclinic. transformation. In figure 25, the relative positions of the oxygen atoms in the tetragonal phase are indicated and the probable directions of movement of the atoms involved in the transformation are shown by arrows.

An alternative mechanism for the hydrolytic polymerization was put forward by Bilinski and Tyree (1969). This involved a changed species $\left[Zr_4(OH)_{15}\, xH_2O\right]^+$, in solution. This species, on taking up one more hydroxyl group, formed an insoluble colloidal, tetrameric unit $Zr_4(OH)_{16}\, xH_2O$. Growth of the colloid, and presumably also crystal growth, then was thought to occur by the reaction of other tetrameric species in solution with the precipitated ones. This proposed mechanism differed slightly from that of Clearfield (1969) in that his mechanism involved crystal growth in solution. However, the two mechanisms are not incompatible beyond this.

In an X-ray and neutron diffraction study of zirconia, Livage, Doi and Mazieres (1966, 1968a, b) proposed a structure for freshly precipitated zirconia, dried and dehydrated at 350°C. The basis for their model was the tetragonal phase of ZrO_2, as described by Teufer (1962) and Smith and Newkirk (1965). The model was supported by inter-atomic distances derived from the X-ray and neutron diffraction data and was a layer structure, based on the (III) planes of ZrO_2, as shown diagramatically in fugure 26 in which the Zr atoms A, B, C and D are in the (III) plane. The proposed structure was based on distances of 2.2, 3.3, 3.7m 4.7 and 6 Å, which were ascribed to BH, AB, AC, CF and AD respectively in figure 26. Since no distances between Zr atoms in adjacent (III) layers were recorded, the authors concluded that the platelets consisted of a single layer of Zr atoms, between the oxygen layers. By means of Wilson's theory, (1949) relating the distribution /

FIGURE 25

(100) projection of ZrO_7 groups in monoclinic ZrO_2, showing relationship with tetragonal phase.

After Smith and Newkirk (1965).

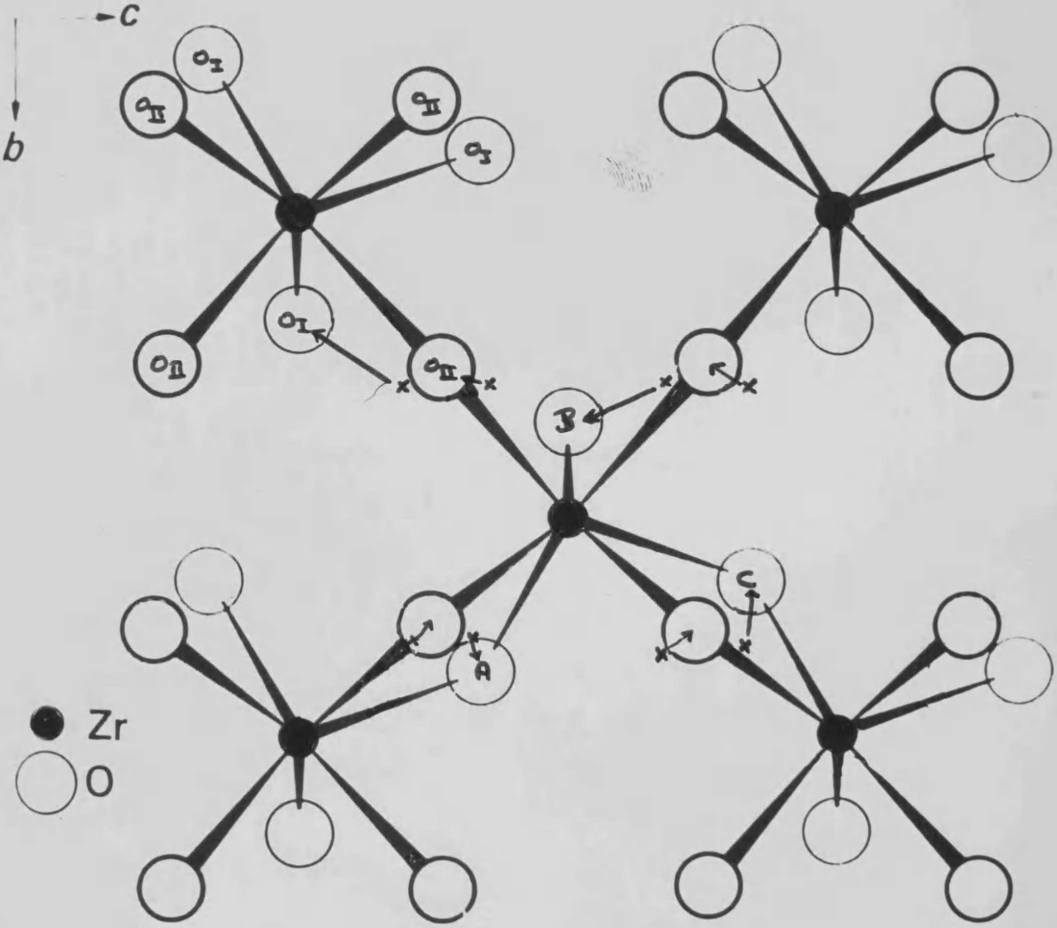
c
b
O_I
O_II
O_II
O_I
O_I
O_II
O_II
B
C
A
Zr
O

FIGURE 26

Layer structure of tetragonal ZrO_2 based on (III) planes.

After Livage et al.

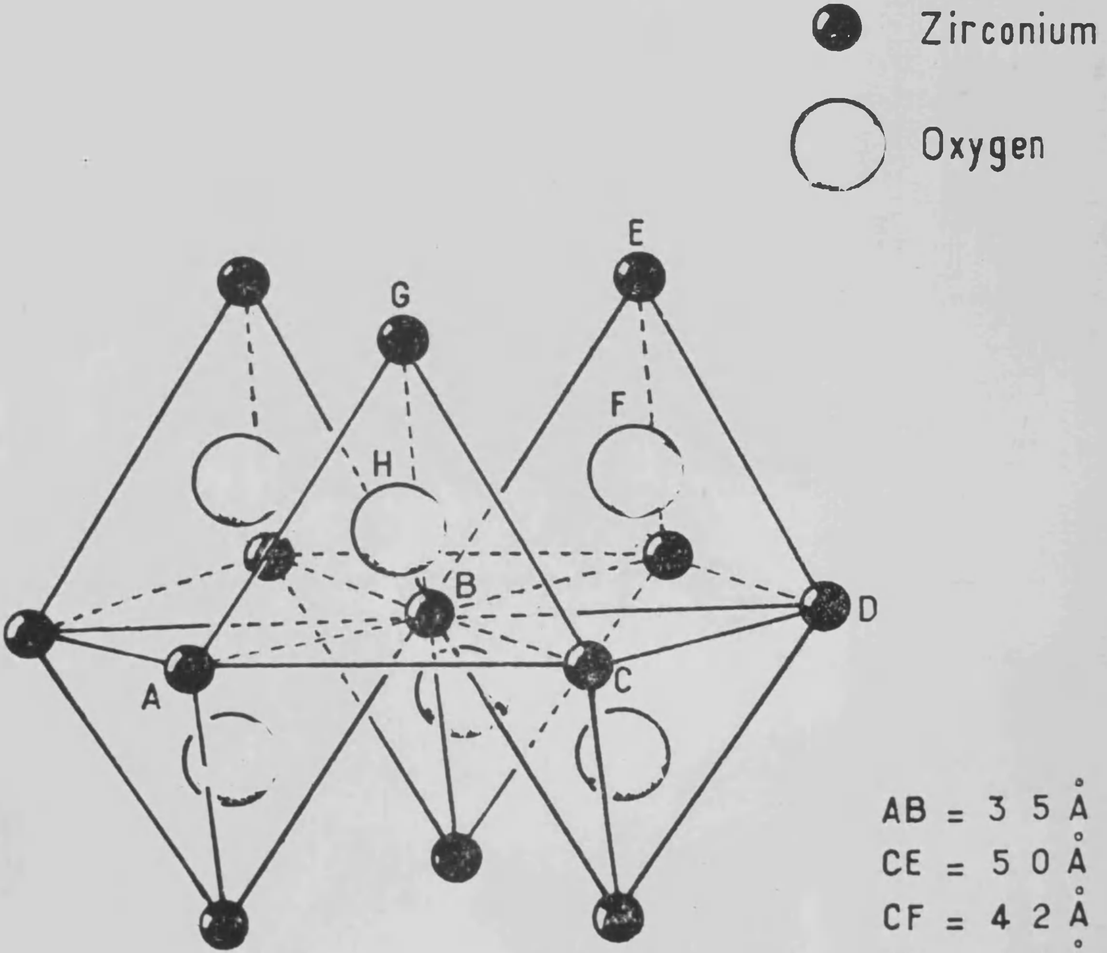
Zirconium
Oxygen
E
G
F
H
B
D
A
C

AB = 3 5 Å
CE = 5 0 Å
CF = 4 2 Å
AD = 6 1 Å
BH = 2 1 Å

FIGURE 27

Model proposed for amorphous zirconia by Livage et al.

After Livage.

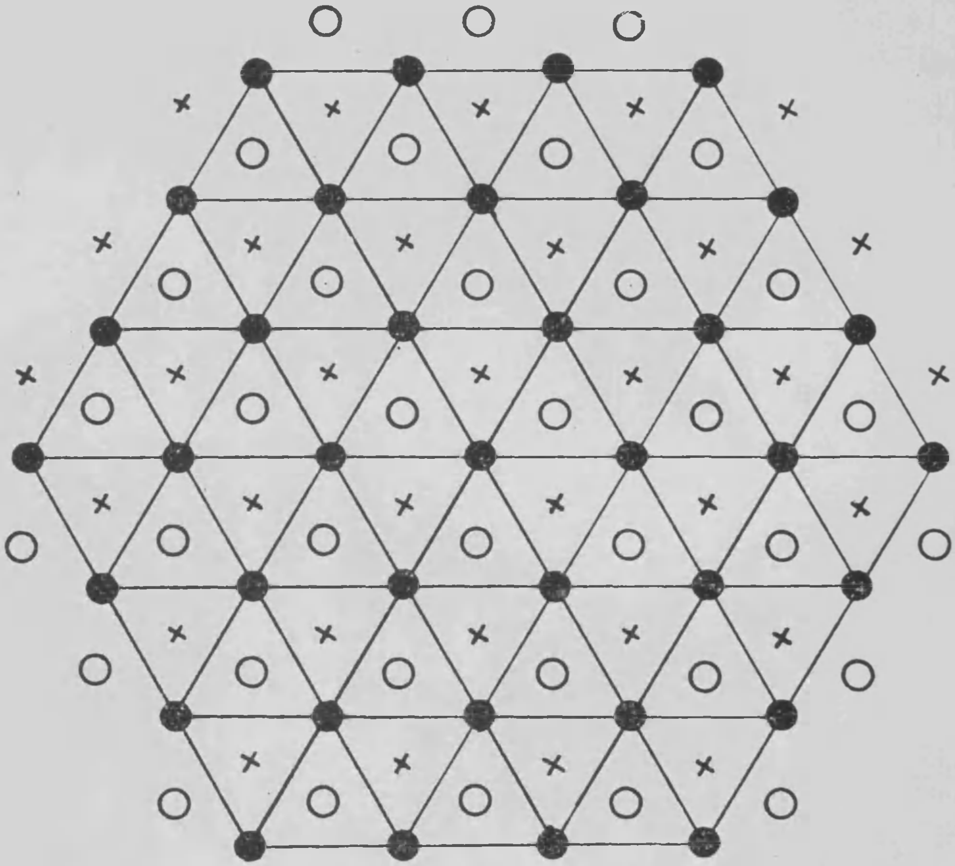

/ distribution of intensity in the reciprocal lattice to the size of the diffracting layers, a mean diameter of 20 Å was calculated, the plate thickness being 4 Å. However, Wilson's theory relates to random layers, and the fact that the authors suggested some ordering in the plates would cast doubt on the validity of their productions. A diagram of their proposed structure is shown in figure 27.

Examination of the (III) planes (~~shaded~~) in figures 21 and 22 will show that link-up of tetramers cannot directly give rise to a structure of this type and it is obvious that the mechanism by which such a structure would be formed, and that which involved tetramer link-up must be mutually exclusive and the electron microscope evidence, combined with pH correlations, would seem to favour the latter mechanism.

Since Livage et al dried and dehydrated the amorphous zirconia at 350°C, it is not strictly valid to compare the structure proposed by these workers with that proposed by Clearfield. However, it is unlikely that the dehydration would result in major structural changes, particularly since Clearfield (1964b) has shown from X-ray powder photographs that the phases of hydrous zirconia and the corresponding calcined oxide phases are virtually identical in overall structure.

B. Hydrous Oxides

(i) β-FeOOH: Although it is not possible to derive a detailed structure for the "pods" and "stars" of monoclinic zirconia from the available data considerable information may be implied from a consideration of an other hydrous oxide, β -FeOOH.

Crystals of this material were first isolated by Böhm (1925) from refluxing solutions of ferric chloride. He identified them as a new form of ferric oxide hydrate. Later work by Koetholf and Moskevitz (1936) showed that such compounds were oxide hydroxides, usually called oxyhydroxides, the form here considered being β -FeOOH, which occurs naturally as akaganeite.

A /

/ A notable feature of β-FeOOH is that it possesses, when freshly precipitated, a hollandite or BaMnO2 structure, with 5 Å-square channels, running parallel to the c-axis (Mackay, 1960). The tetragonal unit cell dimensions have been given by Mackay (1960) as a = 10.48 Å, c = 3.023 Å. An unusual feature of β-FeOOH is its morphology, as revealed by electron microscopy. Feitknecht (1960) observed that the crystals had the appearance of bundles of parallel needles. Later investigations by Watson, Cardell, and Hellen (1962) provided more accurate information concerning the peculiar cigar-shaped crystallites, which they called "somatoids" because of their crystallographically irregular shapes. A pattern of striations, parallel to the main axis, with a repeat distance of about 60 Å was accounted for, using sectioning and shadow-casting methods.

The authors deduced that the crystals were square in cross-section, with a side length of about 550 Å; the crystals were up to 5000 Å in axial length, along what was shown to be the c-axis (Mackay, 1960). Watson et al (1962) suggested that the structure within these crystals probably consisted of an oriented bundle of orthogonally-packed rods, fairly loosely packed. The repeat distance was about 60 Å, the rods being about 30 Å thick, and 30 Å apart. The rods were longer towards the centre of a crystal, and were themselves crystals. There was some evidence from the cross-sections that the rods were (in fact) hollow and an alternative model was proposed, taking this into account. In this case, the rods were packed more closely together. The not infrequent star-shaped, and Y-shaped crystals were regarded as twins.

Gallagher (1970), using electron microscopy, X-ray diffraction and gas absorption techniques extended this work and confirmed the presence of pores in β-FeOOH. The mean pore diameter was found to be 28 Å. A structure was proposed for the rods, to account for these pores, involving the hollandite structure.

Clearfield (1964) considered the crystalline forms of zirconia as "hydrated" /

/ "hydrated oxo-hydroxides", with the general formula $ZrO_b(OH)_{4-2b}\propto H_2O$.

Structure of monoclinic hydrous zirconia

The appearance of the monoclinic "pods" was so similar to that of the β-FeOOH "somatoids" that at first sight it seemed an extremely attractive idea to propose that the structures of the two species were in fact closely related, particularly since crystalline hydrous zirconia is known as a "hydrated oxohydroxide". Also, the fact that both were prepared by reflux of aqueous solutions seemed further evidence for a close similarity in structures. It was therefore thought that the zirconia "pods" were composed of bundles of subcrystals which were either hollow rods, or loosely packed solid rods, to allow for the appearance of the 30 Å striations. The "stars" were supposed to be twinned versions of the "pods". The N.M.R. data, which was consistent with a porous material, was regarded as additional evidence for the proposed structure. Electron diffraction patterns of single, isolated crystallites showed that the above reasoning did not apply to the zirconia. The "stars" were shown to be single crystals, or oriented bundles of subcrystals, in general agreement with the proposed β-FeOOH structure. Twinning on (100) was found to take place parallel to an edge rather than a diagonal of the "square". The diffraction patterns obtained from the few isolated "pods" were interpreted in terms of "stars" in a different orientation with respect to the electron beam. The fact that the so-called "pods" also showed (100) twinning was taken as additional evidence that the two forms were in fact identical.

It was not possible from the available data, to present a complete structure for these platelets. A schematic model for a platelet is shown in figure 28.

/ -

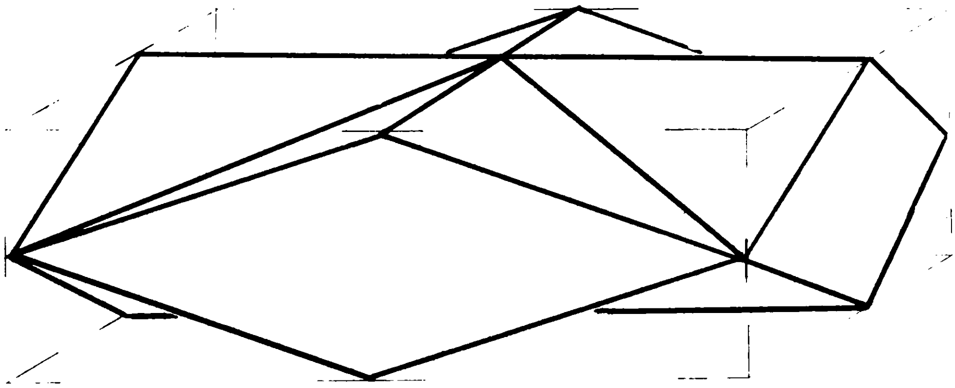

Figure 28.

This is not a real representation of the species concerned but is probably sufficiently close, dimensionally, for the purposes of the discussion. In order that a surface area could be calculated, the possibility of curved faces was discounted.

Taking the dimensions of the model as shown in figure 28 , the total surface area of the model is found to be 1.34 x 10^{6}(A), the volume being 8.3 x 10^{7}(Å)^{2} . The density has been calculated by Smith and Newkirk (1965) and given as 5.8 g.cm.$^{-3}$. Thus the weight of the structure shown in figure 28 would be 4.8 x 10^{-16}g., and the specific surface area is then shown to be 28 m.^{2}g.$^{-1}$. If, on the other the zirconia consisted of spherical particles 450 Å in diameter, the surface area would be 13 m.^{2}g.$^{-1}$, while if the particles were simply 670 Å square and 280 Å thick, the surface area would be 27 m^{2}g^{-1}. Conversely, an increase in the puckering of the surface would give a corresponding increase in the surface area, although this increase would not be large. Thus for particles of average dimensions similar to those found in monoclinic zirconia, a surface area in the approximate range 10 - 40m^{2}g^{-1} is to be expected.

The /

/ The measured surface area was 143 m^2g^{-1} which is higher, by a factor of about five, than would be expected for "solid" particles. This suggests a porous structure for the stars as it is unlikely that any simple shape, in the given size range would approach this value of surface area.

The evidence for a porous structure may be summarized as follows:-

(i) Electron diffraction suggests that the platelets are highly oriented bundles of crystallites, which may be in the form of rods or layers. Ultra-sonic treatment did not disperse these crystallites.

(ii) N.M.R. signals from aqueous solutions or suspensions showed a broadening which was consistent with a highly porous structure.

(iii) A high surface area was also indicative of a porous material.

(iv) Infra-red absorption in a powdered sample showed the presence of water of hydration, possibly in pores.

Twinning As has already been mentioned, most crystals of both synthetic ZrO_2 and natural baddeleyite exhibit twinning on (100). This was interpreted by McCullough and Trueblood (1959) as being a result of the relatively low energy difference between the ZrO_7 configuration found in the "normal" structure, and that in another related arrangements. The relationship between these two arrangements is shown in figure 25 where the O_I atoms are below the plane, the O_{II} atoms above the plane of the paper. The proposed relationship was this:-

Groups of these O_I atoms, such as A, B, C, were rotated by 180° about an axis which was perpendicular to the plane defined by the four O_{II} atoms. This gave rise to a minor plane parallel to the (100). However, McCullough and Trueblood failed to consider that neither the O_I nor the O_{II} planes were quite parallel to the (100) plane, with the /

/ the result that a simple reflection of the structure across a plane parallel to (100), or a rotation about an axis parallel to the c-axis, would not given an acceptable twin boundary configuration. Smith and Newkirk (1965) suggested an alternative arrangement which gave a more suitable boundary by rotation of the structure about a two-fold axis through $x = y = \frac{1}{2}$. One half of the twin was then shifted $\frac{1}{2}$ a with respect to the other. This could also be visualized in terms of alternate ZrO_7 groups, as a rotation of the O_{II} group about an axis nearly perpendicular to the O_I plane. Small adjustment in bond lengths were required to allow the O_{II} atoms to occupy positions in the twin plane, averaged between both halves of the twins.

This twinning arrangement gave an appropriate configuration for the boundary and a twinning angle approximately 10°, in agreement with the present work.

It was not possibly to correlate this twinning with the features observed in the zirconia although it seems likely that monoclinic hydrous zirconia is very similar to baddeleyite in crystallographic structure. A porous arrangement of subcrystals would allow for the presence of water, without disturbing the crystal lattice, and the weight of evidence in the present work tends to favour this.

Crystallite size distribution

An interesting feature of the monoclinic zirconia was the narrow size range, which was reached quite rapidly under the reflux conditions, and subsequently did not change at all. Similar features have been observed in other studies of hydrous oxides. Thus -FeOOH was shown to consist of crystallites about 5,000 Å in length, and 550 Å in cross section, (Watson, Cardell and Heller, 1962) and in Praesodimium hydroxide, initial studies have shown similar tendencies (Haire and Willmarth, 1970). Since crystal growth in solution evidently takes place by oxolation, this process must be a major controlling factor in determining /

/ determining the final crystal size.

FUTURE STUDIES

The results presented in this work raise a number of questions which, as yet, cannot be answered fully. The first problem is in the interpretation of the high resolution micrographs of the colloidal amorphous zirconia. In the present state of the subject, and with the limits imposed by the electron microscope, more than tentative suggestions are not feasible.

The broad striations observed on the crystallites of monoclinic zirconia were not accounted for satisfactorily. More detailed surface area and gas absorption studies would probably show the presence of pores, if there were any. Broad line N.M.R. would show the presence of any water in "dry" crystalline zirconia, and could be used to distinguish between various water molecules in different environments. Also, a more detailed study of the line broadening effects in high resolution N.M.R. would give further information on the porosity of the structure.

There was no apparent correlation between the (100) twinning in the "stars" and their morphology. If such a relationship could be established, it may be possible to provide a complete structure for these particles, in terms which account for the pore structure, the matrix of oriented sub-crystals, and the twinning.

Having such a large surface area, it is possible that crystalline hydrous zirconia will be useful as a catalyst support, provided that sintering and phase transitions do not reduce the surface area drastically.

Finally, since amorphous hydrous zirconia is known as an ion exchanger (e.g. Britz and Nancollas, 1969) it seems likely that the crystalline material, which appears to be similar in composition to amorphous zirconia /

/ zirconia, will also possess ion exchange properties.

PART 2

A HIGH RESOLUTION ELECTRON MICROSCOPE STUDY OF CHRYSOTILE.

GENERAL CONTENTS OF PART 2

INTRODUCTION 155
EXPERIMENTAL 161
RESULTS 165
DISCUSSION 180

INTRODUCTION

CHRYSOTILE 155
CRYSTALLOGRAPHIC CLASSIFICATION 158
THERMAL STABILITY 160

EXPERIMENTAL

(i) SAMPLE PREPARATION 161
(ii)ELECTRON MICROSCOPE 161

RESULTS

RESOLUTION OF CHRYSOTILE LATTICE 165
FIBRE CROSS-SECTIONS 165

UNUSUAL GROWTH FEATURES

(a) FIBRE TIPS 165
(b) THIN FIBRES 174
(c) OTHER MINERAL PRESENT 174
FIBRE DIMENSIONS 175
ELECTRON BEAM DAMAGE 175

DISCUSSION

RESOLUTION OF LATTICE IMAGES 180
USE OF CHRYSOTILE AS A SPECIMEN
SUPPORT 181
FIBRE DIMENSION 182

INTRODUCTION

As a mineral of practical value, asbestos has a long history, evidence for early applications being found in the writings of Plutarch (438 B.C.). The Romans used Chrysotile from the Italian Alps to make cremation cloths, while the anthophyllite deposits of Finland had an even earlier application, the mineral being used as a reinforcement. Asbestos mines in Russia were recorded by Marco Polo (1250). In spite of these early applications, asbestos did not become commercially important until the discovery of large chrysotile deposits in Canada in 1847.

CHRYSOTILE: Chrysotile, which is commercially the most important asbestos, belongs to a group of minerals known collectively as Serpentine. The first structural information on chrysotile was an X-ray diffraction pattern obtained by Anderson and Clark (1929). As a result of further X-ray studies, Warren and Bragg (1930) proposed a structure based on amphibole-like silica chains, the suggested composition being $Mg_6Si_4O_{11}(OH)_6H_2O$. This gave a reasonable explanation for the fibrous nature of the mineral, but was not consistent with Anderson and Clark's data (1929). Pauling (1930) suggested that if the magnesium analogue of kaolin, $Al_2Si_2O_5(OH)_4$, existed, it would have curved layers, owing to the misfit between the two component layers. Accordingly, Warren and Hering (1941) proposed a disordered layer structure, whereas Aruja (1943) used Pauling's hypothesis to suggest that the curvature of the layers would limit the growth of the chrysotile lattice to narrow ribbons.

The curved layer structure has been shown (Warren and Hering, 1941, Whittaker, 1953, Deer, Howie and Zussman, 1962, 1963) to be based upon a network of SiO_4 tetrahedra, forming a sheet, to which is joined a Brucite /

/ Brucite layer, $Mg(OH)_2$ in such a way that on one side, two out of every three hydroxyl groups are replaced by oxygen atoms at apices of the tetrahedra, as is shown schematically in figure 29.

The first reference to electron microscopy of chrysotile was mentioned in a review by Hillier and Turkevitch (1949), who claimed that the observed fibres had the appearance of hollow tubes. This observation was followed by those of Bates, Sand and Mink (1950) and Noll and Kircher (1950) who made similar claims. The micrographs presented, however, could not be taken as proof in themselves that the fibres were in fact hollow tubes, because the images could equally well have been interpretated as representing thin laths.

Detailed X-ray studies and theoretical calculations by Whittaker (1951, 1954, 1955) showed that observed X-ray intensities from chrysotile fibres were consistent with a cylindrical lattice. The work of Jagodzinski and Kunze (1954 a, b, c) was in broad agreement with this findings, although there was some disagreement in the more detailed postulates. This discrepancy was shown by Whittaker to be due to the use of different lattice parameters. However, the agreement was that chrysotile had a cylindrical lattice, and that the fibres were hollow tubes. Whether they consisted of concentric layers, or a single spiral arrangement was not conclusively shown.

In 1956, Pundsack carried out density measurements on sealed blocks of fibres, and found that the density was greater than would be expected if the fibres were hollow cylinders, as predicted by X-ray studies, and also suggested from some electron micrographs. Thus the idea that chrysotile consisted of curved laths, rather than hollow tubes, was briefly revived.

Whittaker (1957) supported his own claims for a cylindrical lattice by proposing that the void volume within and between the fibrils was filled with fragments of curved lattice. From X-ray intensity measurements /

FIGURE 29

Schematic structure of Clinochrysotile on (010). Sheets are continued in the direction of curvature and normal to the plane of section.

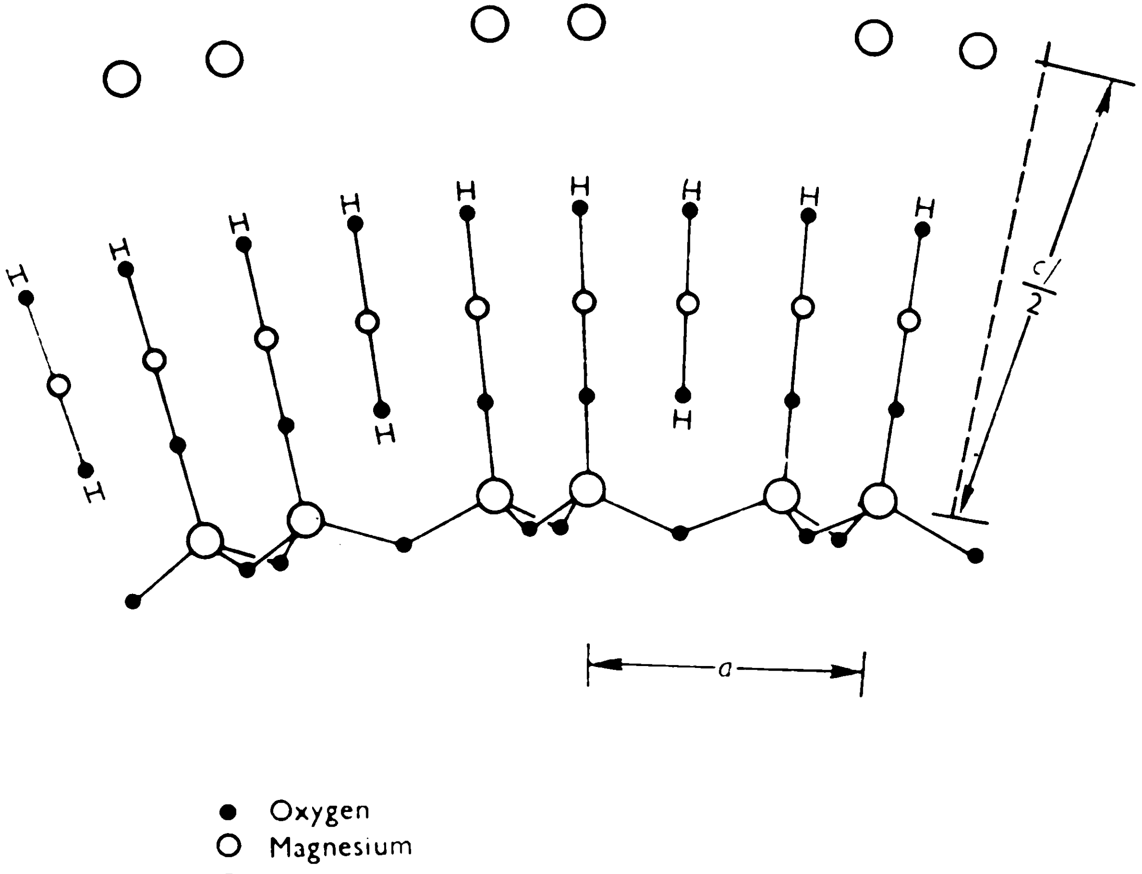
H
a
c/2
Oxygen
Magnesium
Silicon

/ measurements he suggested that the most commonly occurring fibre would be a cylinder 260 Å in diameter, having a hollow centre 110 Å in diameter. The wall of this tube would consist of ten composite Brucite-Silica layers. On this basis, the total void volume would be approximately 25%, this volume being filled with fragmented lattices. Bates and Comer (1959) suggested that the tubes were rather filled with amorphous material, presumably a magnesium silicate gel.

Kheiker, Flantsbaum and Bubeleva (1967) also carried out measurements of (h00) reflections, and small-angle scattering curves from Russian Chrysotile. They deduced that the fibres had an average wall thickness of 20 - 23 layers, the inner radius being about 60 Å. This gave an overall fibre thickness of approximately 370 Å, with 150 Å walls. Thus these fibres appeared to be larger than those mentioned by Whittaker.

Maser, Rice and Klug (1960) obtained evidence for cylindrical chrysotile fibres in electron micrographs of end-on cross-sections of chrysotile fibres, showing what appeared to be concentric and spiral structures. Claims that these micrographs constituted actual proof of such structures were rather optimistic, however, since the dimensions involved were below 10 Å, and the micrographs were not taken under high resolution conditions. A high resolution study by Yada (1967), of chrysotile asbestos gave the first clear evidence for hollow cylinders consisting of spirally-wound layers. Some very striking micrographs of end-on cross-sections of the chrysotile fibrils were obtained, and in several, the spiral arrangements of the layers could be distinguished. More recently, Yada (1970) has shown a concentric arrangement of layers in a small number of fibres.

CRYSTALLOGRAPHIC CLASSIFICATION: Another aspect of the structure of the chrysotile concerns its structural classification. Whittaker and Zussman (1956) have listed three varieties, ortho-chrysotile, clino-chrysotile and para-chrysotile. Ortho-chrysotile (orthohombic) and clino-chrysotile /

/ clino-chrysotile (monoclinic) have similar unit cell dimensions, the only distinguishing parameter being the angle β . The structure of para-chrysotile is analogous to that of ortho-chrysotile, except that its fibre axis, instead of being the b axis, is the a axis. This is the most rare of the three varieties.

The most common modification is clino-chrysotile (Whittaker, 1956) and its lattice parameters, according to a variety of sources, are given in Table 20.

Table 20.

LATTICE PARAMETERS OF CLINO-CHRYSOTILE

Author (s)	a (Å)	b (Å)	c (Å)	α°	β°	γ°
Warren & Bragg (1930)	14.66	18.5	5.33	90	93°16'	90
Warren & Hering (1942)	7.33	9.24	5.33	90	93°16'	90
Aruja (1943)	14.62	9.20	5.32	90	93°12'	90
Padurow (1950)	7.36	9.26	5.33	92°50'	93°11'	89°50'
Whittaker (1951)	14.65	9.20	5.33	90	93° 7'	90
Brindley (1952)	5.33	9.24	7.33	90	93°	90
Jagodzinski & Kunze (1954)	5.33	9.10	7.33	90	93°16'	90
Whittaker & Zussman (1956)	5.34	9.20	14.65	90	93°16'	90
Yada (1967)	5.30	9.10	7.32	90	93°	90

The results of Padurow (1950) would indicate that the mineral is in fact triclinic. However, later work has failed to support these measurements, and they are regarded as unreliable, or non-representative parameters for chrysotile.

It can be seen from the table that, after the results of Brindley (1952) the allocation of a and c axis was interchanged with the resulting c parameter becoming the distance between layers. There has been a lack of /

/ of agreement between the various authors as to whether the value 14.6 Å, or 7.3 Å should be assigned to the length of the unit cell in the c direction. In figure 29. which shows a schematic section of chrysotile on the (010) plane, it can be seen that the $\frac{c}{2}$ distance is taken to be that between two successive Silica layers, a distance of 7.3 Å.

On this basis, the c spacing is 14.6 Å, as proposed by Whittaker and Zussman (1956). However, Yada (1967) pointed out that, if this was the case, then the extra half-plane of an edge dislocation in the (001) plane would correspond to two extra lines in the observed 7.3 Å lattice image, corresponding to the (002) planes. In reality, he found that most lattice dislocations showed only one extra line, and Yada concluded that the repeat period in the c direction should be 7.3 Å.

It has recently been shown by Cockayne and Whelan (1970) that a terminating half-fringe need not represent an edge dislocation. This will be discussed later.

THERMAL STABILITY: Although asbestos is popularly associated with great thermal stability, particularly in its use as a fire-resistant medium, it has been recently shown to decompose on continued heating. The thermal decomposition of chrysotile has been shown by Ball and Taylor (1961) and Brindley and Hayami (1965) to follow a distinct two-stage sequence: dehydroxylation, followed by breakdown to other minerals. The initial loss of hydroxyls takes place in the range 600 - 780°C, whilst at 800 - 850°C, the anhydride breaks down in a sharp transition to forsterite and silica. The overall decomposition may be represented by the following equation:-

$$Mg_6Si_4O_{10}(OH)_8 \longrightarrow 3\,Mg_2SiO_4 + SiO_2 + 4H_2O$$

Below 600°C, chrysotile is accepted as being thermally stable.

Despite /

Despite the thermal stability, it has been observed by Yada (1967) that chrysotile is unstable to even moderate electron beam irradiation. This was evidenced in a loss of crystallinity, as seen in electron diffraction patterns, and an overall deterioration in the lattice images observed. This loss of crystallinity was noted to commence at the outer surfaces of the fibres, which became irregular, and was interpreted as a beam-induced dehydration process, different in some way from the processes involved in the thermal breakdown of the mineral.

EXPERIMENTAL:

(i) SAMPLE PREPARATION: Specimens of chrysotile from a variety of sources were used. By ultrasonic treatment in a bath for 20 minutes, a small sample in water could be reduced to single fibres, or small bundles of two or three fibres. A drop of this suspension was allowed to dry upon a Platinum-Iridium mount. It was found that a network of fibres could be made to span 70μ holes in the mount and the need for a supporting substrate was eliminated.

In this way, background structure was not present in high resolution micrographs, and the quality of the images obtained was thus improved. Charging-up of the specimen was also reduced, since most of the fibres were in contact with the metallic mount itself. Thermal vibration, potentially a serious problem because of the lack of a support film, was minimized by operation of the electron microscope at a low beam intensity, thereby also minimizing the irradiation damage.

(ii) ELECTRON MICROSCOPY: The electron microscope was operated at an instrumental magnification of 160,000X. A pointed filament was used, which gave an increase in beam coherence, and allowed the use of a 100μ condenser aperture. 100μ or 200μ thin foil apertures, made as described earlier were used in the objective lens and in this way high resolution images of the chrysotile fibres were consistently obtainable.

/

PLATE 37

Chrysotile from Valmalenco.
Magnification: 2,000,000X

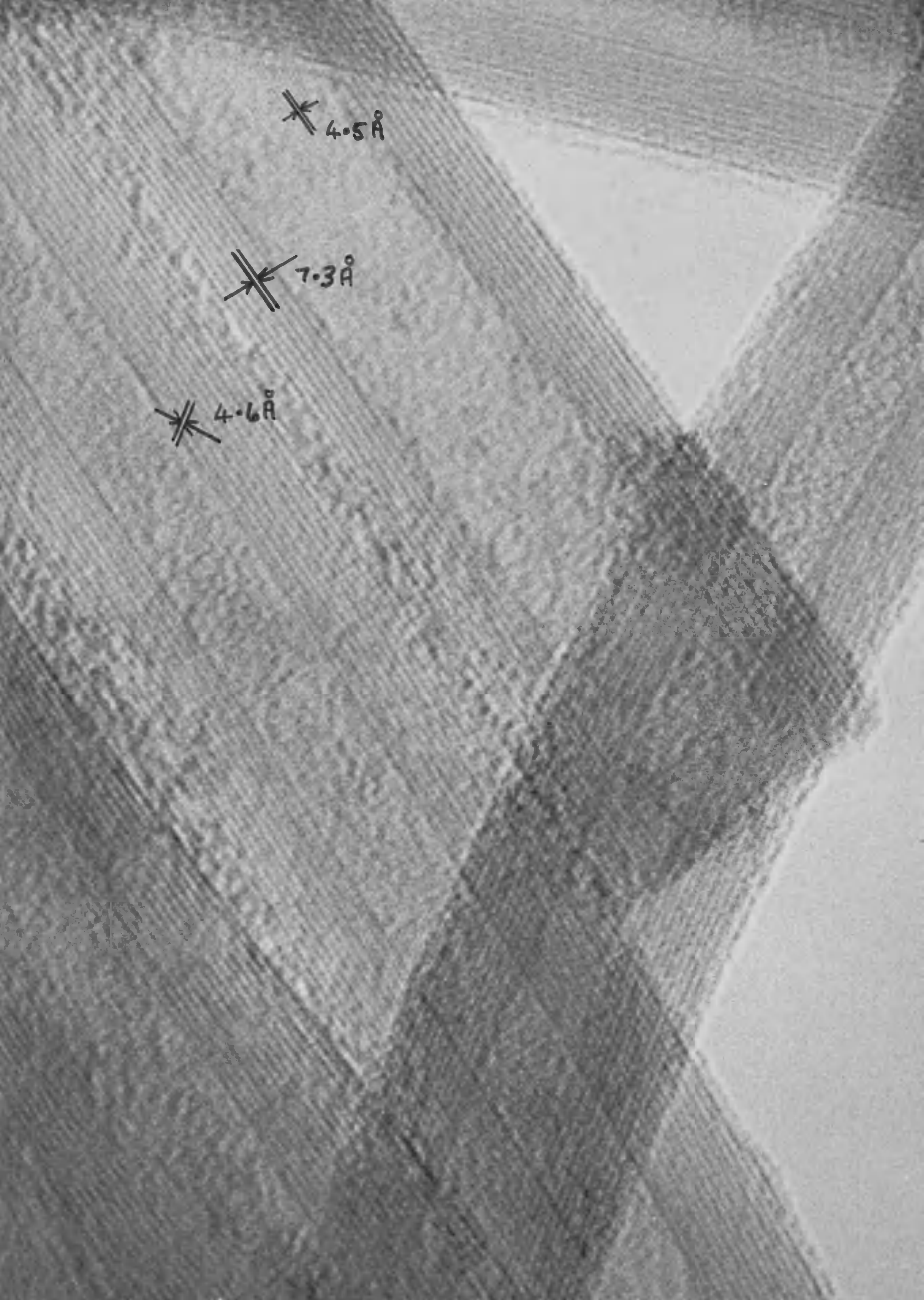
4·5Å
7·3Å
4·6Å

PLATE 38

Chrysotile from Rhodesia.
Magnification: 2,000,000X

PLATE 39

Chrysotile from Clinton, Canada.
Magnification: 2,000,000X

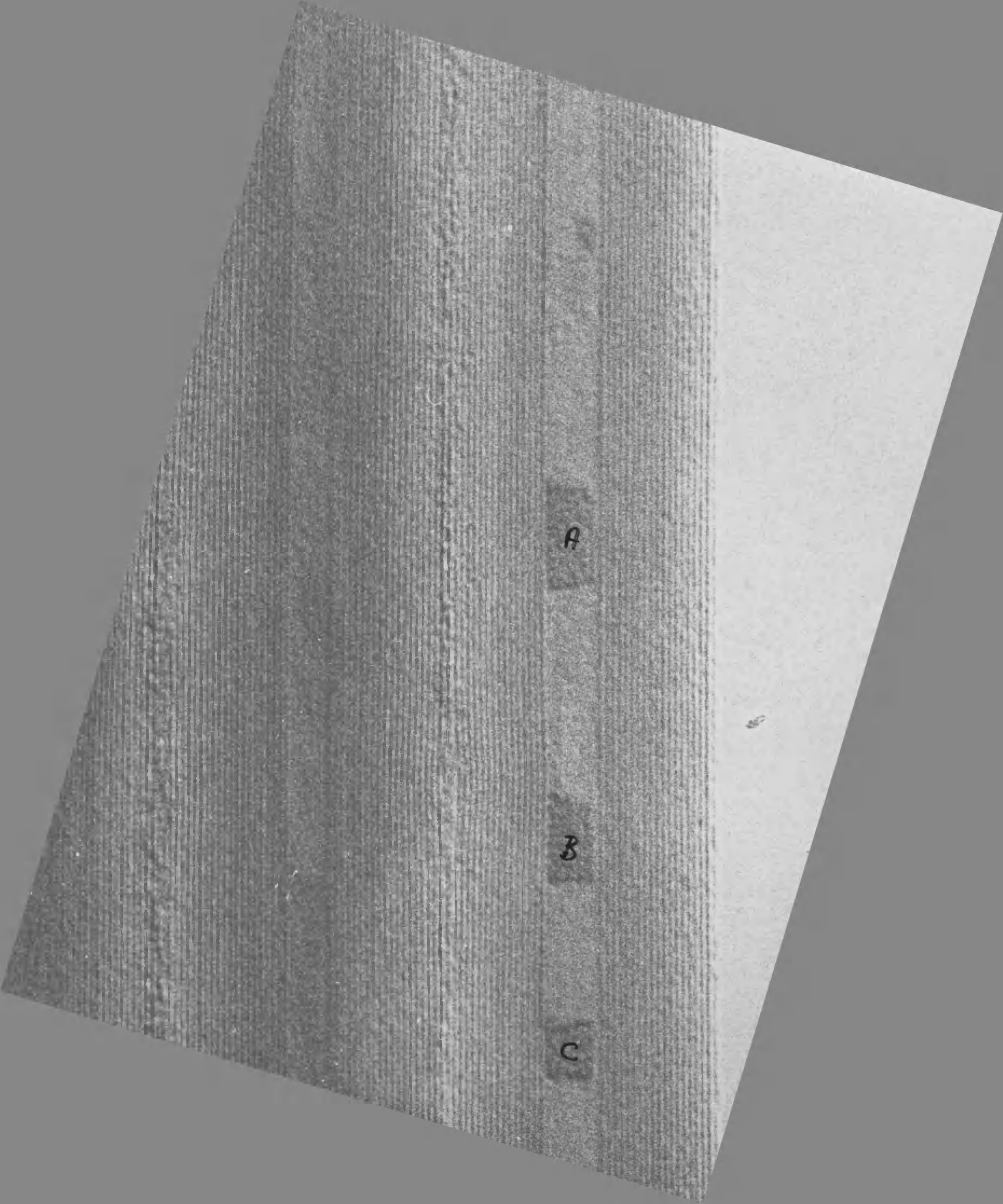
A
B
C

RESULTS:

Specimens of chrysotile were prepared in the manner described and examined in the electron microscope. High resolution electron micrographs were obtained for each of the samples.

RESOLUTION OF CHRYSOTILE LATTICE: Fibrils of chrysotile from different sources are shown in Plates 37, 38 and 39. Resolution of the (001) lattice, with a spacing of 7.3 Å, was achieved for all the samples, and in many instances, the (020) and (110) lattice images, with spacings of 4.5 and 4.6 Å respectively, were also resolved, as shown in Plate 37.

FIBRE CROSS-SECTIONS: Yada (1967) prepared cross-sections of chrysotile fibres, and was thus able to demonstrate spirally wound layers. However, it is felt that the sectioning process would have led to severe deformation of some of the sections which Yada regarded as "unusual growth features". In the present study, a small number of cross-sections were observed, which were apparently broken from fibres as a result of the ultra-sonic treatment. There was no evidence of deformation in these fibres. A thin section is shown at 'A' in Plate 40. This fibre is 270 Å in diameter, and its hollow centre is clearly visible. The dimensions for this fibre of Rhodesian chrysotile are well below the average for that sample. A much thicker cross-section from the same source is shown in Plate 41, the overall width of the fibre being 750 Å. Twenty-seven layers are clearly resolved, and the fibre probably consists of more than thirty layers. Because the layers were not completely resolved round the circumference of these sections, it was not possible to show the spiral arrangement of the layers.

UNUSUAL GROWTH FEATURES: (a) Fibre tips. Most of the fibres studied terminated in fairly well-defined breaks, usually normal to the fibre axis, as shown in Plate 42. Occasionally, the innermost layers were seen to project well beyond the outer layers, as in Plate 43 /

PLATE 40

Thin cross section of chrysotile
from Clinton.
Magnification: 2,000,000X

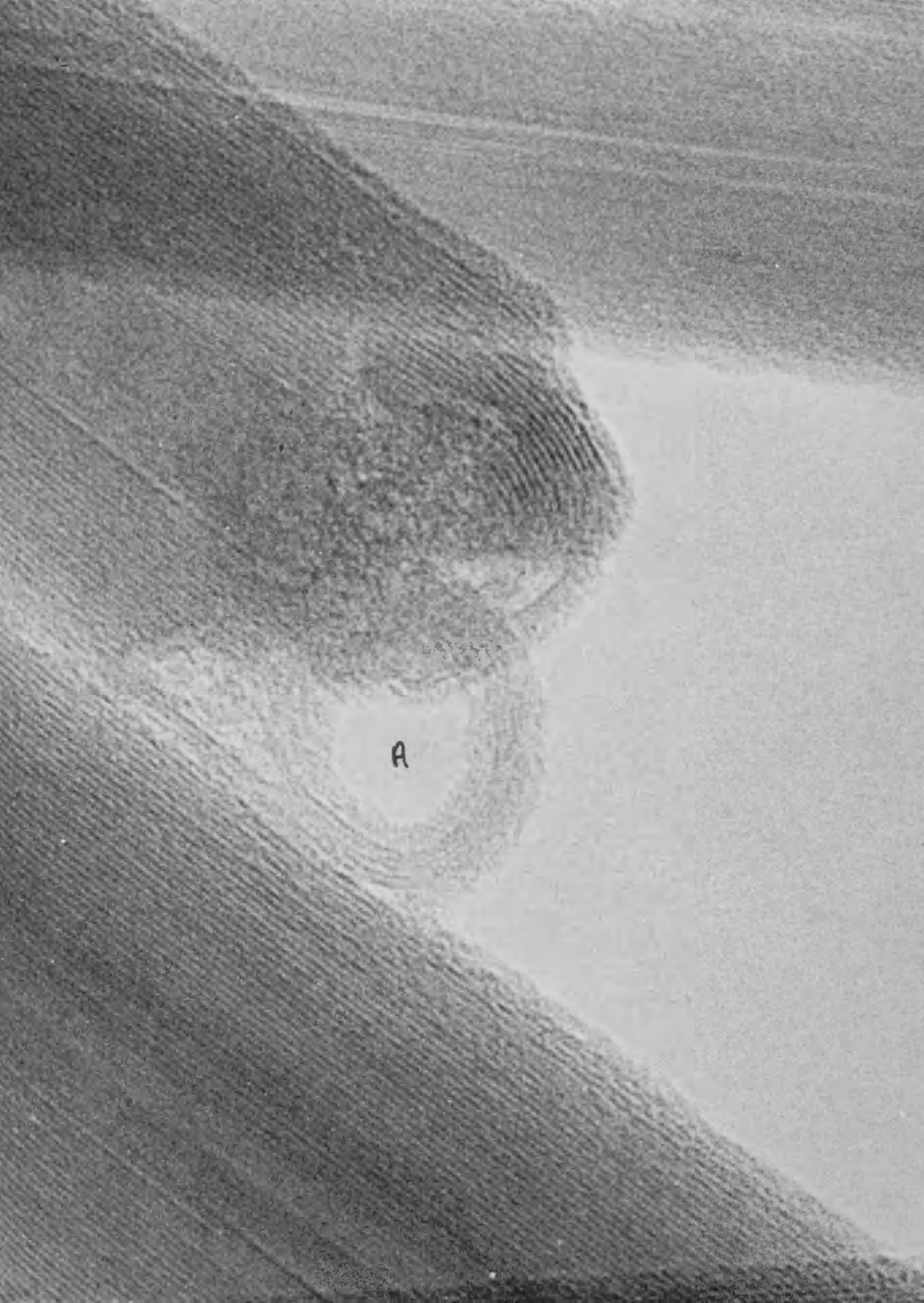
A

PLATE 41

Thick cross section of Chrysotile
from Clinton.
Magnification: 2,000,000X

PLATE 42

Chrysotile fibre tip (Clinton)
Magnification: 2,000,000X

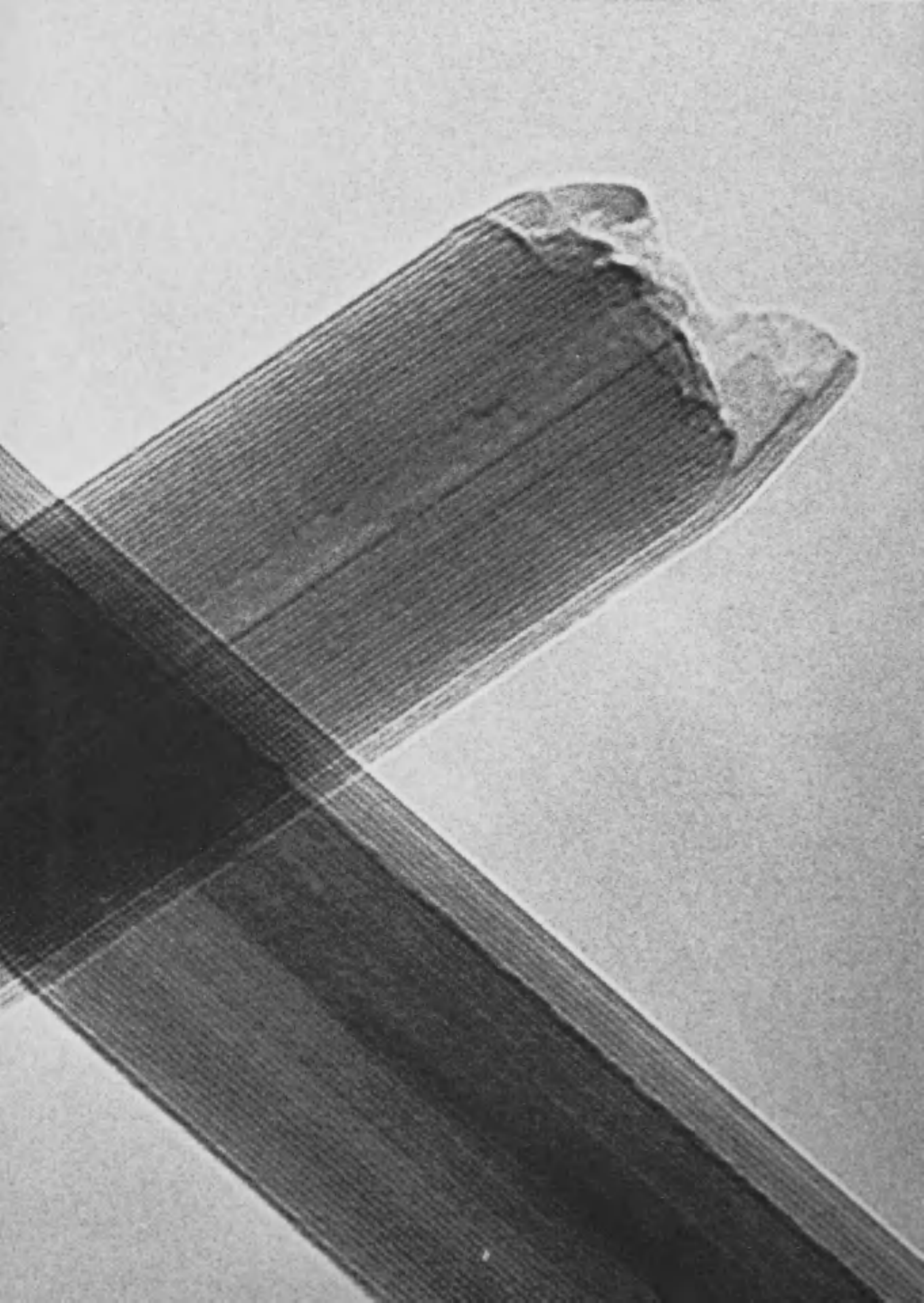

PLATE 43

Protruding layers in fibre
tip (Rhodesia)
Magnification: 2,000,000X

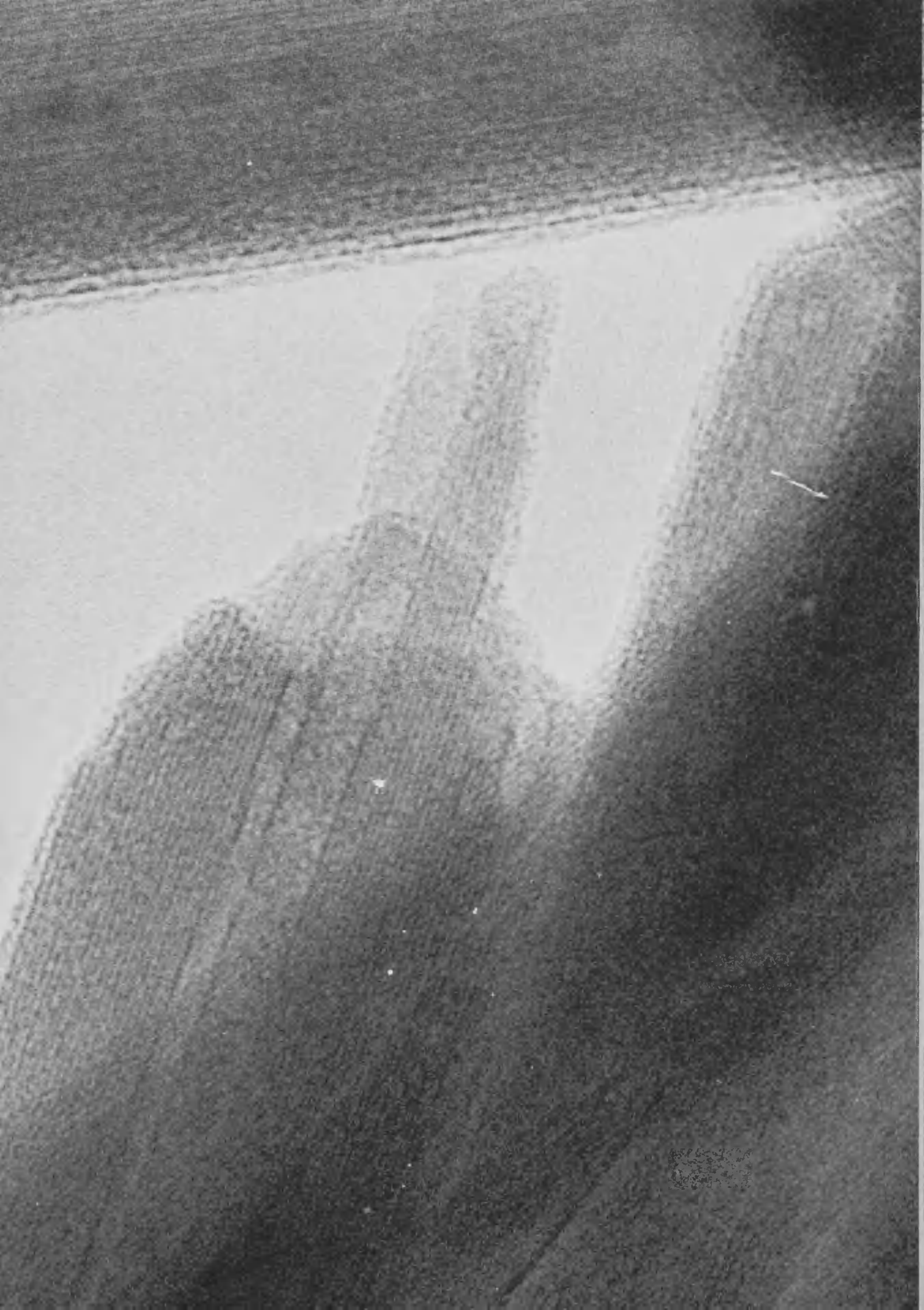

PLATE 44

Unusual growth feature in
fibre tip (Rhodesia).
Magnification: 2,000,000X

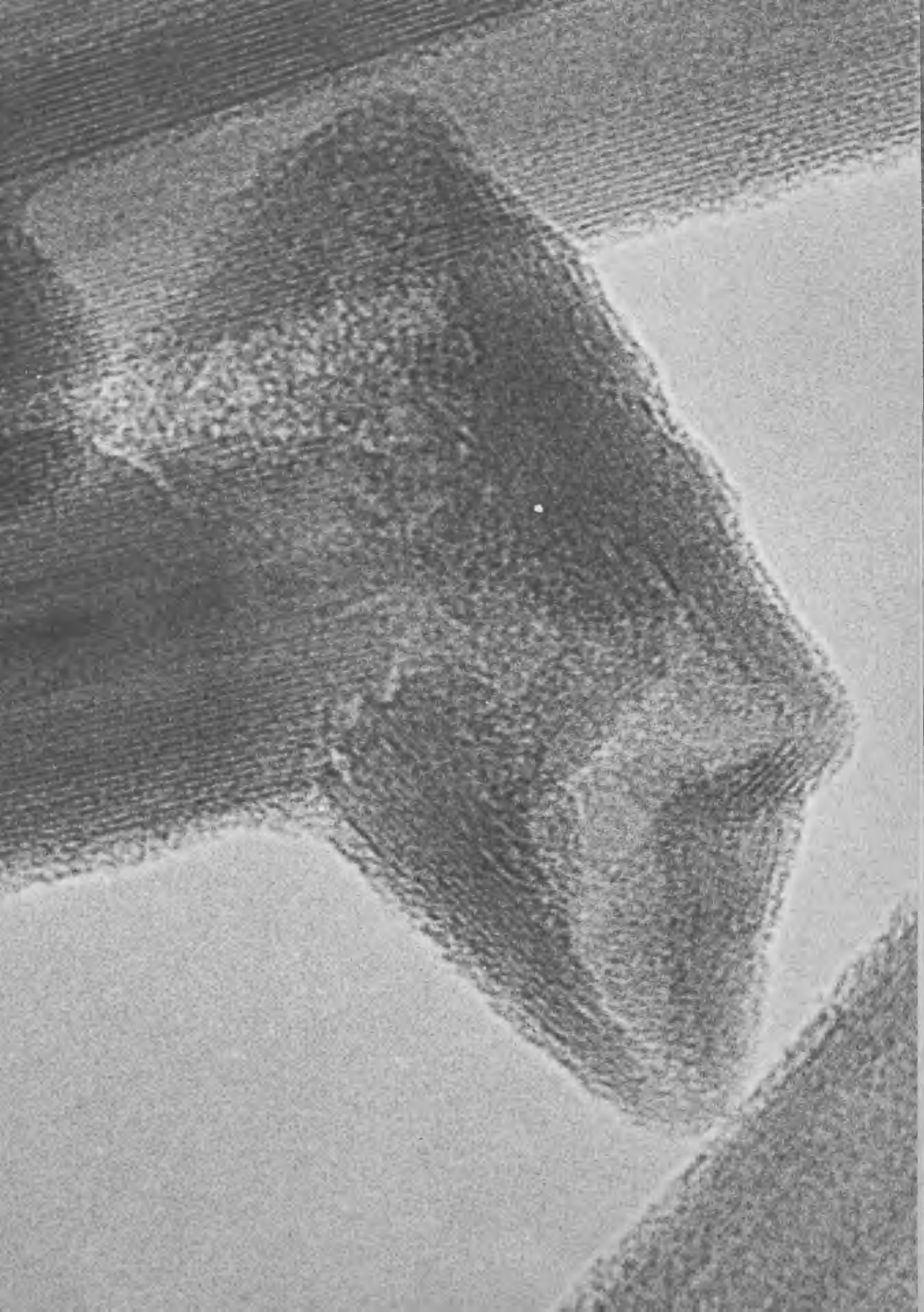

PLATE 45

Thin fibres of Clinton Chrysotile, showing an incomplete fracture at 'A'.

Magnification: 2,000,000X

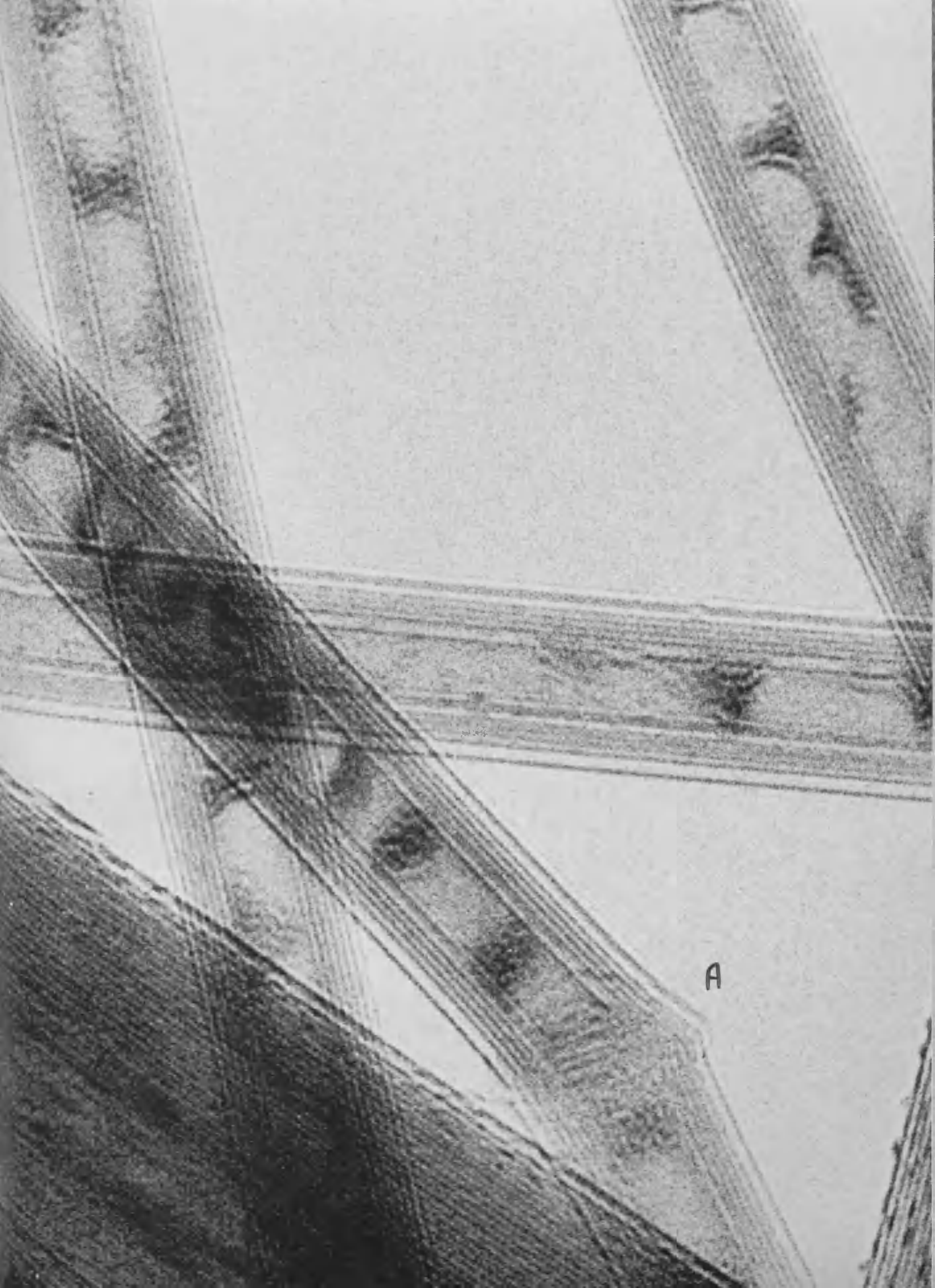
A

PLATE 46

Flake of "Serpentine" showing
7 Å striations.
Magnification: 2,000,000X

PLATE 47

Thin flake showing 5 Å striations.

Magnification: 2,000,000X

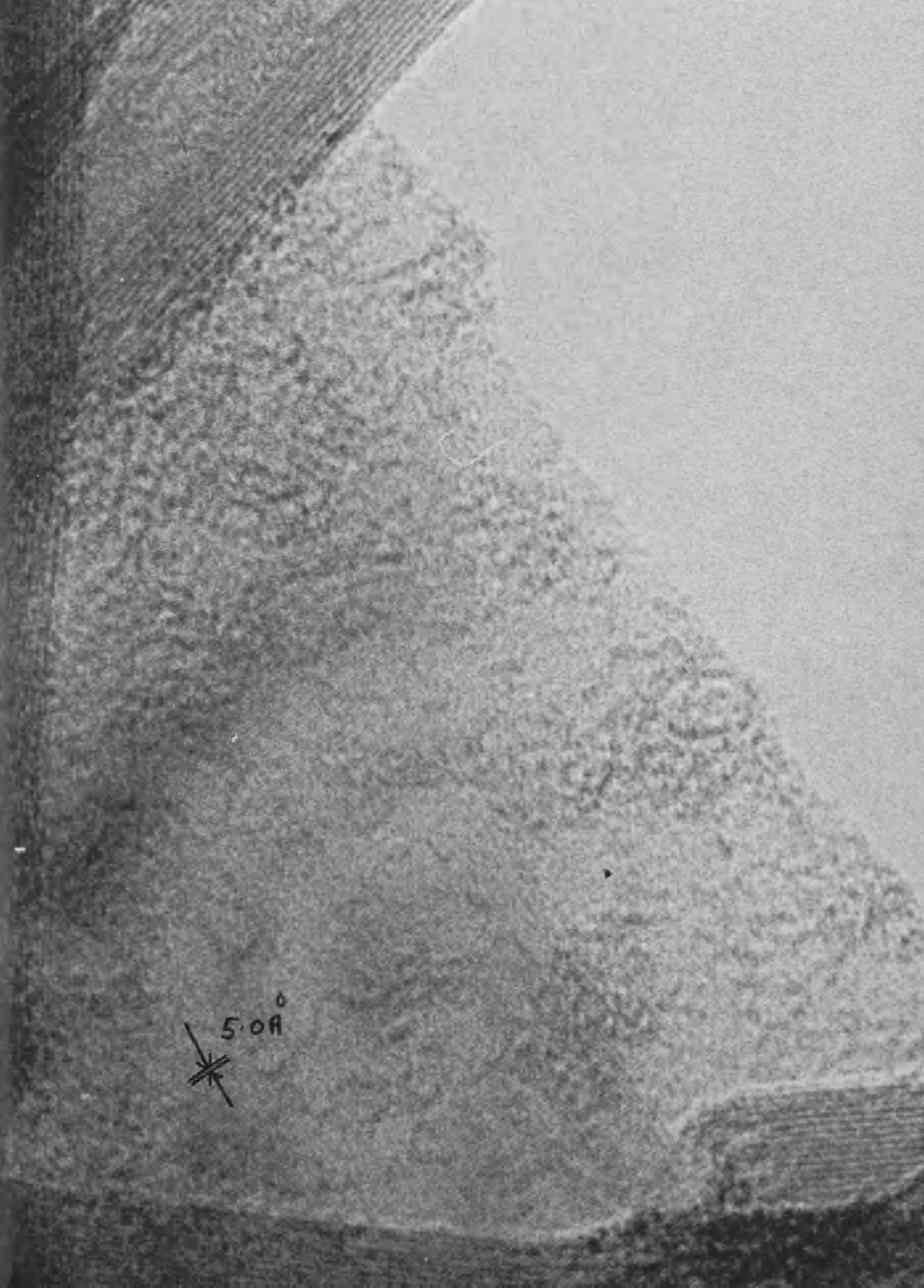

5·0Å

/ 43. In contrast to the "clean" breaks, there was also a number of unusual fibre tips observed, a typical example, from Rhodesia, being shown in Plate 44. Structures very similar to this were found in several fibres from the various sources, and they were assumed to be significant structures, rather than artefacts produced by the specimen preparation technique. An incompletely fractured fibril is shown at 'A' in Plate 45

(b) Thin fibres. The sample from Clinton, Canada contained a number of extremely thin filaments, a number of which are shown in Plate 45 These tubes are only 150 Å in diameter and consist of seven composite layers. The "hollow" centres of these fibres are seen to contain aggregates of dense material. Other fibres from the same locality contained dense material along their hollow centres, as at A, B, C in Plate 39. It has been suggested (Whittaker 1957, Bates and Comer 1959) that the hollow cylinders were filled with fragments of curved lattice, or, alternatively, an amorphous silica-magnesia gel. From the appearance of the fibres in the micrograph, the latter proposal is supported. The aggregation of the amorphous gel into discreet bumps is thought to be the result of its dehydration within the microscope.

(c) Other Minerals Present. In addition to the chrysotile fibres described, some other associated crystalline masses were observed, most of which showed fringe patterns with a spacing close to 7.3 Å, as is shown in Plate 46 . These crystalline masses may consist of fragments of cylindrical lattices. Alternatively, they may be regarded as flakes of serpentine $(Mg_6Al)\ (Si_4Al)\ O_{10}(OH)_8$, the "parent" mineral of chrysotile itself. The (001) spacing of serpentine has been recorded by Gillery (1959) as 7.09 Å. On other thin flakes, however, were observed striations with considerably smaller spacings. Plate 47 shows a thin crystalline flake with a fringe system with a spacing of 5.0 Å. These fringes, observed in two directions on the flake, were accurately measured by calibration against the (001) image of the supporting chrysotile network.

/ -

FIBRE DIMENSIONS: Whittaker proposed that the average chrysotile fibre would be a cylinder 260 Å in diameter with an inside diameter of 110 Å, whilst Kheiker et al suggested that these dimensions were respectively 370 and 60 Å, for the particular chrysotile concerned. As a comparison with these predictions, the average outer and inner diameters of the various samples of chrysotile were measured, the values obtained being shown in Table 21.

Table 21.

DIMENSIONS OF CHRYSOTILE FIBRES

Source	Outer Diameter	Inner Diameter	No. of Layers
Whittaker (1957)	260 Å	110	10
Kheiker, Flantsbaun and Bubeleva (1967)	370	60	22
Rhodesia	370	92	19
Canada (Clinton)	360	60	21
Valmalenco	270	90	13

ELECTRON BEAM DAMAGE: This effect presented some difficulty at the outset of the present work. However, by maintaining the electron beam intensity at a sufficiently low level to allow an exposure time of about six seconds, it was possible to minimize the damage. If focussing was carried out quickly, images could be recorded with no visible electron beam damage affecting the specimen, as can be seen in Plate 48, which shows (two) fibres of chrysotile in which the (001) and (020) lattice images are clearly resolved. Where electron beam damage did occur, however, it was usually evident as a loss of the lattice image, beginning at the outer layers. This was accompanied by the outer surface becoming irregular, and it was possible to detect this change in successive micrographs, as at 'X' in Plates 24, 25 and 26.

In /

PLATE 48

Fibres of Clinton Chrysotile, showing (001) and (020) lattice images.

Magnification: 2,000,000X

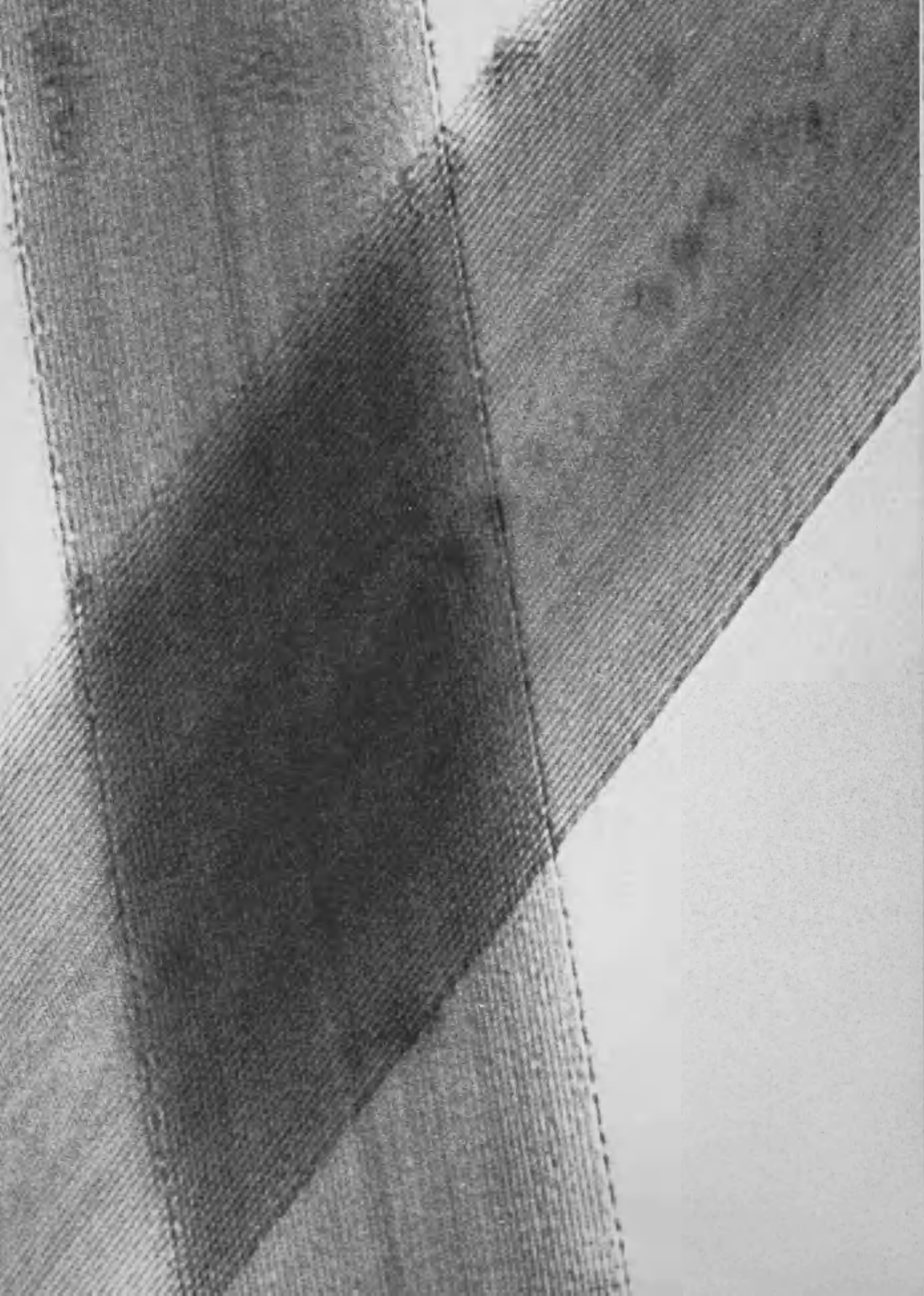

PLATE 49

Fibres of Rhodesian Chrysotile,
showing effect of electron beam
damage in the region AA'.
Magnification: 2,000,000X

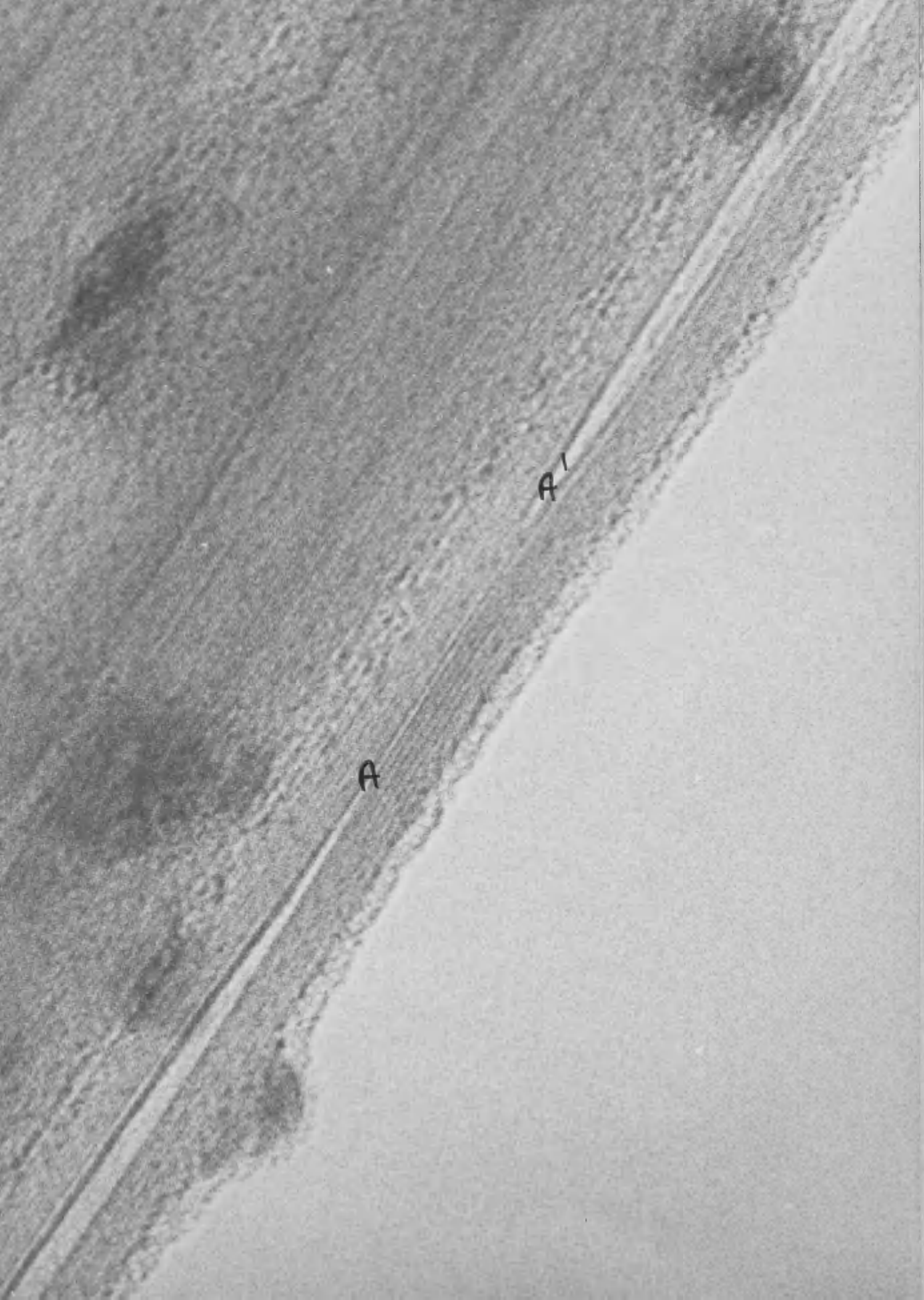
A'
A

PLATE 50

Same area as Plate 49 showing further irradiation damage.
Magnification: 2,000,000X

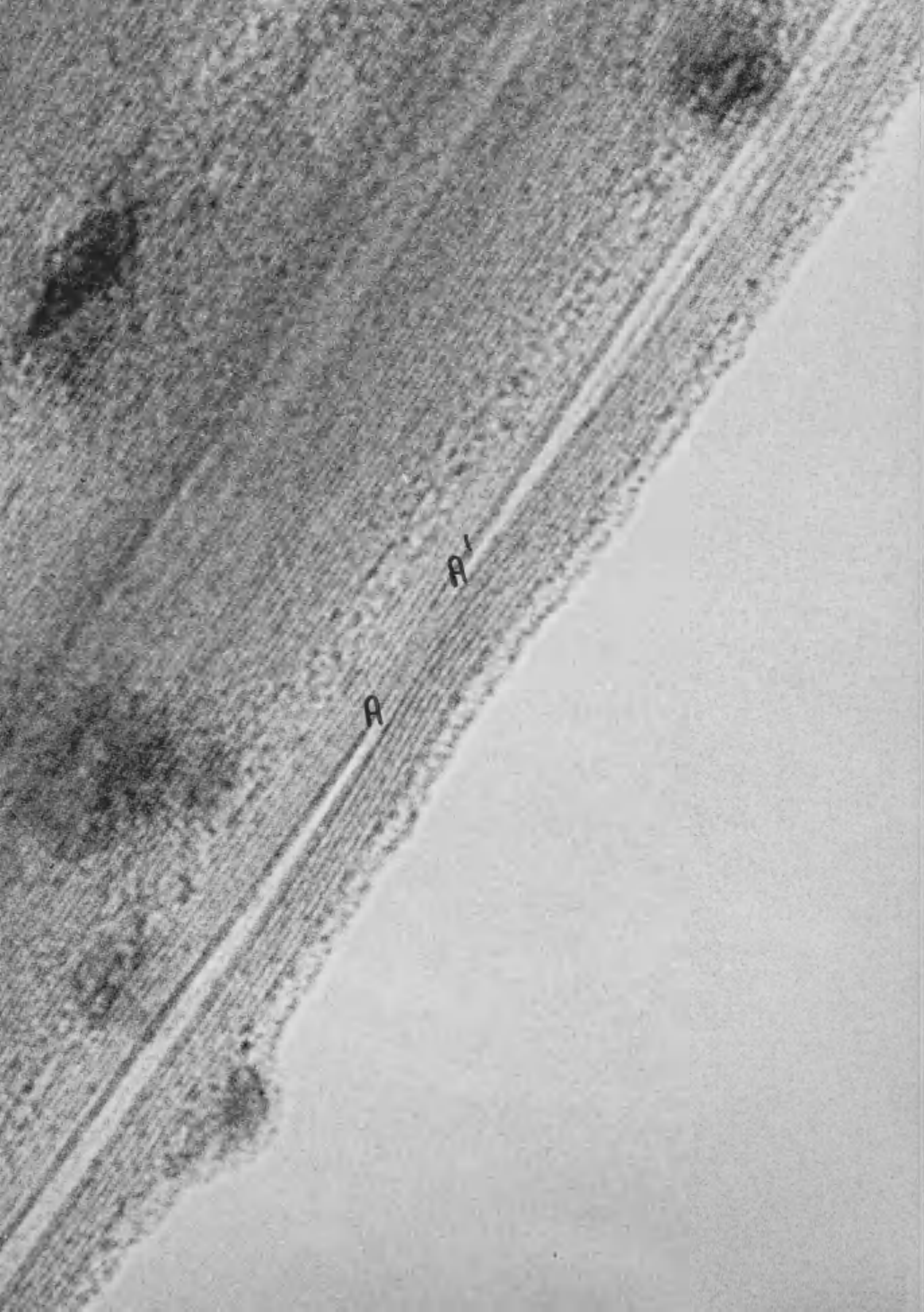
A'
A

PLATE 51

Same area as Plate 49, showing further irradiation damage.
Magnification: 2,000,000X

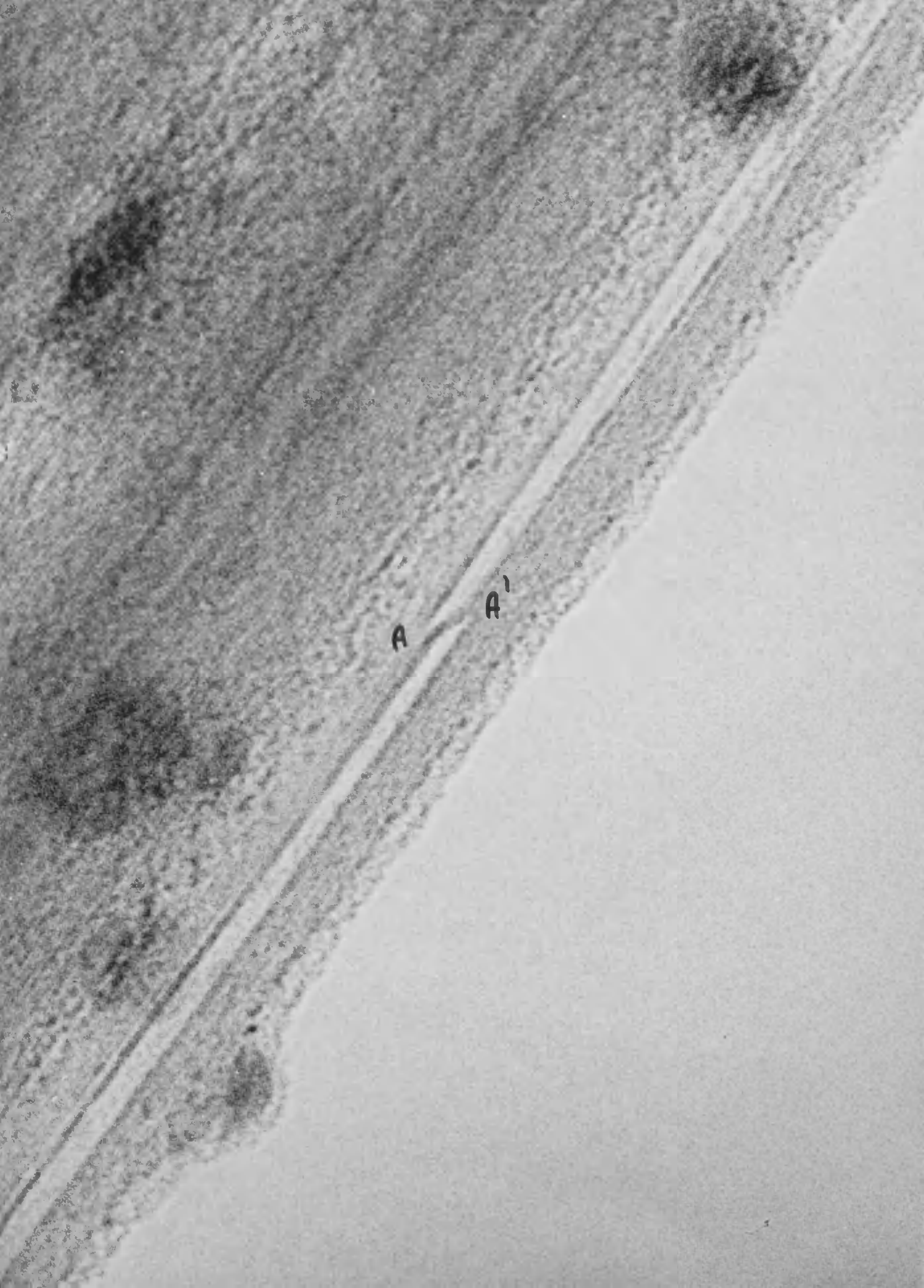
A
A'

In some fibres, however, the effect of beam damage was much more striking, and in a sequence of micrographs the planes could be observed actually coming apart. Such a sequence is shown in Plates 49, 50 and 51 where the time between each micrograph is approximately 10 seconds, with an exposure time of six seconds. The fibre involved has an outer diameter of 180 Å, an apparent inner diameter of approximately 35 Å, and consists of 7 layers, as shown. The exact nature of the defect around which the change takes place is not clear although it appears that an extra layer is involved between A and A'.

DISCUSSION:

RESOLUTION OF LATTICE IMAGES: Since the work of Menter (1956) it has been commonly believed that the fringe profiles observed in thin crystals, arising from the interaction of transmitted and (h k l) diffracted beams, correspond to the (h k l) lattice planes in the crystal. Extra terminating half-fringes are regarded as evidence for edge dislocations, and the technique of "lattice resolution" has been applied to the study of defect structures in thin crystals (Chadderton, 1962; Phillips and Hugo, 1968, 1970; Parsons, Hoelke and Rainville, 1968, 1969, 1970).

However, Cockayne, Ray and Whelan (1968) pointed out that a correct interpretation of fringe perturbations depends upon a knowledge of the phase relationship between the contributing beams and the perturbations were shown to be due to the variations in beam intensities and to the changes in the phase relationship between the diffracted beams, across the lower face of the crystal. Cockayne and Whelan (1970) have extended this work, calculating theoretical fringe profiles using the dynamical theory, and have shown that a one-to-one correspondence between lattice planes in the specimen, and the fringe distribution in the image, need not necessarily be true. On this basis then it is perhaps doubtful whether Yada (1967) was fully justified in suggesting that the c-parameter in clino-chrysotile was 7.3 rather than 14.6 Å.

The /

The fact that crystals were cylindrical would mean, however, that some of the (001) planes would always be in an appropriate orientation, when the fibres were normal to the beam.

An exact interpretation of the fringe perturbations shown in Plates 49 - 51 , as an electron beam damage effect, is not possible, although it seems reasonable that at least one extra plane is involved.

USE OF CHRYSOTILE AS A SPECIMEN SUPPORT: The high resolution study of chrysotile was carried out in order to evaluate the possible use of the fibres as a specimen support technique for the colloidal particles under investigation. There were a number of advantages which its use offered, over the use of the more conventional support films, and they include the following:-

(i) If the specimen could be supported between fibres, background-free micrographs may be obtained. Low resolution micrographs showing asbestos fibres as a support were mentioned by Hall (1953).

(ii) Since a Brucite layer, $Mg(OH)_2$, forms the outer layer of the cylindrical chrysotile lattice, the external curved surfaces will be composed entirely of hydroxyl groups, thus exerting a strongly attractive force towards positively charged species, such as were being studied in this work.

(iii) The (001) lattice planes ought to be readily resolvable, there being no orientation problems. These lattice images would serve as an internal calibration for size determination within the specimen.

Against such advantages, there were the following disadvantages:-

(i) Chrysotile fibres are unstable to intense electron beam irradiation.

(ii) There would be a tendency for the fibres to be mechanically unstable /

/ unstable, since, in order to avoid charging effects, they would not be supported by an underlying film.

Both of these problems were overcome by avoiding prolonged exposure of the specimen to the electron beam, the use of a low beam current, and the use of double condenser illumination.

FIBRE DIMENSIONS: Table 21 shows that the calculations of Whittaker (1957) give theoretical dimensions smaller than those found for most fibres. In general, the hollow centres are narrower and the overall diameters greater, than predicted. However, the measured dimensions correspond much more closely to the predictions of Kheiker et al (1967) and it would seem that these authors provide a more accurate study. It is also possible that varieties of chrysotile used in both these studies contained fibres of different average dimensions, which may account for the discrepancy, as in the present study, where the sample from Clinton corresponded quite closely to the dimensions given by Kheiker et al., whereas the Valmalenco sample was nearer to Whittaker's model.

APPENDIX

HYDROLYSIS OF THORIUM

HYDROLYSIS OF THORIUM

The hydrolysis of thorium has been less widely studied than that of zirconium. In one of the earliest studies, Denham (1908) measured pH in various $Th(SO_4)_2$ solutions. He found that the pH varied with time, which immediately presented a complication in the interpretation. Hildebrand (1913) and Britton (1925) titrated Th IV salt solutions with base, in an attempt to investigate the precipitation of the hydroxide, or of basic salts. However, both the Ionic Strength and thorium concentration varied, and quantitative results were rather inconclusive.

Chauvenet and Tonnet (1930) carried out conductimetric and calorimetric measurements on the addition of hydroxyl to the $Th\ Cl_4$ solutions and concluded that, as pH increased, the following hydrolysis took place:-

$$Th^{4+} + 4H_2O \longrightarrow Th\ (OH)_2^{2+} + 2H_3O^+$$

A similar scheme was postulated by Chauvenet and Soteyrand-Franck (1930) for the hydrolysis of Th^{4+} as the nitrate.

On the other hand Kasper (1941), on the basis of his e.m.f. studies of base hydrolysis of $Th(NO_3)_4$, suggested that $Th(OH)^{3+}$ was formed.

The first suggestion of polymeric Th(IV) ions was made by Schaal and Fouchère (1947), who performed e.m.f. measurements on thorium perchlorate and nitrate solutions. They assumed that the following reaction occurred -

$$nTh^{4+} + 2nOH^- \longrightarrow (ThO)_n^{2n+} + nH_2O$$

and from /

/ and from the data obtained, concluded that n had a likely value of four. Souchay (1948) claimed that his freezing-point measurements on thorium nitrate solutions supported the existence of a tetrameric Th (IV) species.

The first real evidence for polymeric Th(IV) ions was the analysis of the crystal structure of a basic thorium salt, Th $(OH)_2CrO_4.H_2O$, by Lundgren and Sillen (1949) in which the thorium ions were linked by hydroxyl bridges to form chains, as shown in figure 30 with the composition $\left[\mathrm{Th}\ (OH)_2^{2+}\right]_n$. Layers of these chains were linked by the CrO_4^{2-} counterions. Lundgren (1950) was able to demonstrate the existence of similar chains in Th $(OH)_2SO_4$.

Dobry, Guinand and Mathieu-Sicaud (1953) studied amorphous thorium hydroxide using a variety of techniques which included viscosity measurements, light scattering, and electron microscopy. The claim was made that the colloidal particles consisted of chains 18 Å thick, with an average length 700 Å. The authors suggested that these could represent bundles of 20 to 30 of the $\left[\mathrm{Th}\ (OH)_2^{2+}\right]$ chains found in the basic Th IV salts by Lundgren and Sillen (1949, 1950). Although the electron microscope evidence was supported to some extent by the other measurements, the authors pointed out that the microscope used, an R.C.A. - E.M.U.2.D. had a resolving power of only 18 - 20 Å, so that an exact interpretation of the electron micrographs was difficult. The possibility that the specimen preparation method, dipping carbon coated grids into a dilute suspension, would have an effect on the morphology was not discussed.

An extensive series of potentiometric measurements was carried out by Kraus and Holmberg (1954), on Th (IV) in perchlorate, and chloride solutions. From measurements carried out in 1M $NaClO_4$, they concluded that Th $(OH)_2^{2+}$ and $Th_2(OH)_2^{6+}$ were formed, while the species $Th(OH)^{3+}$ was unstable. There was some evidence that more highly polymerized species were also present but it was felt that there were insufficient data available to establish their identity.

FIGURE 30

$[Th(OH)_2]_n^{2n+}$ chains in $Th(OH)_2SO_4$.

(After Lundgren, 1950)

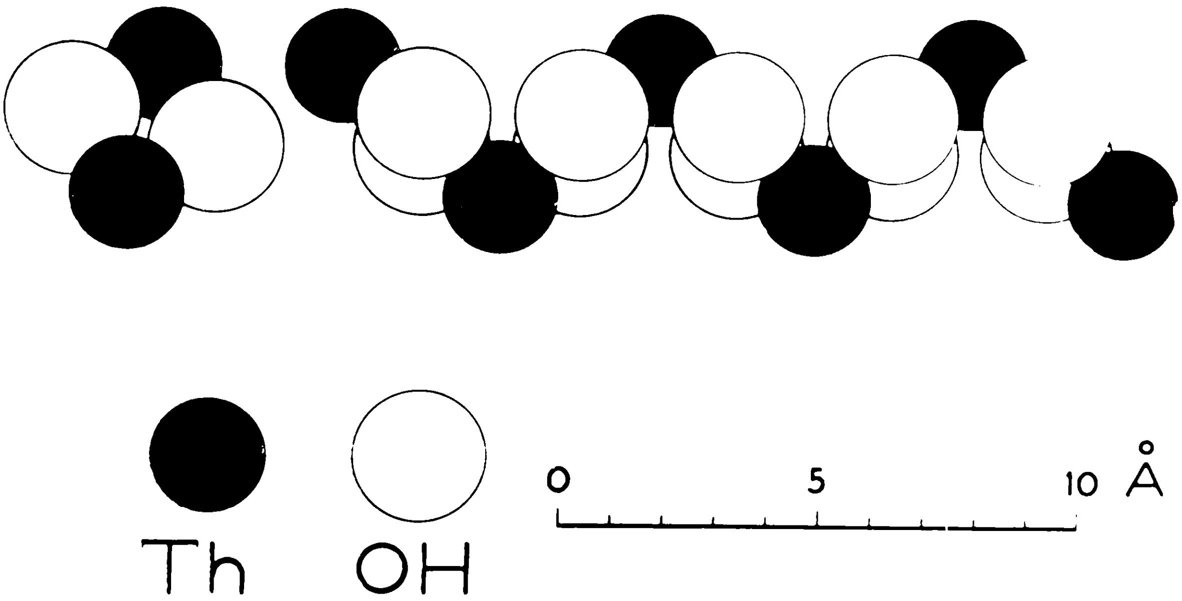
Th
OH
0
5
10 Å

In a similar study by Hietanen and Sillen (1954, 1956) a "core and link" mechanism was developed, as first carried out by Graner and Sillen (1947) for the hydrolysis of Bi-III perchlorate. The pH data (1954, 1956) was interpreted in terms of this mechanism and a series of complexes of the form

$$Th\left[(OH)_3Th \right]_n^{(4 + n)+} , \text{ or } Th_x(OH)_{3x - 3}^{(x + 3)+} ,$$

were postulated.

Lefebvre (1958) examined the data by Kraus and Holmberg (1954) and Hietanen (1954, 1956) and concluded that a simpler scheme would account adequately for both sets of observations. He suggested that only three polymeric species were involved:

$$Th(OH)_2^{2+} , \quad Th_2(OH)_2^{6+} \text{ and } Th_5(OH)_{12}^{8+} .$$

The first two complexes belonged to the series proposed by Kraus and Holmberg, the third belonging to the system of Hietanen.

Although the evidence for polymeric Th IV species in solution was well documented, the idea that Th IV was only monomeric still lingered, and indeed evidence was put forward that this was the case. Pan and Taseu (1955) carried out pH measurements of 0.05 - 0.5 M $Th(No_3)_4$ in $NaClO_4$ and, although they agreed that tetrapositive ions usually showed a strong tendency to polymerize on hydrolysis, they concluded that, in the system studied, only Th^{4+}, $Th(OH)^{3+}$ and $Th(OH)_2^{2+}$ were present. Similar conclusions were reached by Matijevic, Abramson, Schultz and Kerker (1960), from coagulation studies of $Th(NO_3)_4$ solutions. They suggested the following equilibrium:-

$$Th(H_2O)_x^{4+} + H_2O \rightleftharpoons \left[Th(H_2O)_{x+}(OH)\right]^{3+} + H_3O^+$$

and as pH was increased the dimerization:-

/ -

/ $$2\left[Th(H_2O)_{x-1}(OH)\right]^{3+} \rightleftharpoons \left[Th\ (H_2O)_{x-1}(OH)\right]^{6+}$$

was suggested as being likely.

Bilinksi et al (1963), from turbidity and pH measurements, suggested the principal species in Th IV solutions were Th^{4+} and $\left[Th(OH)_2\right]_n^{2n+}$, with Th $(OH^{3+}$ an additional possibility, while ion exchange studies by Zhukov et al (1962, 1963) led them to propose the form $\left[Th(OH)_4Th\right]_n^{4n+}$.

Hentz and Tyree (1965), studying aqueous solutions of Th (IV) perchlorate, found a continuous series of polymers. With n, the average number of hydroxyls per Th IV ion, between 1.5 and 2.0, binuclear, and tri-nuclear species were formed. This eventually led to the formation of large particles, with the precipitation of hydrous oxides or basic salts with n greater than 3. Polymers of intermediate weight were formed when n was between 2 and 3.

To account for pH and solubility measurements of Th (IV) in 1$\underline{M}$ $NaClO_4$, Baes, Meyer and Roberts (1965) postulated four possible series of polymers, with a general composition:-

$$Th_x\ (OH)_y\ ^{(4x - y)^+}$$

with the following sets of , y values being consistent with the data.

(i)	x, y =	1,1	1,2	2,2	5,12	
(ii)		1,1	1,2	2,3	6,15	
(iii)		1,1	1,2	2,2	3,6	6,15
(iv)		1,1	1,2	2,2	4,8	6,15

There is a close similarity between this work and that of Hietanen (1954d, 1950) and Kraus and Holmberg (1954), although neither of these studies showed evidence for $Th(OH)^{3+}$

/-

Larsen and Brown (1964) studied X-ray scattering in acid solutions of $Th(NO_3)_4$ and since the radial distribution curves showed no evidence of Th - Th interactions, it was presumed that only monomers were present as stable species. Similarly, Bacon and Brown (1969) found only evidence for mononuclear species in perchloric acid solutions of Th(IV) perchlorate. The Th-O distance of 2.50 Å, showed evidence of 11 interactions, suggesting 11-fold coordination around each Th IV ion. In an aqueous solution of the oxyperchlorate, however, a Th - Th distance of 4.00 Å was found, with evidence for each Th IV ion having three nearest neighbour Th IV ions. This led Bacon and Brown to propose a tetrahedral model, having Th IV ions at the apices, linked along the edges by six hydroxyls, with the formula $Th_4(OH)_6^{10+}$. Although the Th - Th distance in this complex of 4.00 Å was very close to the Th - Th distance in cubic ThO_2 (3.96 Å) the two species are not directly related, their geometry being quite different.

Much of the published work on thorium hydrolysis is consistent with a chain structure, thorium (IV) ions being bound together by hydroxide bridges. Many reports, however, give evidence for monomers only and it seems that the polymerization is controlled by the conditions prevailing in the solution. Thus acid solutions of thorium nitrate show mainly evidence for monomers and dimers, whilst in perchlorate solutions there appears to be evidence for higher polymers.

RESULTS OF PRELIMINARY INVESTIGATION

In the present work the electron microscope study was extended to the hydrolysis of Thorium (IV), in order to test the applicability of the high resolution technique to other systems. 0.1 M solutions of $Th(NO_3)_4.5H_2O$ and $ThCl_4(\propto H_2O)$ were used as starting materials. One particular difficulty in the initial stages was that both the nitrate and the chloride did not recrystallize easily from water, so that identification of initial crystalline material was not possible.

Whilst a fresh solution of zirconyl chloride gave no observable deposit on chrysotile fibres, a fresh solution, of thorium nitrate, gave extensive areas of chain-like material suspended between fibres. (In the study of thoria, a 200 μ objective aperture was used in order to increase phase contrast effects.) Plate 52 shows such chains, which are about 80 Å in width. The central parts of the chains, 40 Å thick, appear much more electron dense and it is concluded that they represent a higher concentration of thorium atoms. Features in the 5 - 10 Å range were reproducible in successive micrographs. The fresh solution had a pH of 2.24, which remained unchanged after one hour or reflux. In the microscope, however, structural changes were revealed, in that larger, coherent sheets were now observed, as shown in Plate 53. Here, and in other micrographs, the sheets are seen to contain a chain-like substructure, the "chains" being approximately 6 Å in diameter. These may in fact represent the $\left[Th(OH)_2^{2+}\right]$ chains found in basic thorium salts by Lundgren and Sillen (1949, 1950), since they are of a comparable apparent diameter. However, without a knowledge of the defocus value, Δ Lo, and other factors, as described earlier it is not possible to give an accurate interpretation. However, the reproducibility of these structural features does suggest that they may be real. A sample refluxed for six hours, by which time the pH was 2.21, showed signs of aggregation, as a slow increase in opalescence, and /

PLATE 52

Colloidal thoria, from a fresh $Th(NO_2)_4$ solution.
Magnification: 2,000,000X

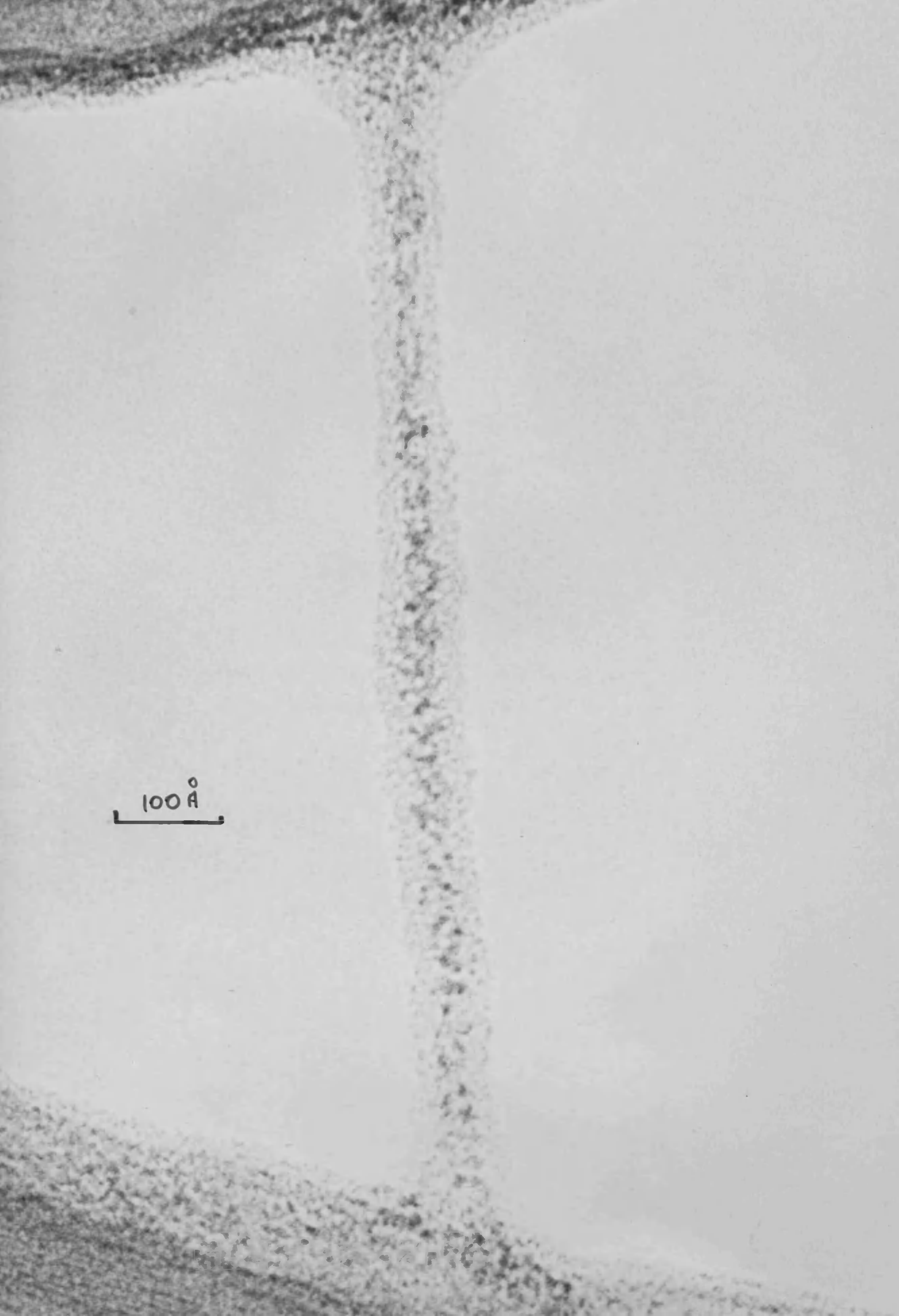
100 Å

PLATE 53

Colloidal thoria after one
hour reflux of $Th(NO_3)_4$ solution.
Magnification: 2,000,000X

/ and also in terms of the observable features in the microscope. Plate 54 shows several such aggregates, as at 'X' and 'Y'. There was as yet no evidence of crystalline thoria. Prolonged reflux brought about crystallization, the final product being shown to be cubic ThO_2, in a hydrous form. The electron diffraction results are presented in Table 21.

Table 21.

d (measured)	d (ThO_2)
3.24 Å	3.23
2.83	2.80
2.00	1.98
1.71	1.69
1.41	1.40
1.29	1.28

Crystalline particles of thoria are shown in Plate 55. It was observed that these particles are much less regular than those of crystalline zirconia and occur over a wide size range. Essentially similar results were found for the hydrolysis of thorium chloride.

DISCUSSION

No model has yet been devised to account for the structural changes occurring during the hydrolysis of thorium salts and the transformation from amorphous to crystalline thoria, although numerous studies of thoria have been made, as by Prasad, Beasley and Milligan (1967). Without such a model, it is difficult to propose a sequence of events, based entirely upon electron micrographs. It would appear, however, that the films of colloidal thoria are quite different from thos of amorphous zirconia. In particular any suggestion of chain structure in /

PLATE 54

Aggregation in colloidal thoria, after six hours reflux of $Th(NO_3)_4$.
Magnification: 2,000,000X

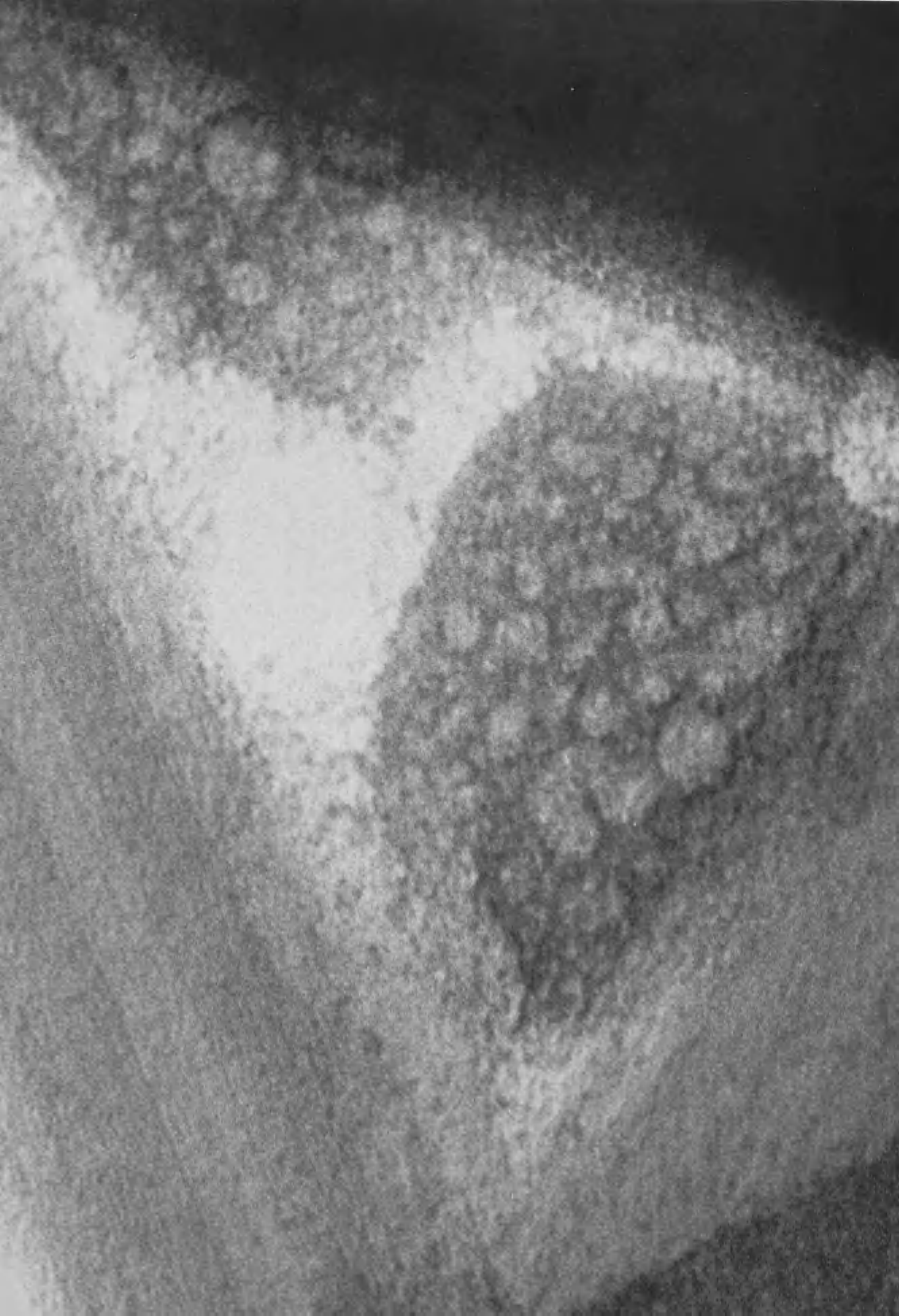

PLATE 55

Crystalline thoria particles,
after prolonged reflux of
$Th(NO_3)_4$.
Magnification: 2,000,000X

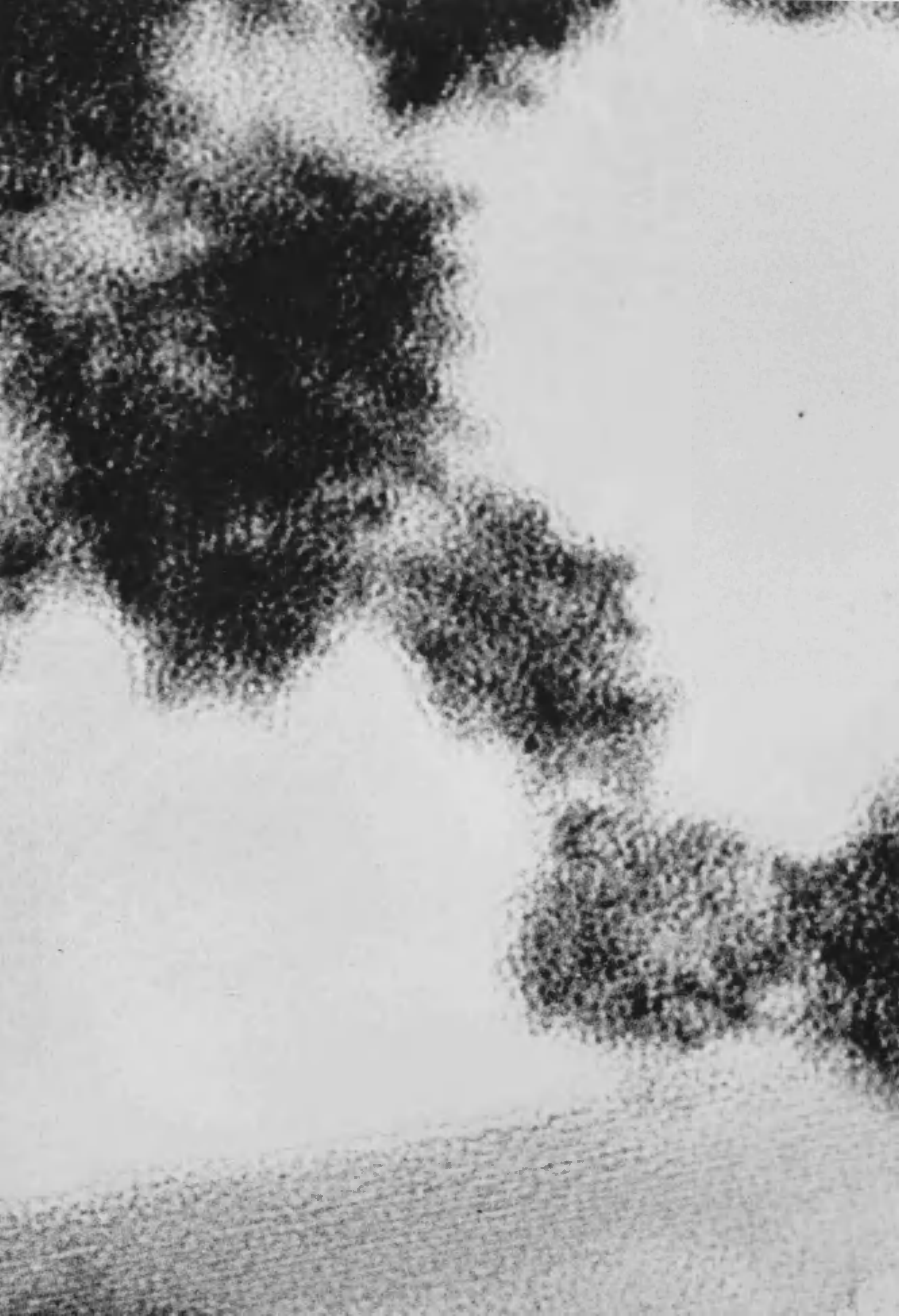

/ in zirconia is not at all pronounced, whereas in the thoria films there is abundant evidence for this.

Cross-linking of thoria chains may take place more or less at random, whilst the formation of zirconia sheets, and their cross-linking, is to some extent more controlled by the structure of the initial tetramer, $\left[Zr(OH)_2 4H_2O\right]_4^{8+}$. Elimination of water from aggregates of thoria chains will eventually give the hydrated ThO_2, which is identifiable in the terminal stages of the hydrolysis.

BIBLIOGRAPHY

BIBLIOGRAPHY

(a) ZIRCONIUM

ADAM, J. & ROGERS, M.D., Acta Cryst., 12 951 (1959).

ADOLF, M. & PAULI, W., Kolloid-Z., 29 173 (1921).

AMPHLETT, C.B., MCDONALD, L.A. & REDMAN, M.J., J. Inorg. Nucl. Chem., 6 236 (1958).

ANGSTADT, R.L. & TYREE, S.Y., J. Inorg. Nucl. Chem., 24 913 (1962).

Van ARKEL, A.E., Physica, 4 286 (1924).

BLUMENTHAL, W.B., Ind. Eng. Chem., 46 528 (1954).

BLUMENTHAL, W.B., "The Chemical Behaviour of Zirconium", Princetown, New Jersey (1958).

BOHM, J. & NICLASSEN, H., Z.anorg. allgem. Chem., 132 6 (1924).

BRITTON, H.T.S., J. Chem. Soc., 127 2120 (1925).

BRITZ, D. & NANCOLLAS, G.H., J. Inorg. Nucl. Chem., 31 3861 (1969).

CABANNES-OTT, C., Ann. Chim., 5 905 (1960).

CHAUVENET, E., Comptes Rendus 154 821, 1234 (1912).

CHAUVENET, E., Comptes Rendus 164 630 (1917).

CHAUVENET, E., Ann. Chim., 13 59 (1920).

CLABAUGH, W.S. & GILCHRIST, R., J. Am. Chem. Soc., 4 2104 (1952)

CLARK, G. & REYNOLDS, D.H., Ind. Eng. Chem., 29 711 (1937).

CLEARFIELD, A. & VAUGHAN, P.A., Acta Cryst., 9 555 (1956).

CLEARFIELD, A., Rev. Pure & Appl. Chem., 14 91 (1964).

CLEARFIELD, A., Inorg. Chem., 3 146 (1964).

CLEARFIELD, A., Private Communication (1969).

COHN, W.M., Trans. Electrochem. Soc., 68 65 (1935).

COHN, W.M. & TOLKSDORF, S., Z.physik.Chem., (B) 8 331 (1930).

CONNICK, R.E. & MCVEY, W.H., J. Am. Chem. Soc., 71 3182 (1949).

CONNICK, R.E. & REAS, W.H., J. Am. Chem. Soc., 73 1171 (1951).

CURTIS, C.E., DONEY, L.M. & JOHNSON, Z.R., J. Am. Ceram. Soc., 37 458 (1954).

DOI, K., Bull. Soc. Franc. Mineral Crist., 89 (2) 216 (1966).

DUWEZ, P. & ODELL, F., J. Am. Ceram. Soc., 33 274 (1950).

DUWEZ, P., ODELL, F., & BROWN, F.H., J. Am. Ceram. Soc., 35 107 (1952).

ERMAKOV, A.N., MAROV, I.N. & BELYAEVA, V.K., Zh. Neorg. Khim., 8 (7) 1623 (196

FISCH, H.A., KINDNESS, C.A. & LANDIS, F.P., "Application of I.R. techniques to the study of Corrosion Film in Zircaloy" KAPL - 2052 (1959).

GARVIE, R.C., J. Phys. Chem., 69 (4) 1238 (1965).

GILLESPIE, R.J., Can. J. Chem., 39 2336 (1961).

GOROSHENKO, Ya G. & SPASIBENKO, T.P., Russ. J. Inorg. Chem., 7 (5) 595 (1962).

GOROSHENKO, Ya G. & SPASIBENKO, T.P., Russ. J. Inorg. Chem., 12 156 (1967).

GRANÉR, F. & SILLÈN, L.G., Acta Chem. Scand., 1 631 (1947).

HAIRE, R.G. & WILLMARTH, T.E., 7th Int. Congr. Electron Microscopy (Grenoble) 1 385 (1970).

HOYASHI, T. & DOIHARA, T., Japan 68 19,877.

JANDER, G. & JAHR, K.F., Kolloid-B. 43 295 (1935).

JOHNSON, J.S. & KRAUS, K.A., J. Am. Chem. Soc., 78 3937 (1956).

KOMISSAROVA, L.N., Russ. J. Inorg. Chem., 5 281 (1960).

KOMISSAROVA, L.N., SIMANOV, Ya.P. & VLADIMIROVA, Z.A., Russ. J. Inorg. Chem., 5 687 (1960).

KRAUS, K.A. & JOHNSON, J.S., J. Am. Chem. Soc., 75 5769 (1953).

KRAUS, K.A. & TYREE, S.Y., Chem. Div. 1/4 y report ORNL - 499 (1949) 26.

LANGE, H., Z. Naturwiss., 82 1 (1910).

LAUBENGAYER, A.W. & EATON, R.B., J. Am. Chem. Soc., 62 2704 (1940).

LARSEN, E.M. & GAMMIL, A.M., J. Am. Chem. Soc., 72 3615 (1950).

LISTER, B.A.J. & MCDONALD, L.A., J. Chem. Soc., 1952 4315.

LIVAGE, J., Bull. Soc. Chim. Fr., 1968 507.

LIVAGE, J. et al, J. Am. Ceram. Soc., 51 349 (1968).

LUNDGREN, G., Svensk. Kemisk. Tidskrift, 71 200 (1959).

MCCULLOUGH, J.D. & TRUEBLOOD, K.N., Acta Cryst., 12 507 (1959).

MATIJEVIC, E., MATHAI, K.G. & KERKER, M., J. Phys. Chem., 66 1799 (1962).

MISSENDEN, J., Chem. News, 124 326 (1922).

MUHA, G.M. & VAUGHAN, P.A., J. Chem. Phys., 33 194 (60).

MURRAY, P. & ALLISON, E.B., Trans. Brit. Ceram. Soc., 53, 335 (1954).

NÁRAY-SZABO, S.V., Z. Krist, 94 414 (1936).

PASCAL, P., "Traité de Chimie Minerale", Masson & Co. Paris 1931.

PASSERINI, L., Gazz. chim. ital., 60 762 (1930).

PAYKULL, S.R., Ber., 6 1467 (1873).

PRAKASH, S., J. Ind. Chem. Soc., 9 193 (1932).

PRAKASH, S., Ind. J. Phys., 8 231 (1933).

PRAKASH, S., Ind. J. Phys., 8 243 (1933).

ROBINSON, F.J. & AYRES, G.H., J. Am. Chem. Soc., 55 2288 (1933).

ROY, A.P., J. Chim. Phys., 65 (3) 475 (1968).

RUER, E., Z.anorg. Chem., 43 282 (1905).

RUFF, O. & EBERT, F., Z.anorg. allgem. Chem., 180 19 (1929).

SCHMID, P., Z.anorg, Chem., 167 369 (1927).

SHARMA, R.D. & DHAR, N.R., J. Ind. Chem. Soc., 9 455 (1932).

SMITH, D.K. & NEWKIRK, H.W., Acta Cryst., 18 983 (1965).

SPASIBENKO, T.P. & GOROSCHENKO, Ya.G., Russ. J. Inorg. Chem., 14 757 (1969).

TANANAEV, I.V. & BOKMELDER, M.Y., Zh. Neorg. Khim., 3 1273 (1958).

THOMAS, A.W., "Colloid Chemistry", New York (1934).

THOMAS, A.W. & OWENS, H.S., J. Am. Chem. Soc., 57 1825 (1935).

VENABLE, F.P., J. Am. Chem. Soc., 16 469 (1894).

VENABLE, F.P., "Zirconium and its compounds", New York (1922).

VENABLE, F.P. & BASKERVILLE, C., J. Am. Chem. Soc., 20 119 321 (1898).

VENABLE, F.P. & JACKSON, D.H., J. Am. Chem. Soc., 42 2531 (1920).

VIVIEN, D., LIVAGE, J. & MAZIÈRES, C., J. Chem. Phys., 1970 199.

VIVIEN, D., LIVAGE, J., MAZIÈRES, C., GRADSZTAJN, S. & CONARD, J., J. Chim. Phys., 1970 205.

WEBER & SCHWARTZ, Ber.d.keram ges., 34 391 (1957).

WILLIAMS-WYNN, D.A., J.Phys. Chem., 63 2065 (1959).

WITTILS, M.C. & SCHIMMIL, F.A., J. Appl. Chem., 27 643 (1956).

YARDLEY, K., Min. Mag., 21 168 (1926).

ZEILEN, A.J. & Connick, R.E., J. Am. Chem. Soc., 78 5785 (1956).

(b) ELECTRON MICROSCOPY

AGAR, A.W., Brit. J. Appl. Phys., 11 185 (1960).

ANDREWS, K.W., DYSON, D.J. & KEOWN, S.R., "Interpretation of Electron Diffraction Patterns", London (1967).

BASSETT, G.A. & MENTER, J.W., Phil. Mag., 2 1482 (1957).

BOIKO, B.T., PALATNIK, L.S. & DERVYANCHENKO, A.S., Dokl. Akad. Nauk. SSSR, 179 316 (1967).

BRADLEY, D.F., Brit. J. Appl. Phys., 5 65 (1954).

BUSCH, H., Ann Phyzik, 81 974 (1926).

CHADDERTON, L.T., Proc. 5th Int. Congr. Electron Microscopy (Philadelphia) 1962 G - 9.

COCKAYNE, D.J.H., RAY, I.L.F. & WHELAN, M.J., Proc. 4th Eur. Conf. Electron Microscopy (Rome) 1 129 (1968).

COCKAYNE, D.J.H. & WHELAN, M.J., Proc. 7th Int. Congr. Electron Microscopy (Grenoble) 1 29 (1970).

COSSLETT, V.E., "Practical Electron Microscopy", London (1951).

CREWE, A.V., New Scientist, July 9th (1970).

DOWELL, W.C.T., 5th Int. Congress for Electron Microscopy (Philadelphia) 1962 KK - 12.

DOWELL, W.C.T., Abhandl. Fritz-Haber Inst. Max Planck Ges. Berlin.Dahlen, 39 233 (1962).

DOWELL, W.C.T., FARRANT, J.L. & WILLIAMS, R.C., Proc. 6th Int. Congr. for Electron Microscopy (Kyoto) 1 635 (1966).

ENNOS, A.E., Brit. J. Appl. Phys., 5 27 (1954); 4 101 (1953).

FERNÁNDEZ-MORÁN, H., Proc. Nat. Acad. Sci. U.S., 56 801 (1966).

FERNÁNDEZ-MORÁN, H., Proc. 6th Int. Congr. Electron Microscopy (Kyoto) 1 13 (1966).

FERNÁNDEZ-MORÁN, H., Proc. 6th Int. Congr. Electron Microscopy (Kyoto) 1 27 (1966).

GRIVET, P., Biochim et Biophys. Acta, 7 1 (1951).

HAINE, M.E., "Electron Microscopy", New York (1961).

HAINE, M.E. & MULVEY, T., Proc. Third Int. Conf. on Electron Microscopy (London) 1954 698.

HALL, C.E. "Introduction to Electron Microscopy", London (1953).

HANSEN, K.J. & MORGENSTEIN, B., Z.ang. Phys., 19 215 (1965).

HEIDE, H.G., J. Cell Biol., 13 147 (1962).

HEIDE, H.G., Z.ang. Phys., 15 116 (1963); 17 70, 73 (1964).

HEIDE, H.G., Proc. 4th Int. Congr. Electron Microscopy (Berlin) 1 82 (1958).

HEIDENREICH, R.D., Bell System Tech. Journal, 45 65 (1965).

HEIDENREICH, R.D., Bell System Tech. Journal, 45 (4) 657 (1966).

HEIDENREICH, R.D., J. Electron Microscopy, 16 23 (1962).

HEIDENREICH, R.D., Bell System Tech. Journal, 47 265 (1968).

HEIDENREICH, R.D., J. Electron Microscopy, 16 (1) 23 (1967).

HEIDENREICH, R.D., Siemens Review, 34 1 (1967).

HEIDENREICH, R.D., HESS, W.M. & BANN, L.L., J. Appl. Cryst., 1 1 (1968).

HIBI, T., Proc. Int. Conf. on Electron Microscopy, (London) 1954 636.

HIBI, T., 5th Int. Congr. Electron Microscopy (1962). KK-1

HILLIER, J., J. Appl. Phys. 19 226 (1948).

HIRSCH, P.B., HOWIE, A., NICHOLSON, R.B., PASHLEY, D.W. & WHELAN, M.J., "Electron Microscopy of Thin Crystals", London (1965).

HOPPE, W., Naturwiss., 48 736 (1961); Optik, 20 599 (1963).

KAMIYA, Y. & UYEDA, R., J. Phys. Soc. Japan, 16 1361 (1961).

KIKUTCHI, Y., Hitachi Sales & Service Information, 93 (1967).

KNOLL, M. & RUSKA, E., Ann. d. Physik, 12 607 (1932).

KONIG, H., Z.Phys., 129 483 (1951).

LANGER, R. & HOPPE, W., Optik, 24 470 (1967).

LE POOLE, J.B., Philips Techn. Rundech, 9 33 (1947).

LENZ, F., Z. Naturf., 9a 185 (1954).

LENZ, F., Z.Physik, 172 498 (1963).

LENZ, F. & SCHEFFELS, W., Z. Naturf., 13 226 (1958).

LOCQUIN, M., Z. wiss Mikr., 62 220 (1955).

LOCQUIN, M. & BESSIS, M., C.R. Soc. Biol. Paris, 142 1947 (1948).

MENTER, J.W., Proc. Roy. Soc., (A) 236 119-135 (1956).

PARSONS, J.R. & HOELKE, C.W., J. Appl. Phys., 40 866 (1969).

PARSONS, J.R., HOELKE, C.W. & RAINVILLE, M., Proc. 4th Eur. Reg. Conf. Electron Microscopy (Rome) 1 133 (1968); 7th Int. Congr. Electron Microscopy (Grenoble) 1 31(1970).

PHILLIPS, R., Brit. J. Appl. Phys., 11 504 (1960).

PHILLIPS, V.A. & HUGO, J.A., Appl. Phys. Letters, 13 67 (1968).

PINES, D., Rev. Mod. Phys. 28 184 (1956); "Elementary Excitations in Solids," New York (1963).

RIEKE, W.D., Optik, 18 278, 373 (1961).

RUSKA, E., Proc. 3rd Int. Conf. on Electron Microscopy 673 (1954).

SCHOTT, O. & LEISEGANG, S., Proc. Eur. Reg. Conf. Electron Microscopy (Stockholm) 27 (1956).

STABENOW, J., Siemens Review, XXXV 24 (1968).

THON, F., Eg-Berichte, 1 52 (1964).

THON, F., Z.Naturf., 20a 154 (1965), 21a, 476 (1966).

THON, F., Proc. 4th Eur. Conf. Electron Microscopy (Rome) 1 127 (1968).

Van DORSTEN, A.C. & PREMSELA, H.F., Proc. 6th Int. Congr. Electron Microscopy(Kyoto)(1966) 1 21.

Von BORRIES, B. & RUSKA, E., Zwiss Mikøroscop, 56 317 (1939).

Von BORRIES, B. & KAUSCHE, G.A., Kolloid - Z., 90 132 (1940).

WATSON, J.H.L., J. Appl. Phys., 18 153 (1947).

WHELAN, M.J., J. Inst. Metals, 87 392 (1959).

YADA, K. & HIBI, T., Proc. 4th Eur. Conf. Electron Microscopy (Rome) 1 143 (1968).

YADA, K. & HIBI, T., (Jap) J. Electronmicroscopy, 18 266 (1969).

ZWORYKIN, V.K., MORTON, G.A., RAMBERG, E.G., HILLIER, J. & VANCE, A.W., "Electron Optics & the Electron Microscope", New York 1945.

(c) CHRYSOTILE.

ANDERSON, H.V. & CLARK, G.L., Ind. Eng. Chem., 21 924 (1929).

ARUJA, E., Ph.D. Thesis, Cambridge (1943).

BALL, M.C. & TAYLOR, H.F.W.. Min. Mag., 32 754 (1961).

BATES, T.F. & COMER, J.J. "Clays and Clay Minerals", New York (1959).

BATES, T.F., SAND, L.D. & MINK, J.F., Science, 111 512 (1950).

BRINDLEY, G.W., "X-ray Identification & Xtal. Structures of Clay Minerals," ch. 2. London (1952).

BRINDLEY, G.W., & HAYAMI, R.Min. Mag. 35 189 (1965).

DEER, W.A., HOWIE, R.A. & ZUSSMAN, J., Rock Forming Minerals, vol1 (1962) vol.2 (1963).

HILLIER, J. & TURKEVITCH, J., Anal. Chem., 21 475 (1949).

JAGODZINSKI, H. & KUNZE, G., Neues Jb.Min.Mh., 95, 113, 137 (1954).

KHEIKER, D.M., FLANTSBAUM, I.M. & BUBELEVA, L.V., Kristillografiya, 12 430 (1967).

NOLL, W. & KIRCHER, H., Naturwiss., 37 540 (1950).

PADUROW, N.N., Acta Cryst., 3 200 (1950).

PUNDSACK, F.L., J.Phys.Chem., 60 361 (1956).

PAULING, L., Proc. Nat. Acad. Sci., 16 578 (1930).

WARREN, B.E. & BRAGG, W.L., Z. Krist., 76 201 (1930).

WARREN, B.E. & HERING, K.W., Phys.Rev., 59 925 (1941).

WHITTAKER, E.J.W., Brit. J. Appl. Phys., 1 162 (1950).

WHITTAKER, E.J.W., Acta Cryst., 4 187 (1951)., 6 647 (1953); 7 827 (1954); 8 571 (1955); 9 855, 862, 865 (1956); 10 149 (1957).

WHITTAKER, E.J.W. & ZUSSMAN, J., Min. Mag., 31 107 (1956).

YADA, K., Acta Cryst., 23 (5) 704 (1967).

YADA, K., 7th Int.Congr. of Electron Microscopy 2 629 (1970.

ZUSSMAN, J., BRINDLEY G.W. & COMER, J.J., Amer. Min. 42 133 (1957).

(d) THORIUM

BACON, W.E. & BROWN, G.H., J. Phys. Chem.,73 4163 (1969).

BAES, C. F., MEYER, N.J. & ROBERTS, C.E., Inorg. Chem.,4 518 (1965).

BILINSKI,H.,Croat.Chem. Acta,35 19 (1963).

BRITTON, H.T.S., J. Chem. Soc.,127 2110 (1925).

CHAUVENET, E. & TONNET, J., Bull. Soc. Chim. Fr.,47 701 (1930).

DENHAM, H.G., J. Chem. Soc.,93 62 (1908).

DOBRY, A., GUINAND, S. & MATHIEU-SICAUD,A.,J. Chim. Phys.,50 501 (1953).

HENTZ, F.C. & TYREE, S.Y., Inorg. Chem.,4 873 (1965).

HIETANAN, S. & SILLÉN, L.G., Acta Chem. Scand.,8 1607 (1954).

HIETANEN, S., Acta Chem. Scand.,8 1626 (1954).

HIETANEN, S., Rec. trav. chem.des Pays-Bas,75 711 (1956).

HIETANEN, S. & SILLÉN, G., Acta Chem. Scand.,13 533 (1959).

HILDEBRAND, J.H., J. Am. Chem. Soc.,35 865 (1913).

KASPER, J., Diss.,John Hopkins Univ.,Baltimore Md. (1941).

KRAUS, K.A. & HOLMBERG, R.W., J. Phys. Chem.,58 325 (1954).

LARSEN, R.D. & BROWN, G.H., J. Phys. Chem.,68 3060 (1964).

LEFEBVRE, J., J. Chim. Phys.,55 227 (1958).

LUNDGREN, G., Arkiv Kemi 2 535 (1950).

LUNDGREN, G. & SILLÉN, L.G., Arkiv Kemi,1 277 (1949).

MATIJEVIĆ, E., ABRAMSON, M.B., SCHULZ, K.F. & KERKER, M., J. Phys. Chem.,64 1157 (1960).

PAN, KUAN & HSEU, TONG-MING, Bull. Chem. Soc. Jap.,28 162 (1955).

SCHAAL, R. & FAUCHERRE, J., Bull. Soc. Chim. Fr.,14 927 (1947).

SOUCHAY, P., Bull. Soc. Chim. Fr.,15 143 (1948).

(e) MISCELLANEOUS

BAIRD, T., Private Communication (1970).

BÖHM, J., Z.anorg. allgem. Chem., 149 203 (1925).

FEITKNECHT, W., 4th Int. Symposium on Reactivity in Solids, Amsterdam (1960).

GALLAGHER, K.J. & PHILLIPS, D.N., Trans. Farad. Soc., 64 785 (1968).

GALLAGHER, K.J., Nature, 226 1225 (1970).

GILLERY, F.H., Am. Min., 44 143 (1959).

KOHLSCHUTTER, V., EGG, C. & BOBTLESKY, M., Helv. Chim. Acta, 8 457 (1925).

KOLTHOFF, I.M. & MOSKOVITZ, B., J. Am. Chem. Soc., 58 777 (1936).

MACKAY, A.L., 4th Int. Symposium on Reactivity in Solids, Amsterdam (1960).

MACKAY, A.L., Min. Mag., 32 545 (1960).

MARSHALL, W.L. & GILL, J.S., J. Am. Chem. Soc., 79 1300 (1957).

POPLE, J.A., SCHNEIDER, W.G. & BERNSTEIN, H.J., "High Resolution Nuclear Magnetic Resonanance", London (1959).

PRASAD, R., BEASLEY, M.L. & MILLIGAN, W.O., J. Electron Microscopy, 16 101 (1967)

SLUSHER, R., J. Inorg. Nucl. Chem., 25 283 (1963).

VAN DEN BERGHE, E.V., VANDER KELEN, G.P. & EECKHAUT, Z., Bull. Soc. Chim. Belges, 76 79 (1967).

WATSON, J.H.L., CARDELL, R.R. & HELLER, W., J. Phys. Chem., 66 1757 (1962).